3

500

AFML-TR-78-127

SA
VO
II A065521

LEVEL

2

STRUCTURAL PROPERTIES OF ADHESIVES
Volume I

W. J. RENTON

VOUGHT CORPORATION
ADVANCED TECHNOLOGY CENTER, INC.
POST OFFICE BOX 226144
DALLAS, TEXAS 75266

SEPTEMBER 1978

TECHNICAL REPORT AFML-TR-78-127
Final Report April 1976 — September 1978

DDC

MAR 9 1979

C

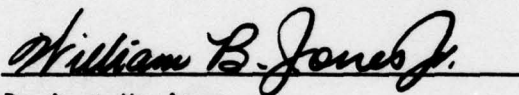Approved for public release; distribution unlimited.

AIR FORCE MATERIALS LABORATORY
AIR FORCE WRIGHT AERONAUTICAL LABORATORIES
AIR FORCE SYSTEMS COMMAND
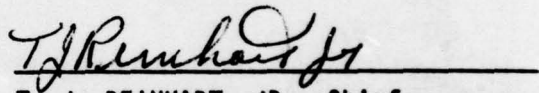WRIGHT-PATTERSON AIR FORCE BASE, OHIO 45433

79 03 06 021

NOTICE

When Government drawings, specifications, or other data are used for any purpose other than in connection with a definitely related Government procurement operation, the United States Government thereby incurs no responsibility nor any obligation whatsoever; and the fact that the government may have formulated, furnished, or in any way supplied the said drawings, specifications, or other data, is not to be regarded by implication or otherwise as in any manner licensing the holder or any other person or corporation, or conveying any rights or permission to manufacture, use, or sell any patented invention that may in any way be related thereto.
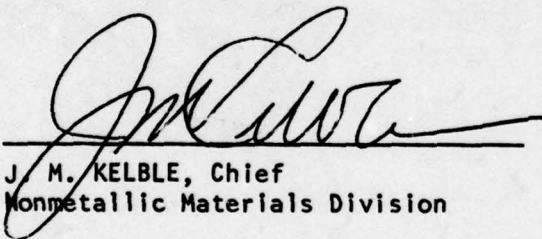
This technical report has been reviewed and is approved for publication.

William B. Jones Jr.

Project Monitor
FOR THE COMMANDER

T. J. Reinhart Jr

T. J. REINHART, JR., Chief
Composite & Fibrous Matls Branch
Nonmetallic Materials Division

J. M. Kelble

J. M. KELBLE, Chief
Nonmetallic Materials Division

REPORT DOCUMENTATION PAGE	READ INSTRUCTIONS BEFORE COMPLETING FORM

1. REPORT NUMBER	2. GOVT ACCESSION NO.	3. RECIPIENT'S CATALOG NUMBER
AFML-TR-78-127-VOL-1		

4. TITLE *(and Subtitle)*	5. TYPE OF REPORT & PERIOD COVERED
STRUCTURAL PROPERTIES OF ADHESIVES. Volume I	Technical Final TECHNICAL REPT. VLI April 1976 - September 1978
	6. PERFORMING ORG. REPORT NUMBER
	2-53500/8CRL-96

7. AUTHOR(s)	8. CONTRACT OR GRANT NUMBER(s)
W. J. RENTON	F33615-76-C-5205

9. PERFORMING ORGANIZATION NAME AND ADDRESS	10. PROGRAM ELEMENT, PROJECT, TASK AREA & WORK UNIT NUMBERS
Vought Corporation Advanced Technology Center, Inc. P. O. Box 226144 Dallas, Texas 75266	7340-02-24

11. CONTROLLING OFFICE NAME AND ADDRESS	12. REPORT DATE
Air Force Materials Laboratory (MBC) Wright-Patterson AF Base, Ohio 45433	September 1978
	13. NUMBER OF PAGES
	177

14. MONITORING AGENCY NAME & ADDRESS *(if different from Controlling Office)*	15. SECURITY CLASS. *(of this report)*
	Unclassified
	15a. DECLASSIFICATION/DOWNGRADING SCHEDULE

16. DISTRIBUTION STATEMENT *(of this Report)*

Approved for public release; distribution unlimited

17. DISTRIBUTION STATEMENT *(of the abstract entered in Block 20, if different from Report)*

18. SUPPLEMENTARY NOTES

19. KEY WORDS *(Continue on reverse side if necessary and identify by block number)*

Structural Adhesives, Adhesive Bonding, Adhesive Mechanical Characterization

20. ABSTRACT *(Continue on reverse side if necessary and identify by block number)*

To enable primary structures to be adhesively bonded in future aerospace hardware structural response prediction procedures must be improved upon. One task in accomplishing this overall objective is a requirement that a set of standardized adhesive test specifications be formulated. It was the objective of this "Structural Properties of Adhesives" program to develop low cost adhesive test procedures required to generate the required rigorous engineering structural property data.

over

DD FORM 1473 EDITION OF 1 NOV 65 IS OBSOLETE
1 JAN 73
S/N 0102-014-6601

79 03 06 0219

389 797

The desired engineering structural properties were specified as was their accuracy requirements. Optimum adhesive test specimens were designed as was a new adhesive deformation measurement system; a parallel plate capacitor. An extensive review of the literature on adhesive testing enabled the formulation of ASTM type adhesive test specifications for static, viscoelastic, and fatigue characterization of adhesives. A fabrication specification was also formulated. Selected test data were generated to verify that the test procedures were easy to perform and repeatable. Additional improvements in the butt joint test procedure were recommended.

FOREWORD

The efforts reported herein were accomplished with the sponsorship of the Air Force Materials Laboratory, Air Force Systems Command, Wright-Patterson Air Force Base, Ohio, 45433. Dr. W. B. Jones, Jr., MBC, was the Air Force Project Engineer. The report is published in two volumes. The second volume contains Appendix A, "The Symmetric Lap Shear Test" and Appendix B, "Adhesive Joint Fabrication and Test Specifications".

iii

TABLE OF CONTENTS

TABLE OF CONTENTS (CONT'D)

LIST OF TABLES

LIST OF ILLUSTRATIONS

LIST OF SYMBOLS

A	Cross sectional area of adherend (in^2)
$A_1, A_2, A_3, B_4, B_5, B_6$	Materials property and specimen geometry constants
D_{11}	Flexural stiffness (in-lb)
E	Primary Young's modulus of adherends (psi)
G	Effective shear modulus of adhesive (psi)
L_1, L_2, L_4	Specimen lengths (in)
M_1, M_4	Bending moment (in-lb)
$N(x)_i^T$	Axial load due to thermal effects (lb)
Q_{11}	Primary stiffness modulus of adherend (psi)
S_i	Boundary value constants
T	Axial load (lb)
V_1, V_4	Transverse shear (lb)
$g(x)$	Temperature distribution function
h_1, h_2, h_3, h_4	Specimen thickness (in)
x, z	Orthogonal axes
β_i	Constants dependent on material properties
λ_i	Eigenvalues of characteristic equations
η	Adhesive thickness (in)
σ_o	Adhesive normal stress (psi)
τ	Adhesive shear stress (psi)

SUBSCRIPTS

L	Upper
u	Lower
1, 2, 3, 4	Part designation

SUPERSCRIPTS

"T"	Temperature

xiii

SECTION I

RESEARCH OBJECTIVE

Adhesive bonding technology has been improved over the last several years. Improvements in materials, processes, surface preparations and analyses for predicting the structural response of adhesive bonded joints are evident. However, structural response prediction procedures are hindered by a lack of accurate viscoelastic adhesive structural property data for various types of loadings and environments.

The reason structural property data are not available is that neither a unified test method nor instrumentation required for obtaining structural property data are available. Presently, numerous bulk, thin film and bonded joint test procedures are indiscriminately used to obtain structural property data on adhesives. Their ability to accurately characterize the structural response of adhesives is questionable. A definitive study was needed to review existing test procedures and develop new ones, as needed, that provide accurate, reproducible low cost adhesive structural property data.

The problem was two fold: (1) the data needs and accuracy requirements had to be unequivocally specified and (2) a set of standardized adhesive test procedures had to be developed to meet this need. Only then can one hope to derive adequate data for accurate prediction of bonded joint behavior in aircraft structures. It was the objective of the "Structural Properties of Adhesives" program to assess and develop the low cost test procedures required to generate rigorous engineering structural property data on adhesives so that items (1) and (2) are satisfactorily resolved for metal adherend bonded structures. To meet this objective, a program consisting of four separate tasks was performed. These four tasks and their stated goals were:

TASK I - REVIEW OF DATA REQUIREMENTS

The goal of this task was to provide a ranked list of adhesive property data required to predict the response of the adhesive in a bonded joint under a variety of load and environmental conditions experienced by aircraft structures. These results are presented in Section II.

TASK II - ASSESSMENT OF EXISTING TEST METHODS

It was the goal of this task to determine the capabilities of existing test procedures to provide the adhesive property data determined in Task I and to determine the merits and deficiencies of these test procedures based on the considerations listed above. The results are presented in Section III.

TASK III - DEVELOPMENT OF IMPROVED TEST METHODS

It was the goal of this task to develop a set of standard recommended test procedures for providing reliable, low cost data meeting the requirements generated in Task I. The recommended test procedures are presented in Volume II.

TASK IV - DATA GENERATION

The goal of this task was to demonstrate the utility, ease of performance and low cost of these various test methods for adhesives representing brittle and ductile structural behavior. The results are presented in Section X.

2

SECTION II

REVIEW OF DATA REQUIREMENTS

To meet the requirements of this task a three phase effort was undertaken:

o Review existing bonded joint analyses to ascertain the adhesive parameters required in the various analytical procedures. Supplement the list derived during this review to reflect time, temperature, and humidity effects as required.

o Perform a sensitivity analysis to ascertain the accuracy within which one should obtain the required adhesive mechanical properties.

o Rank the required adhesive properties in order of their importance to the various analytical routines with their associated accuracy requirements.

2.1 REVIEW OF EXISTING BONDED JOINT ANALYSES

A thorough review of existing bonded joint analyses was made which included a review of articles from NTIS, ASTM, Forest Product Laboratory Reports, Chemical Propulsion Information Agency documents and the various technical journals. Such a review was completed and is summarized in Table I. Only bonded joint configurations typically used in structural attachment configurations were considered. Those bonded joint configurations used to obtain adhesive mechanical property data (e.g. butt joint) will be discussed in detail in Section III. Moreover, the subject of adhesive fracture mechanics was not considered within this program.

A number of individuals have developed analytical or finite element analyses to determine the load and stress distribution for isotropic adherend bonded joints. Significant contributions to the state-of-the-art have been made in references 1 through 40.

The basic approach to analyzing adhesive joints has been to idealize the joint in terms of a mathematical model whereby the material properties and joint geometry are related to the applied loads, resulting in a fourth order or high differential equation. Its solution should result in a realistic description of the stress distribution in the joint. The analyses reviewed for the most part assumed that: (1) all elements are linearly elastic; (2) a state of plane strain

TABLE 1. SUMMARY OF ADHESIVES MECHANICAL PROPERTIES REQUIRED IN BONDED JOINT ANALYSIS

REFERENCES	ULT. SHEAR STRESS G	ULT. SHEAR STRESS E	POISSON'S RATIO	COEF. OF THERMAL EXPANSION	ELASTIC LIMIT SHEAR STRAIN	ULT. SHEAR STRAIN	E_{sec}	G_{sec}	TYPE OF BONDED JOINTS ANALYZED	TYPE OF ANALYSIS
Goland & Reissner	✓	✓							Single lap	*
Srinivas	✓	✓							Single, Butt & Double lap	*
Niskanen									Single & Double lap	*
Hahn & Fouser									Single & Double lap	*
Barker & Hatt	✓	✓							Single & Scarf lap	0
Pirvics	✓	✓							Single & Butt	0
Adams & Peppiatt	✓	✓	✓						Single & Double lap	0
Volkersen	✓								Single & Double lap	*
Erdogan & Ratwani					✓				Single, Stepped Scarf	*
Hartsmith (4 reports)	✓	✓				✓ (Need Adhesive Stress-strain curve)			Single, Double, Scarf, Stepped lap & Non-Classical Geometries	**,*
Dickson et.al.	✓	✓					✓	✓	Single, Double & Stepped lap	*,**
Grimes, Wah et. al.	✓	✓		✓(Plastic)			✓	✓	Single, Double & Stepped lap	**,0
Lehman et al.						✓ adhesive shear stress-strain curve			Single, Double Scarf & Stepped lap	0,0
Renton & Vinson(3)	✓	✓	✓						Single & Symmetric lap	*
Sharpe & Muha	✓	✓							Single lap	Survey Paper

TABLE 1. SUMMARY OF ADHESIVES MECHANICAL PROPERTIES REQUIRED IN BONDED JOINT ANALYSIS (CONT).

REFERENCES	G	E	ULT. SHEAR STRESS	POISSON'S RATIO	COEF. OF THERMAL EXPANSION	ELASTIC LIMIT SHEAR STRAIN	ULT. SHEAR STRAIN	E_{sec}	G_{sec}	TYPE OF BONDED JOINTS ANALYZED	TYPE OF ANALYSIS
Dietz	Coefficient of hygroscopic expansion									Butt Joint	x
Sainsbury & Carter	✓						✓			Tapered lap joint	o
Terekova & Skoryi	✓	✓	✓							Cylindrical lap joint	*
Kelsey & Bensen	✓	✓	✓							Single lap	x
Pahoja	✓	✓	✓							Single lap	x
Harrison & Harrison	✓	✓	✓							Butt & Single lap	o
Cornell	✓	✓	✓							Single lap	*
Wooley & Carver	✓	✓	✓							Single lap	o
Plantema	✓	✓	✓							Single lap	*
Szepe	✓	✓	✓				✓			Double lap	□
Corvelli	✓	✓	✓		✓		✓			Single & Stepped lap	o
Nastran	✓	✓	✓	✓	✓		✓			Single, Double, Scarf & Stepped lap	o, ▣
Das Gupta & Sharma	✓	✓	✓	✓						Single lap	*, *
Wah	✓	✓	✓	✓						Single lap	*
Goodwin	✓	✓	✓	✓			✓			Single & Double lap	▣, o
Gehring et. al.	✓	✓	adhesive tensile and shear stress-strain curves								x

** approximate elastic-plastic closed form analysis   * semi-experimental method

* approximate linear elastic closed form analysis   ▣ elastic-plastic finite element method

o linear elastic finite element analysis   x analytical minimum energy method

or plane stress is assumed to exist across the width of the lap; (3) there is
no stress variation through the thickness of the adhesive; (4) the adherends
follow classical plate theory; (5) the adhesive is fully bonded to the adhe-
rends; (6) adhesive properties are uniform throughout the joint; and (7)
linear small deflection theory is valid. However, because many of the duc-
tile adhesives and resins in use today exhibit physical and/or kinematic
nonlinear behavior at relatively low percentages of their ultimate
strength and because the generally orthotropic behavior of composite materials
add further complexities, the traditional analytical techniques available have
become less reliable. More realistic approaches to this problem have been
advanced in references 23 and 25, among others, by using linear and nonlinear
discrete element analysis of the joint. Such analyses are more costly to run
and require additional time in data preparation and in the interpretation of
results. Thus, closed form analytical methods are preferable whenever possible.
Several of the more prominent analytical methods will now be enlarged upon.

In 1944, Goland and Reissner[3] determined the stresses in a single lap joint
for a relatively inflexible cement layer ($\frac{\text{thickness adherend}}{\text{elastic modulus adherend}} \gg \frac{\text{thickness adhesive}}{\text{elastic modulus adhesive}}$) in which the cement layer is ignored, and for a rela-
tively flexible cement layer whereby the properties of the cement are taken into
account in the analysis. They assumed the joint acted as a cylindrically bent
plate of variable cross section and neutral plane location. Their analytical
results are among the most accurate in characterizing the peak adhesive shear
and tensile stresses in a single lap joint as evidenced by reference 37.

Hart-Smith[32-34] developed an approximate continuum mechanics solution to
determine the static load carrying capability of a scarf, single lap, double
lap and a stepped-lap joint. He accounted for adhesive plasticity effects,
thermal mismatch and variable step lengths in the analysis. The analysis is
restricted to isotropic adherends while the tensile stresses in the adhesive
are ignored and the stresses in the adherends are inadequately quantified. His
analysis takes the form of a infinite series. Results indicate that the adhesive
film strain energy in shear per unit bond area obtained from the thick adherend
symmetric lap joint can be used most effectively in predicting the adhesive fail-
ure in a bonded joint. He emphasized an ultimate strain failure criterion.

6

The most ambitious attempt to analyze a bonded joint is presented by Grimes et. al.[23] His assumptions of plane strain, orthotropic adherends, mid-plane symmetry and the inclusion of plasticity effects in the adhesive and adherends resulted in the solution of two non-linear, non-homogeneous differential equations. The solution is of the same form for stepped-lap, single lap and scarf joints. Experimental verification by Sharpe and Muha[37] of the single-lap joint data found the analysis lacking in its ability to predict the adhesive stress distribution.

Renton and Vinson[35] developed a closed form analytical solution for generally dissimilar adherends, which satisfied all boundary conditions and accounted for the effects of traverse shear and normal strains in the adherend. Sharpe and Muha,[37] experimentally verified that this method of analysis predicted the adhesive shear stress distribution in the most realistic manner of the nearly twenty closed form and finite element methods analyzed. They stated that "there are significant normal stresses present, and it is presumed that the theory that can best predict the measurable shear stress under these complicated conditions will be the best theory". Additionally, the results of a photoelastic study of the symmetric lap joint[48] further substantiates the adequacy of the analysis by verifying that the predicted adherend stresses are in direct agreement with the photoelastic test results.

A problem of increasing importance is the swelling strain introduced into a bonded structure when the structure is in a high humidity environment. Papers by Dietz and Reissner[4] and by Harrison and Harrison[24] describe specific attempts to analyze the severity of the problem. The problem is handled analytically analogously to the thermal strain problem since the form of the field equations is the same.

Viscoelastic analysis per se is absent in the articles reviewed to date. However a quasi-elastic[69] approach to the linear viscoelastic problem can often lead to practical results in some situations. The quasi-elastic method simply involves replacing the modulus, E, in the elastic analysis with its time dependent counterpart $E(t)$.

A summary of the adhesive mechanical properties required for the various bonded joint analyses is summarized in Table 1.

Based on the review of existing analytical techniques, which are inconclusive in their ability to thoroughly characterize the response of an adhesive bonded joint, and a parametric study conducted by Renton and Vinson,[44] the material property variables which appear most important are:

o The adherend primary modulus (E_{11})

o The adhesive shear and tensile moduli

o The adhesive's ductility and ultimate properties in tension and shear

o Coefficients of thermal and hygroscopic expansion

2.2 SENSITIVITY ANALYSIS

The objective of this analysis was to determine the sensitivity of the peak adhesive shear and normal stresses to a prescribed change in adhesive shear and tension moduli for adhesive bonded joints (Figure 1). With this knowledge, the accuracy can be defined within which adhesive moduli should be measured to enhance the accurate analytical prediction of peak adhesive stresses in bonded joints. The accuracy of adhesive property data required is important as it determines:

o The test specimens' allowable geometric tolerances

o The sensitivity requirements of the measurement system by which deformation or strain measurements are taken

o The overall test method accuracy one must employ in obtaining meaningful adhesive structural property data

The accuracy of adhesive property data required for meaningful input in rigorous structural analysis routines can best be determined through a parametric study on the sensitivity of peak adhesive stresses to variations in select nondimensional bonded joint parameters. Studies by Renton and Vinson[44] and DeBruyne[7] have pinpointed those parameters which have a significant influence on the adhesive stress distribution in a bonded structure. They are:

o Adherend inplane and flexural stiffness - this is a function of the primary Young's modulus (Q_{11}) and the adherend's thickness (h). Generally, stiff adherends result in a uniform adhesive shear stress distribution with minimal tearing stresses along the overlap length.

8
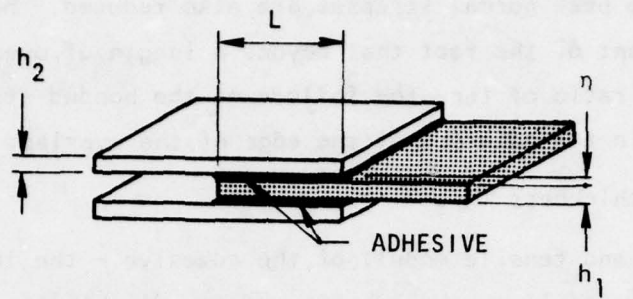
(a) DOUBLE LAP
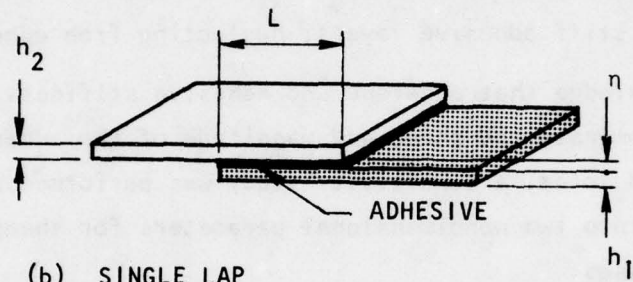
(b) SINGLE LAP
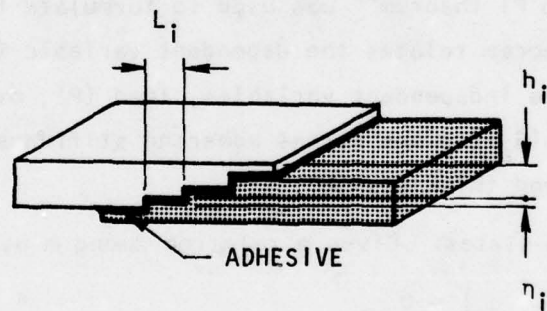
(c) STEPPED LAP

FIGURE 1. VARIOUS BONDED JOINT DESIGNS.

9

o Overlap length - as this parameter increases in magnitude the adhesive
   shear stress becomes more uniform, approaching a (Load/Area) distribu-
   tion. The peak normal stresses are also reduced. However, one should
   be cognizant of the fact that beyond a length of overlap to adherend
   thickness ratio of ten, the failure of the bonded structure is likely
   to occur in the adherend at the edge of the overlap.

o Adhesive thickness (η).

o The shear and tensile moduli of the adhesive - the influence of the
   adhesive's moduli on the adhesive stress distribution is important
   for bonded joints composed of thick deformable adhesive layers,
   while the adhesive's influence on the stresses is insignificant
   for thin, stiff adhesive layers; neglecting free edge effects.

With the knowledge that adherend and adhesive stiffness, and thickness, and
overlap length, dominate the shape and magnitude of the adhesive stress distri-
bution in a bonded joint, a sensitivity study was performed by incorporating
these parameters into two nondimensional parameters for shear and two for adhe-
sive tearing stresses.

The Buckingham Pi theorem[52] was used to formulate the nondimensional para-
meters. The Pi theorem relates the dependent variable (i.e. τ_{max} = maximum
shear stress) to the independent variables, load (P), overlap length (L), adhe-
sive shear modulus (G_a), plane stress adherend stiffness (Q_{11}), adhesive thick-
ness (η) and adherend thickness (h).

The Pi theorem states: Given a relation among m parameters of the form

$$f_2(q_1, q_2, \ldots, q_m) = 0 \qquad\qquad 1$$

an equivalent relation expressed in terms of n nondimensional parameters can be
found of the form

$$f_3(\pi_1, \pi_2, \ldots, \pi_n) = 0 \qquad\qquad 2$$

where the number n is given by the relation

$$n = m - k \qquad\qquad 3$$

where m is the number of q's in Eq. 1 and k is equal to the minimum number of
independent dimensions required to construct the dimensions of all the parameters
$q_1, q_2 \ldots, q_m$.

The π's to completely define the bonded joint problem in shear for identical adherends are

$$\pi_1 = \frac{\tau_{max} L}{P} \; ; \quad \pi_2 = \frac{G_a L^2}{Q_{11} h\eta} \; ; \quad \pi_3 = \frac{h}{L} \qquad\qquad 4$$

Based on linear elastic theory, two simplifications have been made. They are:

i   Assuming a linear elastic adhesive, the maximum stress (τ_{max})* is proportional to the applied inplane load (P).

ii   The effective shear modulus of the adhesive (G_a) and the adhesive thickness (η) enter into the linear analysis in combination (G_a/η), as the adhesive is being characterized in terms of it's overall shear stiffness.

Hence:

$$f_3(\pi_1, \pi_2, \pi_3) = 0 \qquad\qquad 5$$

which is equivalent to:

$$\pi_1 = f_4(\pi_2, \pi_3) \qquad\qquad 6$$

or

$$\frac{\tau_{max} L}{P} = f_4\left(\frac{G_a L^2}{Q_{11} h\eta}, \frac{h}{L}\right) = f_4\left(\frac{G_a L^2}{A\eta}, \frac{h}{L}\right) \qquad\qquad 7$$

where

p = load/unit width (lb/in)

L = overlap length (in)

P/L = average shear stress (psi)

$Q_{11}h = A$ = adherend inplane stiffness

The parameter π_2, is a measure of the shear strain (stress) in the adhesive due to inplane adherend deformation vs. the average shear strain in the adhesive. Moreover, Debruyne[7] has shown π_2 to be an approximate similitude parameter.

———————————

*The singularity in the shear and normal stress predicted at the edge of the adhesive-adherend interface is not considered.

11

In a similar manner, the sensitivity of the maximum adhesive normal stress (σ_{max}) to the independent parameters P, L, Q_{11}, h, η and E_a can be formulated using the Pi theorem.

For identical adherends they are:

$$\overline{\pi}_1 = \frac{\sigma_{max} L}{P} \quad ; \quad \overline{\pi}_2 = \frac{E_a L^4}{D\eta} \quad ; \quad \pi_3 = \frac{h}{L} \qquad \qquad 8$$

which is equivalent to;

$$\frac{\sigma_{max} L}{P} = f_4 \left(\frac{E_a L^4}{D\eta} , \frac{h}{L} \right) \qquad \qquad 9$$

where

$$D = \frac{Q_{11} h^3}{3} = \text{the adherend's flexural stiffness.} \qquad \qquad 10$$

The use of the E_a/η term follows from simplification (ii) with E_a replacing G_a. The parameter $\overline{\pi}_2$ is a measure of normal strain (stress) in the adhesive due to the adherend's flexural rigidity vs. the average normal strain in the adhesive.

The results of the sensitivity analysis were obtained using the in-house computer routines (BOND 3) for identical adherends and (BOND 4) for dissimilar adherends. The results of the sensitivity analysis are presented in Figures 2-5 for similar and dissimilar adherends. These two conditions establish the bounds on the sensitivity indices, including various degrees of joint flexibility and associated moment and h/L effects. The BOND 4 results are for a limiting case whereby the dissimilarity of the adherends is accounted for (Figure 1). Dimensional analysis of dissimilar adherends requires that two additional π's be considered:

$$\pi_4 = \frac{Q_{11} h_1 + Q_{22} h_2}{Q_{11} h_1} = 1.08 \quad ; \qquad \pi_5 = \frac{Q_{11} h_1^3 + Q_{22} h_2^3}{Q_{11} h_1^3} = 1.00 \qquad 11$$

where: $h_{avg} = (h_1 + h_2)/2$ replaces h in equations 7 and 9.

12
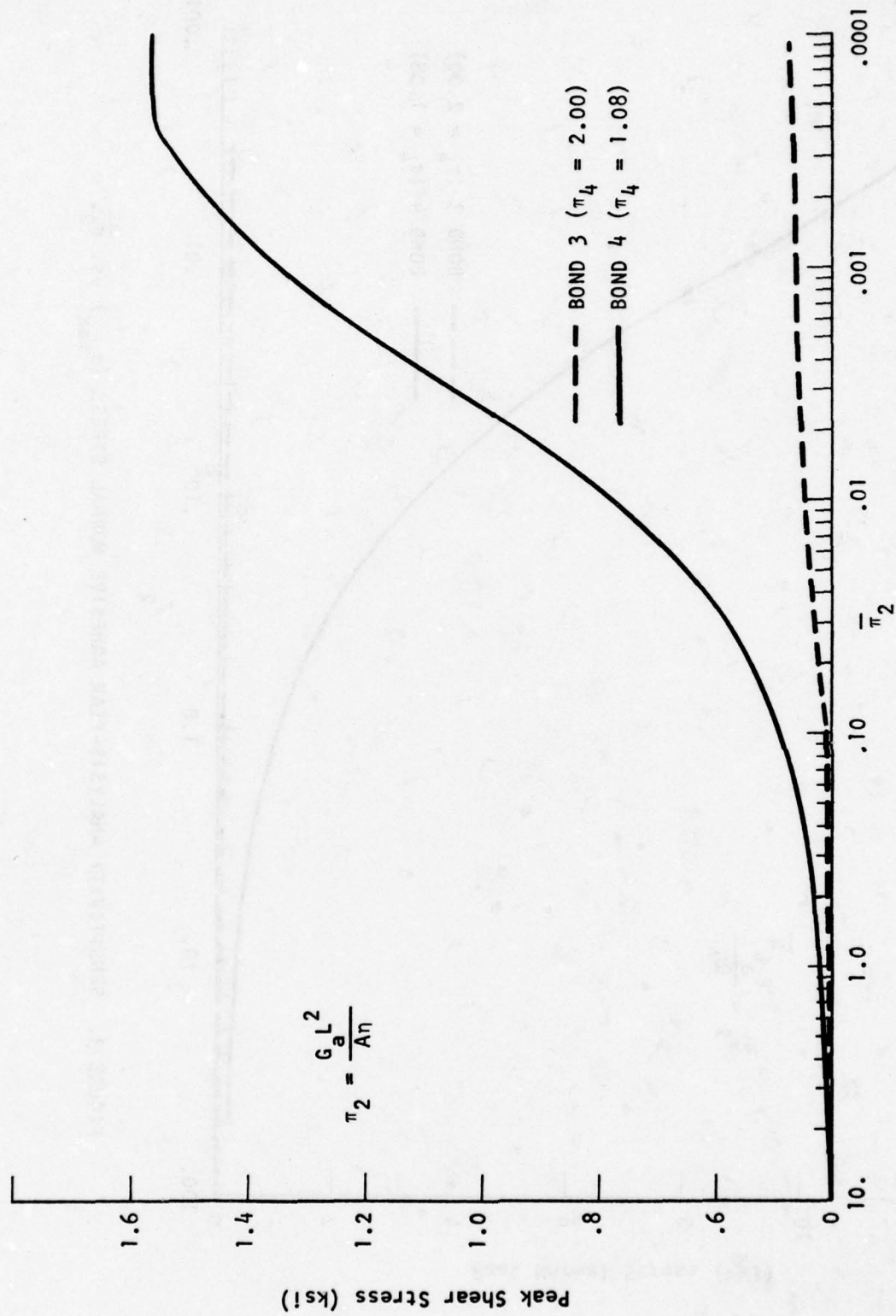
FIGURE 2. SENSITIVITY ANALYSIS—PEAK ADHESIVE SHEAR STRESS (τ_{max}) vs. π_2.

$$\pi_2 = \frac{G_a L^2}{An}$$

BOND 3 ($\pi_4 = 2.00$)
BOND 4 ($\pi_4 = 1.08$)

Peak Shear Stress (ksi)

$\overline{\pi}_2$

13

$$\bar{\pi}_2 = \frac{E_a L^4}{D\eta}$$

Peak Normal Stress (ksi)

BOND 3 (π_4 = 2.00)

BOND 4 (π_4 = 1.08)

$\bar{\pi}_2$
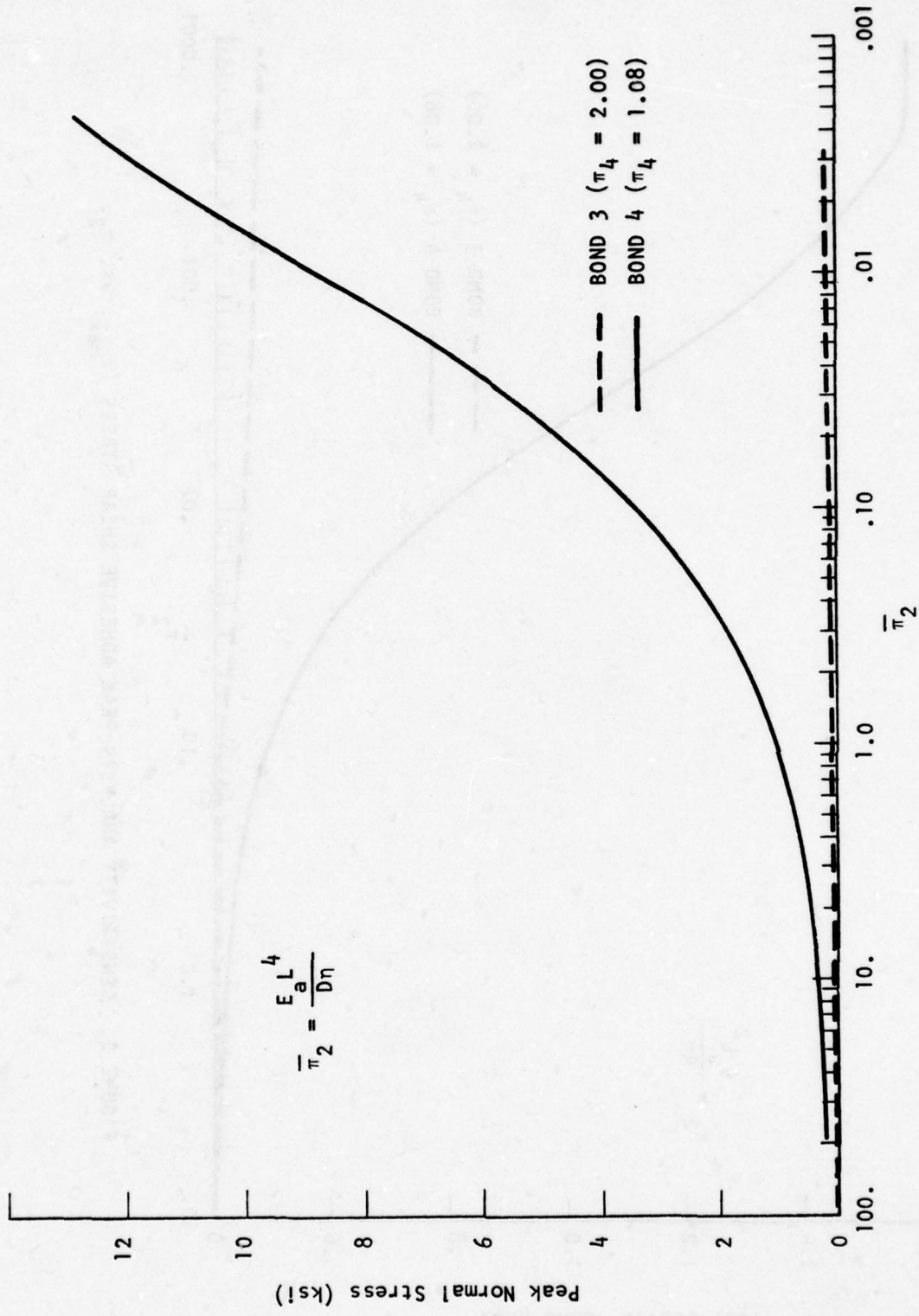
FIGURE 3. SENSITIVITY ANALYSIS-PEAK ADHESIVE NORMAL STRESS (σ_{max}) vs. $\bar{\pi}_2$.

14
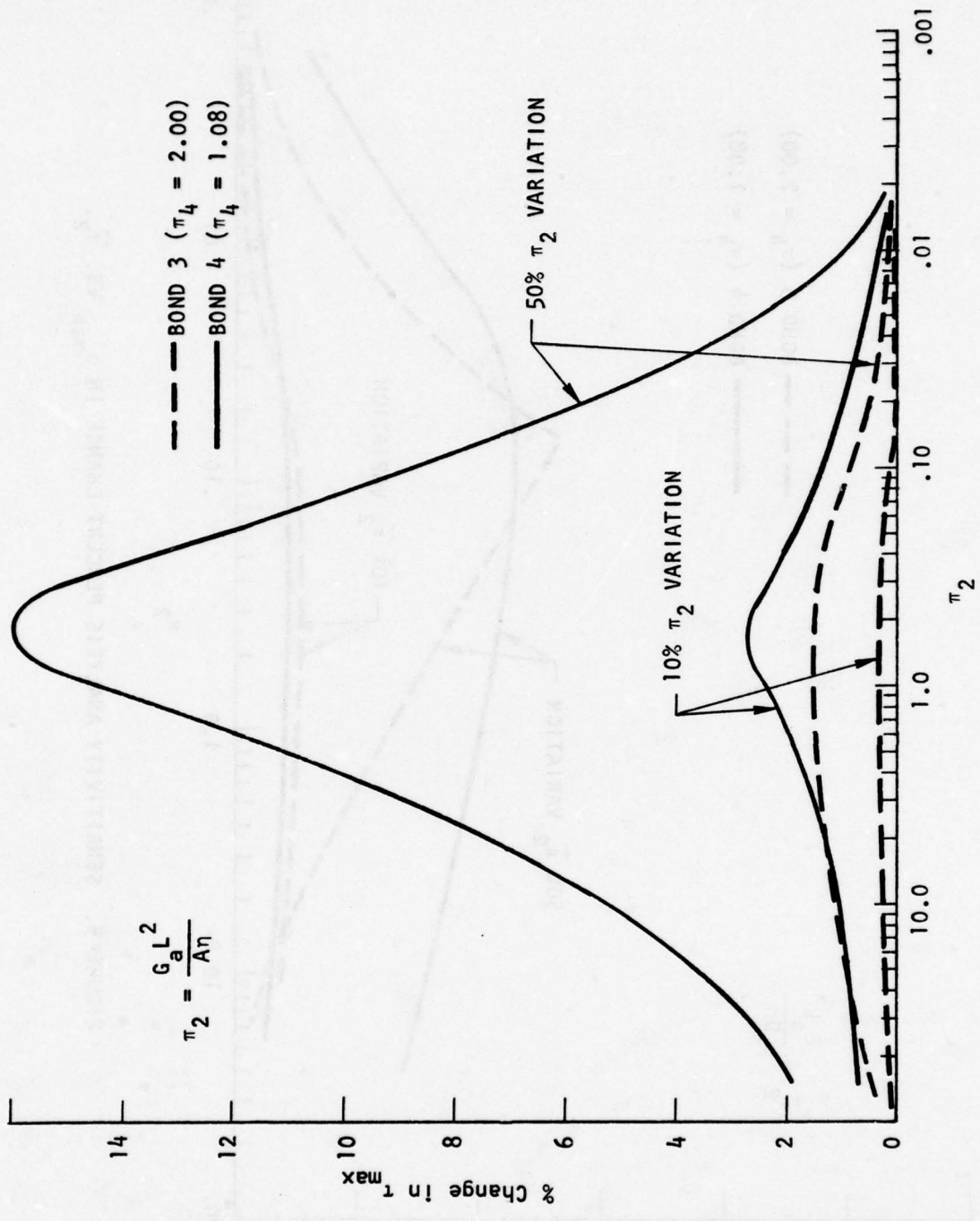
FIGURE 4. SENSITIVITY ANALYSIS PERCENT CHANGE IN π_{max} VS. π_2.

15
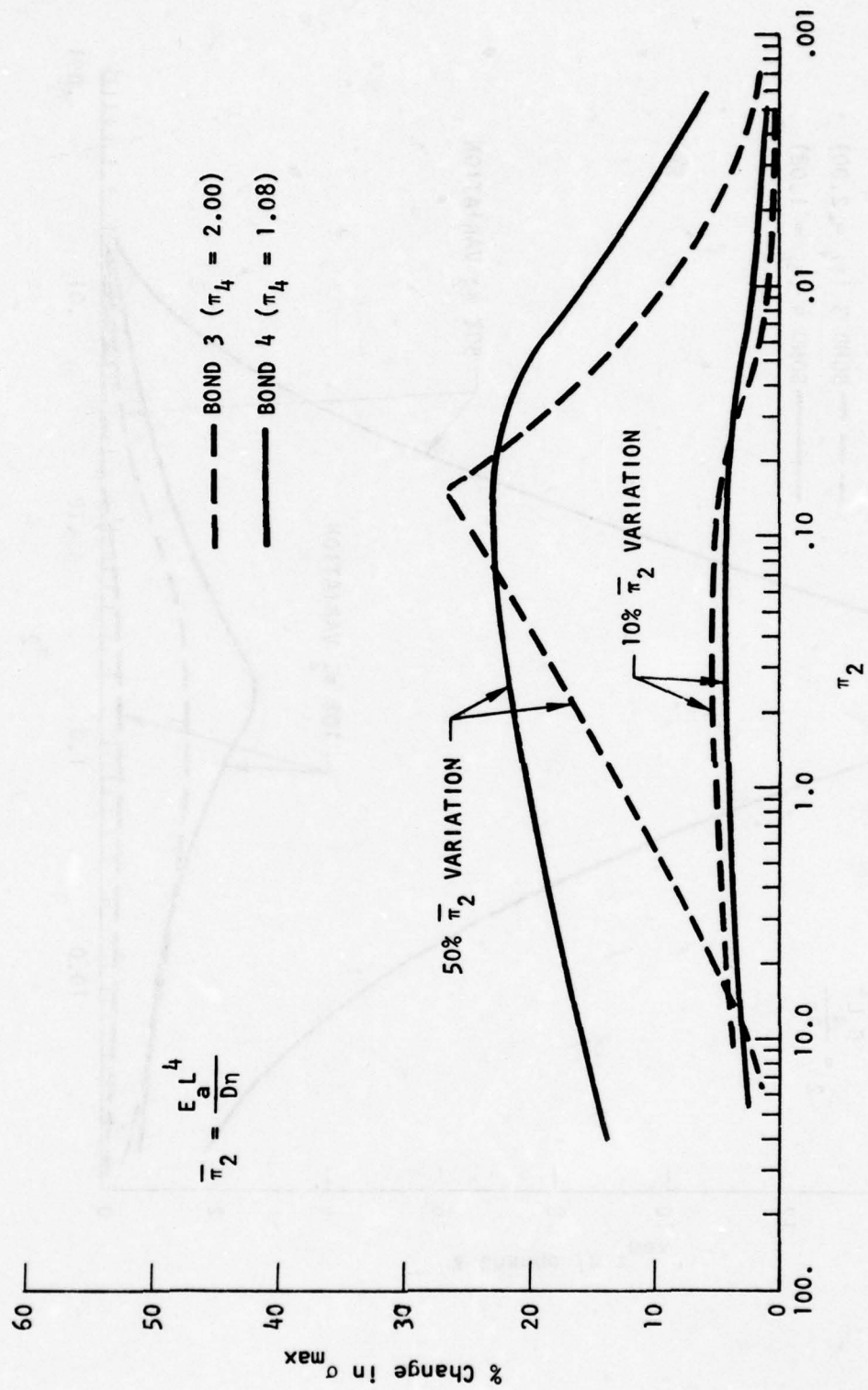
FIGURE 5. SENSITIVITY ANALYSIS PERCENT CHANGE IN σ_{max} VS. $\bar{\pi}_2$.

16

The dependence of τ_{max} and σ_{max} on various h/L ratio's, for all values of π_2 and $\bar{\pi}_2$, was found to produce curves within the envelope formed by the solid and dotted lines in Figures 2 and 3. Therefore, only the limiting cases were used to determine the sensitivity curves presented in Figures 4 and 5.

Figures 4 and 5 show the sensitivity of the peak adhesive stresses to a 10% and 50% variation in the nondimensional parameters. Inspection of Figures 4 and 5 reveals that the normal stress is somewhat more sensitive to its nondimensional parameter than the shear stress. From Figure 4 one can readily observe that the range of significant sensitivity is for $.01 \leq \pi_2 \leq 2.5$. For practical designs, in which adherend failure is absent, the magnitude of adhesive shear moduli corresponding to this spread of π_2 is $300 \leq G \leq 300,000$. A range of extreme sensitivity for the adhesive tension modulus can also be established from inspection of Figure 5. It is $200 \leq E \leq 1,500,000$ for $\bar{\pi}_2 \leq 40.0$. Within these limits, the adhesive properties will significantly influence the adhesive stress distributions for most bonded joint designs.

Review of Figures 4 and 5 dictates that the normal stress sensitivity be used to establish a realistic design goal for the accurate determination of adhesive moduli. A $\pm$ 5% change in adhesive tension modulus ($\bar{\pi}_2$ in Figure 5). would enable one to ascertain the peak normal stress to within $\pm$ 2.5%. This is a desirable modulus determination goal and was used in the Tasks II and III of this program to formulate the accuracy requirements for an adhesive deformation measurement device and for the necessary geometric measurements of the test specimens.

2.3 EXTENSION TO OTHER BONDED STRUCTURES

The results presented, while based on single lap joint analyses, are believed to be upper bounds for the sensitivity of peak adhesive stress vs. adhesive modulus for the stepped-lap and double lap joints, shown in Figure 1 due to eccentric load path effects. More uniform shear stress distributions in these joints necessitates that an applied load divided by surface area shear stress will be approximated. Therefore, the response of these joints should be less dependent on adhesive modulus, being independent of the modulus in the limit. Typical stress distributions are shown in Figure 6.

17
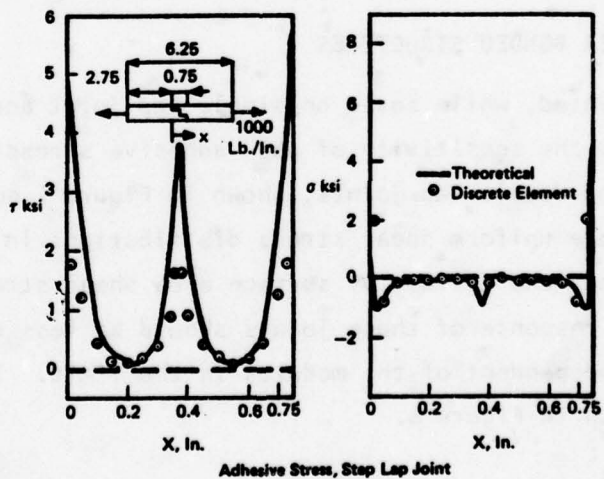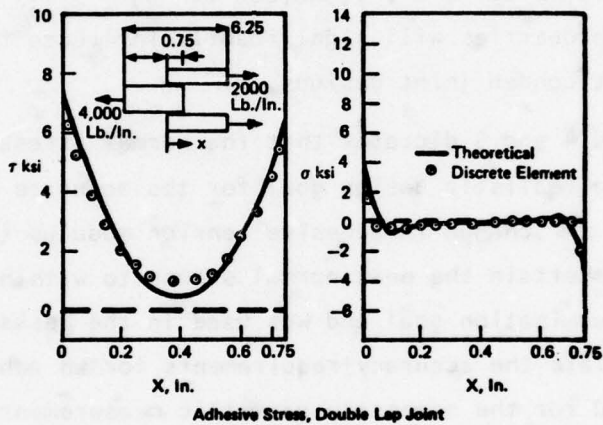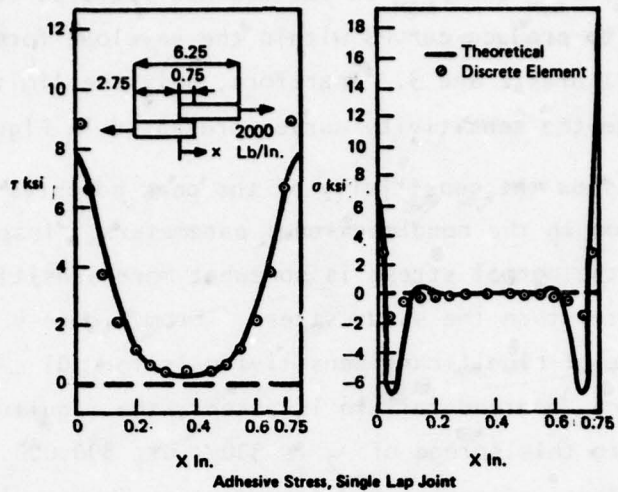
FIGURE 6. TYPICAL ADHESIVE STRESS DISTRIBUTIONS PER REFERENCE (23).

18

2.4 COMPLETE ADHESIVE CHARACTERIZATION

Additional adhesive property data requirements depend on the type of rigorous analysis of aircraft bonded structural components one wishes to perform. Assuming an all encompassing analysis is desired for both brittle and ductile adhesives, an additional list of adhesive property data that must be considered, based on an on-going literature search of applicable continuum mechanics, viscoelastic and fatigue theories of bonded joint behavior has been compiled.

The complete characterization of an adhesive requires that its response to various load, time and environmental conditions be ascertained. The data desired were:

o Stress-Strain response at constant strain rate to failure

o Cyclic stress-strain response vs. number of cycles to failure

o Creep response

o Combined shear and tension response

o The response of the first three items to various moisture and temperature environments

The effects of the innumerable combinations of loading and environment on the mechanical and physical response of adhesives was not ascertained in this program but should be considered for later Air Force programs.

2.5 RANKING OF ADHESIVE PROPERTY DATA REQUIREMENTS

The ranking (relative importance) of specific adhesive property data required to predict the response of the adhesive in a bonded joint under typical aircraft structural loads and environments was the overall goal of this initial task.

The list of desired adhesive properties ranked from most important to least important within the numerical categories only are:

2.5.1 Mechanical Properties Requirements Ranking

o Linear elastic shear and tension moduli[*]

o Creep compliance master curves in shear and tension

---

[*]For an isotropic, homogeneous adhesive layer, the Poisson's ratio may be determined in place of the shear or tension modulus.

o Linear viscoelastic limit shear and tension stress (strain). This
approximates the proportional limit stress.

o Fatigue shear and tension moduli that reflect the adhesive's
wearout and/or stability region just prior to catastrophic failure.

2.5.2 Strength Properties Requirements Ranking

o Ultimate shear, tension and combined shear and tension strength

o Ultimate shear and tensile strain

o Fatigue tensile and shear strength (strain) vs. cycles to failure

o Fatigue endurance limit values

2.5.3 Physical Properties Requirements Ranking

o Coefficient of thermal expansion

o Coefficient of hygroscopic expansion

The effect of adhesive thickness, aging, scrim support, surface roughness
temperature and humidity on all of the above items, and the inclusion of strain
rate effects as applicable should also be determined. This would include the
development of a test to determine when moisture equilibrium of the adhesive has
been attained for a particular environment.

SECTION III

ASSESSMENT OF EXISTING TEST METHODS

It was the goal of this task to determine the capabilities of existing test procedures to provide the adhesive property data required in Task I and to determine the merits and deficiencies of these test procedures based on the constraints defined in Task I.

To meet the requirements of this task a three phase effort was undertaken:

o Formulate and rank a set of evaluation criteria by which the relative merits and deficiencies of the various test specimens and testing procedures could be judged.

o Provide an in-depth review of existing test specimens and test methods for measurement of adhesive properties within the constraints defined in Task I.

o Summarize the results of the evaluation (e.g. test specimen merits and deficiencies) of the currently available test methodology in a matrix format, ranking the test methods and specimen designs as to their capability to obtain the adhesive property data required by the analytical methodology identified in Task I.

3.1 TEST SPECIMEN EVALUATION CRITERIA

To objectively evaluate the adequacy of the various test specimens available from which one can obtain adhesive mechanical property data, the following specimen evaluation criteria were defined.

THE SPECIMEN LOADING MODE IS DOMINANT AND CONTROLLABLE - Tension and shear modes should be separable and their magnitude easily controlled. A biaxial or triaxial stress state should be present in the adhesive.

SPECIMEN IS CAPABLE OF PROVIDING QUANTITATIVE RESULTS - Modulus and strength data in representative environments should be possible to obtain.

TEST SPECIMEN IS REPRESENTATIVE OF MATERIALS AND PROCESSING USAGE IN A PRODUCTION ENVIRONMENT - The specimen should reflect the chemical, physical and mechanical response of an adhesive bonded between two relatively rigid adherends.

21

A REALISTIC ANALYSIS OF THE BIAXIAL OR TRIAXIAL STRESS STATE IN THE ADHESIVE BONDED TEST SPECIMEN IS POSSIBLE - A closed form or finite element analysis should verify the suitability of using the specimen for the generation of static, fatigue and viscoelastic stress-strain response data for representative temperatures and relative humidities. It should account for the constraint effect of the adhesive by the adherend when applicable and for the viscoelastic nature of the adhesive. Nonlinear adherend deformation effects should be avoided. Finally, the analysis should be capable of providing an estimate of the error introduced on the adhesive stress and deformation state by non-uniform adhesive thickness control and geometrical variations of pertinent specimen dimensions.

EASE OF SPECIMEN FABRICATION AND ASSOCIATED COST - Multiple specimen preparation should be possible, relatively easy to achieve and of nominal cost. Uniform dimensional control of adhesive bondline thickness over the normal range of adhesive thicknesses (i.e., .002" → .030") is necessary for proper test data interpretation. Specimen adherend dimensions should not require unusually close tolerances, while the bond surface undulations of the adherends should be minimal to insure uniform adhesive thickness control. Means to attain accurate adhesive thickness control should include considerations of shims, scrim and a precision fabrication fixture.

THE SPECIMEN SHOULD BE USABLE FOR TESTING BRITTLE AND DUCTILE ADHESIVES - The specimens response for both brittle and ductile adhesives should be reflected in the analysis (i.e., elastic vs. viscoelastic). Moreover, any sensitive specimen gripping or instrumentation problems which may make the attainment of meaningful mechanical test data difficult should be avoided.

THE SPECIMEN'S BONDLINE SHOULD BE EASILY ACCESSIBLE, TO ACCURATELY MEASURE ITS THICKNESS - Microscopes, Verniers and gage blocks with a Vernier are several ways one may measure adhesive bondline thickness accurately. A number of measurements along the perimeter of the bondline should be possible to verify bondline uniformity. For visual measurement a sharp contrast between adhesive and adherend is desirable.

THE SPECIMEN'S BONDLINE SHOULD BE EASILY INSPECTED BY NDE MEANS - Inspection of the bondline for debonds, voids and air bubbles should be possible for defects as small as .050 inches. Adherend thickness requirements should not impose any severe restriction on inspection of the bondline using NDE techniques. NDE means to consider are:

o X-ray

o Pulse-echo ultrasonics

o Neutron Radiography

o Transmission ultrasonics

3.2 TEST METHODOLOGY EVALUATION CRITERIA

Once the test specimen has been determined it is mandatory that simple, reliable test procedures be employed to minimize data scatter and cost. The evaluation criteria to be considered were:

ENVIRONMENTAL TEST CONSIDERATIONS - Proper environmental conditioning of test specimens should insure that moisture and temperature equilibrium in the bondline have been attained. Subsequently, long term mechanical tests should be performed within this environment. Moisture and temperature equilibrium times vs. temperature-moisture history should be determined to ensure equilibrium requirements are met. Means to accurately measure temperature from -60°F to 350°F and relative humidity from 10% to 100% before and during the performance of mechanical tests should be determined.

TEST APPARATUS AND INSTRUMENTATION - Adhesive deformation measurement device sensitivity requirements should be established to determine the adhesive properties to within ±3.4%. The maintenance of this sensitivity over the prescribed temperature-humidity test extremes should be ascertained.

Additional factors to be considered in the selection of a deformation measurement device should include:

o Ease of attachment to the test specimens

o Simplicity

o Stability with respect to time and environment

23

o Range of usage

o Linearity

o Durability

o Cost

EASE OF TEST PERFORMANCE AND REPEATABILITY - The actual test methodology used for short and long term testing by various groups were reviewed to ascertain its ease of performance by those familiar with good test procedures. The likelihood of avoiding inadvertent errors (i.e. to insure repeatability) in performance of the test methodology should be considered and verified by selective testing. Errors may be introduced by specimen alignment sensitivity, loading fixture complexity and/or deformation measurement system complexity.

REDUCTION OF RAW TEST DATA - Presently used data reduction techniques were reviewed as pertains to their utility in characterizing adhesive raw data for direct inclusion in bonded joint analysis. Data reduction techniques should reflect the impact of static, fatigue, viscoelastic and environmental effects on adhesive properties.

FAILURE SURFACE EXAMINATION - Visual and microscopic means in use today should be evaluated for their ability to gleen pertinent information from the failed adhesive surfaces. The ease and cost of using the various microscopic devices vs. the potential information to be obtained should be determined.

OVERALL COST - The overall cost to perform a specific test methodology should be determined. The cost should include specimen fabrication, NDE inspection, and environmental conditioning. Additionally, the cost of special grips, fixtures, instrumentation, performance of the actual test, data reduction and reporting should be included in the overall cost.

A summary of the strengths and weaknesses of test specimens and test methodology has been ascertained per these evaluation criteria.

3.3 REVIEW OF THE STATE OF THE ART TEST METHODOLOGY

In implementing the test methodology literature search, the following areas of documentation were searched for their contribution to the state-of-the-art on adhesive test methodology:

o ASTM Standard Adhesive Property Test Methods

o DoD Program Technical Reports

o Space Science Reports

o Forest Product Laboratory Reports

o Federal Test Methods

o Engineering Journals

3.4 CANDIDATE TEST SPECIMEN REVIEW

A summary of the various candidate test specimen geometries already in exist-ance vs. the evaluation criteria is given in Table 2. From this review, the test specimens deemed best suited for the successful accomplishment of this program are:

o Thick Adherend Lap Joint - Shear

o Butt Joint - Tension

o Scarf Joint - Combined tension plus shear

These results are subject to the constraints that:

o Only the use of metal adherends was considered in this review.

o Bulk adhesive specimens were excluded from serious consideration as the "candidate test specimens" as they are not representative of a "real structural application" environment. Their use is significant in understanding and discerning the importance of the different interface effects evident with bulk (e.g. interaction with oxide layer on the adherend surface) vs. constrained specimens (e.g. the chemical plus residual mechanical constraints imposed on the adhesive by the adherend during cure). Such information is necessary to accurately characterize a bonded structure's response in a realistic environment.

In arriving at the selection of the candidate test specimens, a survey questionnaire was mailed to selected individuals ($\cong$ 15) in industrial and governmental positions. These gentlemen were asked to respond to the questionnaire based on their working knowledge of the candidate specimens. This information was most valuable in arriving at final selection of the test specimens. The results of the survey are summarized in Table 3. The

TABLE 2. SUMMARY OF ADHESIV

TEST SPECIMEN / EVALUATION CRITERIA	THICK ADHEREND	BUTT JOINT	SCARF JOINT	NAPKIN-RING Single or Multiple Adhesive Layers
Load Mode* Controllable	II	I, II	I, II	I, II
Specimen Can Provide Quantative Results	Yes	Yes	Yes	Yes
Representative of Real Struct. Applic. (Reflects Phys., Chem., Mech., Response of Adhes. Between Adherends for Load - Environ.)	Yes	Yes	Yes	Physical } Yes Chemical } Mechanical-Questionable may be geometry effect
Specimen Introduces Biaxial or Triaxial Stress State In Adhesive	Yes	Yes Can Provide a Near Triaxial Stress State	Yes	Yes
Specimen** Analysis Performed	E	E,P	E,P	E-Incomplete
Adhesive Thickness 1. Control 2. Can measure in several locations	Easy Yes	Easy Yes	Modestly Difficult Yes	Difficult Only on Outside
Specimen Fabrication 1. Ease of Multi. Specimens 2. Relative Cost	Easy Low	Easy Yes	Modestly Difficult Modestly Expensive	Difficult High
Ease of NDI Inspectability	Easy	Modestly Difficult Angular Scan Required	Modestly Difficult Angular Scan Required	Modestly Difficult Reduced Access to Bond From Inside
Spec. Can Be Used With Brittle and Ductile Adhesives	Yes	Yes	Yes	Yes
References	35,45, 55, 71, 72, 73, 155	7, 22, 72, 76, 77, 78, 82, 87, 126,143, 150, 151, 160, 166, 168, 174	7, 23, 72, 78, 82, 102, 103, 174	7, 18, 28, 53, 54, 70, 74, 83, 88, 94, 164, 167, 174

* Tension = I
  Shear = II

** E = Elastic
   V = Viscoelastic
   P = Photoelastic

TABLE 2. SUMMARY OF ADHESIVE TEST SPECIMEN EVALUATION

	SCARF JOINT	NAPKIN-RING Single or Multiple Adhesive Layers	BALANCED DOUBLE LAP	SINGLE LAP	BULK-DOG BONE OR STRIP BIAXIAL	BULK THIN WALLED TUBE	
	1, 11	1, 11	11 – Thick Adherends	None	1	1, 11	
	Yes	Yes	Yes-Thick Adherend Mode 11 only	Yes Of Limited Value	Yes	Yes	
	Yes	Physical } Yes Chemical } Mechanical-Question-able may be geometry effect	Yes	Yes	No Adhesive-Adherend Interface Effect Absent	No Adhesive-Adherend Interface Effect Absent	Ad... Int... Ab...
...ar	Yes	Yes	Yes	Yes	No	Yes	
	E,P	E-Incomplete	E,V	E,V Adherends can fail or exceed yield	E,V,P - Biaxial Strip E - Dog Bone	E, V	
	Modestly Difficult Yes	Difficult Only on Outside	Modestly Difficult Yes	Easy Yes	Modestly Difficult Yes	Difficult Yes	
	Modestly Difficult Modestly Expensive	Difficult High	Modestly Difficult Modestly Expensive	Easy Low	Strip Biaxial-diffi-cult Dog Bone - Easy Low - Dog Bone High - Strip	Difficult High	M... M...
...ult	Modestly Difficult Angular Scan Re-quired	Modestly Difficult Reduced Access to Bond From Inside	Modestly Difficult Defect in Bondline Separability Problem	Easy	Easy	Easy	
	Yes	Yes	Yes	Yes	Brittle-Grip Problem	Brittle-Grip Problem	Bri...
..., 78, 150, ..8,	7, 23, 72, 78, 82, 102, 103, 174	7, 18, 28, 53, 54, 70, 74, 83, 88, 94, 164, 167, 174	7, 18, 23, 72	7, 23, 72, 88, 100, 143, 152 – 154, 156-159, 161, 162, 165, 174	77, 82, 163	77, 82, 163	7...

26

	BULK-DOG BONE OR STRIP BIAXIAL	BULK THIN WALLED TUBE	BULK SOLID ROD	TUBULAR LAP JOINT
	I	I, II	I, II	II
	Yes	Yes	Yes	Yes
	No Adhesive-Adherend Interface Effect Absent	No Adhesive-Adherend Interface Effect Absent	No Adhesive-Adherend Interface Effect Absent	Yes
	No	Yes	No	Yes
II or	E,V,P - Biaxial Strip E - Dog Bone	E, V	E	E,V
	Modestly Difficult Yes	Difficult Yes	Difficult Yes	Modestly Difficult No
	Strip Biaxial-difficult Dog Bone - Easy Low - Dog Bone High - Strip	Difficult High	Modestly Difficult Modestly Expensive	Modestly Difficult Modestly Expensive
	Easy	Easy	Easy	Modestly Difficult
	Brittle-Grip Problem	Brittle-Grip Problem	Brittle-Grip Problem	Yes
00, 156- 65,	77, 82, 163	77, 82, 163	72, 82, 163	78, 173, 174

26

TABLE 3. SUMMARY OF SURVEY ON TEST SPECIMEN SELECTION AND USAGE.

Candidate Specimens	Ease of Fabricating Multiple Specimens	Ease of Fabricating Thickness Control	Cost of Fabrication	Ease of NDI	Ease of Uninitiated to Fabricate Test Specimens	Cost of Test Performance With Subject Specimens
Thick Adherend	1.125	1.25	1.37	1.12	1.50	1.25
Butt Joint	2.25	2.50	2.00	3.37	2.00	1.62
Scarf Joint	3.37	3.12	3.25	2.62	3.75	2.75
Napkin Ring	4.87	4.87	4.87	3.37	4.50	4.62
Double Lap Joint	3.37	3.12	3.50	2.50	3.12	2.25

1 = easiest or least expensive

5 = hardest or most expensive

specimens are evaluated with respect to six criteria on a 1 through 5 basis, according to their ability to satisfy a particular item, with 1 representing the easiest or least expensive specimen to use.

The strengths and weaknesses of the various test specimens, as detailed in Table 2, make the selection of the test specimens to be used throughout the remainder of the test program obvious. A summary of selected pertinent information gathered during the performance of this task will now be presented.

3.4.1 Thick Adherend Symmetric Lap Joint

Renton and Vinson[35,55] conducted an analytical and experimental program on joints. A segment of the program involved a systematic analytical and experi-bonded mental effort to obtain effective adhesive properties in tension and shear between metal and composite material adherends. A closed form analytical model was developed to analyze the thick adherend symmetric lap joint specimen, Figure 7, which was used to obtain adhesive shear properties. From this analysis, the influence of adherend material properties and geometry and the importance of proper location of the measurement device on the specimen were ascertained. The conventional butt joint was used to obtain adhesive tensile properties. Overall, the results looked quite realistic with Poisson's ratio for EA951 adhesive in the .425 to .472 range.

Frazier et al[71] conducted an extensive development program on the generation of mechanical property data for adhesives joined between metal and composite adherends. They also investigated the influence of various surface preparation methods on the adhesives mechanical response, while seeking to develop or improve adhesive durability testing methodology. They used the thick adherend lap shear specimen shown in Figure 7. Although they didn't account for the influence of shear stress distribution in the shear property determinations, their efforts contributed significantly to the understanding of joint behavior. The cost of specimen fabrication and testing was quite reasonable.
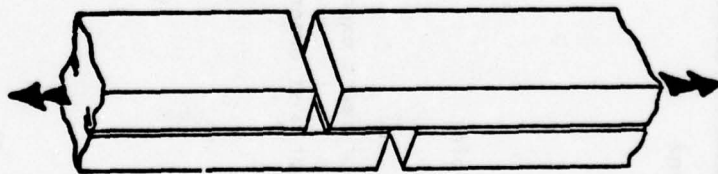
FIGURE 7. THICK ADHEREND SPECIMEN

Marceau and Scardino[72] conducted an extensive evaluation, based on specific criteria, on the adequacy of certain tests to determine adhesive durability under stress and adverse environments. They compiled an extensive test reference list and a summary of advantages and disadvantages of specific test techniques. Their objective was to ascertain which test methods, for a reasonable cost, could be used to evaluate the stress durability of adhesive bonded structures subjected to cyclic or steady state loads in various environments. They looked at a minimum of eighteen distinct test methods. Their evaluation criteria were:

o The test specimens must relate to real structural loading modes

o Mode I loading must be controllable

o Mode II loading must be controllable

o The test method must yield quantitative results and not be subjective

o Fabrication of specimens must be reasonable in that the specimens are relatively simple, do not require unusually close dimensional tolerances and fabrication costs are reasonable for programs involving large numbers of test specimens.

Of the three specimens selected, two were for fracture toughness studies and do not concern us. The third specimen was the thick adherend lap shear specimen.

A similar thick adherend lap joint test specimen to obtain adhesive shear properties has also been advocated by Kreiger[73] for aluminum adherends. The specimen is presently being used on the PABST Program and by several aerospace companies. However, the influence of optimum specimen geometry is neglected. The positioning of the deformation measurement device away from the adhesive-adherend-interface further clouds the accuracy of the adhesive properties obtained.

3.4.2 Butt Joints

Numerous attempts to analyze the butt joint have been made by Norris[74] and Lindsey[77] among others.[7,76,78,79,83,88] Norris assumed the adhesive was isotropic and predicted the joint's failure based on Von Mise's failure criterion. He then tested both tubular butt joints and bulk adhesive specimens. He determined that a meaningful difference existed between bulk vs. constrained tension moduli of the adhesive systems tested. He suggested characterizing an adhesive in a butt joint in an orthotropic manner.

29

The butt joint (poker chip) specimen illustrated in Figure 8, has been rigorously analyzed by elastic methods by Lindsey, et al[77] and Messner[171] and photoelastically by Dixon[172] and verified by finite element analysis. A tri-axial stress field is approximated in the center of the specimen when bending of the rigid adherends is negligible, the ratio of the disc diameter to thickness of the adhesive is greater than ten and the Poisson's ratio of the adhesive is approximately .50. The effect of lower Poisson's ratios on the stress distribution is also discussed.
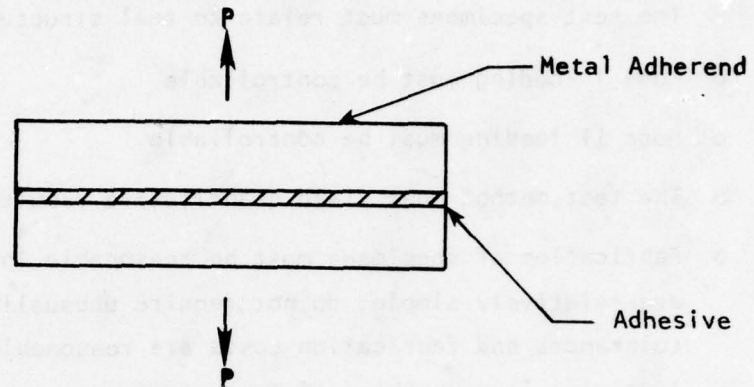
FIGURE 8. POKER CHIP SPECIMEN

Overall, the potential problems in using this specimen are adhesive thickness control, accurate adhesive deformation measurement of the bondline under load, and the significance of eccentric load and adherend geometry (i.e., rectangular vs. circular cross section) effects on the adhesive stress distribution. The cost is modest.

3.4.3 Scarf Joint Specimen

The scarf joint (Figure 9) specimen offers the advantages of a controllable tension and shear loading mode. This control is achieved by the angle of the scarf across the adherend's surface to be bonded. Analytical studies by Lackman,[103] Lubkin,[102] and photoelastic studies by McClaren[104] have shown that the stress in the middle plane of the specimen is triaxial with a superimposed shear stress. These specimens can pose bondline thickness control and alignment difficulties; this is more severe with composite materials.[71,72] However, it's projected problems appear less risky and the specimen is less costly than the alternate selection, namely the napkin-ring specimen.

3.4.4 Napkin-Ring Specimen

Many of the instrumented adhesive characterization tests done, to date, used the napkin-ring specimen, (Figure 10). One of its principle attributes

FIGURE 9. SCARF JOINT

ADHESIVE BOND LINE
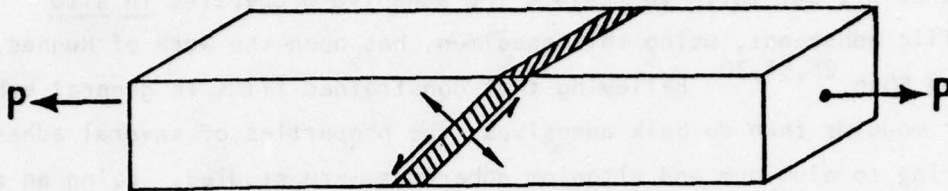
NAPKIN RING SPECIMEN
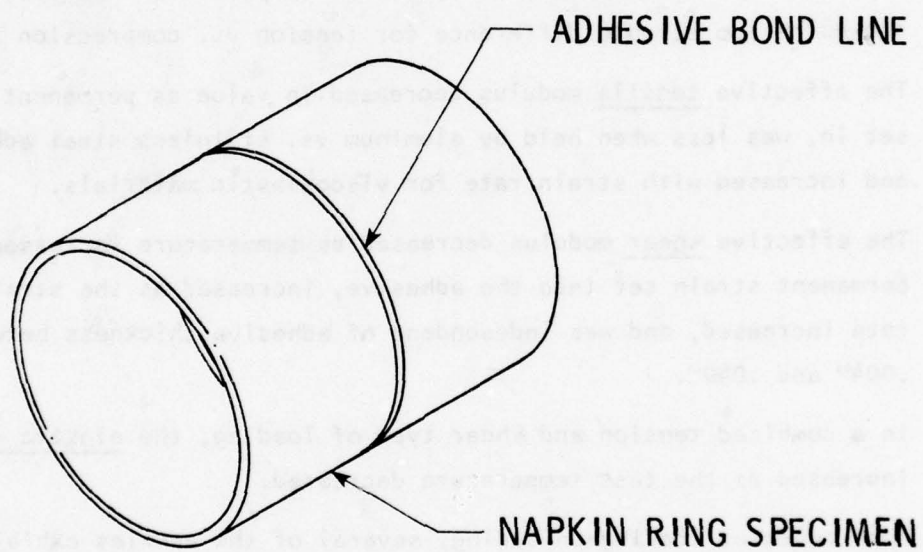
FIGURE 10.   NAPKIN - RING TEST SPECIMEN

31

is that it can be used to determine the stress-strain response of an adhesive material in shear, tension, or a combination thereof. An accurate analysis of the stress (strain) distribution in the adhesive of this specimen is not presently in the open literature. It is known to be biaxial or triaxial.

The best effort put forth to measure the adhesive properties in situ between metallic adherends, using this specimen, has been the work of Hughes, Rutherford and Shen.[28,53,70] Believing that constrained films in general exhibit a greater modulus than do bulk adhesives, the properties of several adhesive systems adhering to aluminum and titanium adherends were studied. Using an air-gap capacitance extensometer with a resolution of 1×10^{-7} inches attached to a napkin-ring type specimen, they determined for the adhesives Epon 9601, Epon 828/V40, EC2214 and Metlbond 329 that:

o The effective tensile modulus increased as the adhesive thickness of the bondline decreased, decreased as temperature increased, and showed no appreciable difference for tension vs. compression loads.

o The effective tensile modulus decreased in value as permanent strain set in, was less when held by aluminum vs. stainless steel adherends, and increased with strain rate for viscoelastic materials.

o The effective shear modulus decreased as temperature increased and permanent strain set into the adhesive, increased as the strain rate increased, and was independent of adhesive thickness between .004" and .040".

o In a combined tension and shear type of loading, the elastic limit increased as the test temperature decreased.

o Upon repeated loading-unloading, several of the epoxies exhibited work hardening, changing their material property values at high stress levels, while remembering the stress from which they were unloaded.

o For the adhesives tested, they determined that the elastic limit was lower and the viscoelastic flow higher for shear vs. tension loading.

32

o Raising the test temperature and reducing the strain rate produced similar effects (i.e. the moduli were softer).

o Poor bonding procedures and out-of-date adhesives proved to be the most damaging to material property values.

In general, their data exhibited scatter of as much as 70% while the Poisson's ratio values were seemingly low, being in the .26 to .38 range.

Overall, their work emphasizes the complexity and high cost associated with obtaining reliable adhesive property data in this manner. Variables included cure condition, joint thickness, test temperature and humidity, pre-strain, strain rate, stress level, time between loads, time at load and adherend modulus.

Using a napkin-ring specimen in shear and a thin-walled cylindrical butt joint in tension, Zabora et al[54] developed test techniques to determine adhesive properties in shear and tension. Results are presented for low, intermediate and high modulus adhesives. The overall program suffered from several problems as related to the proposed program herein:

o The cost of specimen preparation, test set up and data measurement was quite high.

o Fabrication variables were not accounted for in the study and the adherend specimens were reused. This leaves unanswered the question of what effect these uncontrollables had on the data output and its associated scatter.

o The test procedure was somewhat complex, being susceptible to mechanical linkage and specimen eccentricity errors.

o A comparison of shear and tensile moduli test results for the same adhesive resulted in the Poisson's ratio being larger than + .50, which is impossible.

Lin and Bell,[93] Kuenzi and Stevens,[83] Lehman[18] and others have also made use of the napkin-ring specimen in various adhesive characterization efforts. Overall, the napkin-ring specimen is shown to be adaptable to a controlled tension plus shear loading with use of rather elaborate gadgetry. However, bondline thickness control, NDI inspection problems, high fabrication and testing costs, and load linkage errors are detriments to using this test specimen on a high volume basis.

33

3.4.5 Balanced Double Lap Joint Specimen

In principle, the balanced double lap joint could be used in a shear mode with modestly thick adherends. Increased fabrication, NDI Inspection and cost problems would be associated with such a design. The selection of the joint's geometry would be extremely important in obtaining a somewhat uniform shear stress condition.

3.4.6 Other Test Specimens

Several other test specimens to characterize the structural response of adhesives are available. The insufficiencies of using block shear (ASTM-D905), cross-lap tension, and glueline cleavage methods are enumerated by Stanger and Bloomquist.[81] The single lap joint is excluded by it's inability to have separable and controllable loading modes in tension and shear.

3.4.7 Summary - Test Specimen Selection

The thick adherend, butt and scarf joint test specimens were selected as the author believes, based on an extended literature search and communications with knowledgable individuals in the field, that the specimens are most able to fully meet the evaluation criteria set forth. The primary advantages of the specimens selected are:

o Their load mode is controllable

o Specimen fabrication is relatively easy

o They experience the stress states that are experienced by joints in structural applications

o They produce quantitative results

o Their cost is minimal

3.5 TEST METHODOLOGY EVALUATION

The specifics of a proper test procedure by which one obtains accurate data must next be ascertained. The procedure must be formulated in accordance with the type of test being run (e.g. shear, tension, fatigue, creep etc.), and account for specimen fabrication, environmental conditioning, measurement of

34

adhesive bondline thickness and deformation, ease of test performance, repeat-
ability expected using a particular test procedure, data reduction, failure sur-
face examination, error analysis and overall cost. Within this segment of the
program such topics were considered with regards to defining potential test
methodology problem areas to be resolved in Task III.

3.5.1 Specimen Fabrication

The importance attached to fabrication of test specimems is that the proce-
dure, when completed, should produce adhesive bonds of uniform quality, of pre-
dictable adhesive thickness within specific limits, and for a minimum cost. In
addition, the fabrication procedure should yield reproducible results and be
relatively easy to accomplish.

Based on the results of Task I it was determined to be desirable to ascer-
tain the peak stresses in the adhesive to within ± 2.5%. To obtain this goal,
the bondline thickness must be accurately controlled during fabrication, be of
uniform thickness and be measured to within ± 2.5% of it's true value. There-
fore, the adherend's surface preparation, specimen fabrication and associated
bondline thickness control, and bondline thickness measurement should encompass
the following attributes.

o The surface preparation should yield uniform, reproducible adherend
   surfaces of prescribed surface roughness.

o The fabrication procedure should provide good, void free bonds, of
   predictable adhesive thickness, over a prescribed adhesive thickness
   range.

o A means to measure the adhesive thickness (gage length) to within
   ± .00010 inches.

3.5.1.1 Adhesive Bondline Uniformity

It has been repeatedly demonstrated that adhesive properties vary with adhe-
sive thickness. Cuthrell[138] has shown an adhesive property gradient to exist
from the interface into the center of the adhesive thickness. Bulk properties
were approached in the center of the joint. Rutherford, et al,[53] among others,
also determined that the adhesive material properties were a function of thick-
ness.

To obtain uniform strain in the adhesive, a uniform bondline thickness
(i.e., gage length) is necessary. This criterion requires an accurate and

reproducible method for holding the specimen's surfaces that are to be bonded parallel to one another. It also necessitates that if adherend surfaces are to be bonded together their surface roughness including the oxide layer must be within prescribed limits. This would minimize the variation observed in bond-line thickness when adherends with an ill controlled surface finish are bonded together and minimize gage length and associated adhesive property determination errors.

Assume two metal surfaces are to be bonded together by a 4 mil bondline between centerlines. Their surfaces are prepared, including the oxide layer, to an average roughness height of $\pm 63 \times 10^{-6}$ inches. The maximum peak-to-valley height between centerlines is then $\pm 63 \times 10^{-6}$ inches. The surfaces are unprimed.

The error in gage length determination and in adhesive mechanical property determination is:

Gage Length = .004 ± .000252 inches

Gage Length Error = $\dfrac{.004252 - .004000}{.004000}$ = 6.3%

Therefore, consistent and reproducible specimen machining and chemical surface preparation procedures must be instituted to maintain the adhesive thickness (i.e., gage length) error within a specified tolerance.

3.5.1.2 Fabrication Procedure Vs. Adhesive Thickness Control

A lack of bondline uniformity can also introduce an error of similar magnitude to that shown in the previous example. Nominal adhesive thickness control is a direct function of the fabrication procedure employed during cure of the adhesive.

For a general solution to bondline thickness control, precision tooling offers the best hope. Such a fixture can guarantee specimen alignment. Tools used for bonding should be designed to minimize the thermal expansion between the parts and the tool. The elements of the tooling must not cause bridging

36

or any interference which would prevent proper transmission of pressure to the bond areas. A typical bonding fixture is seen in ASTM Specifications D2094 and E229. In the latter instance, a precision screw is used to maintain thickness of the bondline

3.5.2 Bondline Thickness Measurement

Once a specimen has been fabricated, various adhesive (bondline) thickness measurement techniques can be employed. These include direct observation of the specimen with the use of a microscope, the use of a Vernier with the establishment of reference marks on the specimen, or the use of precision gage blocks and a high resolution Vernier to measure the relative distance between two points on the adherends before and after curing. Often times, the lack of a sharp contrast between the adhesive and the interface may necessitate using the latter means. Throughout this program an optical measurement system was found to be more than adequate.

3.5.3 Non-Destructive Inspection-Thick Metal Adherend-Adhesive Joints

Once a bonded specimen is fabricated, assurance that the bonded area is free of voids, air bubbles and associated imperfections is of paramount importance. Failure to attain a near defect free bond will result in poor bond strengths and unreliable adhesive characterization data. The test results will possess significant scatter. Therefore, accurate, sensitive inspection of adhesive bondlines for these defects when located beneath thick metallic adherends is a must.

Based on evaluation of the applicability of several candidate techniques to thick-adherend joints, two NDI techniques, neutron radiography and ultrasonics are recommended for inspecting the adhesive bondline in the specimens used in this study. Recommendation of these NDI techniques for the specimens of this study results from laboratory experience at Vought Corporation and a consensus of NDT personnel polled from within and outside the Vought Corporation. Consideration was given to factors such as ease of data interpretation and availability of the techniques to the average fabricator of bonded structures, in addition to its basic ability to detect bondline flaws. This comparison is summarized in Table 4, which ranks the techniques in the order 1 through 6 according to their capability or desirability, with 1 representing greatest desirability.

37

TABLE 4. COMPARISON OF NDI TECHNIQUES FOR DETECTION OF ADHESIVE BONDLINE FLAWS IN THICK ADHEREND METAL/EPOXY JOINTS.

TECHNIQUE	SENSITIVITY FOR ADHESIVE VOIDS	INDEPENDENCE FROM ADHEREND/BONDLINE GEOMETRY	"NATURE OF FLAW" INFORMATION	EASE OF INTERPRETATION	AVAILABILITY OR ACCESS TO TECHNIQUE OR SYSTEM
Neutron Radiography	1	2	1	2	5
X-ray Radiography	6	3	4	3	4
Ultrasonic Through Transmission	4	4	3	1	1
Ultrasonic Pulse Echo	2	5	5	5	2
Ultrasonic Holography	3	1	2	6	3
Thermal Scan	5	6	6	4	3

Column 1 ranks the flaw detection sensitivity, or the minimum size (typically measured by the diameter) adhesive void detectable by the method in a thick adherend specimen.

Column 2 ranks the degree of independence of the method's flaw detection capability with respect to variations in the adherend-bondline geometry, e.g., thick adherend, scarf, and butt joints.

Column 3 ranks the techniques ability to define the nature of the flaw, i.e., whether the flaw is a void, an inclusion, an unbond or an adherend/bondline separation.

Column 4 ranks the ease of interpretation of the inspection data for the specimens in question, for average NDI personnel. This takes into account factors such as ambiguity arising from scatter effects, multiple reflections, geometric complexity, etc. This ranking is an indication of the extent of additional training which would be required of NDI personnel to utilize the results of the technique.

Column 5 ranks the availability of or accessibility to the technique, for the average potential fabricator of adhesively bonded structures. This ranking considers factors such as cost, complexity or sophistication level of the required apparatus or facility, availability of properly trained users of the technique, etc.

Of the two more sophisticated techniques, neutron radiography and ultrasonic holography, neutron radiography was chosen as the recommended technique, for several reasons: The image is more easily interpreted as to the presence of and the nature of flaws, The sensitivity is believed better for imaging adhesive voids than is ultrasonic holography.

3.5.4 Environmental Considerations

Environment is hereby defined to be the interrelated parameters of temperature and moisture. The effects of moisture on the response of adhesives in bulk or in bonded structures has received little attention until recently. The fundamental mechanisms of moisture penetration are only now beginning to be understood.

Kinlock and Gledhill[107-109] among others, have determined that the primary mechanism by which water migrates into the bondline is by diffusion of water

through the epoxy interface and surface cracks, displacing the adhesive at the interface. Moreover, as oxidation forms on the interface, the mode of failure is changed from cohesive to adhesive. Capillary action is generally thought to be a secondary mode of moisture penetration. Temperature in turn, acts as an accelerator by reducing the time it takes to reach moisture equilibrium in a bonded joint.

The adverse effect of moisture absorption in an adhesive joint is that the adhesive expands in a purely dilatational manner. This introduces swelling stresses and lowers the glass transition temperature of the adhesive. As a result, the adhesive loses its structural integrity at a temperature it was thought to be able to survive. Serious degradation of its properties may result.

Initial moisture distribution at equilibrium in an adhesive bondline is thought to be highly nonuniform. The peak moisture content occurs near the joint edges, while the center part is saturated to a significantly less degree. The cross-sectional distribution is parabolic. As time at equilibrium continues, the migration of moisture inwards results in a more uniform moisture distribution.

In general, temperature levels above ambient have been shown to be detrimental to the performance of adhesive joints. Kuenzi[118] and Frazier, et al[71] among others have substantiated this. Eickner, et al,[114] while supporting Kuenzi's observation based on tests of fourteen different adhesives, is one of several to verify that sub-zero temperatures are not nearly as detrimental as elevated ones. This may not be the case for high temperature cure adhesives.

3.5.5 Considerations For A Successful Environmental Test

With the knowledge that time, temperature and moisture interact to have a potentially profound effect on adhesive properties, the components necessary for a successful and meaningful environmental test are all important. They are:

o ENVIRONMENTAL TEST CHAMBER - It must maintain prescribed environmental requirements for given time periods within specific constraints.

o TEMPERATURE-RELATIVE HUMIDITY MEASUREMENT DEVICES - They should be able to record temperature and relative humidity within prescribed limits.

o SPECIMEN CONDITIONING - The time necessary for a test specimen to reach environmental equilibrium for a given set of environmental conditions should be specified.

o PHYSICAL TESTING - Proper test procedures to follow should be formulated so as to insure that environmental equilibrium effects will be reflected in the mechanical property test results.

o DATA REDUCTION - Proper, universal means to report test results, for a specific set of environmental and load test conditions should be specified.

3.5.5.1 Environmental Test Chamber

Environmental conditioning will be defined for this program, as the exposure of a test specimen of a predetermined material, to the influence of a prescribed environment for a stipulated time period or until equilibrium has been attained. Throughout this program, where practicable, environmental equilibrium was attained so that a fair and equable comparison of material test results was possible.

Environmental (temperature and relative humidity) chambers should be designed to maintain the working space within specific limits of temperature and relative humidity. Good air distribution is the essential factor in obtaining close control of environmental conditions. This necessitates that the air outlets must be positioned such that conditioned air reaches all parts of the working space in sufficient quantity. Another important factor in control of the environment, is the positioning and design of the control elements. They must receive a representative sample of conditioned air and any change must be adjusted for as quickly and as uniformly as possible. The saw-tooth effect, whereby, the parameter being controlled is cycled between two specific limits of an on-off sensing circuit should be held to a minimum. This drift of temperature can cause a more severe variation in the relative humidity (Table 5).

An alternate means of controlling relative humidity at prescribed levels for a specific temperature is the use of saturated salt or acid solutions. Such a slush provides a stable relative humidity environment if accurate temperature control is possible. Its cost to maintain is minimal, but purity of the salt and water which form the slush are important if specific relative humidities are to be attained. It's use in hygrothermal testing should be given

41

TABLE 5[*]

EXPANDED SCALE RELATIVE HUMIDITY TABLE
WET BULB DEPRESSION vs. DRY BULB TEMPERATURE

This table facilitates the determination of exact relative humidity values when a differential recorder or any other measuring device is used that is capable of measuring depression to .1°F. Expanded range covers a maximum of 4°F. depression in .1°F. increments. This is the area of greatest interest in relation to current military specifications.

Wet Bulb depression In °F.	DRY BULB TEMPERATURE — °F.											Wet Bulb depression in °F.
	77 to 81	82 to 87	88 to 95	96 to 103	104 to 113	114 to 127	128 to 141	142 to 149	150 to 161	162 to 171	172 to 200	
	% RELATIVE HUMIDITY											
0.0	100.0	100.0	100.0	100.0	100.0	100.0	100.0	100.0	100.0	100.0	100.0	0.0
.1	99.6	99.6	99.6	99.6	99.7	99.7	99.7	99.7	99.8	99.8	99.8	.1
.2	99.2	99.2	99.2	99.2	99.4	99.4	99.4	99.4	99.6	99.6	99.6	.2
.3	98.8	98.8	98.8	98.8	99.1	99.1	99.1	99.1	99.4	99.4	99.4	.3
.4	98.4	98.4	98.4	98.4	98.8	98.8	98.8	98.8	99.2	99.2	99.2	.4
.5	98.0	98.0	98.0	98.0	98.5	98.5	98.5	98.5	99.0	99.0	99.0	.5
.6	97.6	97.6	97.6	97.6	98.2	98.2	98.2	98.2	98.8	98.8	98.8	.6
.7	97.2	97.2	97.2	97.2	97.9	97.9	97.9	97.9	98.6	98.6	98.6	.7
.8	96.8	96.8	96.8	96.8	97.6	97.6	97.6	97.6	98.4	98.4	98.4	.8
.9	96.4	96.4	96.4	96.4	97.3	97.3	97.3	97.3	98.2	98.2	98.2	.9
1.0	96.0	96.0	96.0	96.0	97.0	97.0	97.0	97.0	98.0	98.0	98.0	1.0
.1	95.5	95.6	95.6	95.7	96.6	96.7	96.7	96.8	97.7	97.7	97.8	.1
.2	95.0	95.2	95.2	95.4	96.2	96.4	96.4	96.6	97.4	97.4	97.6	.2
.3	94.5	94.8	94.8	95.1	95.8	96.1	96.1	96.4	97.1	97.1	97.4	.3
.4	94.0	94.4	94.4	94.8	95.4	95.8	95.8	96.2	96.8	96.8	97.2	.4
.5	93.5	94.0	94.0	94.5	95.0	95.5	95.5	96.0	96.5	96.5	97.0	.5
.6	93.0	93.6	93.6	94.2	94.6	95.2	95.2	95.8	96.2	96.2	96.8	.6
.7	92.5	93.2	93.2	93.9	94.2	94.9	94.9	95.6	95.9	95.9	96.6	.7
.8	92.0	92.8	92.8	93.6	93.6	94.6	94.6	95.4	95.6	95.6	96.4	.8
.9	91.5	92.4	92.4	93.3	93.4	94.3	94.3	95.2	95.3	95.3	96.2	.9
2.0	91.0	92.0	92.0	93.0	93.0	94.0	94.0	95.0	95.0	95.0	96.0	2.0
.1	90.6	91.6	91.7	92.6	92.7	93.7	93.7	94.7	94.7	94.8	95.8	.1
.2	90.2	91.2	91.4	92.2	92.4	93.4	93.4	94.4	94.4	94.6	95.6	.2
.3	89.8	90.8	91.1	91.8	92.1	93.1	93.1	94.1	94.1	94.4	95.4	.3
.4	89.4	90.4	90.8	91.4	91.8	92.8	92.8	93.8	93.8	94.2	95.2	.4
.5	89.0	90.0	90.5	91.0	91.5	92.5	92.5	93.5	93.5	94.0	95.0	.5
.6	88.6	89.6	90.2	90.6	91.2	92.2	92.2	93.2	93.2	93.8	94.8	.6
.7	88.2	89.2	89.9	90.2	90.9	91.9	91.9	92.9	92.9	93.6	94.6	.7
.8	87.8	88.8	89.6	89.8	90.6	91.6	91.6	92.6	92.6	93.4	94.4	.8
.9	87.4	88.4	89.3	89.4	90.3	91.3	91.3	92.3	92.3	93.2	94.2	.9
3.0	87.0	88.0	89.0	89.0	90.0	91.0	91.0	92.0	92.0	93.0	94.0	3.0
.1	86.6	87.6	88.6	88.7	89.7	90.7	90.8	91.8	91.8	92.8	93.8	.1
.2	86.2	87.2	88.2	88.4	89.4	90.4	90.6	91.6	91.6	92.6	93.6	.2
.3	85.8	86.8	87.8	88.1	89.1	90.1	90.4	91.4	91.4	92.4	93.4	.3
.4	85.4	86.4	87.4	87.8	88.8	89.8	90.2	91.2	91.2	92.2	93.2	.4
.5	85.0	86.0	87.0	87.5	88.5	89.5	90.0	91.0	91.0	92.0	93.0	.5
.6	84.6	85.6	86.6	87.2	88.2	89.2	89.8	90.8	90.8	91.8	92.8	.6
.7	84.2	85.2	86.2	86.9	87.9	88.9	89.6	90.6	90.6	91.6	92.6	.7
.8	83.8	84.8	85.8	86.6	87.6	88.6	89.4	90.4	90.4	91.4	92.4	.8
.9	83.4	84.4	85.4	86.3	87.3	88.3	89.2	90.2	90.2	91.2	92.2	.9
4.0	83.0	84.0	85.0	86.0	87.0	88.0	89.0	90.0	90.0	91.0	92.0	4.0

[*]Reference 186

42

serious consideration. However, problems relating to the breakdown of the salts for extended test periods and their deposition of corrosive deposits on the test specimens should be resolved. Relative humidity control in the (1-2%) range should be expected. The salt slush is maintained in a dessicator which can be maintained at a constant temperature by insertion into a laboratory oven.

3.5.5.2 Specimen Conditioning

Equilibrium Relative Humidity, i.e., the relative humidity of the air at which the specimen moisture is in balance with that of the air so that the specimen neither gains nor loses moisture, is what one wishes to attain prior to the initiation of mechanical property testing.

Moisture absorption tests to determine the moisture equilibrium weight gain and the time to attain this weight gain have been performed for FM-73M and FM-400 adhesives in bulk and bonded joint specimens. The bonded joint dimensions of 1.0" wide x .36" long duplicates the dimensions of the thick adherend test specimens and approximates that of our butt and scarf joint test specimens.

Our goal was to determine a moisture absorption vs. time curve Figure 11, to ascertain the time required for the thick adherend, butt and scarf joint specimens to attain moisture equilibrium for 75% and 95% relative humidity environment.

In a bonded joint, the moisture absorption process is a two dimensional diffusion problem. A one dimensional analytical solution can be used to approximate the two dimensional moisture absorption process for a bonded structure. In this particular instance, the one dimensional approach has been exploited and is guided by existing bulk adhesive test data.

Reduction of the bulk adhesive data at 140°F enabled one to determine the one-dimensional diffusivity coefficient. For FM-73M it was 6.05×10^{-6} in^2/hr, and for FM-400 it equalled 6.96×10^{-6} in^2/hr. With this information and one-dimensional diffusion theory, one can estimate the time for a bonded specimen of a given length and width to attain its 95% saturation level for a given relative humidity level at 140°F. The adhesive's moisture equilibrium weight gain for a particular relative humidity level, independent of temperature, can be obtained from the bulk data for which moisture equilibrium at 75% and 95% R.H. was attained. A summary of 99% saturation weight gain for both adhesives is given in Table 6 along with the source of the data.

43

TABLE 6. SUMMARY OF BULK ADHESIVE MOISTURE ABSORPTION DATA.

CONDITION (TEMP/R.H.)	WEIGHT GAIN AT 99% SATURATION		REMARKS
	FM 400	FM 73M	
140°/100%	3.50	2.10	"Fatigue Behavior of Adhesively Bonded Joints, Quarterly Progress Report No. 3, 1977, J. Romanko, Contract No. F33615-76-C-5220
140°/75%	2.10	1.45	ATC IR&D Data
140°/95%	3.21	1.97	Estimated Data

With the moisture equilibrium weight gain, the Vought test data for bonded sandwiches (solid lines of curves in Figure 11) and the time to attain 95% of moisture equilibrium weight known, the predicted moisture weight gain vs. time curves (2-dimensional approximation) in Figure 11 could be determined for the thick adherend specimens at 95% - 100% relative humidity.

The projected moisture absorption vs. time curves in Figure 11 for 75% relative humidity makes use of the 99% saturation data in Table 6. Since the long time bonded joint specimen data are lacking, the moisture absorption vs. time curves were estimated such that the net change in moisture absorption as a percent of the known moisture equilibrium value vs. time is identical to that for the 95 - 100% R.H. data curves while the temperature remained at 140°F.

These data were subsequently used in Tables 17, 18, 22, 24, 25 to predict the amount of moisture weight gain for thick adherend, butt (.30" x 1.0") and scarf joint specimens.

3.5.5.3 Physical Testing

Once a test specimen has attained temperature and moisture equilibrium, the proper means by which one carries out adhesive characterization tests must be ascertained. Long term tests (i.e., creep, fatigue) and elevated temperature/relative humidity static tests should be run within the prescribed environment. Room temperature static tests, can be performed outside of a controlled environment.

3.5.6 Data Reduction

In the test report, all pertinent environmental data must be recorded that will make the data useful in design of bonded structures. This should also eliminate the uncertainties which presently exist in comparing adhesive test data for similar environmental conditions. The specific information required to resolve the concerns over making valid data comparisons, based on the work of independent investigators, is defined in each adhesive test specification (Volume II).

3.6 SUMMARY-CURRENT TEST SPECIFICATION WEAKNESSES AND/OR ITEMS OF PARAMOUNT IMPORTANCE FOR AN ACCURATE TEST METHODOLOGY

The major deficiency in adhesive characterization, is the arbitrary test and report procedures followed by the various investigators. Incomplete information on the tests is disseminated. This makes data results questionable and
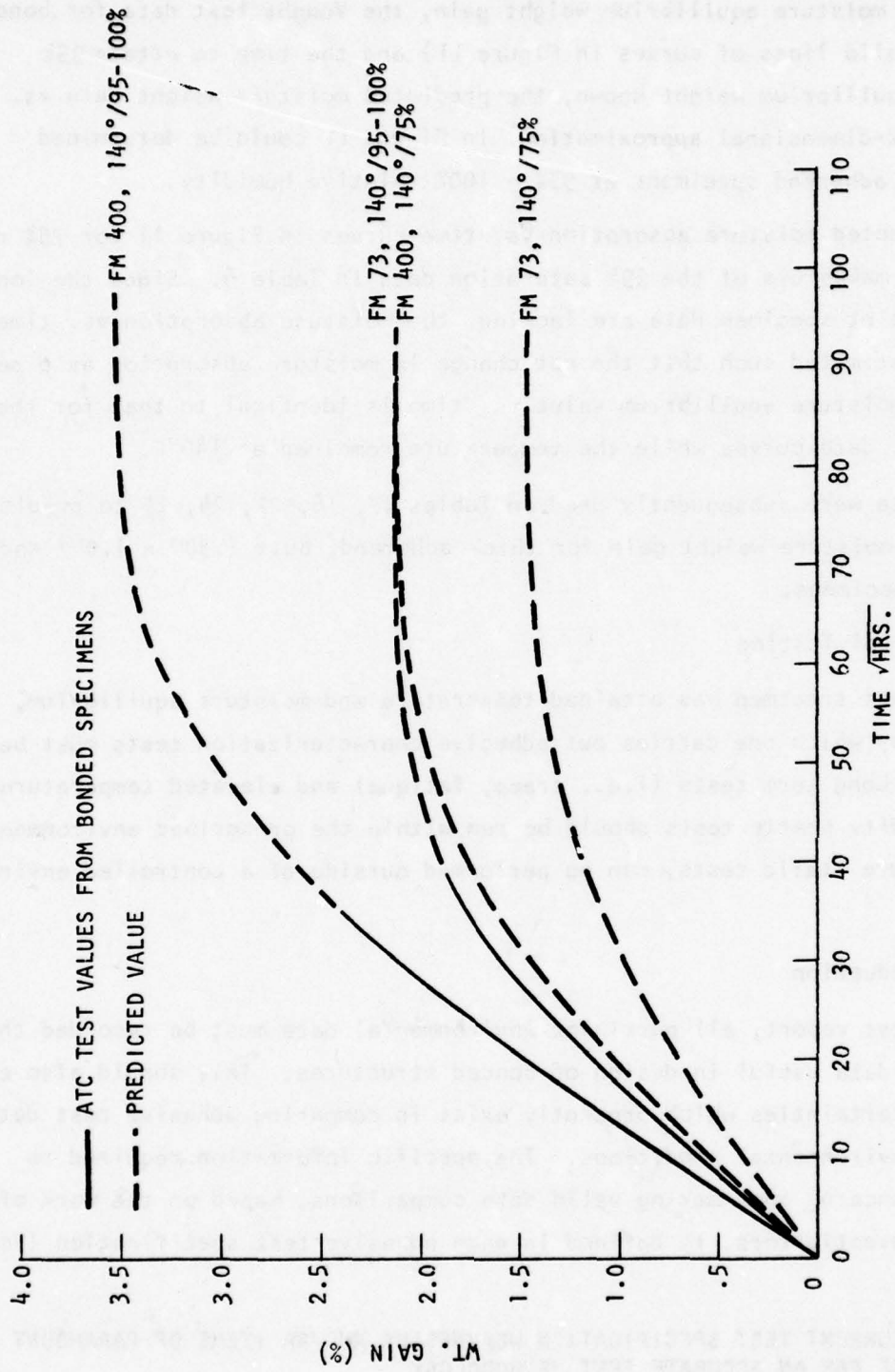
data comparisons impossible. This may be due in part to the lack of ASTM test specifications in this area. Only a standard adhesive shear modulus test (E-229) using a Napkin-ring test specimen, presently exists for characterizing thin film adhesives. Creep testing is defined but uses an unsatisfactory test specimen, the single lap joint.

As a result of the review conducted in this task, the items which were given serious consideration during the formulation of the adhesive test specifications in Task III were.

3.6.1 Test Specimen

o The effect of specimen geometry on the stress state (biaxial, uniform etc.) was not specified. Optimum specimen design considerations were absent and were considered.

3.6.2 Specimen Fabrication

o A fabrication procedure for the three test specimens selected was in need of development. It had to ensure bondline thickness control, prevent specimen eccentricities and avoid thermal cool down problems. Also, it had to be verified by physical tests that the fabrication procedure employed resulted in a high quality bond.

3.6.3 Bondline Thickness Measurement

o For optical measurement methods, specify the surface polishing procedure to insure a good measurement is made and that the bond is not degraded during the polishing procedure.

o Specify the adhesive thickness measurement device accuracy.

o Specify the number and location of the bondline thickness measurements one should make to insure that bondline uniformity is maintained.

3.6.4 Environmental

o A test chamber with a demonstrated ability to maintain a uniform environment within a prescribed accuracy had to be specified. This may be an oven with a saturated salt solution in a dessicator or an environmental chamber.

47

o The constraints within which the percent relative humidity should be maintained at elevated temperatures and the measurement means to insure this should be specified.

o A test procedure to ascertain when environmental equilibrium has been attained should be specified. This should include the time to reach equilibrium for a specific temperature and relative humidity.

o An analytical technique which can predict the time for a specimen to attain moisture equilibrium, and the equilibrium content is desirable.

3.6.5 Ease of Test Performance and Repeatability

o There must be developed test procedures for the test specimens selected that minimize the chance for inadvertent error.

o Specification of the number of specimens per set of test parameters to guarantee believability of data must be made.

3.6.6 Data Reduction

o A universal reporting format to insure that data results by various parties are readily comparable must be specified.

o The equations required to reduce the test data for easy use in rigorous bonded joint analysis must be specified.

o Specification of how the test specimen was conditioned (i.e. time, temperature, relative humidity) and the accuracy within which the environmental conditions were maintained is critical.

o Whether the mechanical testing was performed in the specimen conditioning environment must be reported. If not, the time elapsed from specimen removal from the conditioning environment until the testing was completed should be reported as should the new environmental parameters.

3.6.7 Failure Surface Examination

o The type of adhesive failure observed - adhesive or cohesive should be specified.

o Microscopic analysis of the adhesive failure surface may be desirable in specific instances.

3.6.8 Error Analysis

An appreciation for the magnitude of the error incurred during the performance of the test should be ascertained. The parameters of concern are:

- o Specimen geometry

- o Grip eccentricity

- o Deformation measurement system linearity, sensitivity and its location with respect to the bondline.

- o Bondline thickness eccentricity.

- o Load readout accuracy.

- o Data Reduction Methodology Accuracy

SECTION IV

EVALUATION OF INSTRUMENTATION FOR BONDLINE DEFORMITY MEASUREMENT

The purpose of this evaluation is to determine the instrumentation best suited to measure adhesive deformation so as to obtain specific structural properties of adhesives to within a prescribed accuracy. The problem associated with the measurement of changes in bondline dimensions during loading is related to the small changes in bondline thickness usually encountered. For example, in a tensile test, 1% strain in a 5 mil bondline is 50×10^{-6} inches. Careful workers in the field[53-55] express the need for a minimum accuracy in measurement of bondline dimensional changes of 1×10^{-6} inches. This accuracy must be maintained over a very wide temperature and humidity range and for long periods of time. These conditions impose very strict requirements on the stability of the strain sensor.

Study to date indicates that LVDT's, extensometers, Tuckerman gages, air-gap capacity gages, and strain gages are the sensors most commonly used. For the present purpose, direct reading gages are not applicable since the strain history during loading must be recorded on an analog chart or digital printout.

The method of attachment of a sensor to the specimen is also important. For best accuracy and precision, a gage should be attached so that it spans only the bondline. A gage attached to a specimen at an appreciable distance on either side of the bondline must be corrected for strain in the adherend.

4.1 OVERALL ACCURACY REQUIREMENT

Results of the sensitivity study performed in Task I resulted in the peak normal stress being the most sensitive adhesive design parameter. An attempt to determine the peak normal stress within $\pm 2.5\%$ was spiked out as a desirable goal. This in turn stipulates that the nondimensional parameter $\overline{\pi}_2 = E_a L^4 / (D\eta)$ be determined to within an overall accuracy of $\pm 5\%$.

Assuming a mean square error (MSE) analysis is applicable, the mean square error is defined as $MSE^2 = E_1^2 + E_2^2 + E_3^2 + E_4^2 + E_5^2$ 12
It is desired that the MSE be $\leq$ 5%.

Let:

     E_1 = the error in measuring the overlap length (L) magnified by the fourth
          power.

     E_2^* = the error in measuring the adherend thickness (h) magnified by the
          third power

     E_3^* = the error in measuring the adherend's modulus (E).

     E_4 = the error in measuring the adhesive thickness (η)

     E_5 = the error in measuring the adhesive tensile modulus (E_a).

The following assumptions were made in this analysis in order to realistically
estimate E_5.

Parameter	Typical Value	Measurement Accuracy	Probable Error (%)
L	.500"	$\pm$ .001	$\pm$ .80
h	.100"	$\pm$ .0005	$\pm$ 1.5
E	10×10^6	____	$\pm$ 2.0
η	.004"	$\pm$ .00010	$\pm$ 2.5

thus:

$$E_5 = \sqrt{MSE^2 - E_1^2 - E_2^2 - E_3^2 - E_4^2}$$

$$E_5 = \sqrt{(.05)^2 - (.008)^2 - (.015)^2 - (.02)^2 - (.025)^2}$$

$$E_5 = \pm 3.4\%$$

Therefore, the tension modulus must be measured to within an accuracy of
$\pm$ 3.4%, for a bondline thickness of .004 inches. For a .010 inch bondline
thickness, the overall accuracy of $\pm$ 5% can be attained if the adhesive modulus
is measured to a $\pm$ 4.2% accuracy.

$^*D = Eh^3/(12(1-v^2))$

4.2 ADHESIVE DEFORMATION MEASUREMENT ACCURACY REQUIREMENT

The adhesive tension modulus (E_a) and shear modulus (G_a) are obtained from an equation of the form:

$$E_a(G_a) = \frac{P\eta}{A\Delta} \qquad\qquad 13$$

where:

P = the applied load (lb).

A = the cross-sectional area normal to the applied load for tension and the surface area of the adhesive parallel to the applied load for shear (in^2).

η = the adhesive thickness (in).

Δ = the adhesive deformation (in)

The load on a typical closed-loop hydraulic system can be determined to within $\pm$ .5%. Continuing with the accuracy requirements stipulated in the previous section, the cross sectional area (surface area in shear) will be determined to within an accuracy of $\pm$ 1.0%, with (η) being determined to within $\pm$ 2.5%.

The accuracy within which the adhesive deformation (E_Δ) should be determined is again based on a MSE analysis. The MSE must be $\leq$ 3.4%.

$$E_\Delta = \sqrt{(.034)^2 - (.005)^2 - (.01)^2 - (.025)^2}$$

$$E_\Delta = \pm 2\%$$

For 100×10^{-6} inches this necessitates an overall measurement accuracy requirement of $\pm$ 2 microinches. It is with this overall accuracy requirement in mind, that all measurement systems were evaluated.

4.3 ADHESIVE DEFORMATION MEASUREMENT REQUIREMENTS

4.3.1 Strain in Bondlines

In measuring the strain in adhesive bondlines, the available gage length is limited to the bondline thickness. In this program, bondline thickness may vary from 0.002 to 0.20 inches. For example, 1% strain in a 0.005-inch bondline is 50×10^{-6} inches. To plot a load-strain curve over this range with a maximum error of $\pm$ 2%, an absolute accuracy of $\pm 1.0 \times 10^{-6}$ inches is required. Measurements to such an accuracy are difficult to make and beyond the capabilities of most standard strain measuring systems.

4.3.2 Strain Sensor Requirements

To measure the strain in the adhesive bondline directly, it would be necessary to mount the strain sensor so that its active element would bridge the specimen's bondline interfaces. No way has been found to do this. It is necessary to make the gage length greater than the bondline thickness and anchor the ends of the sensor's active element onto the specimen as close to the bondline interfaces as possible. The sensor will then measure not only the strain in the bondline, but also over two small lengths of adherend. The strain in the adherend must be subtracted from the total measured strain. The contribution of the adherend strain must be calculated from accurately known characteristics of the adherend or from simultaneous strain measurement on the specimen. The process of correcting the strain sensor output for the contribution of the adherend will increase the error in measuring the strain in the bondline. Therefore, the strain sensor, to be sufficiently accurate, must be mounted with a minimum of adherend material included between its anchor points.

4.3.3 Other Measuring System Requirements

The criteria for selecting a suitable strain sensor operating principle and physical configuration are as follows:

o Ease of attachment
o Simplicity
o Operating range
o Resolution
o Linearity
o Accuracy
o Durability

53

o Immunity to environment (including frequence response) -must be
   stable with minimum drift in high temperature, humidity environ-
   ments for extended periods of time.

O Cost

4.4 APPLICABLE ADHESIVE DISPLACEMENT MEASUREMENT SYSTEMS

Conventional methods of strain or displacement measurement are not directly
applicable to bondline deformation measurements because of their large gage
lengths and environmental limitations. A survey of the literature and discus-
sions with vendors showed promise for the following operating systems for adapta-
tion to bondline deformation measurements:

Air-gap capacitive sensors
Linear variable differential transformer sensors

A tabular summary of the strengths and weaknesses of the various systems is pre-
sented in Table 7.

4.4.1 Capacitive Displacement Sensor Systems (Two Plate Capacitors)

The capacitance of a parallel plate condensor is:

$$C = \frac{0.0885 \times K \times A}{d}$$

14

where   C = capacitance in picofarads
         K = dielectric constant (for air, K = 1)
         A = area of smaller plate in cm^2
         d = distance between plates in cm

The plates of an air gap capacitor are arranged so that one plate is attached
to a tensile specimen at one interface between adherend and bondline and the
other plate is attached at the other interface. Two different configurations of
the arrangement are shown schematically in Figure 12. Figure 12a shows a capaci-
tor whose plate spacing is varied directly with and is always equal to the bond-
line thickness. Figure 12b shows a capacitor whose area is varied proportional
to bondline thickness.

Referring to equation (14), case (a) capacitance varies inversely with
bondline thickness. The impedance of a capacitor is:

54

| SYSTEM OR COMPONENT	OPERATING PRINCIPLE	SENSOR MANUF.	SIGNAL COND. MANUF.	SIMPLE OR COMPLEX	EASY OR HARD TO ATTACH	DISPLACEMENT RANGE	RESOLUTION	LINEARITY	ACCURACY	STABILITY RELIABILITY DRIFT	TEMPERATURE	HUMIDITY	SENSITIVITY GAGE FACTOR	MISC.	
Parallel Plate Air Capacitor (Sensor only)	Annular Parallel Plates Across Bondline	Custom Design At ATC Shop	N.A.	Simple Design But Close Tolerances	Specimens Must Be Cut to Close Tolerances	0.005 in.	0.82×10^{-9} in	Non-linear But Electronics Can Make it Linear	Function of Construction of the Sensor But $>7 \times 10^{-7}$ in	HIGH HIGH LOW	Typical 2.5×10^{-6} in Reading Per °C	Condensation Can be a Problem	Typical 7×10^{-3} pf/µ" @ 100,000 Hz gμ"/µ"	Integrates if Active Area Capacitor is Surrounding the Specimen	Used need atta blen
Impedance Comparator (Signal Cond. Only)	Transformer Bridge Measures Against STD. Cap. Imp. Diff.	N.A.	General Radio	Easy to Operate Analog Out Prop. to change in imp.	N.A.	Min 0.1% ΔZ f.s. 10^{-5} to 10^{-7} pf	0.001% f.s.*	3% f.s.	3% f.s.	HIGH HIGH LOW	Use at Room Ambient	Use at Room Ambient	N.A.	Measures the Difference Between an unknown and a standard. Has analog output for recorder	
Manual Displacement Meter Model 1055 (Signal Cond. Only)	Inductive Bridge Indicates Bridge Unbalance (Change in Capacitance)	N.A.	Automatic System Lab. "England"	Easy to Operate Analog Out Prop. Displ.	N.A.	Function of Transducer	10^{-6} p.f.	0.1% f.s. if Calib. At 0 & f.s.	0.1% f.s.	HIGH HIGH LOW	Ambient	Ambient	N.A.	Variable Bandwidth For Noise Reduction	Meas sett rec
LVDT Ultra-Precision Gage Heads (Sensor Only)	Linear Variable Differential Transformer	Schaevitz	N.A.	Simple	Require Fixture	Min: 0.005 in. Max: 0.100 in.	4×10^{-6} in Repeatability	Linear Within 0.05% of Linear Range	Accurate Within 0.04%	GOOD GOOD	40° to 140°F	Needs Low Humidity and to be Kept Clean	3.7mv/ mil in/volt	Single Point Measurement	Has rang Pote tric liai
LVDT (Sensor Only)	Linear Variable Differential Transformer	Schaevitz	N.A.	Simple	Requires Fixture	Min: 0.005 in. Max: 0.100 in.	Infinite	Linear Within 0.25% of Linear Range	Accurate Within 0.25%	HIGH HIGH LOW	Available in High Temperature Model $-65°$ to 300°F	No Effect	4.8×10^{-3} Volts Per 1×10^{-6} in	Single Point Measurement	Reso conn ture be a
LVDT Extensometer (Sensor Assembly)	LVDT in Fixture 3 Point Mtg. To Specimen	ATC Shop Per Krieger American Cyanamid	N.A.	Simple	Requires Fixture Kreiger Design	Min: 125×10^{-6} in Max: > 0.010 in.	1.25×10^{-6} in	Linear Within ± 0.5% of Linear Range	Accurate Within ± 0.5%	Depends on Fab. & Design of Jig. Gen. Good	Metal Expansion Effect Should Be Calculated	No Effect	3×10^{-4} volt Per 1×10^{-6} in	Specifically Designed For Thick Adhered Lap Shear Specimen	Erro off syst Adhe Envi
LVDT Extensometer Strain System (Total Assembly)	LVDT in Fixture Using Knife Edges	Tinius Olsen	Tinius Olsen	Fairly Complex	Easy	Min: 0.01 in. f.s. to 0.04 in. f.s.	Infinite	± 20×10^{-6} in	± 20×10^{-6} in	GOOD GOOD GOOD	500°F	Little Effect	3×10^{-4} volt Per 1×10^{-6} in	Not Good For Dynamic Use Per Present Design	unit hard samm in r
Serrated Capacitor (Sensor Only)	Multi-Plate Cap.Plates Parallel to Strain	Custom Built at ATC	N.A.	Close Tolerances	Easy	Dependent on Construction	0.01×10^{-6} in	Sensor Itself Non-Linear But Electronics Can Make it Linear	Function of The Construction of the Sensor But $> 1 \times 10^{-7}$ in	GOOD GOOD UNKNOWN	May be Water cooled But should Have Little Effect	Effected by Condensation	1×10^{-2} pf Per 1×10^{-6} in	Large Output Impedance	Use jum
CAS 025 ALT LVDT Signal Conditioner (Conditioner Only)	Synchronous Demodulator	N.A.	Schaevitz	Simple	N.A.	± 0.03 in	N.A.	Linear Within 0.05%	N.A.	± 0.05% GOOD LOW	0° - 130°F 0.02% Per °F of Sensitivity	Room Ambient	100 mv Input RMS Gives 10v D.C. Out		Exce
Differential Screw Translator (Calibrator)	Micrometer Head With Differential Screw	Lansing Research Corp Ithaca, NY	N.A.	Simple	N.A.	0.01 in	1×10^{-6} in 0.01% f.s.	0.1% f.s. (NBS)	0.1% f.s.	HIGH HIGH LOW	Metal Expansion	No Effect	N.A.	Visual Micrometer Scale With Vernier	Aptm
SLVC + Man. Displacement Meter System	See Item 3 Differential Capacitor With Spring Loaded Shaft	A.S.L.	A.S.L.	Straight Forward Operation	Requires a Custom Fixture	Min: 0.2 in.	2×10^{-6} in	Analog Output Linear to 0.1% of f.s.	Same As Linearity	HIGH HIGH LOW	Offered in NILO 36 T.C. < 2ppm Per °C	Condensation Can be A Problem	N.A.	N.A.	Aptm
Automatic Tracking Tuckerman Extensometer (Sensor Only)	Mech. Device To Rotate Mirror and Deflect Light to Beam Tracker	STD Tuckerman Gage	Phisltech Optical Tracker	Complex System	Attachment Tricky Req. Much Optical Lineup	Min: 100×10^{-6} in Max: 2000×10^{-6} in	2×10^{-6} in	3% f.s.	Deflection Error 3% f.s.	Not Given	Effects Could Be Calculable	Condensation Could Fog Optics	N.A.	Gage Length 0.25 in.	This use comp
Optical Strain Gage	Laser Interferometer Light Reflection Off Grooves on Specimen	No Sensor in Usual Sense to Mounted Specimen (2) Lines on Specimen	Assemble Laser Slits Electrometer Etc. (Interferometer)	Total System Is Complex	(2) Grooves on Flat polished Specimen Laser Interferometer Mounted to Test Machine	200 µε = 1×10^{-6} in. Linear 1250µε = 6×10^{-6} in Non-Linear But Repeatable	1×10^{-8} in	Non-Linear	1×10^{-6} in	25 µε/24 HR	Specimen Expansion Effects Reading	Condensation Can Obstruct Operation	±2 Micro-Strain	Gage Length 0.005 in	Upon nigh use moni comp
Boeing High Temperature Capacitive Strain Gage System	Welded Gage Using Differential Capacitor	HITEC	HITEC	Complicated Gage Assembly	Welded to Specimen Specimen Material Limited	2% Strain Range or .02 in.	Infinite	Same As Linearity	± .5% to 300 µε 70°F ± 1% to 1500 @ 1500°F ± 2% to 20,000 µε @70°F	0.1 µε/Day At 1100°F	± 300 µε to 1500°F Cryogenic-1500°F	No Effect	.018pf/ 1000 µε	Single Point Measurement	Prob and
Carl High Temperature Capacitive Strain Gage	(2) Plate Capacitor Plates Parallel to Strain	G.V. Planer LTD England	N.A.	Simple	Welded	800×10^{-6} in	Not Given	Not Given	Not Given	Drift 20°C-Sue/mth. 600°C-Sue/day	-269°C To +650°C	Could Be Affected By Condensation	Gage Factor 100	Gage Length 20 mm (0.8 in)	Not
Metal Foil Strain Gage -015 CK	Wire Strain Gage	Micromeasurements	Any Good Strain Gage Sig. Cond.	Simple	Yes	Min: 1500 µε Max: 10,000µε	Infinite	0.2% f.s.	0.2% f.s. (1500 µε) 3µε	GOOD GOOD GOOD	Can Be Temp. Comp For Specimen Material	Creep of Strain Gage Adhesive Problem	Gage Factor 2	Gage Length .015 in	Tra slve min foc mid perf
Dilatometer System	Laser Beam Interferometer	Hewlett Packard	Hewlett Packard	Complex	Easy	0-51 feet	$.6 \times 10^{-6}$ in	Not Given	± 0.5 ppm ± 1 Count	HIGH HIGH LOW	± 32° to ± 130°F	To 95%	N.A.	Single Point Measurement	Too

*f.s. = Full Scale

MENT MEASURING SYSTEM - EVALUATION AND COST ESTIMATE

RESOLUTION	LINEARITY	ACCURACY	STABILITY RELIABILITY DRIFT	TEMPERATURE	HUMIDITY	SENSITIVITY GAGE FACTOR	MISC.	NOTES	ESTIMATED COST OF COMPONENTS
0.82×10^{-3} in	Non-linear But Electronics Can Make It Linear	Function of Construction of the Sensor But $>71 \times 10^{-7}$ in	HIGH HIGH LOW	Typical 2.5×10^{-6} in Reading Per °C	Condensation Can be a Problem	Typical 7×10^{-3} pf/μ" @ 100,000 Hz gl/μ"	Integrates If Active Area Capacitor is Surrounding the Specimen	Useable at elevated temperature and has needed resolution. Potential specimen attachment and electrical shielding problems. ATC DESIGN / SHOP FAB. / TOTAL / SUBSEQUENT	$ 800 / 700 / 1500 / 500
0.001% f.s.*	3% f.s.	3% f.s.	HIGH HIGH LOW	Use at Room Ambient	Use at Room Ambient	N.A.	Measures the Difference Between an unknown and a standard. Has analog output for recorder.	G. R. 1654 Comp. / 1422 Precision Reference Capacitor	$1600 / $1000
10^{-6} p.f.	0.1% f.s. if Calib. At 0.6 f.s.	0.1% f.s.	HIGH HIGH LOW	Ambient	Ambient	N.A.	Variable Bandwidth For Noise Reduction	Measures an unbalance from initial setting. Has analog output for recorder. MODEL 1055	$2715
4×10^{-6} in Repeatability	Linear Within 0.05% of Linear Range	Accurate Within 0.04%	4×10^{-6} in GOOD GOOD	40° to 140°F	Needs Low Humidity and to be Kept Clean	3.7mV/mil in/volt	Single Point Measurement	Has good resolution over ± 50% of total range. Resolution inferior to capacitor. Potential specimen attachment and electrical shield problems. Temperature limited.	$158 - $221
Infinite	Linear Within 0.25% of Linear Range	Accurate Within 0.25%	HIGH HIGH LOW	Available in High Temperature Model -65° to 300°F	No Effect	4.8×10^{-3} Volts Per 1×10^{-6} in	Single Point Measurement	Resolution will be dependent on physical construction of holding system. Temperature limited. Electrical shielding may be a problem.	$ 110
0.25×10^{-6} in	Linear Within ± 0.5% of Linear Range	Accurate Within ± 0.5%	Depends on Fab. & Design of Jig. Gen. Good	Metal Expansion Effect Should Be Calculated	No Effect	3×10^{-4} volt Per 1×10^{-6} in	Specifically Designed For Thick Adhered Lap Shear Specimen	Error due to Attachment off of Bondline. A dummy Adherend System to Factor Out Adherend Displacement and Environmental errors needed. LVDT DESIGN / FAB. / SIG. COND. / TOTAL / ADDL UNITS	$ 125 / 400 / 350 / 375 / $1250 / 850 / $2100
Infinite	± 20×10^{-6} in	± 20×10^{-6} in	GOOD GOOD GOOD	500°F	Little Effect	3×10^{-4} volt Per 1×10^{-6} in	Not Good For Dynamic Use Per Present Design	Unit is bulky and may be hard to handle. There seems to be room for slop in the moving parts. GAGE / BREAKAWAY SUPPORT / X-Y RECORDER / SIG. COND.	$ 725 / 75 / 1200 / 342 / $2342
0.01×10^{-6} in	Sensor Itself Non-Linear But Electronics Can Make It Linear	Function of The Construction of the Sensor But ± 1×10^{-7} in	GOOD GOOD UNKNOWN	May be Water cooled But should Have Little Effect	Effected by Condensation	1×10^{-2} pF Per 1×10^{-6} in	Large Output Impedance	Use for rotational measurement in conjunction with parallel plate capacitor.	> $1500
N.A.	Linear Within 0.05%	N.A.	± 0.05% GOOD LOW	0° - 130°F 0.02% Per °F of Sensitivity	Room Ambient	100 mv Input RMS Gives 10v D.C. Out		CAS 025 WLT / Excellent unit design and should do well.	$ 342
1×10^{-6} in 0.01% f.s. (NBS)	0.1% f.s.	0.1% f.s.	HIGH HIGH LOW	Metal Expansion	No Effect	N.A.	Visual Micrometer Scale With Vernier	Accuracy not good enough. TRANSLATOR / STAGE / TOTAL / N.B.S. CALIBRATION	$ 80 / 215 / 295 / 250
3×10^{-6} in	Analog Output Linear to 0.1% of f.s.	Same As Linearity	HIGH HIGH LOW	Offered in NILO 36 T.C. < 2ppm Per °C	Condensation Can Be A Problem	N.A.	N.A.	Accuracy not good enough (2) SLVC / FIXTURE DESIGN / FAB. FIXTURES / MODEL 1055 / TOTAL	$1200 / 400 / 375 / 2715 / $4690
2×10^{-6} in	3% f.s.	Deflection Error 3% f.s.	Not Given	Effects Could Be Calculable	Condensation Could Fog Optics	N.A.	Gage Length 0.25 in	This extensometer would not be easy to use. Requires lots of adjusting. Too complex and expensive	(?) Best Guess Is very Costly
1×10^{-8} in	Non-Linear	1×10^{-6} in	25 μ∊/24 HR	Specimen Expansion Effects Reading	Condensation Can Obstruct Operation	±2 Micro-Strain	Gage Length 0.005 in	Useful only on flat polished specimens might not be useable across a bondline. Has shortest gage length and appears to measure very small displacements. Too complex and expensive.	(?) Best Guess Is very Costly
Infinite	± .5% to 300 μ∊ 70°F ± 1% to 1500 @ 1500°F ± 2% to 20,000 μ∊ @70°F	Same As Linearity	0.1 μ∊/Day At 1100°F	± 300 μ∊ to 1500°F Cryogenic-1500°F	No Effect	.018 pf/ 1000 μ∊	Single Point Measurement	Probably not adaptable to bondline measurement. Must be welded to specimen and the cost is too high. GAGE / TEMP. COMP. / SIG. COND. / TOTAL	$ 890 / 190 / 2715 / $3795
Not Given	Not Given	Not Given	Drift 20°C-5μ∊/mth 600°C-5μ∊/day	-269°C To +650°C	Could Be Affected By Condensation	Gage Factor 100	Gage Length 20 mm (0.8 in)	Not Adaptable For Our Use	$208 Quant. 1-5
Infinite	0.2% f.s.	0.2% f.s. (1500 μ∊) 3μ∊	GOOD GOOD GOOD	Can Be Temp. Comp For Specimen Material	Creep of Strain Gage Adhesive Problem	Gage Factor 2	Gage Length .015 in	Trouble conding across adhesive bondline - not accurate enough performance, not satisfactory at high relative humidities for extended time period.	
6×10^{-6} in	Not Given	± 0.5 ppm ± 1 Count	HIGH HIGH LOW	± 32° to ± 130°F	To 95%	N.A.	Single Point Measurement	Too expensive. DILATOMETER HEAD / LASER AND READOUT UNIT	$4500 / $12000
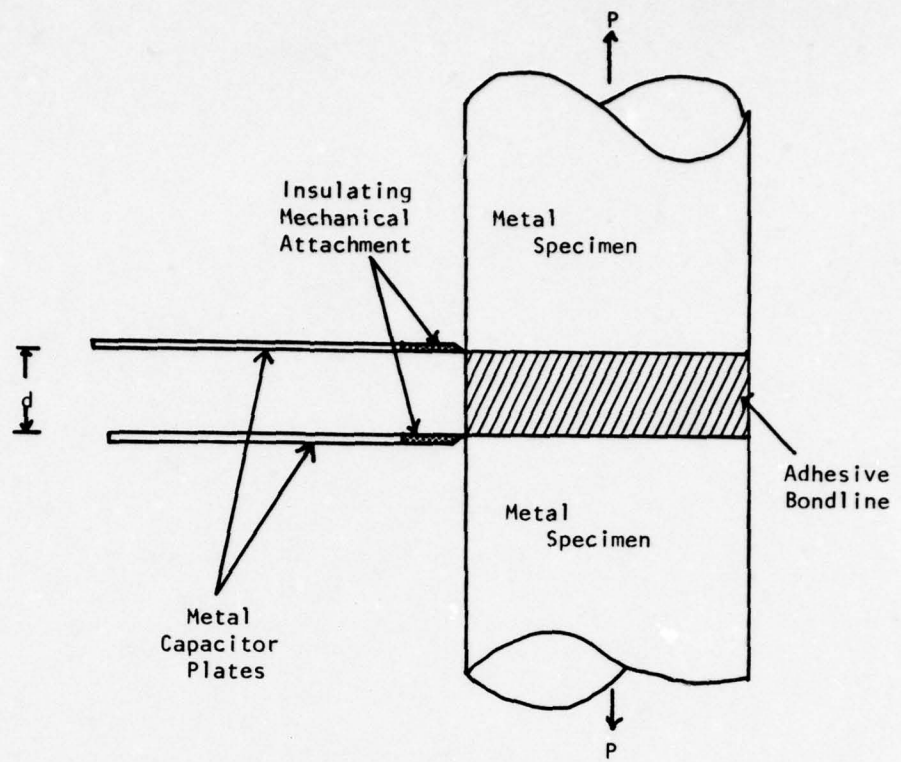
Case (a)   Variable Spacing Capacitive Displacement Sensor
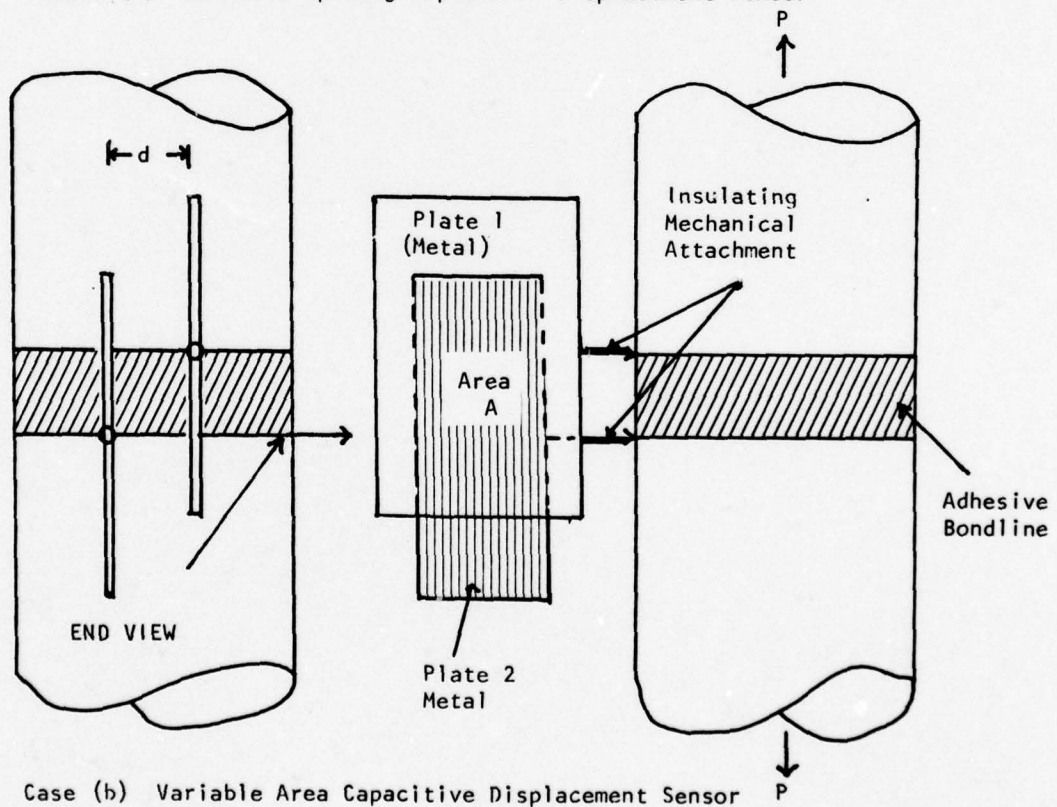
Case (b)   Variable Area Capacitive Displacement Sensor

FIGURE 12.   CAPACITIVE DISPLACEMENT SENSOR CONFIGURATIONS.

56

$$\overline{Z}_c = \frac{1}{\omega C}$$

where $\overline{Z}_c$ = magnitude of impedance

ω = $2\pi f$

f   = frequency in Hz.

The impedance is seen to vary inversely as the capacitance. Therefore, the impedance will vary directly as the distance between the plates and hence the bondline thickness.

4.4.2 Candidate Capacitive Sensors

A search of the literature and discussions with vendors showed several embodiments of the capacitive displacement sensor systems as possibilities. These were:

o Systems reported by Rutherford et. al. in 1968,

o System reported by Yeakley and Lindholm in 1973,

Discussions with General Radio indicated a signal conditioning system of exceptional adaptibility in their Model 1654 impedance comparator.

4.4.2.1 Rutherford System

Rutherford designed and used a capacitive displacement sensor similar in conception to that of Brown.[58] The sensor was used in measuring properties of adhesives in bonded joints and is directly applicable to the present study. Figure 13 shows the basic design of the sensor. Figure 14 illustrates his method of gage attachment close to the bondline-specimen interfaces. As a signal conditioner he used either a General Radio capacitance bridge type 1615A (10^{-5} pf resolution) or a Robertshaw Fulton Proximity Meter. An x-y recorder was also used. Sensitivities on the order of 5×10^{-4} pf/div were routinely obtained. Reference 58 makes no comment on linearity, stability, or accuracy.

4.4.2.2 Yeakley System

Yeakley designed and used a parallel plate sensor similar to Rutherford's for tension specimens. The plates are water cooled. Figure 15 shows the sensor plates and the mounting arrangement on a cylindrical specimen. The signal conditioner shown in Figure 16 was designed specifically for this sensor. The sensor capacitor is used as the feedback capacitor in a charge amplifier. The gain
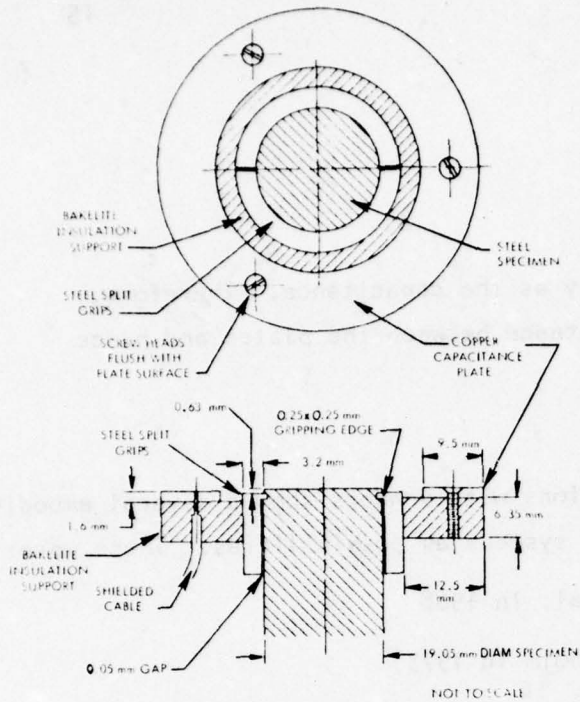
FIGURE 13. EXTERNAL AIR-GAP CAPACI-
TANCE EXTENSOMETER ASSEMBLY
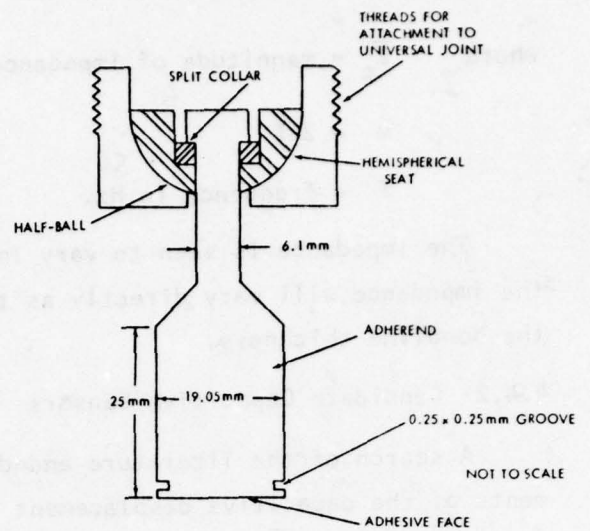
FIGURE 14. SCHEMATIC CROSS SECTION OF
ADHEREND AND GRIPPING
ASSEMBLY
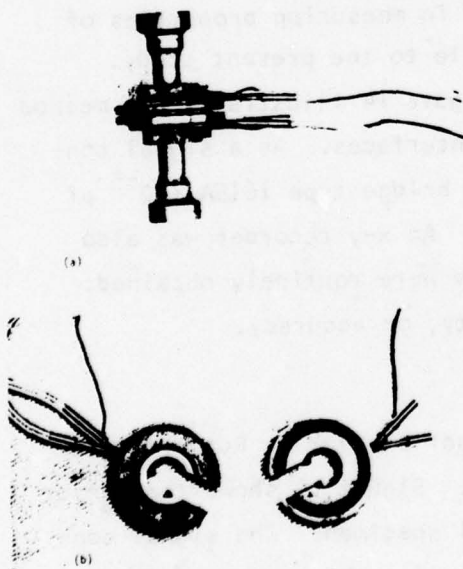
FIGURE 15. UNIAXIAL CAPACITANCE EXTENSOMETER
MOUNTED ON SPECIMEN (A) AND SHOW-
ING PLATE ARRANGEMENT (B)
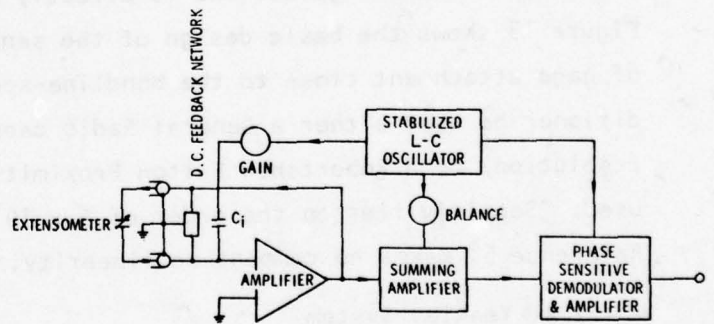
FIGURE 16. CIRCUIT SCHEMATIC FOR UNIAXIAL
EXTENSOMETER.

58

of the charge amplifier is inversely proportional to its feedback capacitor. With a fixed capacitor, C_i as the input element for a carrier signal, the amplifier output is a carrier signal proportional in amplitude to sensor plate spacing.

He also designed a water-cooled biaxial capacitive sensor for measuring axial and torsional strains in a butt bonded tubing specimen. Linearity, stability, and accuracy are not specified in Reference 59.

4.4.2.3 General Radio Model 1654 Impedance Capacitor

The General Radio Model 1654 Impedance Comparator is an ideal instrument for use as a signal conditioner with capacitive displacement sensors. Figure 17 shows the instrument, its controls, and the specifications for the instrument. The instrument is a Wheatstone bridge providing shielded and guarded terminals for connection of a standard capacitor* and an unknown capacitor. The bridge circuit is not adjusted for a balance; instead, the unbalance voltage is measured to give the required impedance difference information. The detector is phase sensitive and selects those vector components of the unbalance voltage that are proportional to the impedance magnitude in percent, as well as the phase angle difference.

The metering circuit and the analog output voltage for the magnitude channel of the 1654 are linearized to ensure accurate readings without correction for up to 30% impedance differences. The combination of four fixed frequencies from 100 Hz to 100 kHz, with a wide impedance range and several different ranges, results in a flexible and extremely versatile impedance comparator.

The impedance difference full scale ranges in percent are: 0.1, 0.3, 1, 3, 10 and 30. If the separation of the plates of a parallel tension gage are set equal to the gage length before loading and a variable capacitor as a standard is adjusted for a zero impedance difference, the comparator will read out in percent elongation (strain). The analog voltage output has a resolution of 0.001% of full scale, and an accuracy of 3% of full scale. The comparator can also be used effectively to compare two similar gages or the two halves of a differential variable capacitor.

---

*The instrument will also handle the comparison of resistive and inductive impedances.

59
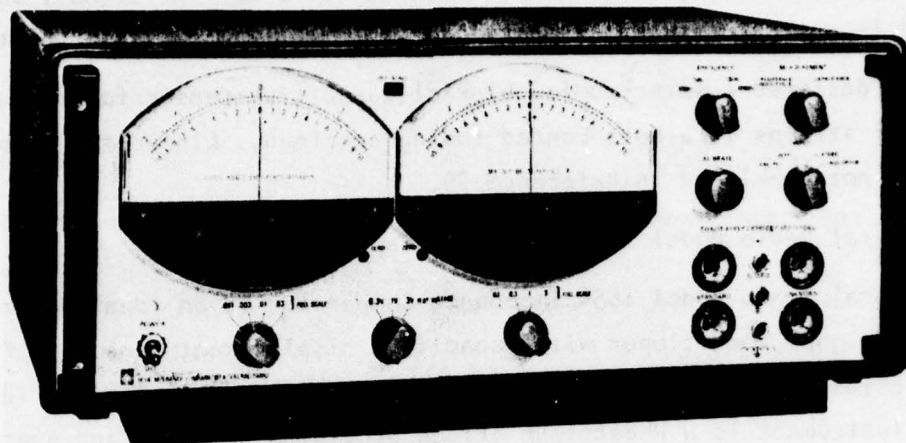
SPECIFICATIONS

Frequencies: Internal only 100 Hz, 1, 10, and 100 kHz, ±1%.

Ranges: 0.1% to 30% full-scale impedance difference; 0.001 to 0.3 radian full-scale phase-angle difference. Available ranges depend on test voltage selected as shown in the following table.

Test Voltage	Impedance Difference Full-scale Range — %						Phase-Angle Difference Full-scale Range — Radian					
	0.1	0.3	1	3	10	30	0.001	0.003	0.01	0.03	0.1	0.3
0.3 V			x	x	x	x			x	x	x	x
1 V		x	x	x	x			x	x	x	x	
3 V	x	x	x	x			x	x	x	x		

Impedance Ranges (0.3-V test voltage*)

Freq	Resistance	Capacitance	Inductance
100 Hz	2 Ω — 20 MΩ	1000 pF — 1000 μF	5 mH — 1000 H
1 kHz	2 Ω — 2 MΩ	50 pF** — 100 μF	500 μH — 100 H
10 kHz	2 Ω — 200 kΩ	50 pF** — 10 μF	50 μH — 1 H
100 kHz	10 Ω — 10 kΩ	50 pF** — 0.1 μF	20 μH — 10 mH

* Low R and L limits are increased and upper C limit decreased by 10:1 for 1-V test voltage and by 100:1 for 3-V.
** To 0.1 pF by substitution method.

Resolution: Meter, 0.003% and 0.00003 radian. Analog-voltage output, 0.001% and 0.00001 radian.

Accuracy: 3% of full scale.

Voltage Across Standard and Unknown: 0.3, 1, or 3 V selected by front-panel control. Test voltage of 2 V (with 0.6 and 6 V) can be obtained on special order.

Analog-Voltage Outputs: Voltages proportional to meter deflections at two rear-panel connectors: ±10 V full scale behind <10 Ω for 1782 Analog Limit Comparator; ±3 V or ±10 V (depending on range) full scale behind 2 kΩ for DVM, A-D converter or other use.

Test Speed: About 1 component per second with meter, max. With analog output voltage, about 4 components per second, except about 1 component per second at 100 Hz.

Power: 105 to 125 or 210 to 250 V, 50-60 Hz, 15 W except 1654-Z1, 35 W.

Supplied: Multiple-contact connector and power cord.

Available: 1782 ANALOG LIMIT COMPARATOR (supplied with -Z1 and -Z3); 1413 PRECISION DECADE CAPACITOR (supplied with -Z2 and -Z3) and other GR decade boxes and standards of resistance, capacitance, and inductance; 1680-P1 TEST FIXTURE for rapid connection of components (includes con-

FIGURE 17. GENERAL RADIO MODEL 1654 IMPEDANCE COMPARATOR

4.4.3 Candidate Linear Differential Transformer Sensors

Hermetically sealed and specially treated LVDT's are available that will operate under conditions of high humidity and modest temperatures (200°F). LVDT's are mechanically rugged and will withstand shock and vibration. Special coatings can be used to protect them from chemical fumes. Two systems of special interest to this program are discussed.

4.4.3.1 Tinius Olsen LVDT Extensometer

The Tinius Olsen Testing Machine Company of Willow Grove, Pa. manufactures a line of extensometers using LVDT's as sensitive elements and strain recorders. Figure 18 shows one of interest for bondline deformation measurements. It can be easily adapted to a short gage length. The gage is designated as S-1000-2A. The gage is easily installed by snapping it on the specimen. The knife edges and the leaf springs hold the gage securely in place. The left hand knife edge and stress spring, support the structure holding the body of the LVDT. The right hand knife edge beam is pivoted at the nut and screw immediately to its right. The other end of the beam which is spring loaded holds the push rod and core of the LVDT. The beam magnifies the displacement of the knife by two. A mechanical zero adjust is provided.

If the left hand knife edge and spring assembly is turned upside down and properly positioned, a very short gage length can be obtained. This arrangement is recommended for attaching the knife edges adjacent to the adhesive-adherend interface.

The performance of the gage in the new configuration would depend on the choice of LVDT. Performance of the gage should be very close to that of the LVDT chosen. Some slight errors might be introduced by the pivot bearing but it should be small.

4.4.3.2 Krieger LVDT Extensometer

R. B. Krieger, Jr. has developed a displacement sensor system specifically for shear measurements on the thick adherend lap-shear specimen. Figure 19 shows the two LVDT assemblies required, mounted on a test specimen. The core is flexure mounted and is driven by a single point. The coil is suspended from the other pair of points. The points can be arranged to be very close to the bondline.
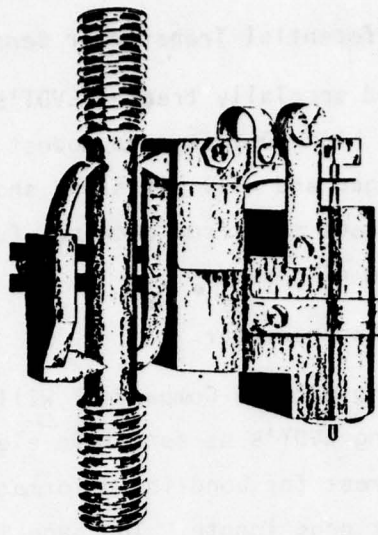
FIGURE 18. TYPICAL LVDT EXTENSOMETER
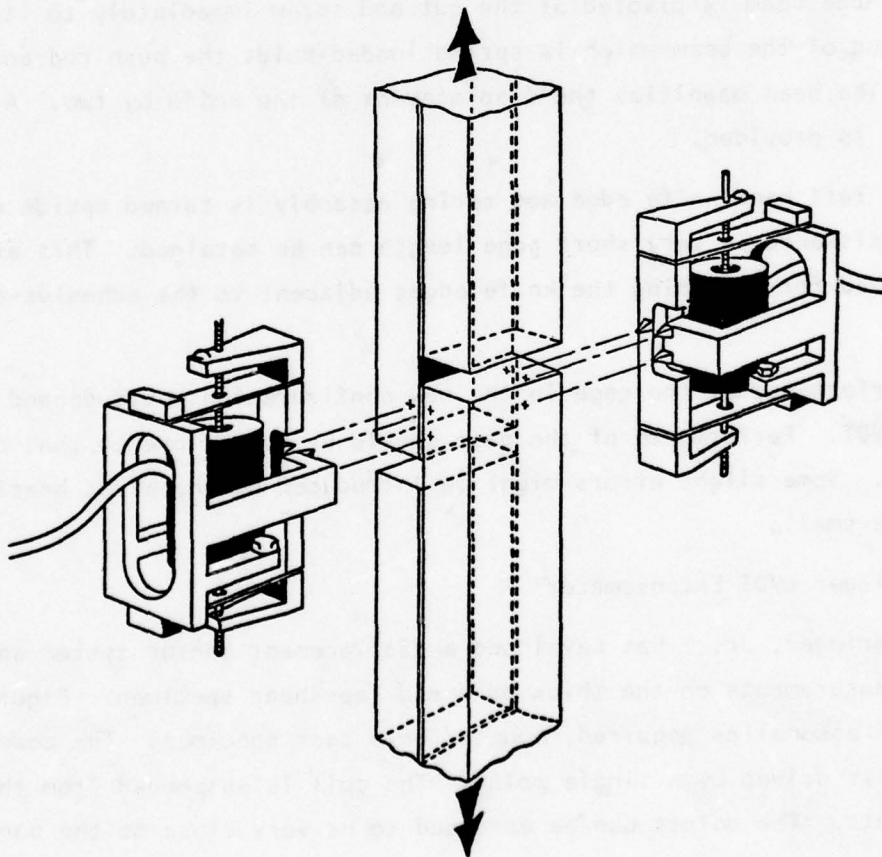
FIGURE 19. NEW ADHESIVE DEFORMATION MEASUREMENT DEVICE

One set of gages may be used on a solid metal specimen to account for metal deformation in the adherends. The accuracy calculated for this displacement sensor based on available information is estimated to be ± 5% if it is assumed that all errors will combine in one direction.

4.5 SUMMARY

In an effort to more easily evaluate the various displacement measurement devices in an objective manner, Table 7 was prepared. All candidate measurement systems have been evaluated against a common set of criteria. It was concluded as a result of the survey that the two candidate measurement systems just discussed be given further consideration, as to their adaptability to measure the adhesive deformation off of adhesive mechanical property test specimens, within the overall accuracy requirement of ± 2.0%.

The uncertainty as to the shape of the test specimens and the potential problems and/or disadvantages of each system required that both systems be given further study during the performance of Task III.

63

SECTION V

TEST SPECIMEN ANALYTICAL MODEL

5.1 SCARF JOINT ANALYSIS

Examination, in a realistic manner, of the stress (strain) state in an adhesively bonded scarf (butt) joint configuration, requires that a specific closed form analytical model be derived. The analysis presented enables one to determine the optimum specimen dimensions to maximize the uniform stress (strain) region in the adhesive, thereby minimizing disruptive edge effects for a particular test geometry. Employing these optimal test specimens, one may obtain accurate adhesive mechanical property data and account for the fact that the apparent adhesive modulus measured during an actual test is a known percentage of the true uniaxial adhesive modulus. This relationship is a function of adhesive and adherend properties and specimen geometry. The mechanical property data obtained using these specimens will be the subject of a future paper.

Several attempts to analyze the scarf[102] or butt[77,194,195] joint have been made. In all instances, the constraining effect of the stiffer adherend material on the adhesive and the viscoelastic nature of the adhesive were neglected. The ensuing analysis accounts for finite adherend properties and uses as a starting point, the analytical model developed in Reference 77. Both the circular and rectangular scarf joint geometries are looked at. Once the stresses (strains) in the rectangular (circular) scarf joint are defined, it is a simple matter to obtain the stresses (strains) in the butt joint.

A rigorously correct mathematical model for the scarf (butt) joint configuration leads to a mixed boundary value problem that is essentially intractable using a classical elasticity approach. This is primarily due to the discontinuous boundary condition the joint presents at the right angled corner where the adherend surface is appreciably stiffer than the adhesive while the adhesive's surface is free of stress. The ensuing stress singularity is not accounted for within the analysis. Its effect can be quantified using the analytical approach found in reference 3. Moreover, its degree of penetration from the adhesive's free surface inward is a function of the specimen's shear modulus and Poisson's ratio. A realistic specimen design ($a \gg \eta$) will restrict the effect of this singularity to within one to two adhesive thicknesses from the adhesive's free surface.

64

5.1.1 Formulation of the Problem (Rectangular Geometry)

The rectangular scarf joint geometry and notation are shown in Figure 20a. The joint is assumed to be infinitely long in the z-direction (i.e., L/a >> 1) and is therefore considered to be in a generalized plane strain state. Linear elastic analysis is used with the inclusion of linear viscoelastic effects by means of the "quasi-elastic" approach. The adherend material is assumed to be linearly elastic, isotropic and homogeneous. Its effect on the adhesive is realized through use of the adherend displacement boundary conditions, while the adhesive is characterized in a linearly viscoelastic manner. It too is assumed to be isotropic and homogeneous. Additional assumptions are that the bond between the adhesive and the adherend is structurally sound, the stresses and displacements vary over the adhesive thickness in a prescribed manner, that adhesive planes originally parallel to the adherend interface remain parallel upon loading and that the adhesive-adherend discontinuity effect is defined by the unknown function f(s).

The adhesive's geometry and notation are shown in Figure 20b. The adhesive half-thickness is taken as unity for simplicity, but without loss of generality.

The adhesive slab is bonded to the two deformable adherends @ $\eta = \pm 1$. The adhesive is loaded in the η-direction by a load (P sin θ) which increases the adhesive thickness by 2ε and a shear load (P cos θ). It is desired to determine the state of stress (strain) in the adhesive for this system of external forces.

5.1.1.1 Elastic Adherend Boundary Conditions

The displacement boundary conditions at the adhesive-adherend interface can be ascertained by determining the displacements in a solid homogeneous linearly elastic, isotropic bar when subjected to a uniform axial tensile stress (σ_x) over its cross-section. The resulting displacements and strains are:

$$u = \frac{\sigma_x x}{\hat{E}} + C_2 y + C_1 \; ; \; v = \frac{-\hat{\nu}\sigma_x y}{\hat{E}} - C_2 x + C_3 \; ; \; w = \frac{-\hat{\nu}\sigma_x z}{\hat{E}} + C_4 \qquad 16$$

$$\hat{\varepsilon}_x = \frac{\partial u}{\partial x} = \frac{\sigma_x}{\hat{E}} \; ; \; \hat{\varepsilon}_y = \frac{\partial v}{\partial y} = \frac{-\hat{\nu}\sigma_x}{\hat{E}} \; ; \; \hat{\varepsilon}_z = \frac{-\hat{\nu}\sigma_x}{\hat{E}} = \text{const.}$$

$$\hat{\gamma}_{xy} = \hat{\gamma}_{xz} = \hat{\gamma}_{yz} = 0 \qquad 17$$

The constants $\hat{\nu}$ and $\hat{E}$ are the Poisson's ratio and Young's modulus of the adherend material while, u, v, and w are the displacements in the x, y and z directions.

65
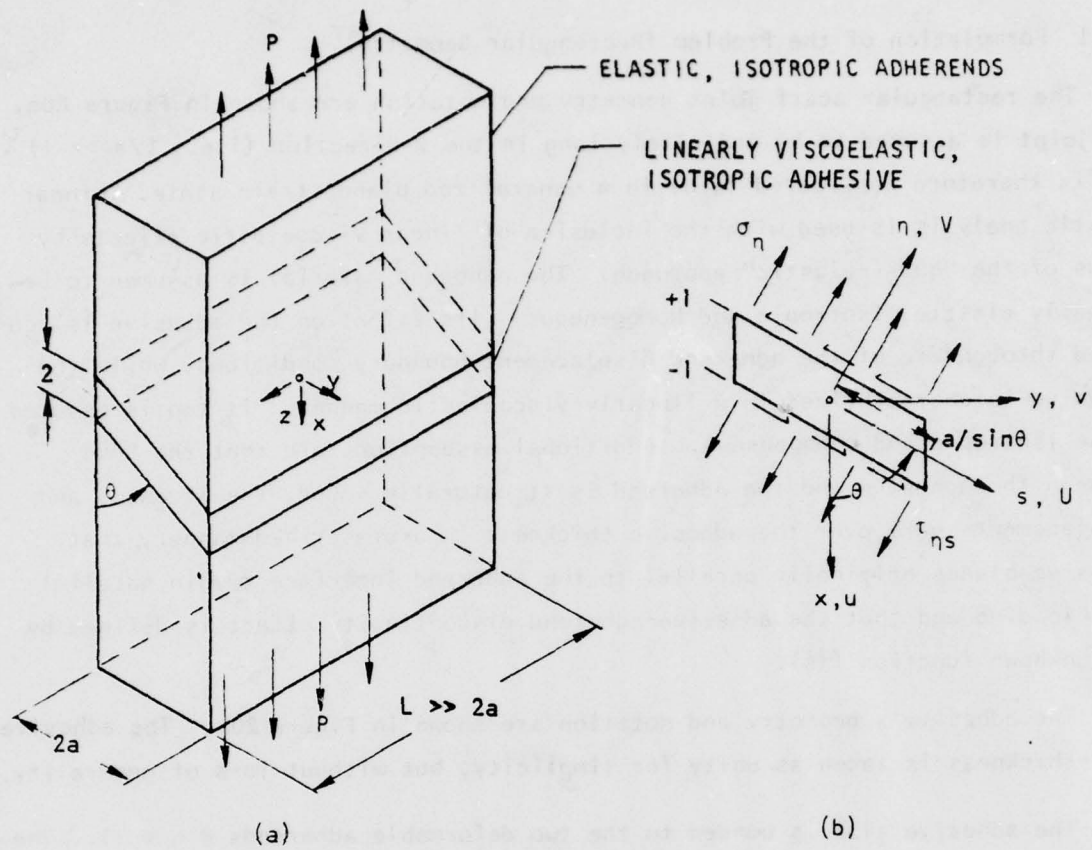
FIGURE 20. RECTANGULAR SCARF JOINT GEOMETRY
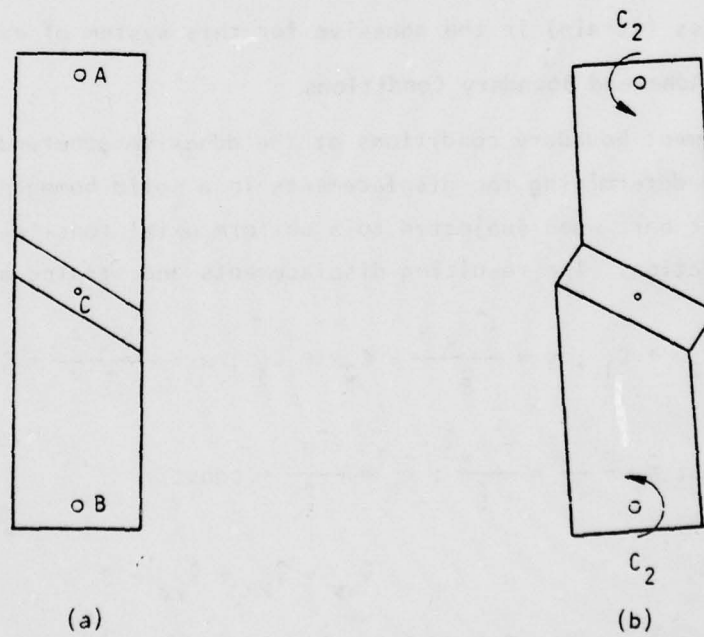
FIGURE 21. ROTATION OF A TYPICAL SCARF JOINT

66

respectively. The constants C_1, C_2 and C_4 define the reference location with respect to the coordinates origin from which all deformation measurements are made. C_1, C_3 and C_4 will be equated to zero.

Lubkin[102] has shown that relative rotation between identical adherends pin loaded at points (A) and (B) is absent. However, it can be shown that the specimen as a whole rotates in the (x-y) plane and that this rotation is given by the (C_2) term in Equation (16). The rotation it refers to is depicted in Figure 21 and is independent of cross-sectional geometry. It can be directly determined by measuring the rotation of a vertical side of the specimen with a high resolution optical measurement device as the specimen is loaded. Alternately, the rotation can be obtained by measuring the specimen's displacement parallel (U) and perpendicular (V) to the adhesive-adherend interface and using the relationship:

$$C_2 = \frac{V \cos \theta - U \sin \theta}{\ell/2}$$

Moreover, it can be shown, by the use of symmetry arguments, that there is no horizontal movement of the center point (C) and that the deformation across the adhesive thickness from right to left is symmetric. Therefore, the rotation of the upper and lower adherends (C_2) must be in the same direction and does occur about pints (A) and (B).

Let $\hat{U}$ and $\hat{V}$ be the adherend displacements in the (s) and (η) directions, respectively. Then per the well-known transformation of axes formulas:

$$\hat{U} = u \cos \theta + v \sin \theta$$

$$\hat{V} = v \cos \theta - u \sin \theta \qquad\qquad 18$$

Similarity, the coordinate transformation from the (x-y) to the (s, η) axes is:

$$x = s \cos \theta - \eta \sin \theta$$

$$y = s \sin \theta + \eta \cos \theta \qquad\qquad 19$$

Substitution of Equation (16) into Equation (18) and employing the coordinate transformation relations (Equation (19)), provides the formulas for the adherend displacement functions with reference to the (s, η) axes, namely:

67

$$\hat{U} = As + B\eta ; \qquad\qquad \hat{V} = \beta\eta - Ds \qquad\qquad 20,21$$

where:

$$A = \frac{\sigma_x}{\hat{E}} (\cos^2 \theta - \hat{\nu} \sin^2\theta); \ D = \frac{\sigma_x}{\hat{E}} (1 + \hat{\nu}) \sin \theta \cos \theta + C_2 \qquad 22$$

$$B = - \frac{\sigma_x}{\hat{E}} (1 + \hat{\nu}) \sin \theta \cos \theta + C_2; \ \beta = \frac{\sigma_x}{\hat{E}} (\sin^2 \theta - \hat{\nu} \cos^2 \theta) \qquad 23,24$$

Because the adhesive is constrained by the stiffer adherend at the adhesive-adherend interface, the displacement relations must satisfy Equations (20, 21) at $\eta = \pm 1$ for a continuous interface to exist. Therefore, the boundary conditions to be satisfied at $\eta = \pm 1$ are:

$$\hat{U} = As \pm B; \qquad\qquad \hat{V} = \pm\beta - Ds \qquad\qquad 25,26$$

5.1.1.2 Adhesive Stress Analysis

Based on earlier work,[77,194] the displacement functions for the adhesive in the (s), (η) and (z) directions, respectively, are assumed to be:

$$U = -f(s) (1 - \eta^2) + As + B\eta \qquad\qquad 27$$

and

$$V = \varepsilon \eta - Ds ; \qquad\qquad w = \Gamma z \qquad\qquad 28,29$$

where:

$$\Gamma = \frac{-\hat{\nu}\sigma_x}{\hat{E}} \qquad\qquad 30$$

The terms A, B, and D are defined by Equations (22 and 23).

The function $f(s)$ is to be determined by employing the stress equilibrium relations. It relates directly to the deformed shape of the adhesive when constrained by the adherends under load for reasonable aspect ratios. The assumed forms for the displacements U and V, satisfy the boundary conditions, namely Equations (25) and (26) provided $\varepsilon = \beta$ at the adhesive-adherend interface. The displacements provide the normal strain relations:

$$\varepsilon_s \equiv \frac{\partial U}{\partial s} = -f' (1 - \eta^2) + A ; \qquad \varepsilon_\eta \equiv \frac{\partial V}{\partial \eta} = \varepsilon \qquad\qquad 31,32$$

$$\varepsilon_z \equiv \frac{\partial w}{\partial z} = \Gamma ; \qquad \gamma_{\eta s} = \frac{\partial U}{\partial \eta} + \frac{\partial V}{\partial s} = 2f\eta + R \qquad\qquad 33,34$$

68

where

$$R \equiv (B - D) \text{ and } f' \equiv df/ds.$$

The stress equilibrium equations are satisfied on an average basis by their integration across the adhesive thickness. For the s-direction the ensuing plane strain relation is

$$1/2 \int_{-1}^{1} \left[\frac{\partial \sigma_s}{\partial s} + \frac{\partial \tau_{\eta s}}{\partial \eta} \right] d\eta = 0 \qquad 35$$

Symmetry considerations require that σ_s and σ_η be even functions of (η) and that $\tau_{\eta s}$ be an odd function of (η). Furthermore, the average normal stresses will be denoted by

$$\bar{\sigma}_s = 1/2 \int_{-1}^{1} \sigma_s \, d\eta; \qquad \bar{\sigma}_\eta = 1/2 \int_{-1}^{1} \sigma_\eta d\eta \qquad 36$$

With this definition Equation (35) reduces to

$$\frac{d \bar{\sigma}_s}{ds} + 1/2 \tau_{\eta s} \Big|_{-1}^{1} = 0 \qquad 37$$

Similarly, the stress equilibrium relation in the η-direction,

$$1/2 \int_{-1}^{1} \left[\frac{\partial \sigma_\eta}{\partial \eta} + \frac{\partial \tau_{\eta s}}{\partial s} \right] d\eta = 0 \qquad 38$$

is identically satisfied by symmetry considerations.

The averaged stresses $\bar{\sigma}_s$ and $\bar{\sigma}_\eta$ are obtained by substituting Equations (31 - 33) into the stress-strain relations and integrating over the adhesive thickness per Equation (36). The ensuing averaged stress relations are:

$$\bar{\sigma}_s = \int_0^1 [\lambda \upsilon + 2G\epsilon_s] d\eta = -(2/3 \, \lambda + 4/3 \, G)f' + (A + \epsilon + \Gamma)\lambda + 2GA \qquad 39$$

$$\bar{\sigma}_\eta = \int_0^1 [\lambda \upsilon + 2G\epsilon_\eta] d\eta = -2/3 \, f' \, \lambda + (A + \epsilon + \Gamma) \, \lambda + 2G\epsilon \qquad 40$$

$$\bar{\sigma}_z = \nu_a (\bar{\sigma}_s + \bar{\sigma}_\eta) - \frac{\nu E_A^2}{\bar{E}} \epsilon_\eta \qquad 41$$

and

$$\tau_{\eta s} = G \, \gamma_{\eta s} = G(2f\eta + R) \qquad 42$$

69

The governing differential equation whereby a solution to $f(s)$ is obtained, is formulated through substitution of Equations (34, 39 and 42) into Equation (37). The ensuing governing differential equation is:

$$f'' - Mf = 0; \tag{43}$$

$$M \equiv \frac{3G}{\lambda + 2G} \tag{44}$$

The governing differential equation is a second order ordinary differential equation with constant coefficients. Since the shear stress $\tau_{\eta s}$ is an odd function of (η) the desired solution is:

$$f(s) = K \sinh (\sqrt{M} s) \tag{45}$$

The unknown constant (K) is determined by the physical requirement that

$$\overline{\sigma}_s \ (a/\sin \theta) = 0. \tag{46}$$

The resulting relationship is:

$$K = \frac{(A + \varepsilon + \Gamma)\lambda + 2GA}{(2/3 \ \lambda + 4/3 \ G) \ \sqrt{M} \cosh (\sqrt{M} \ a/\sin \theta)} \tag{47}$$

Substitution of Equations (45) and (47) into the various adhesive deformation, (Equations 27-29) strain (Equations 31-34) and stress (Equations 39-34) relations gives the final form for these relations.

5.1.2 Formulation Of The Problem (Circular Geometry)

The circular scarf joint geometry and the candidate notation (s, η, ϕ) are shown in Figure 22. Except for deletion of the plane strain condition, all assumptions are identical to that for the rectangular scarf joint. The adhesive disk is bonded between two deformable adherends @ $\eta = \pm 1$ and is two units thick. The disk is loaded in the η - direction by a load $(P \sin\theta)$ which increases the adhesive thickness by $2 \ \varepsilon$ and a shear load of $(P \cos\theta)$.

70
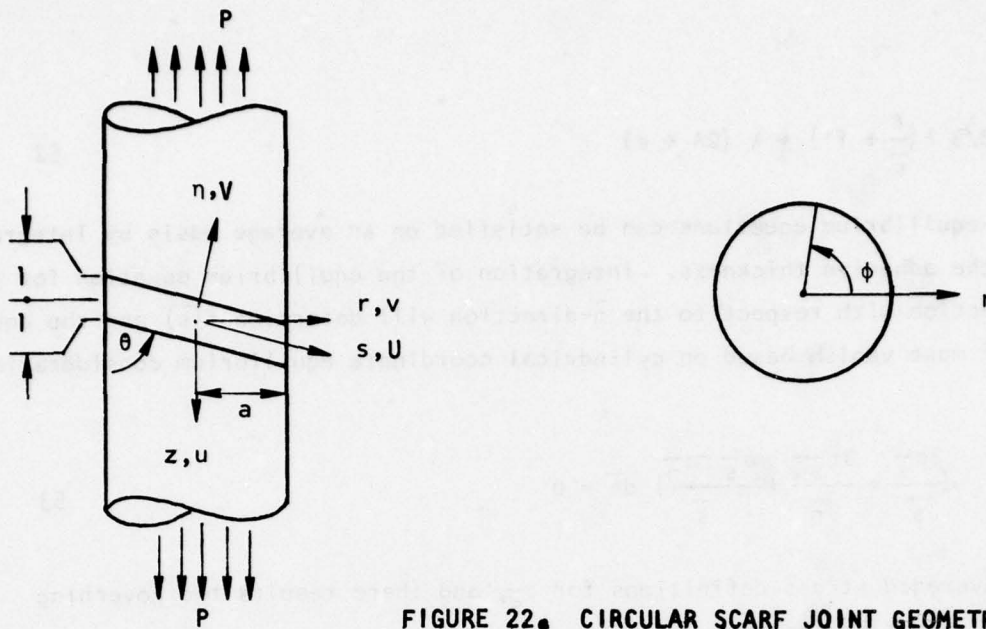
FIGURE 22. CIRCULAR SCARF JOINT GEOMETRY.

5.1.3 Adhesive Stress Analysis

The displacement boundary conditions at the adhesive-adherend interface are ascertained in a manner analogous to that for the rectangular geometry. Thus at $\bar{\eta} = \pm 1$, Equations (25) and (26) are valid. Moreover, Equation (46) must also be satisfied.

The displacement functions for the adhesive in the $(\bar{s})$, $(\bar{\eta})$ and $(\bar{\phi})$ directions are identical in form to those defining U and V in Equations (27-28) The strains corresponding to these displacements are identical to those defined in Equations (31, 32 and 34) for ε_s, ε_η and $\gamma_{\eta s}$, respectively. Moreover,

$$\varepsilon_{\bar{\phi}} = \frac{U}{s} = \frac{-f(1-\bar{\eta}^2)}{s} + A + \frac{B\bar{\eta}}{s} \qquad 48$$

The resulting averaged stress relations are:

$$\bar{\sigma}_{\bar{s}} = \bar{K} - 4/3 \, G \, f' + 2GA \qquad 49$$

$$\bar{\sigma}_{\bar{\phi}} = \bar{K} - 4/3 \, G \, \frac{f}{s} + 2GA \qquad 50$$

$$\bar{\sigma}_{\bar{\eta}} = \bar{K} + 2G\varepsilon \qquad 51$$

71

where

$$\overline{K} = -2/3 \; \lambda \left(\frac{f}{s} + f'\right) + \lambda \; (2A + \varepsilon)$$

52

The stress-equilibrium equations can be satisfied on an average basis by integration over the adhesive thickness. Integration of the equilibrium equation for the radial direction with respect to the $\overline{\eta}$-direction will determine $f(\overline{s})$ and the equation itself must vanish based on cylindrical coordinate equilibrium considerations. Thus:

$$1/2 \int_{-1}^{1} \; \left(\frac{\partial \sigma_{\overline{s}}}{\partial \overline{s}} + \frac{\partial \tau_{\overline{s\eta}}}{\partial \overline{\eta}} + \frac{\sigma_{\overline{s}} - \sigma_{\overline{\eta}}}{\overline{s}}\right) \; d\overline{\eta} = 0$$

53

using the averaged stress definitions for $\sigma_{\overline{s}}$, and there results the governing differential equation, namely:

$$f'' + \frac{f'}{s} - \left(\frac{1}{s^2} + M\right) f = 0$$

54

where $\tau_{s\eta}$ is an odd function of η due to symmetry about the $\eta = 0$ plane. The equilibrium equation for the η-direction is satisfied identically.

Equation (54) is a modified Bessel Equation of order one. A complete solution is of the form

$$f(s) = \overline{A} I_1 \; (s\sqrt{M}) + \overline{B} k_1 (s\sqrt{M})$$

55

where $I_1 \; (s\sqrt{M})$ is a modified Bessel function of the first kind and $k_1 \; (s\sqrt{M})$ is a modified Bessel function of the second kind.

As $s \to 0$, U must be finite. This specifies that $f(s)$ be finite. Therefore $\overline{B} = 0$.

The constant $\overline{A}$ is determined using equation (46) Thus:

$$\overline{A} = \frac{-3\lambda \; (2A+\varepsilon) \; - \; 6GA}{-2(\lambda+2G)\sqrt{M} I_0 \left(\frac{a\sqrt{M}}{\sin\theta}\right) \; + \; \frac{4G}{a} \; I_1\left(\frac{a\sqrt{M}}{\sin\theta}\right) \; \sin\theta}$$

56

Again, the final form for the various adhesive deformation, strain and stress relations is obtained using equations (55) and (56) in an identical manner to that specified for the rectangular geometry.

72

5.2 BUTT JOINT ANALYSIS

For the limiting case whereby $\theta = 90°$, the solution for the butt joint is realized from the scarf joint analysis. The sole analytical difference is that the in-plane shear term previously identified by (R) $\rightarrow$ 0 as θ approaches $90°$. Therefore, the resulting shear strain is

$$\gamma_{ns} = 2\eta K \sinh (s\sqrt{M}) \qquad \text{(rectangular geometry)} \qquad 57$$

$$\gamma_{ns} = 2\eta \overline{A} I_1 (s\sqrt{M}) \qquad \text{(circular geometry)} \qquad 58$$

This strain is a direct result of the material property discontinuity which exists at the adhesive-adherend interface. This readily substantiates that the scarf joint is nothing more than a butt joint with a transverse in-plane shear being superimposed on the adhesive.

5.3 VERIFICATION OF ANALYTICAL MODEL

The analytical accuracy of the present analysis, for the limiting case whereby the adherend modulus approaches infinity, has been verified by comparing it with the *finite* difference results of reference 77 (Figure 23). In turn, the results of reference 77 have been verified by the experimental data of reference 194 and by the energy methods approach of reference 126 and 195.

A singularity region of influence is generally small compared to the distance to the nearest boundary. The region dominated by the stress singularity in Figure 23 and reference 77 is shown to be less than one adhesive thickness for the case of infinitely rigid adherends. While no appreciable growth in the region the singularity influences is anticipated, a numerical solution to evaluate the impact of the singularity for a finite adherend modulus is recommended.

5.4 APPARENT UNIAXIAL MODULUS

The apparent uniaxial modulus E_p (PSI) is defined as the ratio of the average normal stress over the bonded surface area $\sigma_{navg.}$, required to produce a normal displacement (V), to the nominal axial strain $\varepsilon_\eta m$ viz.

$$E_p \equiv \frac{\sigma_{navg.}}{\varepsilon} = \frac{\int_o^{\overline{R}} \overline{\sigma}_\eta ds}{\varepsilon} \qquad 59$$

where $\overline{R} = a/\sin \theta$.

$$\frac{\bar{\sigma}_n}{E_A \varepsilon}$$

Poisson's ratio $\nu = 0.4$

——— Reference (17) Finite Difference Solution

○ Analytical Solution (Special Case of Rigid Adherends)

$Z = \pm 1$

$Z = 0$

$\frac{r}{a}$
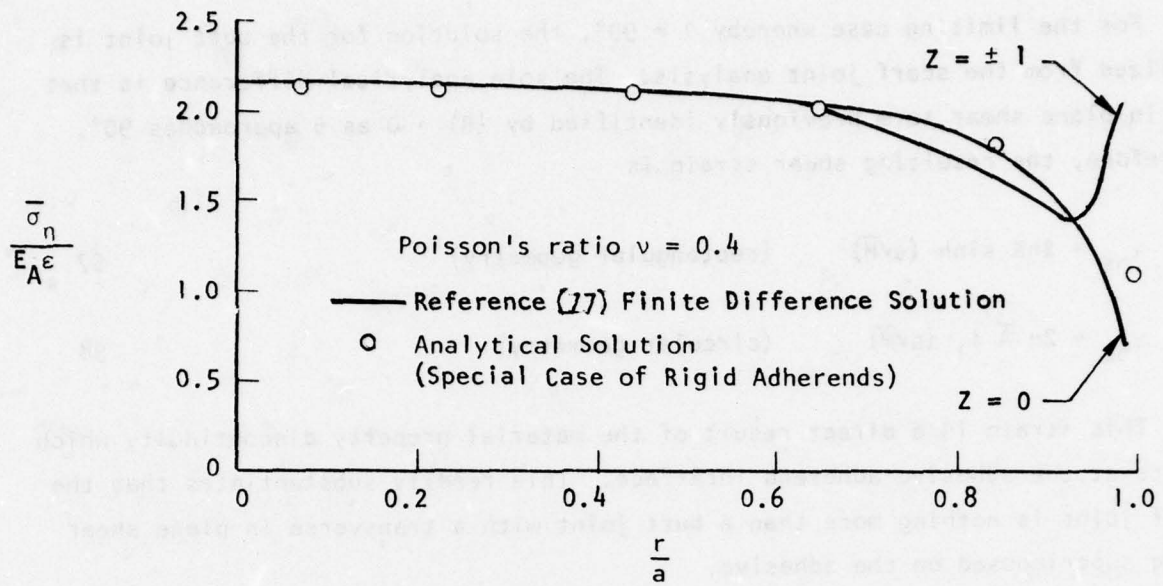
FIGURE 23. COMPARISON OF AXIAL STRESSES OBTAINED FROM THE TWO DIFFERENT METHODS OF SOLUTION FOR CIRCULAR GEOMETRY. ($a = 10$, $\theta = 90°$)

Substitution of Equation (40 and 45) into Equation (59) gives

$$E_P = \frac{-2\lambda}{3R\epsilon} \sinh(\sqrt{M}\,R) \left[\frac{(A + \epsilon)\lambda + 2GA}{(2/3\,\lambda + 4/3\,G)\sqrt{M}\,\cosh(\sqrt{M}\,\bar{R})} \right] \qquad 60$$

$$+ \frac{A\lambda}{\epsilon} + \lambda + \frac{\Gamma}{\epsilon}\lambda + 2G$$

Let $\quad \Gamma = -\frac{\hat{\nu}\epsilon\, E_P}{\hat{E}}; \qquad A = \frac{\epsilon\, E_A}{\hat{E}} (\cos^2\theta - \hat{\nu}\sin^2\theta)$

Then

$$\frac{A}{\epsilon} = \frac{E_P}{\hat{E}} (\cos^2\theta - \hat{\nu}\sin^2\theta) = \alpha$$

Substituting for A/ϵ and Γ in Equation (60) gives

$$E_P = -\frac{2}{3R} \frac{\lambda\,\sinh(\sqrt{M}\,\bar{R})}{(2/3\,\lambda + 4/3\,G)\sqrt{M}\,\cosh(\sqrt{M}\,\bar{R})} [\alpha\lambda + \lambda + 2G\alpha]$$

$$+ \alpha\lambda + \lambda - \frac{\hat{\nu}E_A}{\hat{E}}\lambda + 2G$$

Rearranging terms, the final relationship is:

$$\frac{E_P}{E_A} = \frac{\dfrac{\lambda + 2G}{E_A} - \dfrac{\lambda^2\,\sinh(\sqrt{M}\,\bar{R})}{E_A\bar{R}\,\sqrt{M}\,(\lambda + 2G)\,\cosh(\sqrt{M}\,\bar{R})}}{1 + \dfrac{\lambda}{\hat{E}}\left[(\cos^2\theta - \hat{\nu}\sin^2\theta)\left(\dfrac{\sinh(\sqrt{M}\,\bar{R})}{\bar{R}\,\sqrt{M}\,\cosh(\sqrt{M}\,\bar{R})} - 1\right) + \hat{\nu}\right]} \qquad 61$$

where E_P is the uniaxial tensile modulus.

5.5 OPTIMALLY DESIGNED TEST SPECIMENS

Employing the analytical methodology developed in the previous section, a parametric study was undertaken to ascertain the optimum geometry for adhesive scarf and butt joint test specimens, whereby a uniform adhesive tensile and shear stress state (scarf joint only) exist over as large a segment of the half-span (a) as is practicable. This is accomplished by minimizing the adhesive-adherend discontinuity effect defined by f(s) or f(s̄). Figures 24-26 determined

75
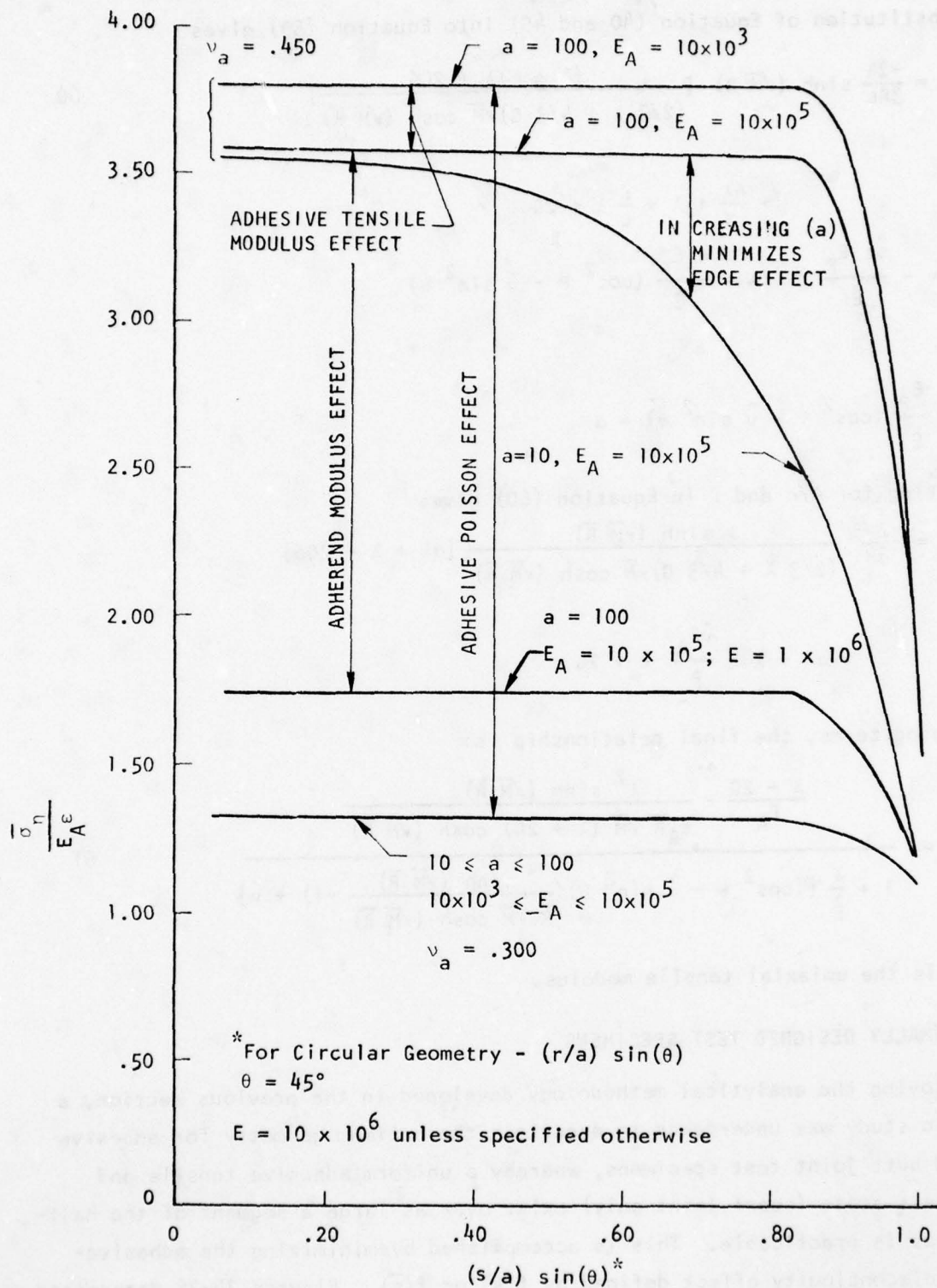
FIGURE 24. PRIMARY NORMAL STRESS DISTRIBUTION IN RECTANGULAR OR
CIRCULAR SCARF (BUTT) JOINTS.
(ϵ = 1.0) ASPECT RATIO ($10 \leq a \leq 100$)
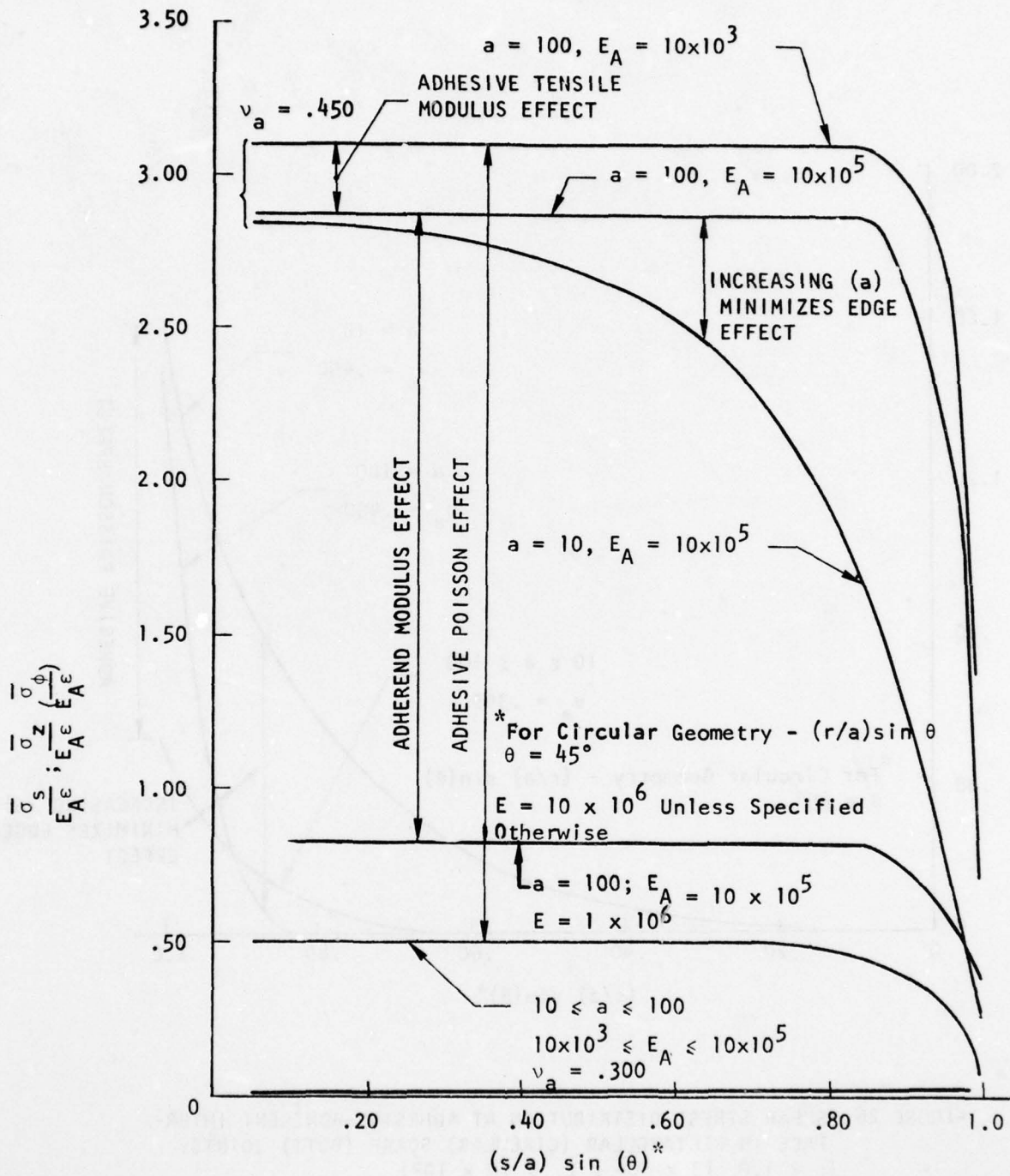
FIGURE 25. SECONDARY NORMAL STRESS DISTRIBUTIONS IN RECTANGULAR OR
CIRCULAR SCARF (BUTT) JOINTS.
(ϵ = 1.0) ASPECT RATIO ($10 \leq a \leq 100$).
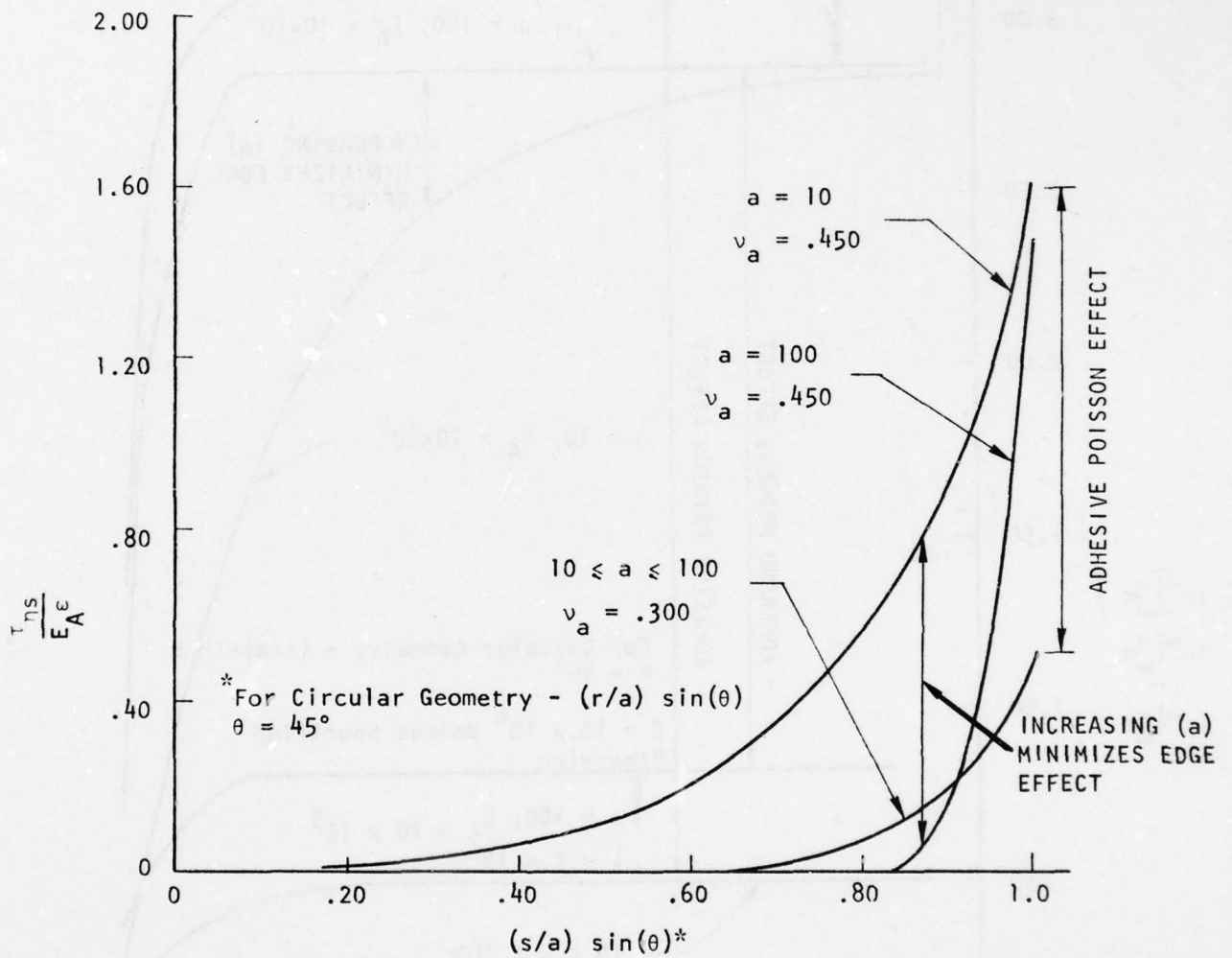
FIGURE 26. SHEAR STRESS DISTRIBUTION AT ADHESIVE-ADHERENT INTER-
FACE IN RECTANGULAR (CIRCULAR) SCARF (BUTT) JOINTS.
($\varepsilon = 1.0$; $10 \times 10^3 \leq E_A \leq 10 \times 10^5$)
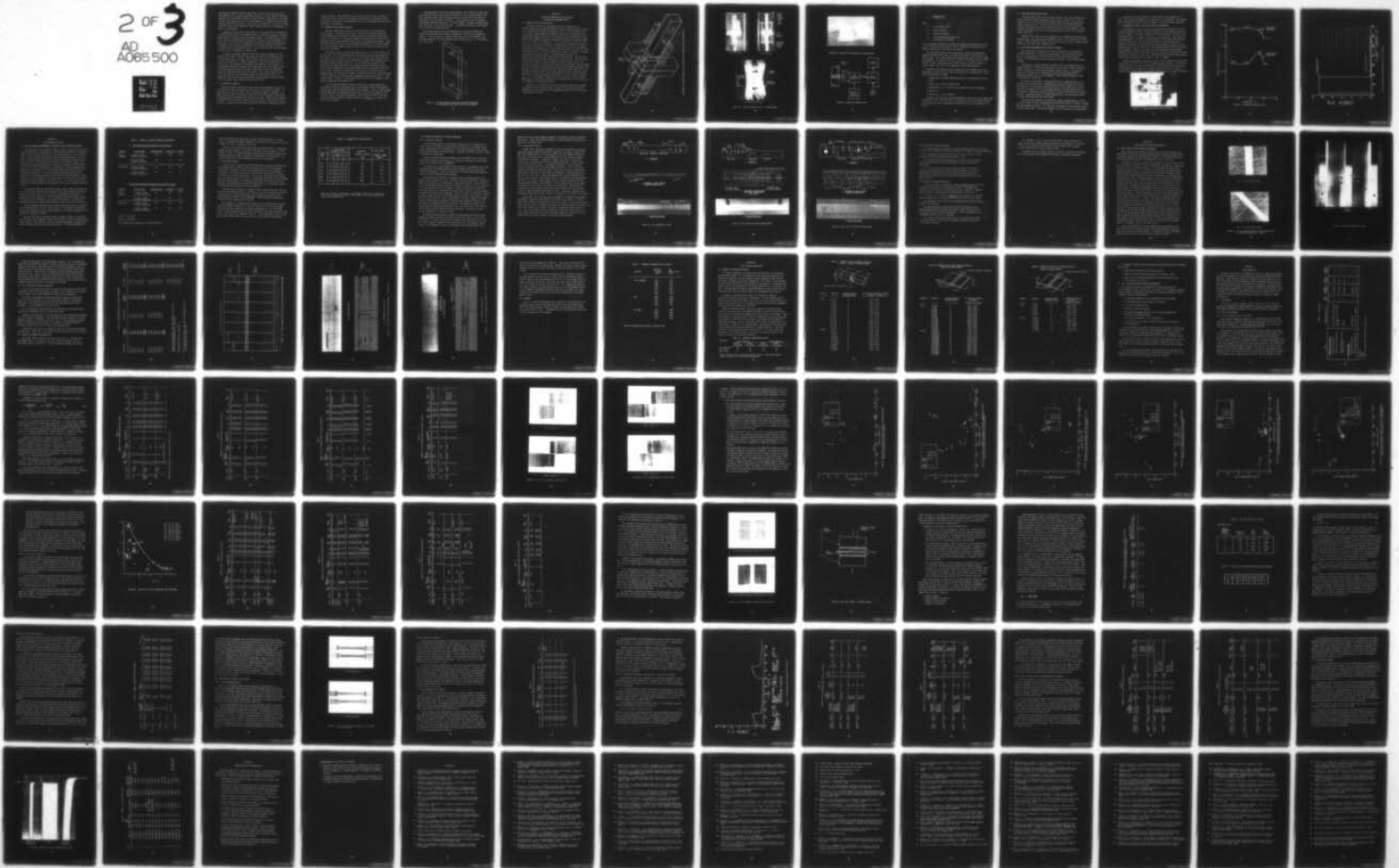
5 500

from Equations (39-42 and 49-51) reveal that a uniform stress state can exist over 90-95% of (a). From such specimens, realistic "in situ" adhesive mechanical properties can be obtained. Moreover, Figures (24-26), reveal that the pertinent variables are aspect ratio (a), the tensile modulus of the adhesive and the adherend (E_A and $\hat{E}$) and the Poisson's ratio (ν_a) of the adhesive. The data is normalized with respect to the adhesive's Young's modulus (E_A) and the displacement (ε) normal to the bondline.

Inspection of the figures reveals that it is the aspect ratio in combination with the Poisson's ratio of the adhesive which influences the spanwise uniformity (edge effect) of adhesive tensile and shear stresses. This edge effect is especially severe as the magnitude of the adhesive's Poisson's ratio approaches 1/2. Additionally, the ratio of the adherend to the adhesive properties combine with the aspect ratio to dictate the magnitude of the normal and shear stresses in the adhesive for a given applied strain. In the limit case ($\hat{E} = E_A$) one attains the solution for a homogeneous, isotropic bar.

In summary, by careful selection of the test specimen geometry one can obtain a near uniform triaxial stress state and impart to the adhesive a controlled shear stress. An aspect ratio of forty (up to 100 if the Poisson's ratio of the adhesive is $\geqslant$ .480) is suggested to maintain the edge effect to within two or three adhesive thicknesses of the adhesive's free surface. As the mechanical properties obtained are average properties of the adhesive constrained between the much stiffer elastic adherends, this minor edge effect should not appreciably effect the test results. Thus, the uniformity of the stress distribution over the bonded surface will enable one to obtain the mechanical linear and nonlinear viscoelastic response effects typical of adhesives at elevated load, temperature and moisture levels.

5.6 VISCOELASTIC EFFECTS

Under sufficiently high strain rates and/or elevated temperature and relative humidity levels, most adhesives will exhibit a viscoelastic response. The applicability of the scarf (butt) joint to attain meaningful viscoelastic response characteristics is possible by selection of a joint geometry within which the adhesive sees an approximately uniform stress state. Routine data reduction techniques[128] are then used to obtain useful design data. This data can easily be used in conjunction with various viscoelastic analytical techniques to design

79

"real structure". One such method is the "quasi-elastic" method, in which at time (t) the elastic moduli are replaced by corresponding viscoelastic relaxation moduli, resulting in the determination of the time dependent adhesive stress response of the component.

5.7 OPTIMUM TEST SPECIMEN SELECTION

Two basic shapes were considered in the selection of the butt and scarf joint geometry: rectangular and circular. The cost of specimen preparation for each geometry was ascertained employing the drill and bonding jigs shown in Figure I-1 of Volume II. Final cost estimates revealed that the circular test specimens would cost approximately twice that of the rectangular geometry. Since analytical difficulties were not anticipated irregardless of the specimen geometry, the rectangular geometry shown in Figure 27 was selected for all butt and scarf joint specimens.

The primary optimum test specimen design objective is that the adhesive normal and shear stress distributions are to be uniform over as large a segment of the span (a) as is realistic. This will tend to minimize the influence of the edge effect seen in Figures 24, 25, enabling one to obtain more accurate and reproducible adhesive moduli properties. As the mechanical properties to be obtained are average properties of the adhesive constrained between the much stiffer elastic adherends, a small edge effects will not appreciably effect the test results. Moreover, the uniformity of the stress distribution over the bonded surface will enable one to handle the mechanical nonlinear response effects typical of adhesives at elevated loads, temperature and moisture levels in a much simpler manner. Finally, it is desirable that the ratio of the apparent to bulk uniaxial modulus be approximately 1.0.

It was assumed that adhesive bondline thicknesses of approximately four and eight mils would be fabricated for all test specimens from which mechanical property data would be obtained throughout this program. Further, it was assumed that an edge effect of approximately ten percent of (s/a) for an adhesive with a Poisson ratio $\leq$ .400 could be tolerated. With these constraints it was possible to determine a realistic aspect ratio (a = 2 $a/t_{adhesive}$ per Figure 27) for our test specimens.

A minimum aspect ratio of forty was selected. This required a plate thickness dimension (2a) of .300 inches for a Poisson's ratio of approximately .400. Such a specimen should limit the edge effects to within two or less adhesive thicknesses from the edges of the joint. If the Poisson's ratio of the adhesive exceeds .400 some redesign for the 8 mil adhesive thickness specimens would have to be made. This was not the case. In addition, the ratio of L/2a should be $\geq$ 4 and h/L $\geq$ 8 (see Figure 27).

The optimum adhesive bond area dimensions for the thick adherend test specimen were obtained earlier and are summarized in Table A-2 of Appendix A, Volume II. Per the results of Table A-2 and Figure A-3 of the appendix, the pertinent dimensions for these specimens were selected to be: h_1 = .750 inches; L_2 = .360 inches.
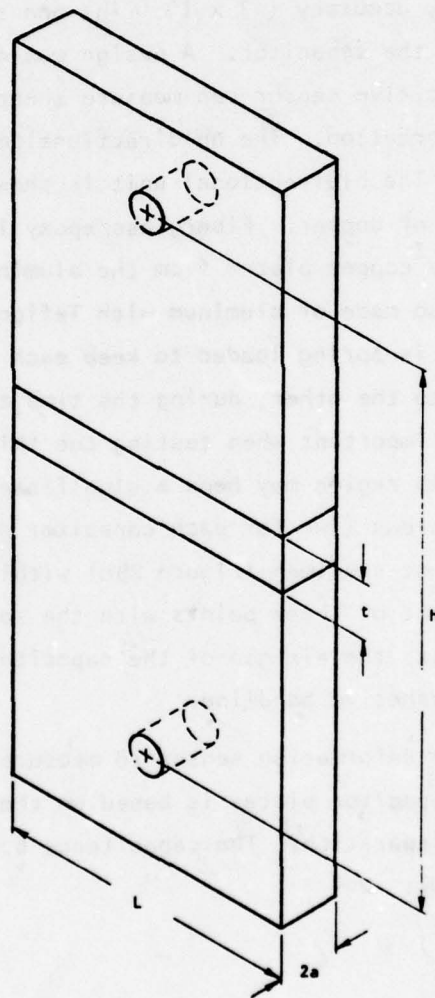
FIGURE 27. TYPICAL GEOMETRIC SHAPE AND PERTINENT DIMENSIONS
OF OPTIMUM BUTT AND SCARF JOINT TEST SPECIMENS.

81

SECTION VI

DESIGN AND FABRICATION OF THE ADHESIVE
DEFORMATION MEASUREMENT DEVICE

6.1 PARALLEL-PLATE CAPACITOR DESIGN

An adhesive deformation measurement sensor was designed with the
intent of measuring the adhesive deformation within ±2.0% as defined in Section
4.2. Further study of potential problems in the use of an air-gap capacitor
vs. an LVDT to measure adhesive deformation resulted in the decision to use a
parallel-plate capacitance device. This decision was motivated mainly by the
superior environmental stability (temperature and humidity), resolution capabi-
lity ($\cong 1.0 \times 10^{-9}$ in), accuracy ($>7 \times 10^{-7}$ in) and sensitivity ($\cong 2.2 \times 10^{-3}$
pf/μ in at 1.0 kHz) of the capacitor. A design was developed whereby one con-
figuration of the capacitive sensor can measure shear, tensile or a combined
shear plus tensile deformation. The unidirectional model of the device is shown
in Figures 28 and 29. The bidirectional unit is shown in Figure 30. The capa-
citive plates are made of copper. Fiberglass/epoxy insulators are
employed to isolate the copper plates from the aluminum body. The anti-plate
rotation guides are also made of aluminum with Teflon rollers. One roller arm
is fixed and the other is spring loaded to keep each capacitor plate from
rotating with respect to the other, during the time the specimen is being loaded.
This can be especially important when testing the thick adherend specimen as the
adherends in the overlap region may bend a significant amount under load. Four
pin point attachment screws (two for each capacitor plate) are used to attach
the capacitor to the test specimen (Figure 29c) within .06 inches of the bond-
line. It is the movement of these points with the specimen, once it deforms
under load, which adjusts the air-gap of the capacitor, which in turn signifies
a displacement in the adhesive bondline.

The ability of the deformation sensor to measure extremely small changes
in separation of the capacitor plates is based on the relationship between
capacitance and plate separation. The capacitance between two parallel plates
is determined as follows:
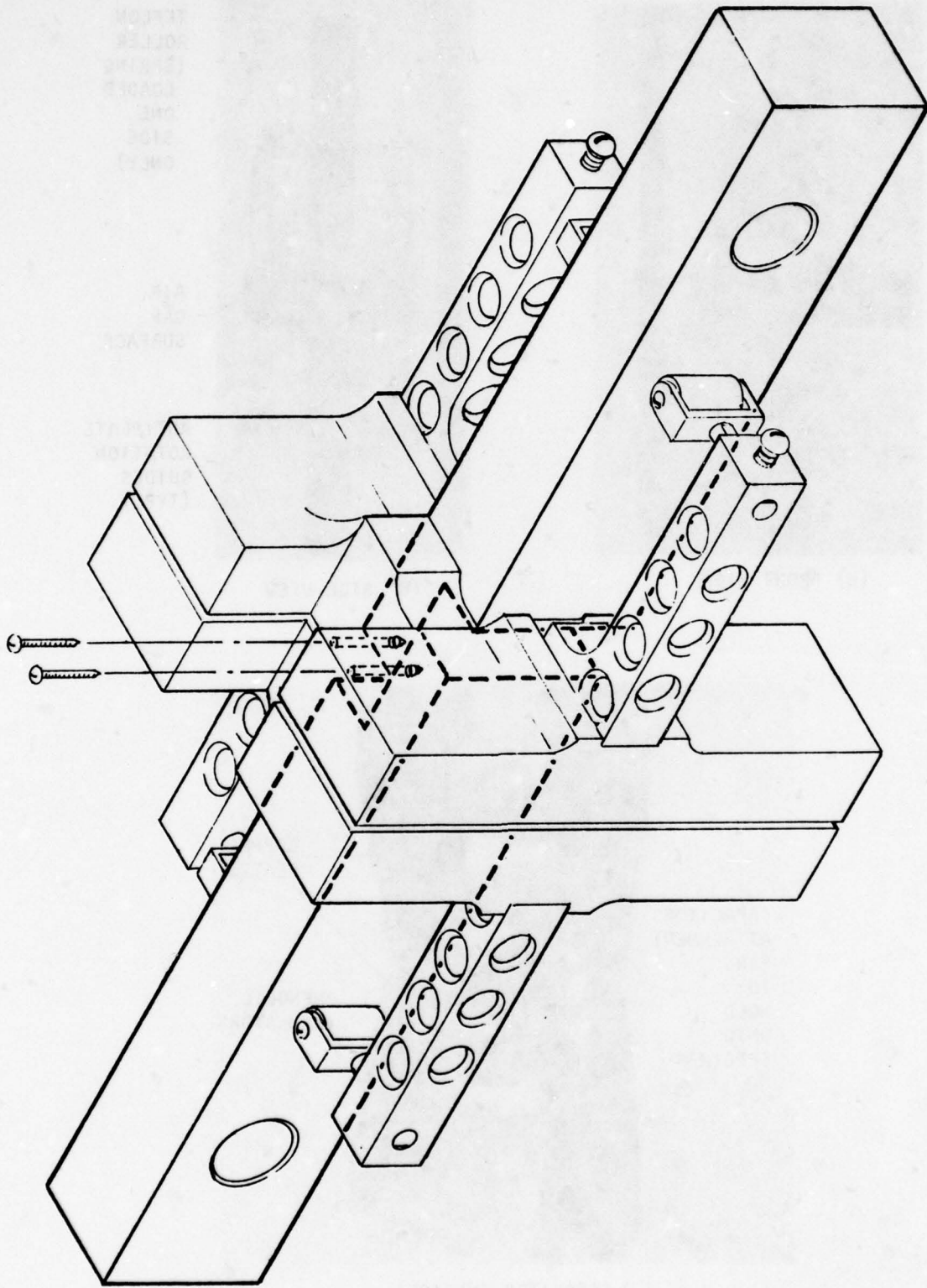
FIGURE 28. SELECTED PARALLEL PLATE CAPACITOR TO MEASURE ADHESIVE DEFORMATION

83
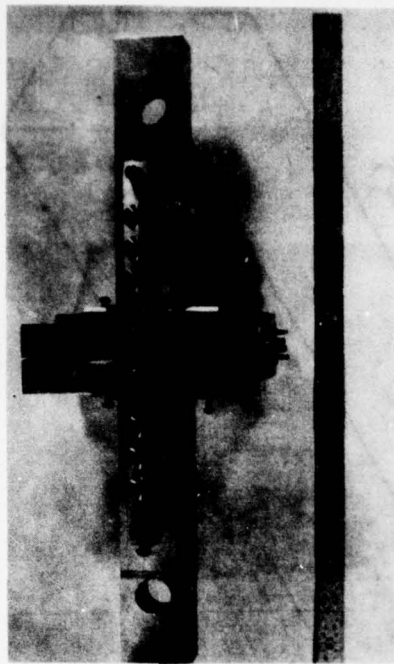
(a) FRONT VIEW
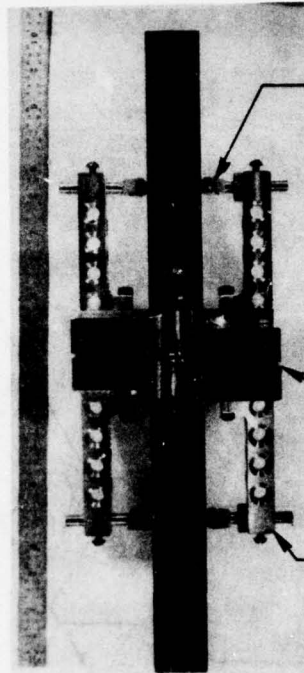
(b) SIDE VIEW

TEFLON
ROLLER
(SPRING
LOADED
ONE
SIDE
ONLY)

AIR
GAP
SURFACE

ANTIPLATE
ROTATION
GUIDES
(TYP.)
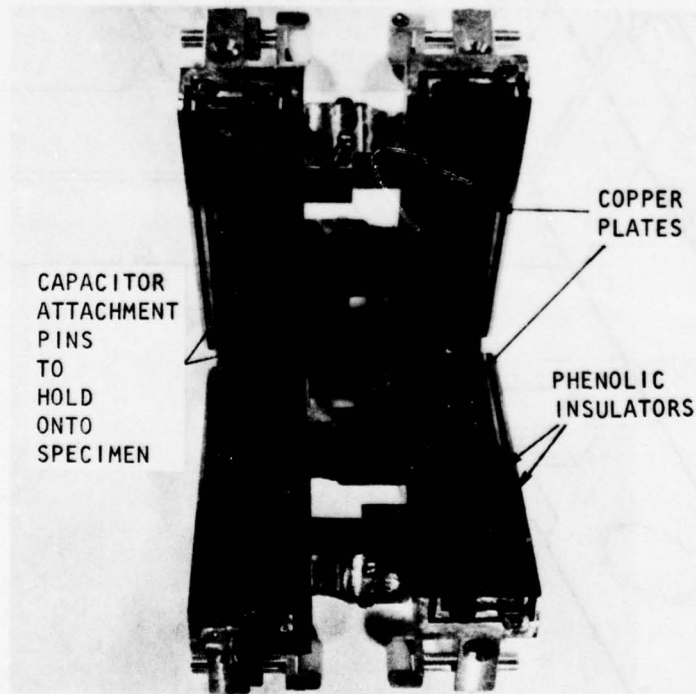
CAPACITOR
ATTACHMENT
PINS
TO
HOLD
ONTO
SPECIMEN

COPPER
PLATES

PHENOLIC
INSULATORS

(c) CAPACITOR SURFACES

FIGURE 29.   PARALLEL-PLATE CAPACITOR - UNIDIRECTIONAL

84
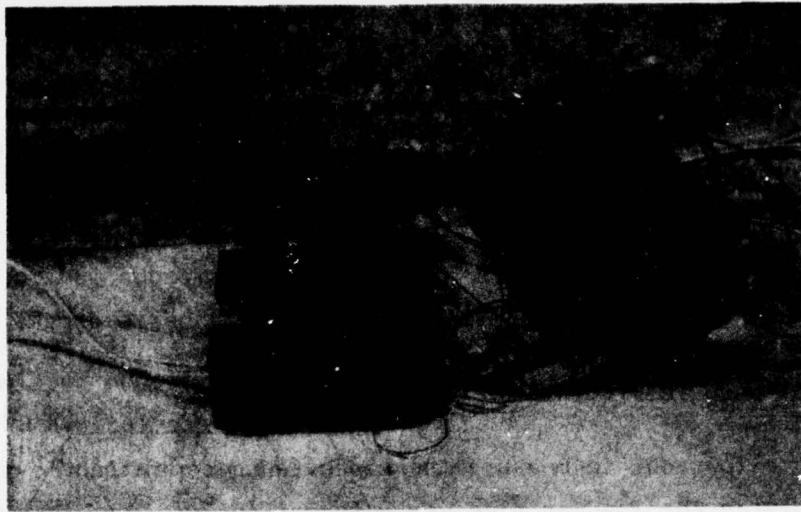
FIGURE 30. PARALLEL PLATE CAPACITOR - BIDIRECTIONAL.
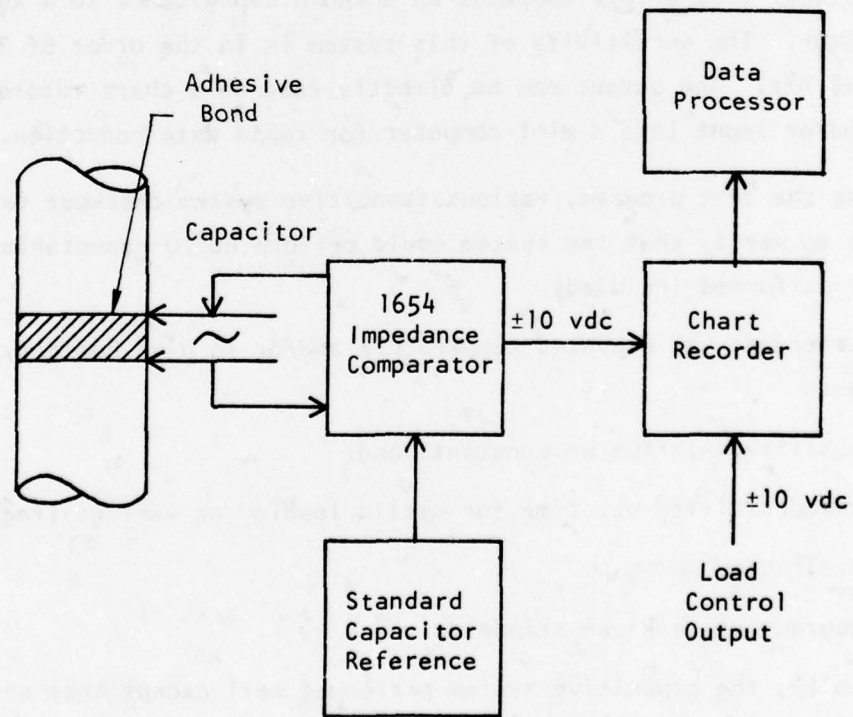
FIGURE 31. CAPACITIVE SENSOR CIRCUIT

85

$$C = \frac{0.255 \, \epsilon'A \, (N-1)}{d}$$

where

A = area of plates (in^2)

N = number of plates

ϵ' = dielectric constant

d = distance separating plates (in)

C = capacitance in picofarads

This relationship allows one to measure the capacitance continuously during a test, thereby giving the load or time vs. deformation information one requires to mechanically characterize the adhesive.

The capacitance sensor circuit (Figure 31), employs a General Radio Comparison Bridge, Model 1654, to evaluate the change in capacitance of the sensor plates. This bridge compares an unknown capacitance to a known standard capacitor. The sensitivity of this system is in the order of 2.2×10^{-3} pf/μin at 1 KHz. The output can be directly read on a chart recorder, x-y plotter and/or input into a mini-computer for rapid data reduction.

During the test program, various capacitive system checkout tests were undertaken to verify that the system could perform up to expectations. Tests which were performed included:

o Performance at elevated temperature and/or in high humidity environments

o Stability vs. time at constant load

o Reproducibility vs. time for cyclic loading at various frequencies

o Sensitivity

o Accuracy vs. a known standard.

Initially, the capacitive system performed well except that stray capacitance entered the system. This was due to the fact that all wiring was not shielded. This problem was readily corrected by shielding all wire in the capacitive circuitry.

86

6.2 CAPACITANCE VERIFICATION TESTS

A bidirectional and two unidirectional capacitors were used to obtain the shear, tensile and biaxial mechanical property data presented in this report. Capacitor static verification tests were performed at various temperature and relative humidity levels. Results, obtained using a solid 7075-T6 aluminum specimen .179 inches thick by .903 inches wide showed system repeatability over several load-unload cycles within one pico-farad with a sensitivity of approximately .007 pf/μin.

Reproducibility tests were also conducted using a bonded thick adherend lap shear specimen. The results were reproducible within ± 10% irregardless of temperature (< 180°F) humidity (< 95%) cyclic load rate (up to 3 cps), or constant load-unload test time (15 minute constant load).

6.3 CAPACITANCE MEASUREMENT DEVICE HUMIDITY PROBLEM

During the tests to ascertain the time wise stability of the capacitors at 180°F and 95% R.H., an instability was observed in the capacitance system due to the susceptibility of the original dielectric material to moisture ingress. This eventually led to the capacitor shorting. A minor design change was made.

The change was required because the phenolic material absorbed water and became conductive. Initial (dry) resistance from the copper contact through the dielectric material to the aluminum contacts ranged from 2.5 - 4.5 giga-ohms. These values dropped (and quite normally should) after extended humidity-temperature exposure down to 100 kilo-ohms. At this value, the guard voltage of the capacitor shorted out.

An empirical reevaluation of candidate materials produced a choice of two materials that could be used in combination to replace the phenolic insulator. The selection of an epoxy-fiberglass sheet which is edge sealed with a polysulfide barrier appeared to solve the adverse dielectric response under high humidity exposure. The epoxy-fiberglass material is Hexcel F-161 with 181 fiberglass which was specially produced by Vought manufacturing. The polysulfide sealant is Proseal 898, obtained from Coast Proseal.

The phenolic was replaced using fiberglass and all exposed edges were under cut 0.050 inches in order to accommodate the polysulfide barrier. Assembly followed the same procedure as before. The fiberglass was bonded to the aluminum and sealed with the Proseal 898. The copper was bonded to the fiberglass with EC 3445 epoxy.

87

The modified device was placed in a 180°F, 95% R.H. environment for 72 hours. The resistance changed from 3.5 giga-ohms to 1.3 mega-ohms. This seemed to be an acceptable change so testing resumed. No further problems developed.

6.4 EXTENSOMETER FOR BULK SPECIMEN DEFORMATION MEASUREMENT

An extensometer, shown in Figure 32 (available from ATC-IR&D) was used to accurately measure bulk tensile specimen extension in high temperature and humidity environments. Two LVDT's (Schaveitz's GCA-121-050 series) are used in the extensometer which is clamped by spring force to the specimen. Gage length for the extensometer is two inches. The aluminum parts were chromic acid anodized to minimize corrosion. The extensometer weighs less than 440 grams and is balanced. Calibration data and curves for two extensometer systems at various temperatures are shown in Figure 33. The calibration was performed by attaching the extensometer and two strain gages to an aluminum coupon under constant temperature then comparing the output data after loading and unloading the aluminum coupon to 12,000 psi three times. Room temperature calibration measurements indicate that the accuracy of the LVDT is within ± .000002".

Long-term extensometer stability was also studied through three cycle creep-recovery tests (one hour per cycle) on aluminum coupon specimens. A forty-five minute soak time to bring the extensometer to environmental equilibrium was required before start of each test. A typical third cycle result is shown in Figure 34 for a 75°F, 55% R.H. environment. We consider this result satisfactory.
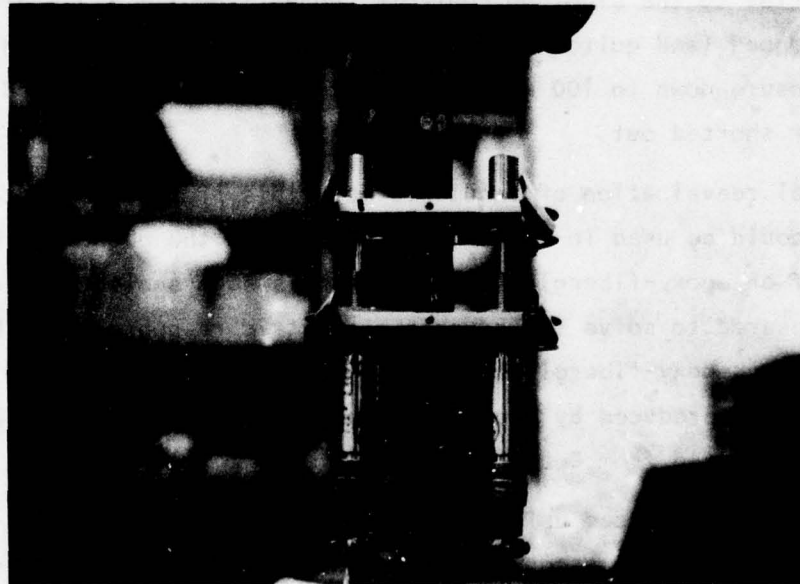
FIGURE 32. EXTENSOMETER SETUP ON TEST SPECIMEN.
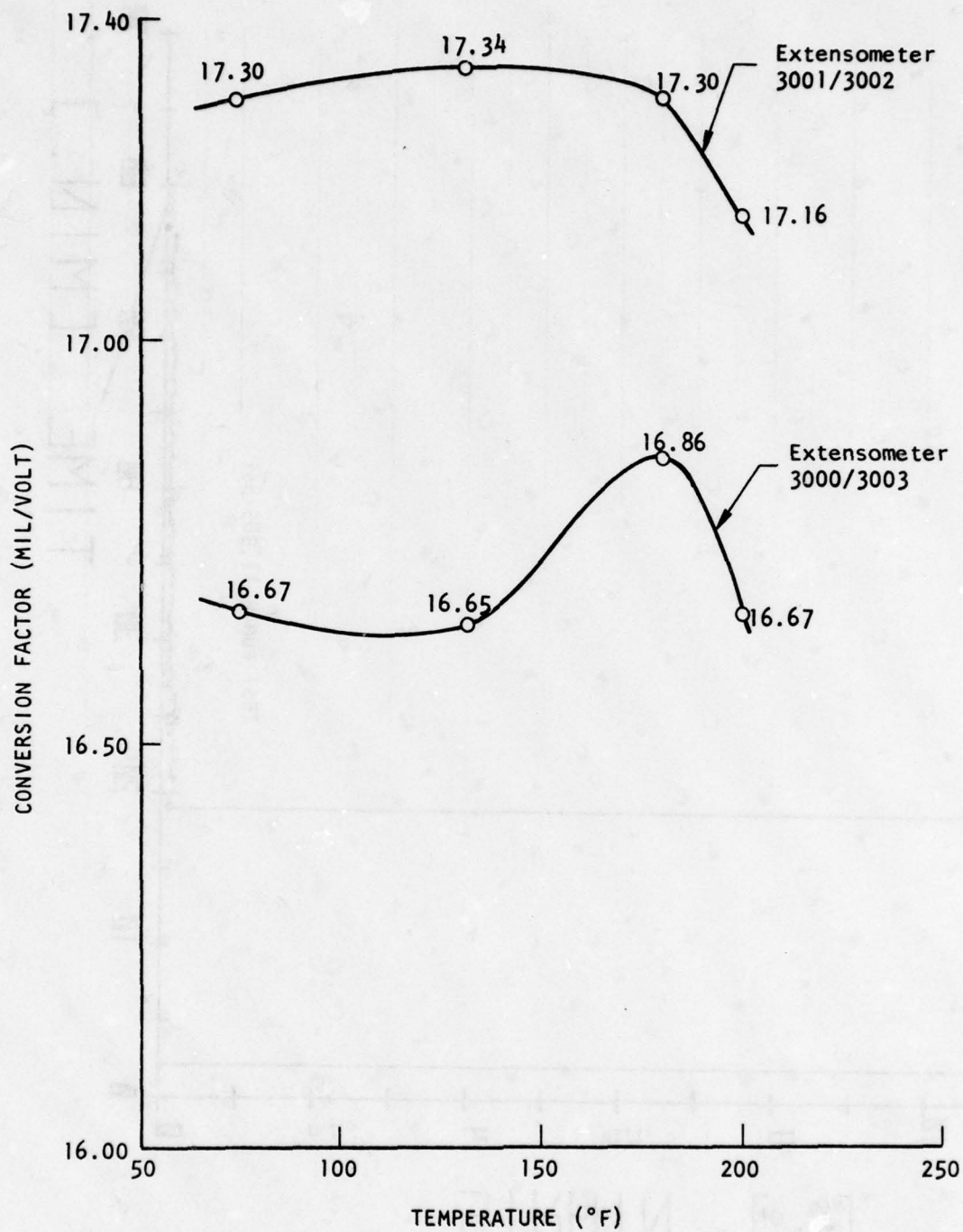
FIGURE 33. EXTENSOMETER CHARACTERISTICS
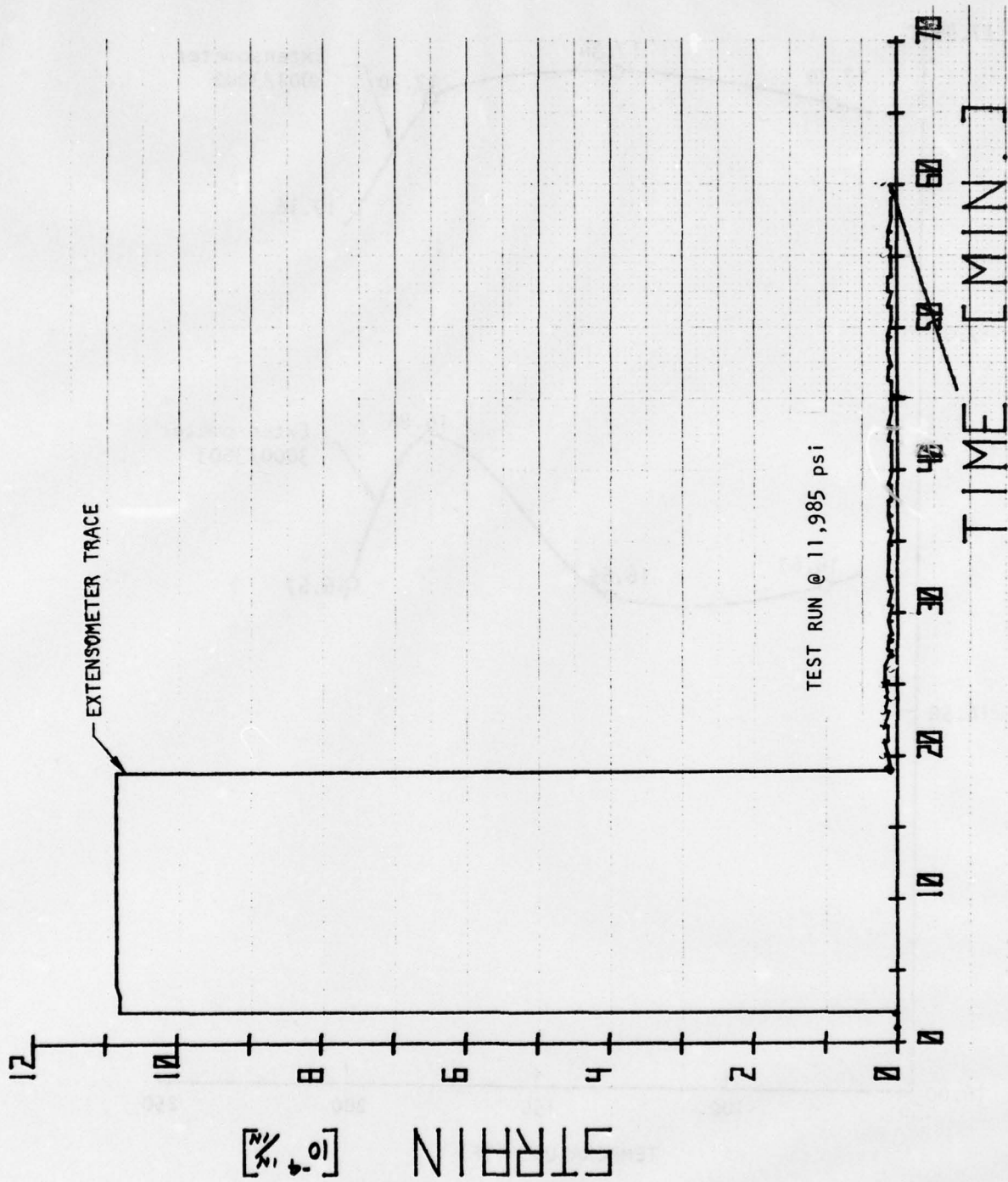
FIGURE 34. ALUMINUM CREEP-RECOVERY TEST AT 75% F AND 55% R.H.

90

SECTION VII

TEST METHODOLOGY FACTORS

7.1 SURFACE ROUGHNESS MEASUREMENTS OF ALUMINUM USED FOR ADHESIVE BONDING

An experiment was performed in order to define the nominal value of sur-
face roughness and its consistency for those aluminum surfaces to be bonded to-
gether to form the test specimens for this research project. The instrument
used in these determinations was the Mitutoyo Surftest-B apparatus. The sur-
faces to be measured were those of bare aluminum 7075-T7651 which were ground
with an end mill in two different directions at two different speeds. The
finished surfaces were representative of those to be bonded in thick adherend,
butt and scarf joint test geometries. Measurement of surface roughness was
taken, once the surfaces had been ground, to substantiate the consistency of
the machining operation. The surface roughness was again measured after
anodization was completed and again after the primer had been applied. Anodi-
zation was with the phosphoric acid process and priming was done with American
Cyanamid's BR-127 chromated anti-corrosion primer. The values reported here
represent an average range for each condition, and are not intended as absolute
values.

Two aluminum blocks were machined at cutter speeds of 400 surface feet per
min. Surfaces were machined with an end mill that represented the faying sur-
faces of lap shear, butt and scarf joint test specimens at feed rates of 2
inches/min and at 4 inches/min. The thick adherend lap shear surface reflects
the surface finish obtained using the side of the end mill. The butt-scarf
specimen reflects the surface finish obtained by using the end of the end mill.

Surface roughness measurements were made by moving the stylus (a) parallel,
and (b) perpendicular to the mill feed direction. An arithmetic (centerline)
average was calculated for each surface between the two sets of readings and the
results are presented in Table 8.

The slow feed rate (2 inches/min) gave the smooth surfaces. At the high
feed rate the surface roughness readings taken parallel to the mill travel direc-
tion increased. This effect carried over through the phosphoric anodize treat-
ment but was obscured when the primer was applied. The surface roughness for

TABLE 8. SUMMARY OF SURFACE ROUGHNESS MEASUREMENTS

a. **For Surfaces Readings Parallel to Mill Travel**

Surface	Travel Speed	Machined Only	&	Anodized	&	Primed
Thick Adherend	2 in/min. @ 400 Surface Feet/Minute	35*		46		42
	4 in/min. @ 400 Surface Feet/Minute	67		72		40
Butt-Scarf	2 in/min. @ 400 Surface Feet/Minute	43		32		30
	4 in/min. @ 400 Surface Feet/Minute	64		49		41

b. **For Surfaces Readings Perpendicular to End Mill Travel**

Surface	Travel Speed	Machined Only	&	Anodized	&	Primed
Thick Adherend	2 in/min. @ 400 Surface Feet/Minute	37		40		38
	4 in/min. @ 400 Surface Feet/Minute	47		49		41
Butt-Scarf	2 in/min. @ 400 Surface Feet/Minute	36		38		32
	4 in/min. @ 400 Surface Feet/Minute	43		45		36

Cutoff = .03 inches

Stroke = 2.00 inches

*All readings are average values in microinch/inch.

the primed surfaces was consistently between (30-40 microinches). In most cases, it appears that surface roughness is incrased with the anodizing step and a smoother surface is regained with priming.

Results of this brief study would seem to substantiate that a reproducible bonding surface, whether it be primed or unprimed, can be attained. For this program in which a 2 inch/minute travel speed was used, anodized surfaces to be bonded should have a surface roughness of approximately 40 microinches. For primed surfaces this should average approximately 35 microinches.

7.2 SPECIMEN ALIGNMENT

Uniaxial tensile testing can be performed quickly and easily but specimen misalignment and its effect on the test results can easily go unrecognized. Misalignment introduces a local stress concentration in the test specimen. It is especially critical at low strain levels and can lead to errors in excess of 20% of the true axial strain level. This in turn can falsely alter fatigue life, and stress rupture life results. Misalignment may be due to loose threads, machining imperfections in the couplings joining the test fixture to the test specimen, top and bottom grip centerline eccentricity or the specimen's centerline being offset from that of the grip centerline.

Alignment may be attained in a number of ways including the use of rod end bearings, nonthreaded couplings, a spherical ball and seat, universal joints and fluid couplings. The rod end bearings, such as shown in the Adhesive Test Specifications of Volume II are recommended. These bearings are commercially available and are inexpensive and reliable.

The alignment of a loading system fitted with rod end bearings was checked using a rectangular aluminum ($E = 10.3 \times 10^6$ psi) bar with four strain gages, one on each surface, bonded to the specimen approximately at its mid-height. A tensile load was applied and the strain recorded for each gage at discrete load levels. The results are presented in Table 9. They substantiate that an alignment accuracy within 4.8% of true axial strain can be routinely anticipated.

93

TABLE 9. ALIGNMENT TEST FIXTURE RESULTS

TENSILE LOAD (LB)	STRAIN GAGE READING $\times 10^{-6}$ in/in Gage*				THEORETICAL READING $\times 10^{6}$ in/in $\varepsilon = \dfrac{P}{AE}$	MAX. ERROR % $\dfrac{\varepsilon_{THEOR.} - \varepsilon_{GAGE}}{\varepsilon_{THEOR.}}$
	1	2	3	4		
500	130	130	130	130	132	0
1056	270	280	290	280	280	±3.5
2160	550	580	590	570	570	±3.5
3250	830	880	890	860	860	±3.5
4400	1110	1180	1200	1150	1160	-4.3
5550	1390	1480	1510	1450	1460	-4.8

*Gages were located at mid-height of rectangular aluminum bar of 7075-T6 of cross-sectional dimensions 1.22" x .30". Gages 1 and 3 were opposite each other as were gages 2 and 4.

94

7.3 DETECTION OF DEFECTS IN ADHESIVE BONDLINES

7.3.1 Inspection Methods

Once a bonded specimen is fabricated, assurance that the bonded area is free of voids, air bubbles and associated imperfections is of paramount importance. Bond defects will contribute to low strength measurement, data scatter and unreliable adhesive characterization. Therefore, accurate, sensitive inspection methods are important.

Several candidate methods applicable to thick adherend joints, were evaluated and discussed in Section 3.5.3. Of these two techniques, neutron radiography and ultrasonics were recommended.

The capability of each method to detect defects in the adhesive were incorporated within the adhesive bondlines of thick adherend lap, butt and scarf joint test specimens. A variety of materials which might offer good detection using the two NDI techniques were employed.

Some materials are more apt to be detected by one technique better than another, such as metals for x-ray. Materials originally proposed for simulating defects in the bondline included metals, porous and non-porous organic materials (with high hydrogen content) and finally inorganic, non metallic, porous materials. Limits were placed on the final number of selections made simply by choosing only those materials or techniques which might offer at least a limited prospect for detection using neutron radiography. Materials finally selected were aluminum planchets, copper and steel wire, glass bubbles, milipore filter material, human hair and nylon cloth with a mylar tape backing. Void sizes ranged from 0.0035 inches to 0.375 inches in diameter so that the lower detection limits of each NDI inspection technique would be ascertained. The specimens prepared using these techniques were thick adherend lap, butt, and scarf joints, thus offering a challenge for correct angle orientation techniques in detection by either neutron radiography or ultrasonic C-scan.

The adhesive used was American Cyanamid FM-73-M epoxy with BR-127 primer. Attempts were made to maintain the bondline thickness as close to 0.010 inches as possible. All defects, regardless of diameter, were maintained at less than this .010" thickness. Spaces for the defects were cut in the adhesive during lay-up. This prevented "flow-out" of the defects during squeeze down of the

adhesive and also allowed adequate movement of the adhesive around the defects during cure. Curing was accomplished using a standard (ATC-built) bonding jig and the 50 ton Wabash press.

7.3.2 Experimental Results

Figures (35a - 37a) show a schematic of each of the different joints and the various defect materials with their respective size ranges. Figures 35b-37b) show reproductions of C-scan recordings of the thick adherend lap joint, butt joint, and scarf joint at 20 dB, obtained with the ultrasonic (through transmission) techniques. Inspection of these scans reveals a "wash-out" of the scan at the lap step of the thick adherend specimen. A loss of detection in the area of the step is considered a draw-back in using ultrasonic C-scan in conjunction with the thick adherend lap joints. This is not a problem with the other two types of joints. Review of the figures revealed that voids down to the order of .125 inches were detectable. No detection was evident for any size of wire. Angle beam transmission C-scan was employed for the butt joint specimen. The general effect is to spread out the area examined. The result is to give a "double image" with the transmission beam reflecting from the bottom surface of the adherend. This in effect gives a mirror image on reception as can be seen from inspection of Figure 36b. Maximum energy transmission and the reception sensitivity are arrived at only with multiple trials for each different configuration of joint. The energy reception level, therefore, (marked on each scan in dB) is not necessarily the same for all joints.

Figures (35c - 37c) show the detection capability achievable using neutron radiography. Comparing these figures with those of the schematic in Figures (35a - 37a) indicates the relative position of each defect. As can be seen from these pictures, small void defects associated with the glass bubble inclusions, with the nylon cloth and with the metal inclusions are measurable down to the 5 mil size. Loss of void definition for the smaller voids on the positive prints is evident when compared to the original radiograph negatives, especially for the 0.0055 inch wire, which is clearly visible only on the negative.

96
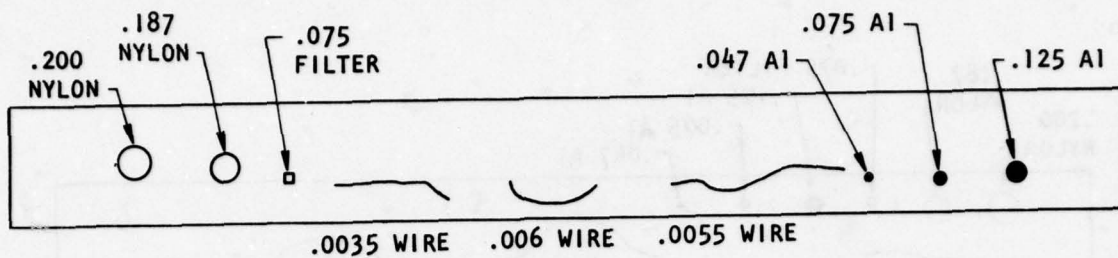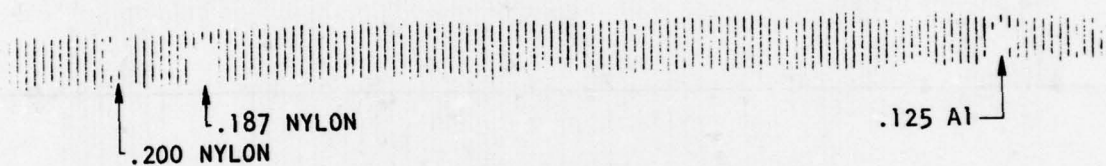
a) **SCHEMATIC**

b) **ULTRASONIC C-SCAN (20 dB)**
   (THROUGH TRANSMISSION)
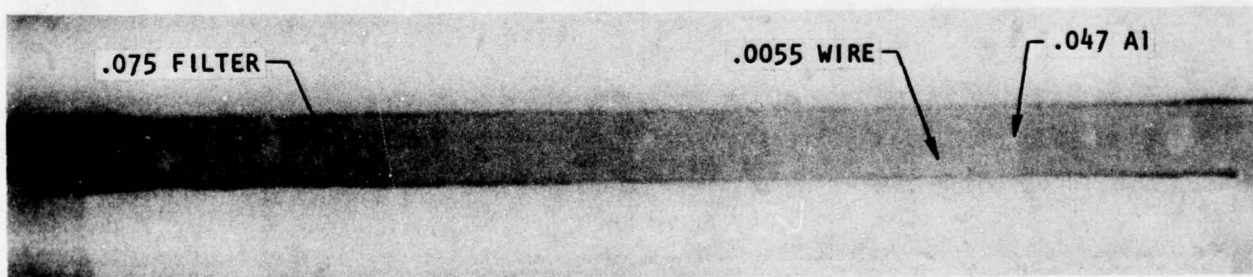
c) **NEUTRON RADIOGRAPH**

FIGURE 35. THICK ADHEREND LAP JOINT

.200 NYLON   .187 NYLON   .075 FILTER   .125 Al   .075 Al   .047 Al

.0055 WIRE   .0035 WIRE   .006 WIRE

a) SCHEMATIC

MIRROR IMAGE EITHER SIDE OF LINE

ALIGNMENT HOLE IN THICK ADHEREND   ALIGNMENT HOLE IN THICK ADHEREND

b) ULTRASONIC C-SCAN (20 dB)
ANGLE BEAM TRANSMISSION
(40° ANGLE)

.047 ALUMINUM
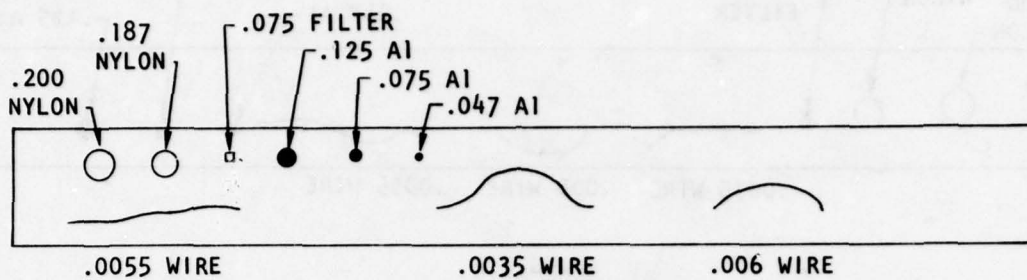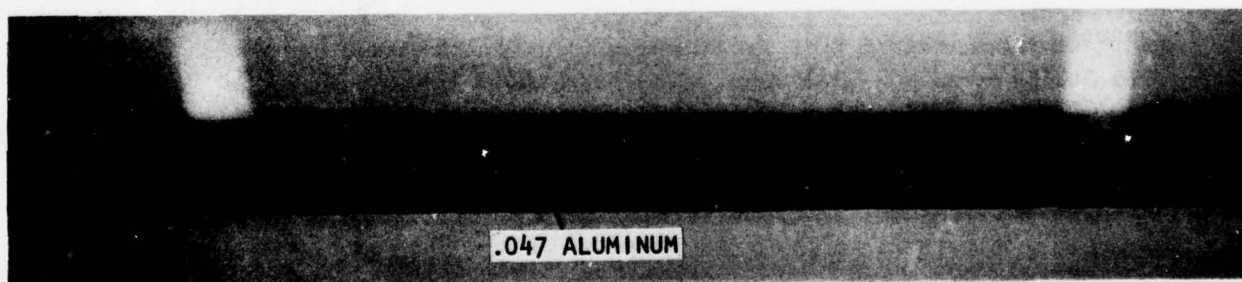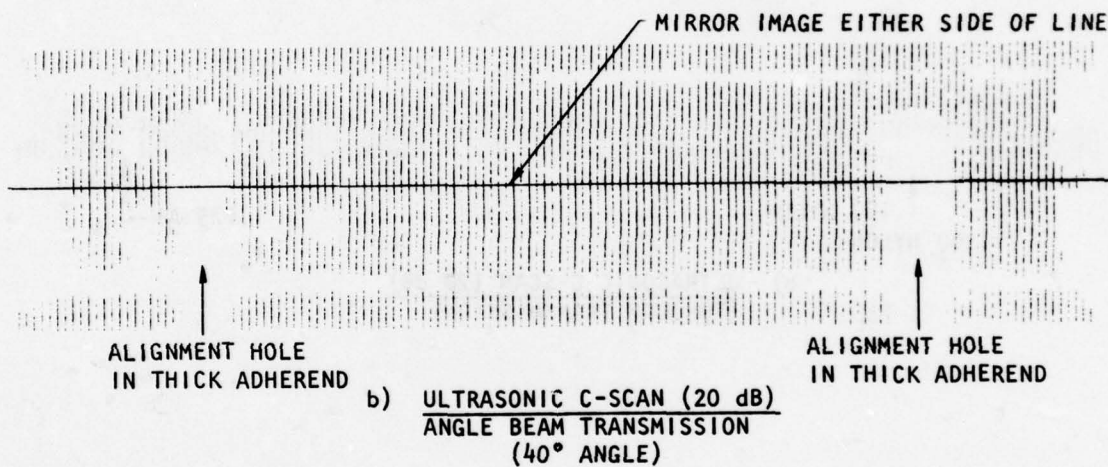
c) NEUTRON RADIOGRAPH

FIGURE 36. BUTT JOINT (45° BEAM INCIDENCE ANGLE)

98
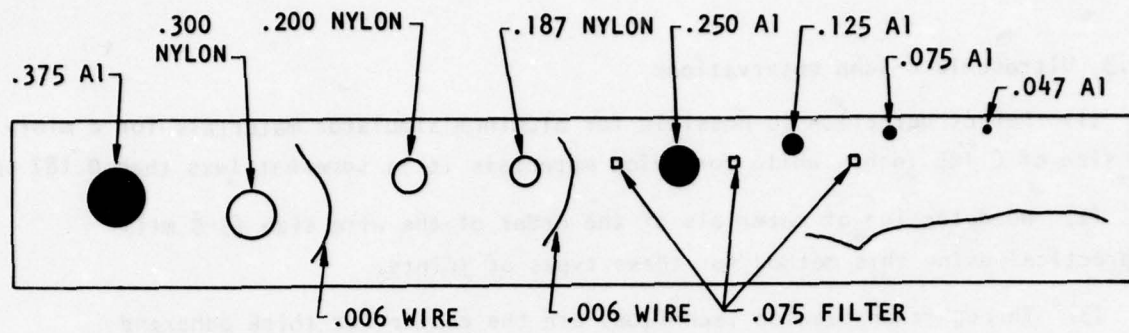
a) SCHEMATIC
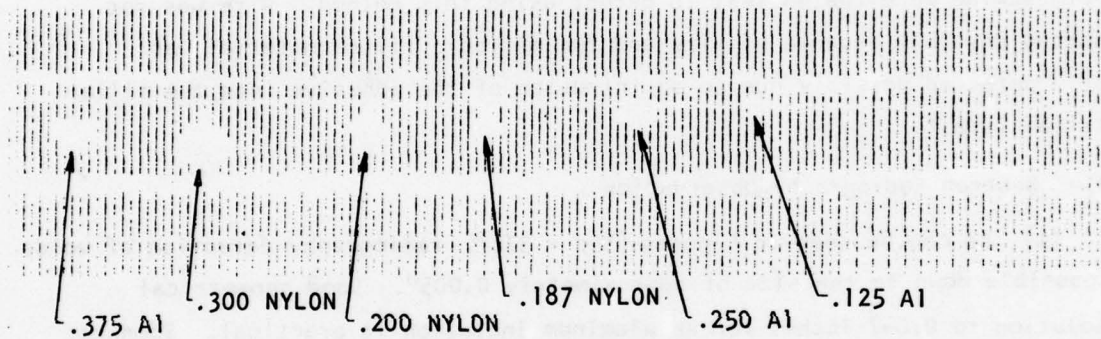
b) ULTRASONIC C-SCAN (20 dB)
(THROUGH TRANSMISSION)
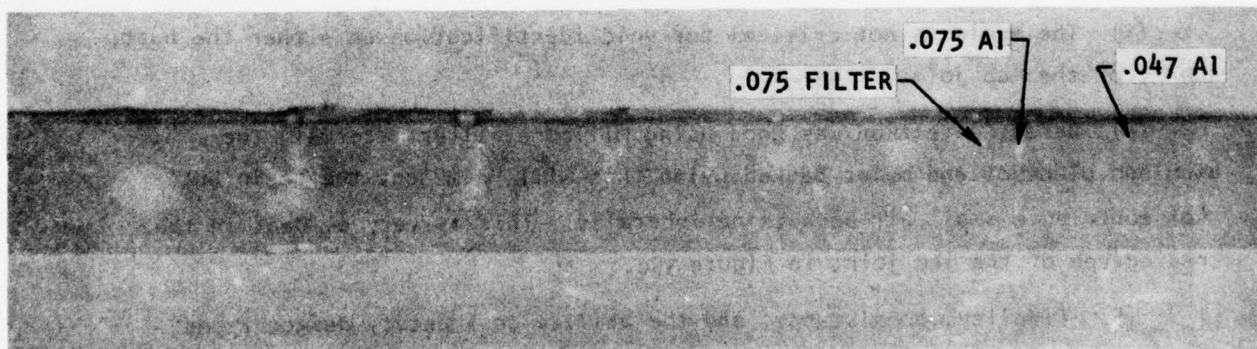
c) NEUTRON RADIOGRAPH

FIGURE 37. SCARF JOINT (45° BEAM INCIDENCE ANGLE)

99

7.3.3 Ultrasonic C-Scan Observations

(1) Defect detection is possible for aluminum simulator materials for a minimum size of 0.125 inches while for nylon materials it is somewhat less than 0.187 inches.

(2) No detection of materials of the order of the wire size (3-5 mil) is practical using this method for these types of joints.

(3) Through-transmission techniques are the choice for thick adherend bonds although angle beam transmission displays the scarf and butt joints satisfactorily.

(4) Of the types of defects used, aluminum planchet and nylon with mylar backing were the easiest to detect using this method. Wire was not detected possibly because of size and the milipore filter material was poorly detected possibly due to an intrusion of the adhesive into the filler material itself.

7.3.4 Neutron Radiography Observation

(1) As can be seen in Figures (35c - 37c), radiography detection of voids is possible down to the size of approximately 0.005". Good geometrical resolution to 0.047 inches for an aluminum inclusion is practical. Somewhat poorer resolution is obtained for the milipore filter and the nylon.

(2) Angle is not critical for <u>resolving</u> voids, although a very good job can be obtained with a very slight angle for both the scarf and butt joints.

(3) The angle is not critical for void identification on either the butt, scarf, or the lap joint.

(4) Defect detection was good using milipore filter material, the aluminum planchet and mylar backed nylon that will "dam" out the resin but not contribute small air pockets peripherally. This is very evident in the radiograph of the lap joint in Figure 35c.

(5) Fidelity, consistency, and the ability to identify defect types in these bondlines are much better with neutron radiography than they are with C-scan ultrasonics.

(6) Although it is not true for the ultrasonic C-scan technique, detection of the very smallest defects using neutron radiography is limited only by the source strength and the distance from the source; smaller objects could be resolved with a higher intensity source.

Throughout this test program, detection of voids in the adhesive bondlines of all test specimens was attempted using neutron radiographic techniques.

SECTION VIII

VERIFICATION OF FABRICATION PROCEDURE

8.1 PANEL FABRICATION AND BONDLINE MEASUREMENT

Three thick adherend test panels and two butt and scarf joint panels were fabricated to verify that an adequate adhesive bonding procedure had been established per the adhesive's specification in Volume II. All adherend material was 3/4" thick 7075-T651 aluminum. The adhesive was FM-73M in all cases.

Subsequent to bonding, the panels were prepared for cutting into the individual test pieces per Section 1.5.3 of the fabrication specification. Panels were cut into six one inch wide test pieces first with the band saw and were then smooth cut using an end mill. Finished cuts of each panel were macroscopically smooth although microscopic irregularities with respect to the adhesive-metal interface offer some challenge in the choice of techniques for accurately measuring bondline widths. The maximum height of metal intrusion into the bondline averaged less than .0002". Figure 38 shows the typical uniformity of bondline thickness achieved, across the full panel width using the fabrication jig designed at ATC. Although polishing of each bondline is to be avoided, it was found necessary for technique development to give a buff finish to one specimen each of both the butt and scarf joints, using fine grit sandpaper and finally a polishing alumina. It was not necessary in the case of the thick adherend lap joints since the bondline direction of these joints lie along the direction of the cut made by the end mill. Irregular lines along the adhesive metal interface for the butt and scarf joints were on only one side of the bondline and this according to the direction of movement of the end mill's bit. Measurements were made at two points on each milled side of each joint, 1/3 of the distance in from the opposite edges (Figure 39) for the butt and scarf joints. Six readings for the thick adherend specimen were obtained. Bondline measurements of the top and bottom surfaces (non-milled) of the butt and scarf joints were not made since the bondline erroneously appeared to have dimensions 2-3 times greater than the milled adhesive sides. This was an anomalous result of the normally present fillet and possibly due to the machining of the bonded panels. It occupied a depth of less than 2 mils.

Bondline measurement profiles were compiled from data obtained using a Bausch and Lomb Filar micrometer mounted on the scope attached to the Wilson Tukon Tester which has a microton stage. It exceeds the accuracy requirement specified in each of the test specifications, namely .001 inches.
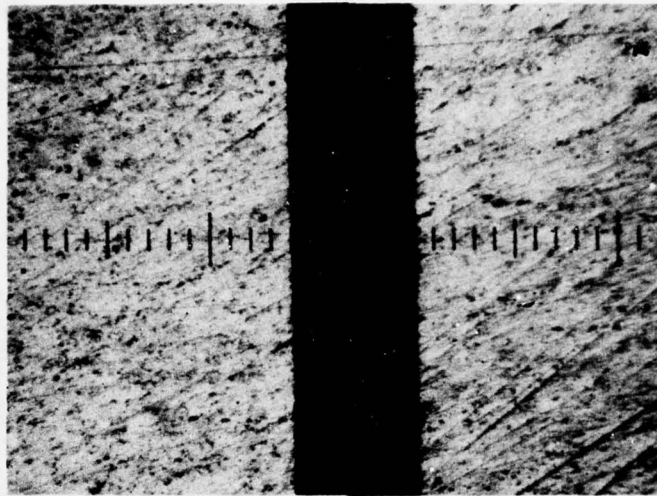
(a) 7 MIL LAP JOINT (100X)

(b) 4 MIL SCARF JOINT (100X)

FIGURE 38. TYPICAL UNIFORM BONDLINES ACHIEVED USING THE
ATC DESIGNED FABRICATION FIXTURE

103
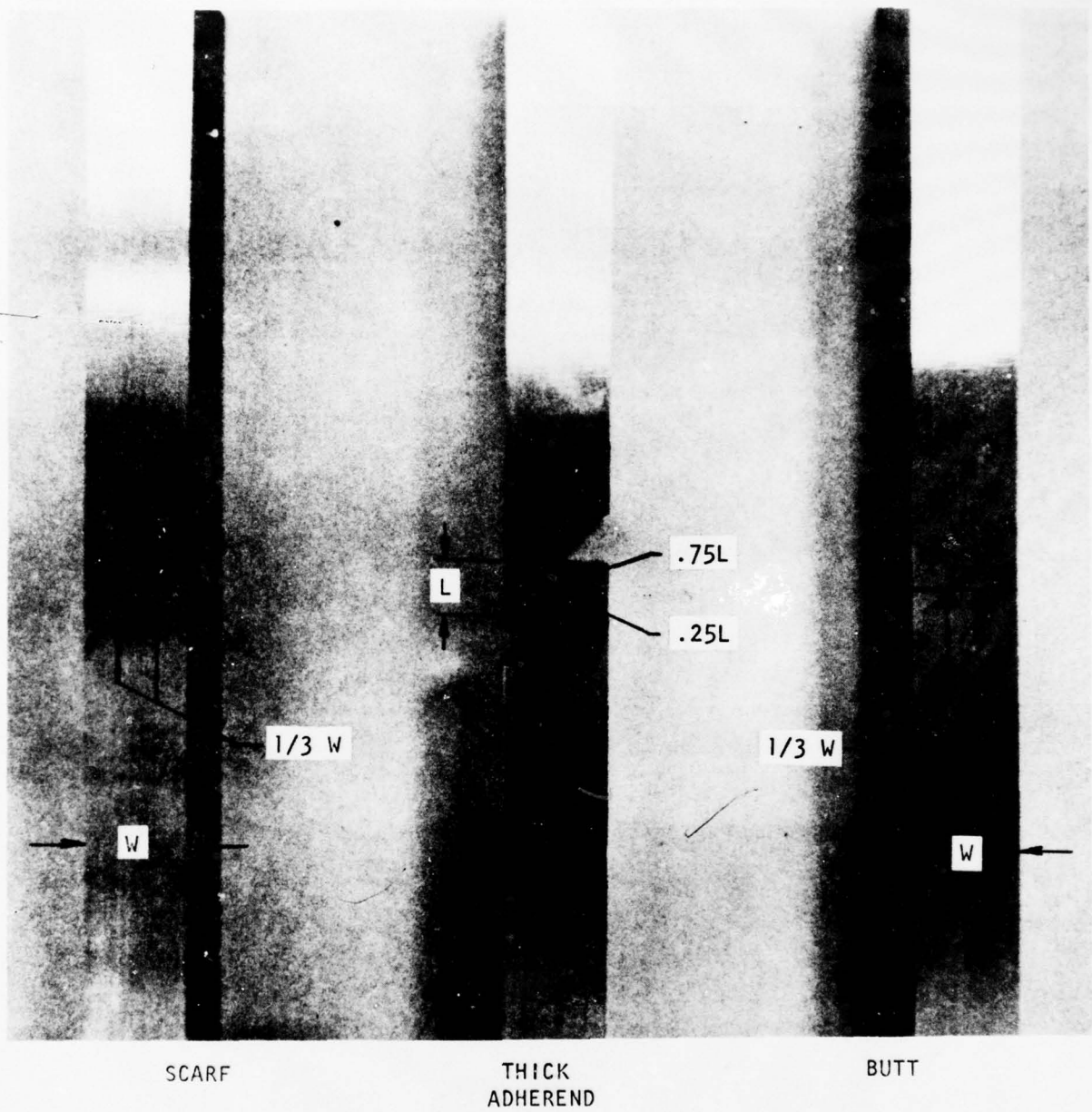
FIGURE 39. BONDLINE MEASUREMENT POINTS.

104

Using the fabrication fixture described in Section 1.5.2 of the Adhesive Fabrication Specification, (Volume II) bondline thickness for the thick adherend panels of .004 inches, .007 inches, and .010 inches were attempted. Only the .004 inch and .010 inch adhesive thicknesses were fabricated for both the butt and scarf joints. Table 10 shows the measured bondline thicknesses obtained from the one inch wide test pieces cut from each panel (Figure 40) for each of the different type joints. The results reveal that by using the fabrication fixture designed by ATC, prescribed boneline thicknesses, of a minimum variation throughout the test panel can be consistently fabricated.

8.2 NDI INSPECTION OF ADHESIVE SPECIMENS

Prior to cutting the test panels into one-inch wide specimens, both neutron radiographic and through transmission ultrasonic C-scan inspection of the bond-lines was made. The through transmission frequency was 5 mega-hertz.

The neutron radiographic technique employed a portable californium-252 source (~2.2 mg) and SR-54 film. The neutron beam's angle of incidence was 90 degrees to the adhesive surface for the thick adherend and scarf joint specimens. It was 45 degrees for the butt joint.

For the ultrasonic C-scan technique, the frequency was optimized and the optimum value accompanies each of the enclosed figures.

Generally, the bondline's clarity and definition were much improved through the use of neutron radiography. Void free bondlines were achieved in all thick adherend specimens. Inspection of the butt joint neutron radiographs revealed several isolated voids of from .003 to .013 inches in diameter (Figure 41). Ultrasonic C-scan results did not reveal these isolated voids.

Inspection of the scarf joint specimens (Figure 42) revealed three possible isolated voids. Again, the C-scan results were not able to verify this finding.

8.3 DESTRUCTIVE GOODNESS-OF-BOND TESTS

Quasistatic tests to failure were run on two of the six specimens from each bonded panel. The stroke rate was .012 inches per minute. The test environment was 80°F and 45% R.H. A total of fourteen specimens were tested

105

TABLE 10. AVERAGE BONDLINE THICKNESS MEASUREMENTS

BUTT JOINT	AVERAGE* (Inches)	SCARF JOINT	AVERAGE* (Inches)	LAP JOINT	AVERAGE* (Inches)
B-4-1***	.0057	S-4-1	.0039	L-4-1	.0047
B-4-2	.0054	S-4-2	.0039	L-4-2	.0046
B-4-3	.0055	S-4-3	.0042	L-4-3	.0050
B-4-4	.0057	S-4-4	.0044	L-4-4	.0051
B-4-5	.0055	S-4-5	.0045	L-4-5	.0050
B-4-6	.0058	S-4-6	.0043	L-4-6	.0050
	.0004**		.0006**		.0005**
B-10-1	.0108	S-10-1	.0110	L-7-1	.0081
B-10-2	.0104	S-10-2	.0109	L-7-2	.0076
B-10-3	.0106	S-10-3	.0111	L-7-3	.0073
B-10-4	.0105	S-10-4	.0109	L-7-4	.0071
B-10-5	.0101	S-10-5	.0105	L-7-5	.0068
B-10-6	.0101	S-10-6	.0103	L-7-5	.0066
	.0007**		.0007**		.0015**
				L-10-1	.0084
				L-10-2	.0087
				L-10-3	.0089
				L-10-4	.0093
				L-10-5	.0094
				L-10-6	.0102
					.0018**

* Average of measurements taken from 4 points on butt and scarf joints and 6 points for lap joints.

** Maximum Variation in test panel.

*** The numbers (1-6) refer to the one inch specimens cut from the test panel per Figure 12b.
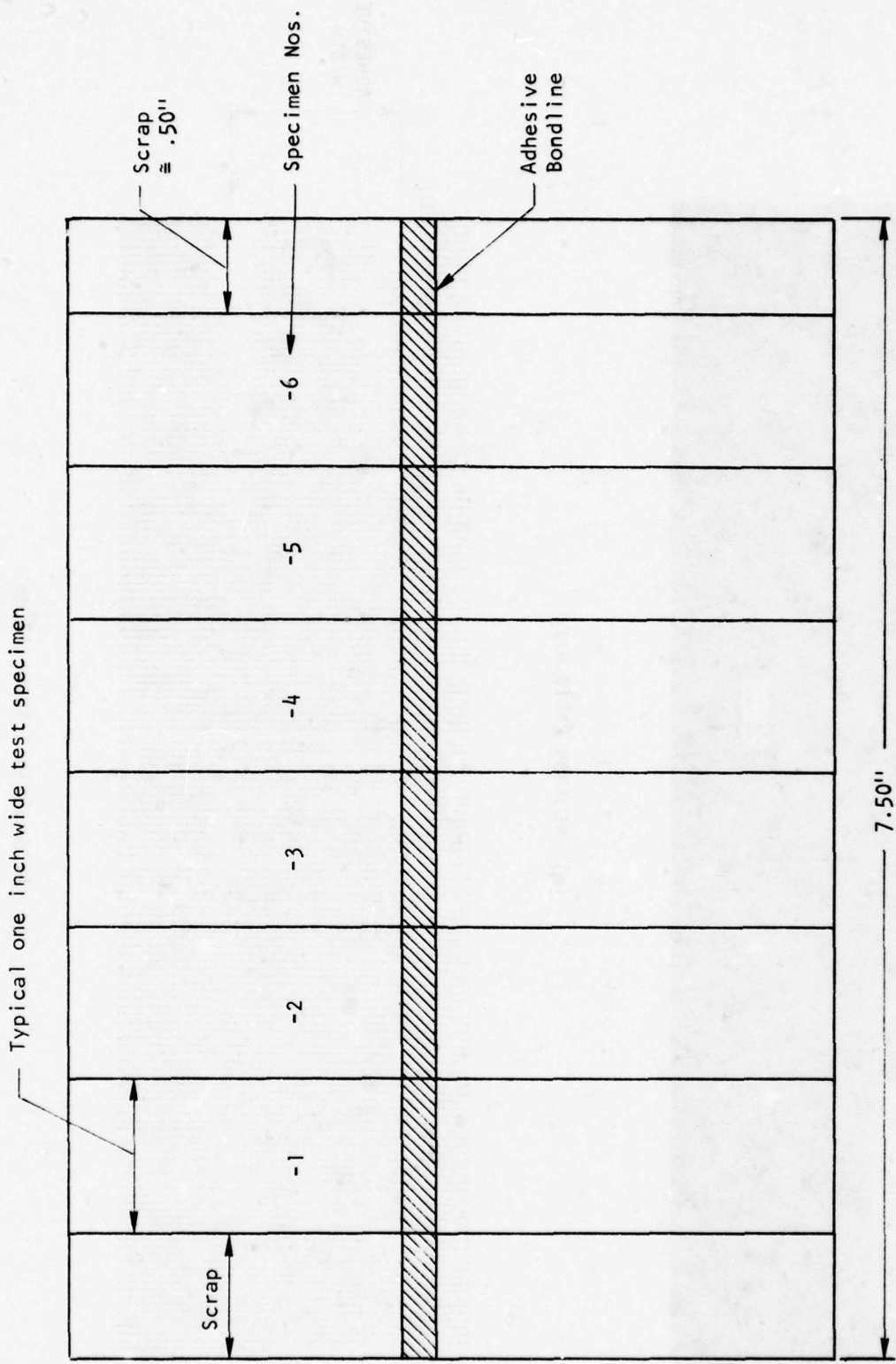
FIGURE 40. TYPICAL BONDED PANEL WITH LOCATION OF ONE-INCH WIDE TEST SPECIMENS

ADHESIVE WIDTH

POSSIBLE VOID AREA

VOIDS
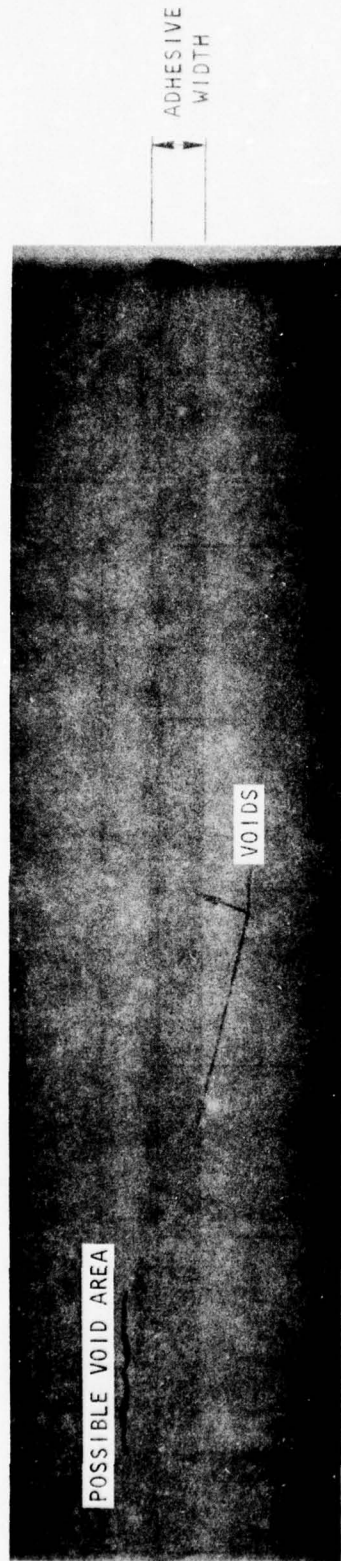
(a) NEUTRON RADIOGRAPH

ADHESIVE WIDTH

(b) ULTRASONIC C-SCAN (17 dB)

FIGURE 41. BUTT JOINT SPECIMEN (FM-73M ADHESIVE - 10 MILS THICK)

108

ADHESIVE
WIDTH

POSSIBLE VOID AREA

(a) NEUTRON RADIOGRAPH

ADHESIVE
WIDTH

Possible difference in
Adhesive Density
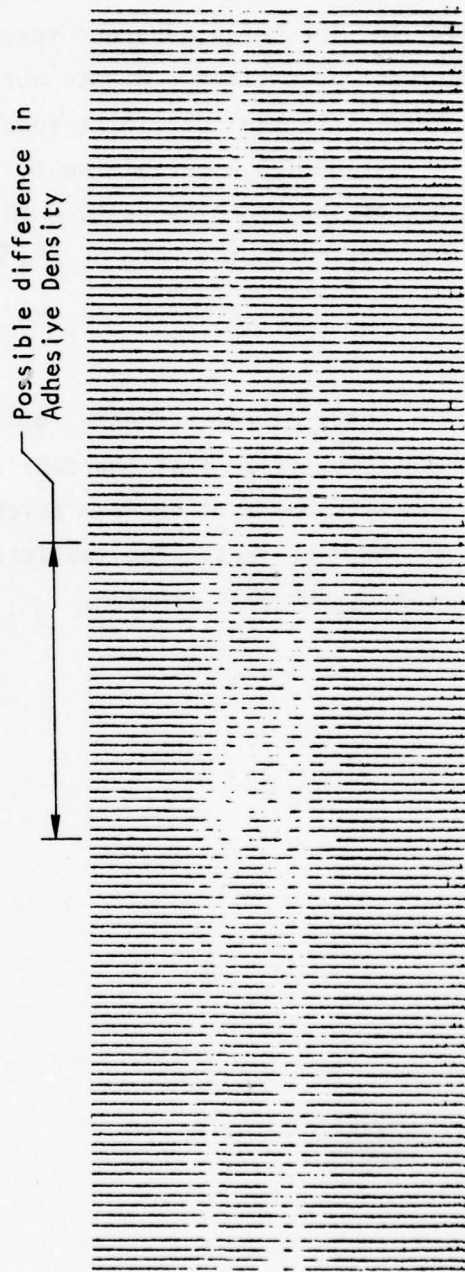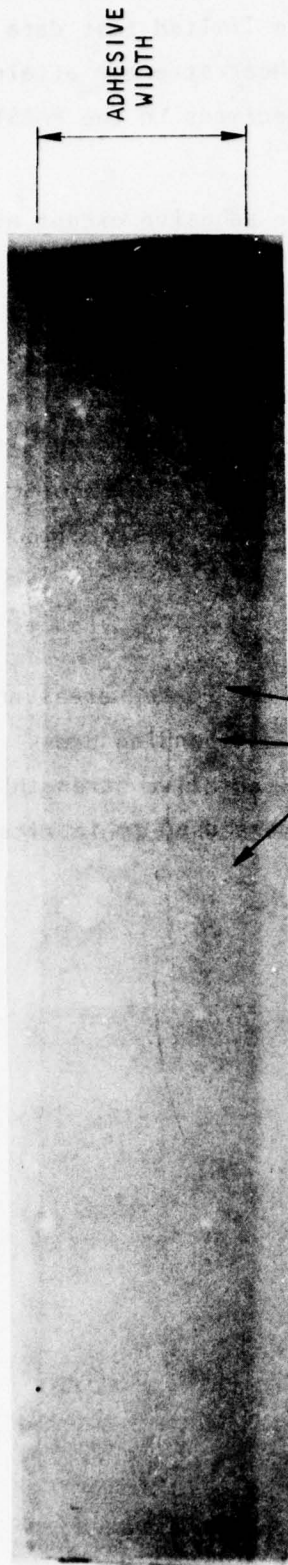
(b) ULTRASONIC C-SCAN (16 dB)

FIGURE 42. SCARF JOINT SPECIMEN (FM-73M ADHESIVE - 10 MILS THICK)

109

and the results are summarized in Table 11. Due to the limited test data definitive trends were not ascertained. However, the shear strength attained compares favorably with values obtained on lap shear specimens in the PABST program.

In all instances the failure was cohesive within the adhesive except at one edge (assumed to be the initial failure region) within which a narrow band (≅ .002" for the thick adherend specimen to .15" for the scarf joint) of adhesive failure was noticed. Minute but scattered voids, ≅ .005 inches or less, were evident in the butt joint specimen. This supported the observation made in Section 7.3.4 pertaining to the butt joint radiographic results. A color change of the adhesive failure surface was also noted. This color change may be related to the rate of the crack propagation as the specimen begins to fail.

8.4 SUMMARY

Results of bondline measurements, NDI inspection of the bonded areas and destructive tests verified that the fabrication fixture and bonding press facilitate adhesive bonds of uniform thickness and representative strength with voids of .005" or less. The fabrication fixtures were used to fabricate all test specimens for this program.

110

TABLE 11. SUMMARY OF DESTRUCTIVE TEST RESULTS

SPECIMEN	ADHESIVE THICKNESS (IN)	MAX STRESS (P/A) (PSI)
THICK ADHEREND	.0046	5611
	.0050	5444
	.0068	5277
	.0076	5222
	.010	5555
	.0094	5500
BUTT	.0055	7933
	.0054	7866
	.0104	6866
	.0103	7133
45° SCARF	.0039	8300*
	.0045	8200
	.0109	8066
	.0105	7933

*Based on projected area normal to applied load.

111

SECTION IX

TEST SPECIMEN FABRICATION

9.1 SUMMARY OF FABRICATION RESULTS

All adhesive bonded test specimens were fabricated per the Fabrication specification (Volume II). Each adherend faying surface was machined, then checked for consistent surface roughness using a Mitutoyo Surftest-B meter. The surface roughness consistently averaged 32×10^{-6} inches. The cure cycles for the primers and adhesives used followed the manufacturer's recommended procedures, taking into consideration the upheat characteristics of the press platens. Although both the FM-73 and the FM-400 adhesives have a broad range of cure cycles, an effort was made to obtain the recommended optimum cycle.

A summary of the fabrication results are presented in Table 12. panels were inspected using neutron radiography. The thick adherend panels were consistently void free (Table 12), while the initial butt and scarf joint panels contained small voids. The bonding fixture was modified and subsequent butt and scarf joint panels were void free.

Adhesive thickness control results are summarized in Tables (13-15). Thickness control for the thick adherend specimens is primarily controlled by the accuracy of the machining procedure along the surfaces to be bonded. Thickness control for the butt and scarf joints is dependent on the shim stock accuracy, degree of parallelism of the surfaces to be bonded and the tapered pin dimensional accuracy. Overall, thickness control across the panel from A to B (see Figures in Tables 13 - 15) was excellent. The ability to fabricate a particular bondline thickness was adequate for thicker bondlines. It was more difficult to fabricate bondlines of 4 mils and less. This may be due to an accumulation of tolerance buildup in the drill jig, bonding jig and in the nominal dimensions of the plates themselves.

TABLE 12. SUMMARY OF FABRICATION RESULTS

SPECIMEN	FM-73 Adhesive		FM-400 Adhesive	
	Number Fabricated	Number With Voids	Number Fabricated	Number With Voids
Thick Adherend	12	1	9	0
Butt Joint	16	9*	15	4*
Scarf Joint	5	4*	6	1

*These resulted prior to modifying bonding fixture. After modification void free panels were consistently fabricated.

112

TABLE 13.   SUMMARY OF THICK ADHEREND FABRICATION
RESULTS - ADHESIVE THICKNESS CONTROL
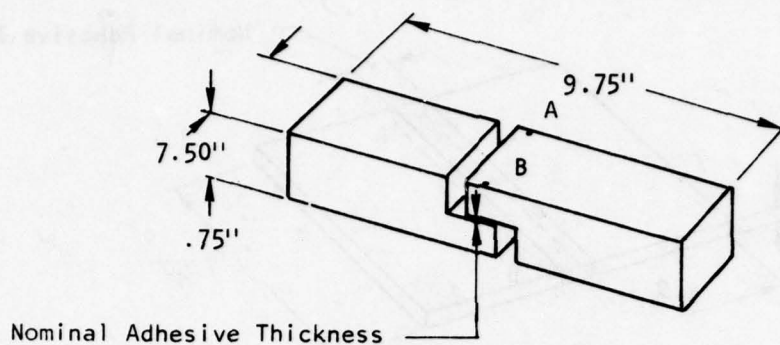
Nominal Adhesive Thickness

ADHESIVE	PANEL NO.	DESIRED ADHESIVE THICKNESS (MILS)	AS FABRICATED ADHESIVE THICKNESS FROM A → B (MILS)
FM-73	2-L-04	4	7.76 → 7.03
	4-L-04	4	7.02 → 6.35
	5-L-04	4	8.46 → 6.20
	6-L-08	8	8.67 → 9.36
	7-L-08	8	9.65 → 10.13
	8-L-08	8	9.80 → 10.50
	9-L-08	8	9.61 → 8.62
	10-L-08	8	9.71 → 9.41
	12-L-08	8	8.77 → 8.35
	13-L-08	8	15.85 → 12.00
	14-L-08	8	10.33 → 8.97
	15-L-08	8	11.65 → 11.03
FM-400	1L-04-F	4	5.40 → 4.50
	3L-04-F	4	10.20 → 7.40
	11L-08-F	8	8.20 → 8.90
	16L-08-F	8	8.10 → 7.70
	17-L-08-F	8	9.50 → 9.40
	18-L-08-F	8	9.50 → 8.90
	19L-08-F	8	8.60 → 8.60
	20L-08-F	8	9.20 → 7.20
	21L-08-F	8	7.90 → 7.60

113

TABLE 14. SUMMARY OF BUTT JOINT FABRICATION RESULTS –
ADHESIVE THICKNESS CONTROL
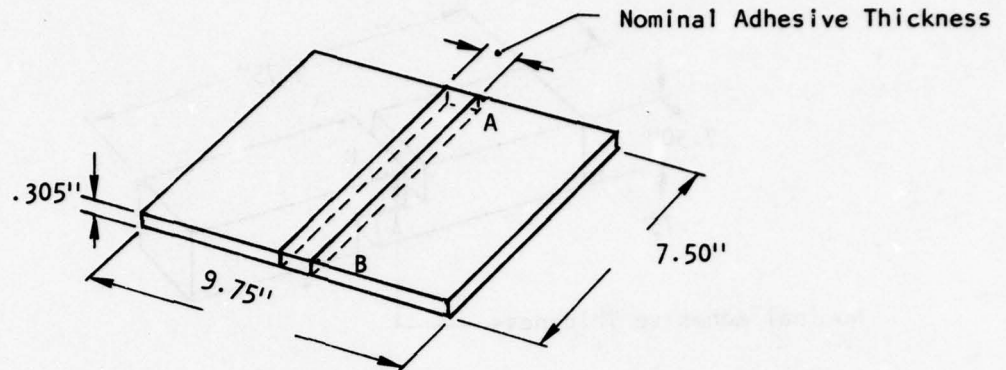
ADHESIVE	PANEL NO.	DESIRED ADHESIVE THICKNESS (MILS)	AS FABRICATED ADHESIVE THICKNESS FROM A → B (MILS)
FM-73	B-1-04	4	5.43 → 5.36
	B-2-04	4	5.60 → 4.80
	B-3-04	4	3.60 → 6.90
	B-4-04	4	4.40 → 4.40
	B-5-04	4	3.82 → 7.26
	B-7-08	8	6.05 → 12.43
	B-8-08	8	8.07 → 10.13
	B-9-08	8	7.91 → 9.22
	B-10-08	8	9.00 → 9.25
	B-11-08	8	8.90 → 8.90
	B-12-08	8	8.80 → 9.20
	B-13-08	8	6.30 → 9.30
	B-14-08	8	7.00 → 8.56
	B-16-08	8	6.93 → 7.93
	B-18-04	4	2.75 → 7.14
FM-400	B-19-04-F	4	7.40 → 7.10
	B-20-04-F	4	7.50 → 7.40
	B-22-04-F	4	7.90 → 7.70
	B-23-08-F	8	9.40 → 11.02
	B-25-08-F	8	9.60 → 10.40
	B-26-08-F	8	9.60 → 10.20
	B-27-08-F	8	5.80 → 12.70
	B-28-08-F	8	7.76 → 8.19
	B-29-08-F	8	12.00 → 12.40
	B-30-04-F	4	6.20 → 7.00
	B-31-04-F	4	5.80 → 6.40
	B-32-04-F	4	5.60 → 6.40
	B-33-04-F	4	6.00 → 7.00
	B-34-08-F	8	8.15 → 8.15
	B-35-08-F	8	9.51 → 9.60

TABLE 15. SUMMARY OF SCARF JOINT FABRICATION RESULTS -
ADHESIVE THICKNESS CONTROL
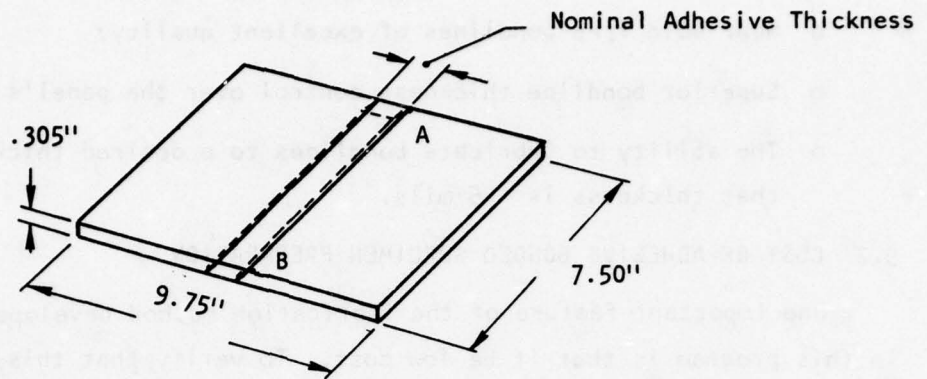
ADHESIVE	PANEL NO.	DESIRED ADHESIVE THICKNESS (MILS)	AS FABRICATED ADHESIVE THICKNESS FROM A → B (MILS)
FM-73	S-1-08	8	8.70 → 8.78
	S-2-08	8	9.22 → 9.06
	S-3-08	8	5.60 → 9.10
	S-4-08	8	9.50 → 10.03
	S-5-04	4	4.50 → 6.20
FM-400	S-6-08-F	8	10.10 → 7.30
	S-7-08-F	8	9.87 → 10.15
	S-8-08-F	8	8.20 → 10.95
	S-9-08-F	8	8.50 → 8.80
	S-10-04-F	4	6.10 → 6.30
	S-11-04-F	4	5.60 → 6.50

In summary, a bonding fixture and fabrication specification were finalized which insure:

- o Near void free bondlines of excellent quality.

- o Superior bondline thickness control over the panel's width.

- o The ability to fabricate bondlines to a desired thickness when that thickness is > 5 mils.

9.2 COST OF ADHESIVE BONDED SPECIMEN PREPARATION

One important feature of the fabrication method developed within this program is that it be low cost. To verify that this has been achieved a cost estimate of the complete fabrication procedure was performed. Items included in the cost estimate were:

- o Initial metal adherend sizing, sanding and milling of edges.

- o Finish machining of metal surfaces to be bonded.

- o Drilling of alignment holes.

- o Cleaning, priming and bonding.

- o Cutting of the bonded panel into one inch wide specimens and drilling of the loading holes.

- o Milling test specimens to final dimensions.

- o The drilling of four holes in each test specimen for attachment of the capacitor.

The cost evaluation was based on making twenty test panels (120 one inch wide test specimens) of either the thick adherend geometrical configuration or the butt (scarf) joint geometrical configuration. It assumes one is familiar with the Fabrication Specification and the Drill and Bonding Jigs.

The results were that it took 45.5 man-hours to completely fabricate the twenty butt (scarf) joint test panels of planar dimensions 9.75" x 7.50". This amounts to 2.3 man-hours per test panel or .4 man-hours per test specimen.

For the thick adherend test panels (extra machining is required to form the gap for the adhesive bondline), it required 70.5 man-hours. This is 3.5 man-hours per test panel or .6 man-hours per test specimen.

116

SECTION X

DATA GENERATION

The goal of this task is to demonstrate the utility, ease of performance, low cost and repeatability of the various test methods for FM-73M and FM-400 adhesives. Thus, the test results will enable one to accurately verify the cost of performing the test methodology, make any necessary modifications to the respective adhesive test specifications, to enhance their ease of performance and support improvements to the adhesive deformation measurement device to enhance data repeatability. Selected bulk uniaxial tensile specimens were also tested to estimate if meaningful differences exist between static and viscoelastic adhesive mechanical properties tested in the neat vs. bonded configuration.

10.1 TEST MATRIX

The scope of the test program is shown in Table 16. The influence of strain rate, temperature, humidity, adhesive thickness, and mode of loading on the mechanical response of bonded joints was experimentally investigated.

10.2 STATIC TEST RESULTS

10.2.1 Thick Adherend Shear Test Results

Shear adhesive mechanical properties for FM-73M (Dacron Mat) and FM-400 (Nylon Knit Fabric) adhesive systems have been determined per the Static Test Specification (Volume II). Aluminum adherends (7075-T651) were .75" thick, 1.0" wide, 10.0" long and had an overlap length of .36".

The specimens, once removed from the saturated salt chamber, were immediately placed in a universal type grip within the controlled environment of the environmental test facility with the ATC designed parallel plate capacitor attached to them (Figure 29). The recording device was set to the proper sensitivity to record the load vs. deformation results. The load range frequency and strain rate parameters were also set to their desired values. The specimen was preloaded to approximately 900 PSI to align the specimen in the test fixture and eliminate any initial adhesive defects. The load was then reduced so as to maintain a small bias load of 25 lbs. on the specimen to preserve all alignment in the assembly prior to applying the test load. The test specimen was then

117

TABLE 16. TEST MATRIX

TEST	TEMPERATURE(°F)/R.H.	LOAD RATE 1	LOAD RATE 2	ADHESIVE THICKNESS	MODE OF LOADING	ADHESIVE SYSTEM 1	ADHESIVE SYSTEM 2
A. OPTIMUM TEST SPECIMEN							
Static Stress-Strain	75/75; 180/75; 75/95; 65/0	X	X	Variable	a,b,c	X	X
Static Creep and Recovery	(72, 120, 140, 160, 180)/ (0, 75)	X		Variable	a,b	X	X
Cyclic Stress-Strain @ 2 Hz and R = + .10	150/dry	X		Variable	a,b	X	X
B. BULK SPECIMENS							
Static Stress-Strain	(75, 180)/175	X		Variable	a	X	X
Static Creep and Recovery	(75, 120, 140, 160)/75	X		Variable	a	X	X

a Tension
b Shear
c Tension + Shear (75°F and 150°F at 0% R.H. only)

118

loaded to failure at the prescribed strain rate in the specified environment. The load vs. deformation data was recorded using a multipoint digistrip chart and transferred to a cassett tape for reduction of the data using an HP 9815 mini-computer and HP-9808 plotter.

A summary of the test results is presented in tabular form in Table 17. The data reduction equations are:

$$G = \frac{\Delta P(\eta)(S.F.)}{A_s(\Delta_s)} \;, \quad F_{su} = \frac{P_u(S.F.)}{A_s} \;, \quad \varepsilon_{ult} = \frac{\Delta_{sult}}{\eta} \qquad \text{62-64}$$

For a load $P_1 > P_2$ and attachment points A and B .126" apart (Figure 29), Δ_s is the displacement measured between loads P_1 and P_2 minus the adherend deformation correction factor for the metal between attachment points A and B.

Also, A_s = surface area of shear specimen (i.e., overlap length x specimen width); F_{su} = adhesive ultimate shear stress (PSI); G = effective shear modulus of the adhesive; $\Delta P = P_1 - P_2$ = applied load; P_u = maximum load specimen attains; S.F. = ratio of constant shear stress of optimum specimen to (P/A_s) shear stress; Δ_s = adhesive displacement in shear specimen; η = adhesive thickness; and ε_{ult} = ultimate adhesive shear strain at centerline of overlap.

The data reproducibility is generally good and it does not seem to be dependent on the capacitance measurement device used. In all cases the shear modulus did change slightly with load. Therefore, for comparison purposes, all shear modulus values were computed at approximately the same time from test initiation for a given load rate. In obtaining the initial test data for FM-73M specimens (2L-04 and 6L-08), the capacitance scale selected precluded an accurate estimate of the ultimate displacement. However, the values are believed to be reasonable approximations.

The FM-73M specimens consistently failed in a cohesive manner as shown in Figure 43. The FM-400 specimens failed in a predominantly adhesive manner at the adhesive-metal interfaces as shown in Figure 44.

The primary purpose of this test program was to demonstrate the utility, ease of performance, and low cost of recently defined test procedures. Moreover, slight modifications to the test procedure were made as the test program

119

TABLE 17

SUMMARY OF THICK ADHEREND SHEAR TEST RESULTS

SPECIMEN	ADHESIVE	LOAD RATE (#/SEC)	COND. ENVIRONMENT TEMPERATURE °F R.H. (%)	TIME IN ENVIRONMENT (HRS)	TEST ENVIRONMENT TEMPERATURE °F	R.H. %	$t_{adh.}$ (in)	G (ksi)	MAX. DISP (in)	MAX. STRAIN (in/in)	F_{su} (ksi)	TYPE FAILURE	CAP. USED
2L-04-1*	FM-73M	1.60	133°F	120	75	75	.0077	71.90	.0027	.3556	6.19	100% Cohesive	2
-2*	(.085 psf)	1.60	95%		75	75	.0076	66.90	.0016	.2158	5.65	"	2
-3*		1.60	Then		75	70	.0075	74.50	.0024	.3306	6.02	"	3
-4*		1.60	133°F		73	73	.0073	67.70	.0014	.1986	5.88	"	3
-5		32.0	70%	≈ 2100	75	74	.0072	99.60	.0021	.2897	5.95	"	2
-6*		32.0			75	74	.0071	91.50	.0015	.2142	5.80	"	2
6L-08-1*	FM-73M	1.60		120	75	70	.0087	42.70	.0019	.2257	4.13	100% Cohesive	3
5L-04-1	FM-73M	32.0			75	67	.0083	74.53	.0014	.1657	5.83	"	3
-3*		1.60			73	73	.0089	49.60	.0024	.2735	4.25	"	2
-4*		32.0		≈ 2500	75	74	.0091	66.60	.0020	.2211	4.68	"	2
-5*		32.0			75	76	.0092	71.21	.0020	.2160	4.53	"	3
-6*		32.0			75	78	.0093	65.81	.0019	.2062	4.51	"	3
1L-04-F1	FM-400	1.60		336	75	75	.0053	58.21	.0010	.1913	4.46	20% Cohesive	3
2	(.100 psf)	1.60			75	75	.0052	61.94	.0009	.1676	4.24	10% Cohesive	2
3		1.60			75	78	.0050	53.33	.0009	.1773	4.39	"	2
4		1.60		≈ 2500	75	78	.0049	48.37	.0009	.1767	4.93	"	3
5			FAILED IN HOLE DRILLING OPERATION										
6		32.0			75	65	.0046	48.26	.0009	.1964	4.95	"	2 & 3

* Approximate Ultimate Displacement - Standard Capacitance Changed during Test.

TABLE 17

SUMMARY OF THICK ADHEREND SHEAR TEST RESULTS (CONT'D)

SPECIMEN	ADHESIVE	LOAD RATE (#/SEC)	COND. ENVIRONMENT TEMPERATURE °F R.H. (%)	TIME IN ENVIRONMENT (HRS)	TEST ENVIRONMENT TEMPERATURE °F	R.H. %	$t_{adh.}$ (in)	G (ksi)	MAX. DISP. (in)	MAX. STRAIN (in/in)	F_{su} (ksi)	TYPE FAILURE	CAP. USED
3L-04-F1	FM-400	1.60	133°F	336	75	77	.0100	104.90	.0011	.1154	6.59	10% Cohesive	2
-2		1.60	95%		75	77	.0095	91.38	.0012	.1211	6.54	"	2
-3		1.60	Then		75	78	.0090	87.44	.0011	.1269	6.60	"	2
-4		32.0	75°F		75	63	.0086	78.64	.0011	.1249	6.79	"	3
-5		32.0	75%	≈2500	75	63	.0081	89.58	.0009	.1093	6.26	"	3
-6		32.0			75	66	.0074	79.10	.0010	.1398	6.32	"	3
4L-04-1	FM-73M	1.60	133°F	1848	180	75	.0070	2.39	.0035	.4964	0.955	100% Cohesive	3
-2		1.60	95%		180	75	.0069	3.48	.0032	.4655	1.006	"	2
-3		1.60	Then		180	75	.0067	1.72	.0030	.4477	0.708	"	3
-4		3.20	133°F		180	75	.0066	3.02	.0039	.5869	2.194	"	2
-5		3.20	70%	≈1100	180	75	.0065	3.06	.0047	.7178	1.222	"	3
-6		3.20			180	75	.0064	2.07	.0043	.6769	1.597	"	2
7L-08-1	FM-73M	1.60	133°F	336	180	75	.0097	0.90	.0084	.7631	1.90	100% Cohesive	2
-2		1.60	95%		180	75	.0098	0.82	.0081	.8309	0.972	"	2
-3		1.60	Then		180	75	.0099	1.11	.0074	.7540	0.966	"	3
-4		3.20	133°F		180	75	.0099	1.33	.0080	.8042	1.158	"	3
-5		3.20	70%	≈1800	180	75	.0100	1.15	.0084	.8375	1.111	"	2
-6		3.20			180	75	.0101	1.10	.0093	.9215	1.305	"	3

121

TABLE 17

SUMMARY OF THICK ADHEREND SHEAR TEST RESULTS (CONT'D)

SPECIMEN	ADHESIVE	LOAD RATE (#/SEC)	COND. ENVIRONMENT TEMPERATURE °F R.H. (%)	TIME IN ENVIRONMENT (HRS)	TEST ENVIRONMENT TEMPERATURE °F	R.H. %	t adh. (in)	G (ksi)	MAX. DISP (in)	MAX. STRAIN (in/in)	F su (ksi)	TYPE FAILURE	CAP. USED
21-L-08-F1	FM-400	1.60	133°F	336	180	75	.0079	72.81	.0006	.0721	3.298	10% Cohesive	3
-2		1.60	95%		180	75	.0078	87.07	.0005	.0602	3.430	"	2
-3		1.60	Then		180	75	.0078	81.10	.0006	.0763	3.236	"	2
-4		32.0	133°F	≈2060	180	75	.0078	67.27	.0005	.0621	3.611	"	3
-5		16.0	70%		180	75	.0077	70.12	.0005	.0621	3.472	"	2
-6		16.0			180	75	.0077	67.81	.0006	.0742	3.542	"	3
16L-08-F1	FM-400	1.60	133°F	336	180	75	.0081	96.64	.0005	.0624	3.333	10% Cohesive	3
2		1.60	95%		180	75	.0080	74.83	.0006	.0758	3.444	"	3
3		1.60	Then		180	75	.0079	71.23	.0005	.0633	3.389	"	2
4		16.0	75°F	≈2688	180	75	.0079	60.69	.0006	.0793	3.416	"	2
5		16.0	75%		180	75	.0078	79.55	.0005	.0669	3.611	"	2
6		16.0			180	75	.0077	73.03	.0006	.0712	3.611	"	3
17L-08-F1	FM-400	1.60	133°F	336	130	75	.0095	102.28	.0009	.0964	4.778	20% Cohesive	2
2		1.60	95%	336	180	75	.0095	87.82	.0011	.1140	3.972	"	3
			Then										
			133°F										
			70%	≈2160									
13L-08-1	FM-73M	1.6	180°F	≈2900	75	95	.0146	83.9	.0011	.0783	3.12	Cohesive	3
-2		1.6	92%		75	95	.0140	90.2	.0014	.1031	3.38	"	3
-3		1.6			75	95	.0134	80.42	.0014	.1020	3.05	"	3

TABLE 17

SUMMARY OF THICK ADHEREND SHEAR TEST RESULTS (CONT'D)

SPECIMEN	ADHESIVE	LOAD RATE (#/SEC)	COND. ENVIRONMENT TEMPERATURE °F R.H.(%)	TIME IN ENVIRONMENT (HRS)	TEST ENVIRONMENT TEMPERATURE °F	R.H. %	$t_{adh.}$ (in)	G (ksi)	MAX. DISP. (in)	MAX. STRAIN (in/in)	F_{su} (ksi)	TYPE FAILURE	CAP. USED
20L-08-F1	FN-400	1.6	180°F 92%	≈ 2800	75	95	.0092		.0002	.0180	3.85	80% Adhesive	3
-F2		1.6			75	95	.0088	126.	.0004	.0508	3.85	"	3
-F3		1.6			75	95	.0084	148.	.0004	.0531	3.81	"	3
9L-08-4	FN-73M	32.	Dessicated	≈ 6400	-65	0	.0090	130.	.0008	.0858	9.16	"	2
-5		32.			-65	0	.0089	416.	.0005	.0578	8.61	"	2
-6		32.			-65	0	.0087	119.	.0016	.1921	8.88	"	2
10L-08-1	FN-73M	16.	Dessicated	≈ 6400	-65	0	.0097	107.	.0010	.0998	9.16	90% Cohesive	2
-2		16.			-65	0	.0096	276.	.0008	.0850	9.44	50% Cohesive	2
-3		16.			-65	0	.0096	113.	.0014	.1445	9.44	90% Cohesive	3
-4		32.			-65	0	.0096	109.	.0010	.1090	9.69	"	3
-5		32.			-65	0	.0095	113.	.0011	.1186	9.16	"	3
-6		32.			-65	0	.0094	139.	.0007	.0772	9.16	"	3
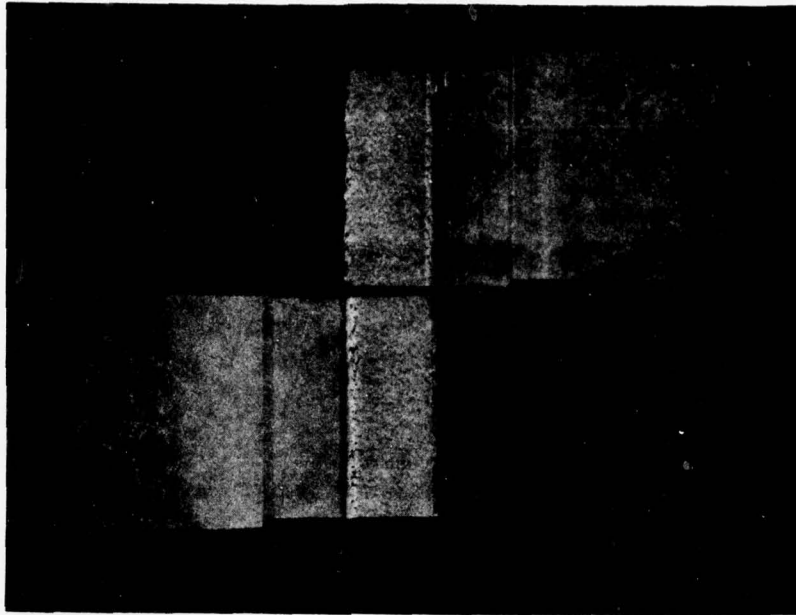
(75°F, 75% R.H.)
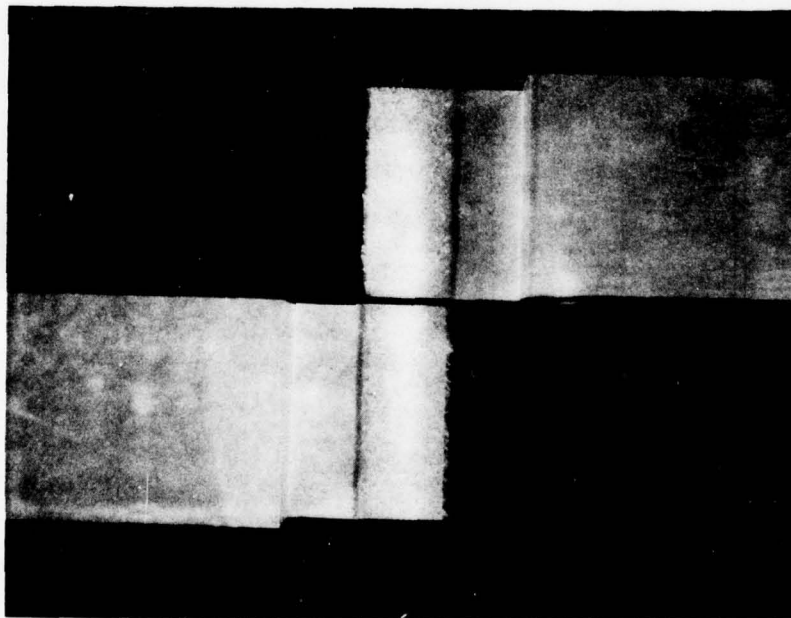
(180°F, 75% R.H.)

FIGURE 43. TYPICAL FM-73 ADHESIVE SHEAR FAILURE
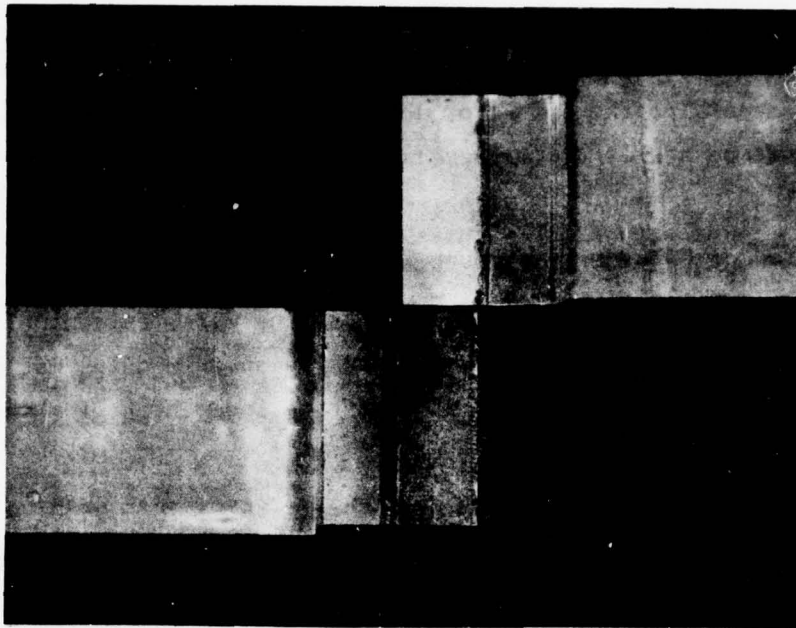
(75°F, 75% R.H.)
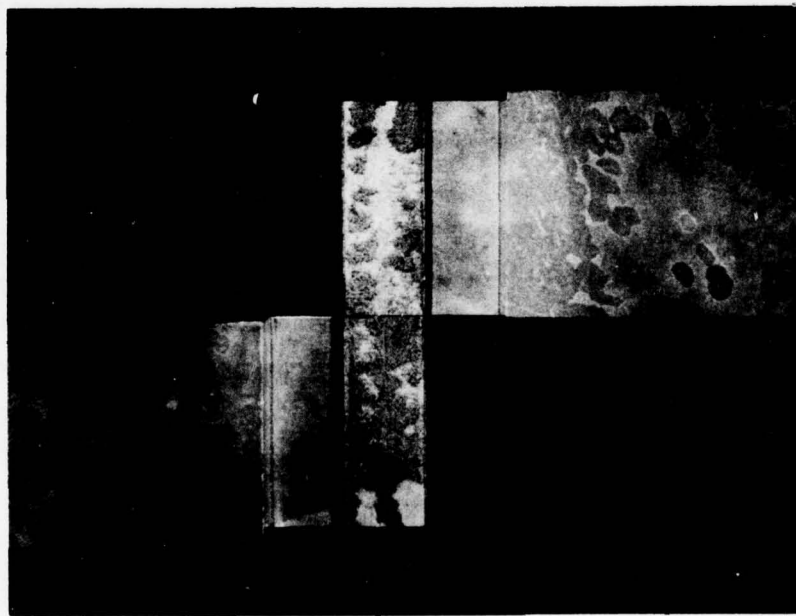
(180°F, 75% R.H.)

FIGURE 44 TYPICAL FM-400 ADHESIVE SHEAR FAILURE

125

proceeded. Certain trends were observed during examination of the shear test results with regard to the effect of load rate, adhesive thickness, relative humidity and temperature. It is recommended that these trends be verified by further testing.

Inspection of Figures 45 through 50 reveals several trends. These are:

o For the two load rates at which specimens were tested, only a modest load rate effect on the FM-73M adhesive shear modulus was observed. All other adhesive properties were rate independent for the range tested.

o In general, for the three temperature (-65°F, 75°F, 180°F) and three relative humidities (0, 75%, 95%) at which test data was obtained for FM-73M adhesive, its shear modulus and ultimate shear strength decreased as temperature and relative humidity increased. Ultimate shear strain increased with an increase in temperature with an anomaly being observed with regard to the 75°F, 95% data.

o For the FM-400 adhesive most of the failures were adhesive, therefore the data is not very informative about the strength characteristics of that adhesive. Regarding response characteristics, the shear-modulus was moderately sensitive to moisture at room temperature while ultimate shear strain decreased in magnitude as temperature and/or moisture increased.

o Where applicable, specific trends in the adhesive's properties directly relatable to adhesive thickness were observed. For the FM-73M material, shear modulus tended to decrease with an increase in adhesive thickness, for 180°F and 75°F at 75% R.H. conditions over the narrow range of adhesive thicknesses tested. The FM-400 modulus tended to increase with an increase in adhesive thickness over a much broader range of adhesive thicknesses. The ultimate shear strain of FM-73M tended to increase with adhesive thickness at 180°F. The effect of 75°F may have been obscured due to the initial data recording limitations of the capacitor as specified on the previous page.
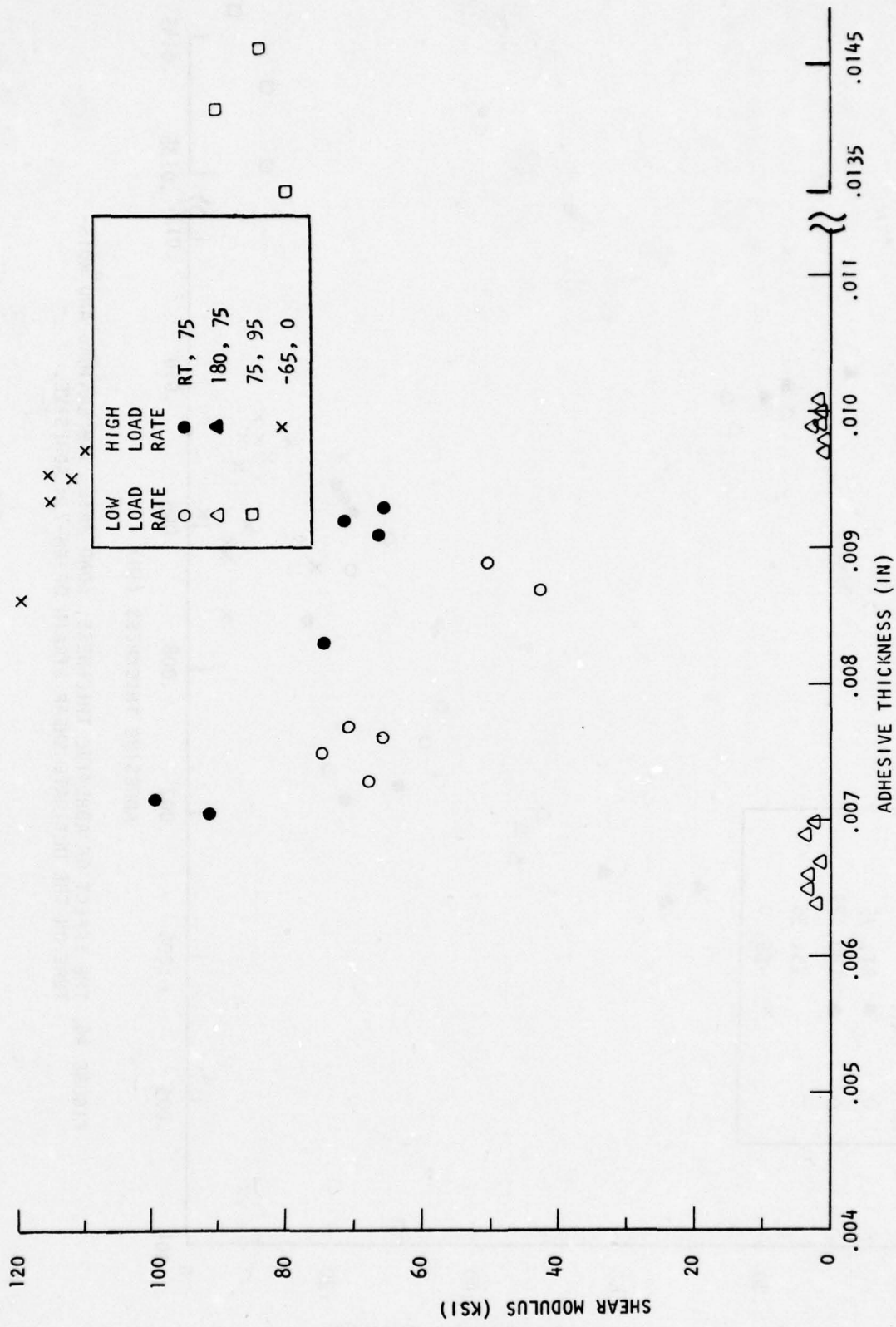
FIGURE 45. THE EFFECT OF ADHESIVE THICKNESS, LOAD RATE, TEMPERATURE AND MOIS-
TURE ON THE SHEAR MODULUS OF FM-73M ADHESIVE.

127
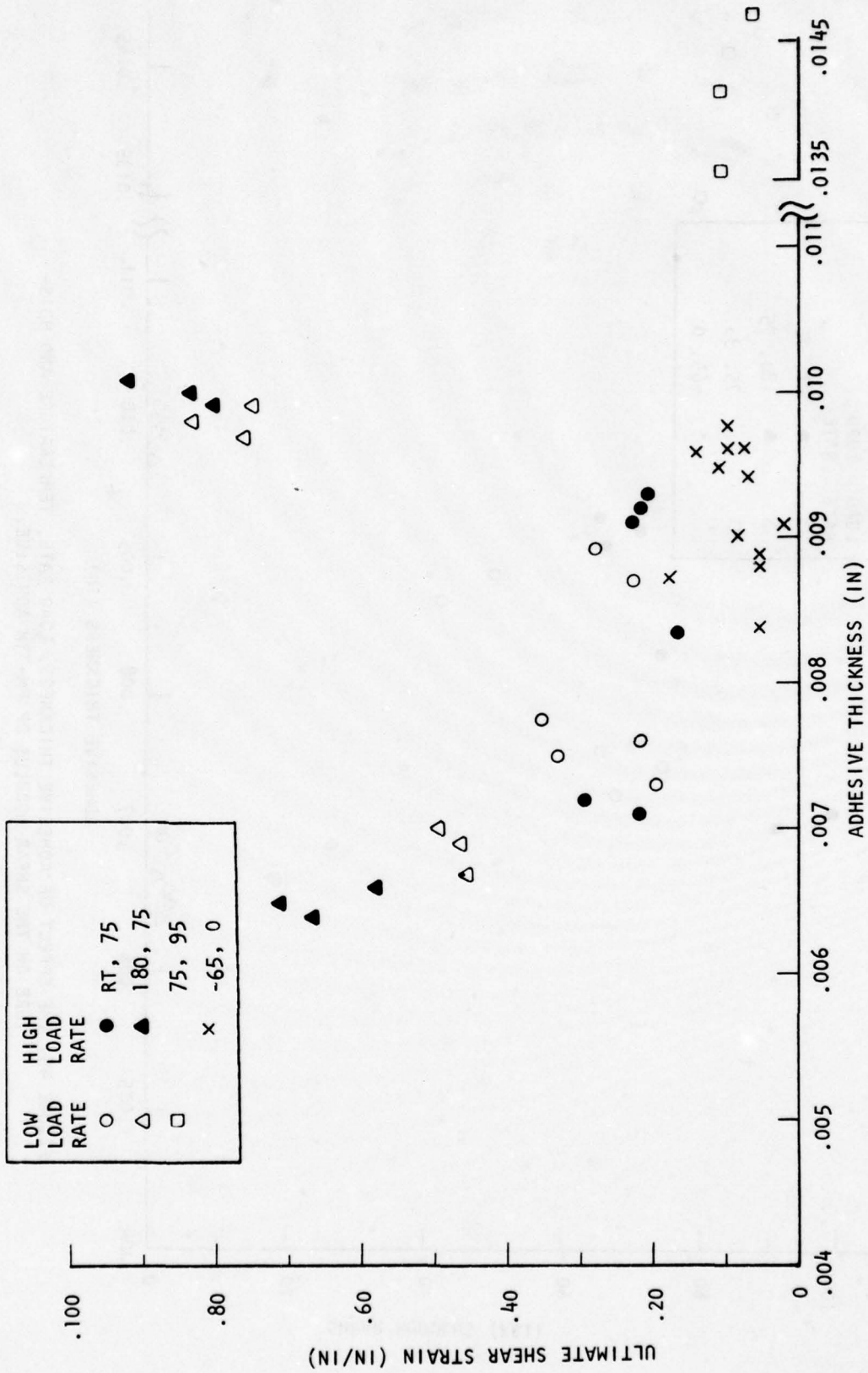
FIGURE 46. THE EFFECT OF ADHESIVE THICKNESS, LOAD RATE, TEMPERATURE AND MOIS-
TURE ON THE ULTIMATE SHEAR STRAIN OF FM-73M ADHESIVE.
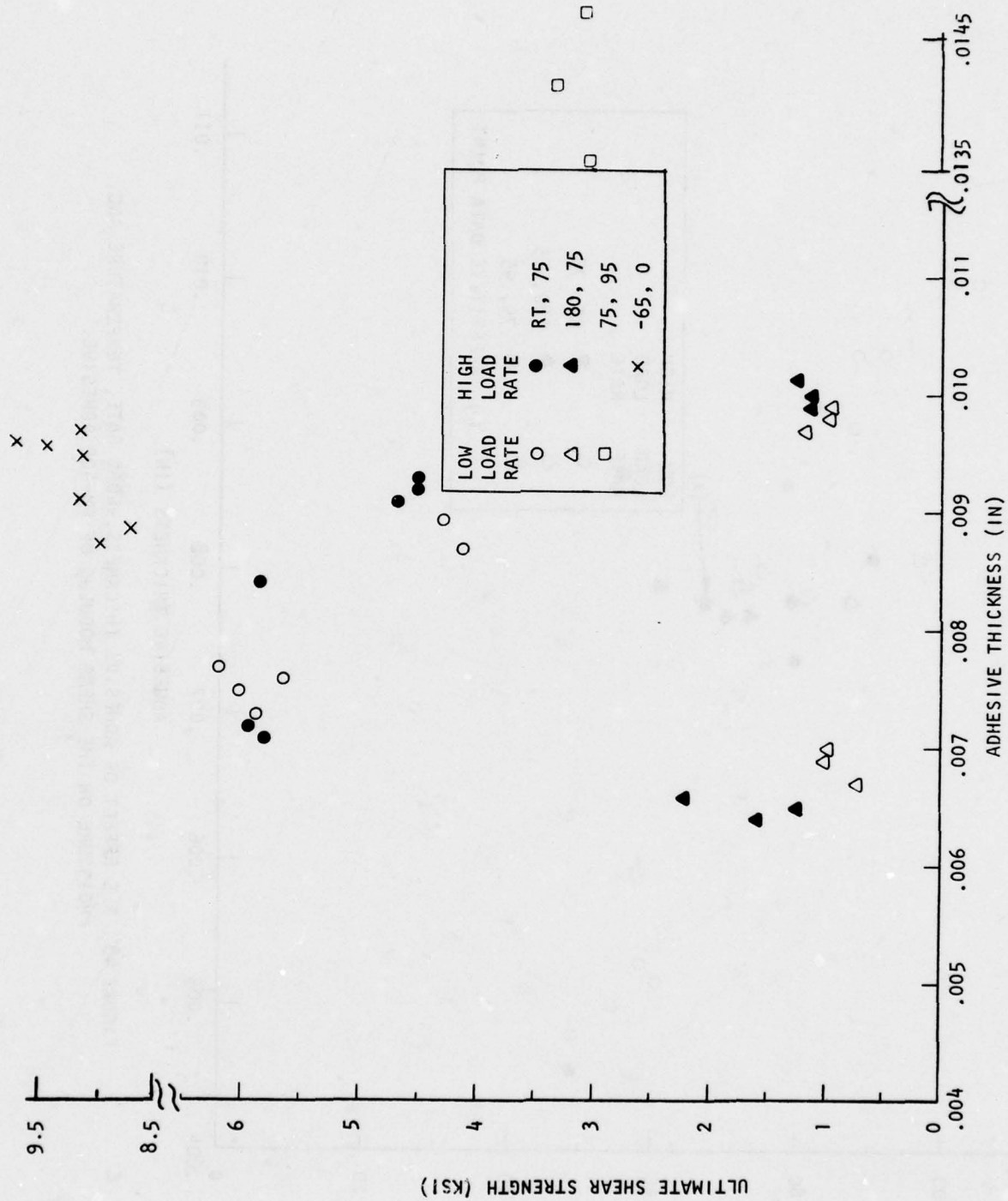
FIGURE 47. THE EFFECT OF ADHESIVE THICKNESS, LOAD RATE, TEMPERATURE AND MOIS-
TURE ON THE ULTIMATE SHEAR STRENGTH OF FM-73M ADHESIVE.

ADHESIVE THICKNESS (IN)

ULTIMATE SHEAR STRENGTH (KSI)

LOW LOAD RATE	HIGH LOAD RATE		
○	●	RT, 75	
△	▲	180, 75	
□		75, 95	
	×	-65, 0	

129
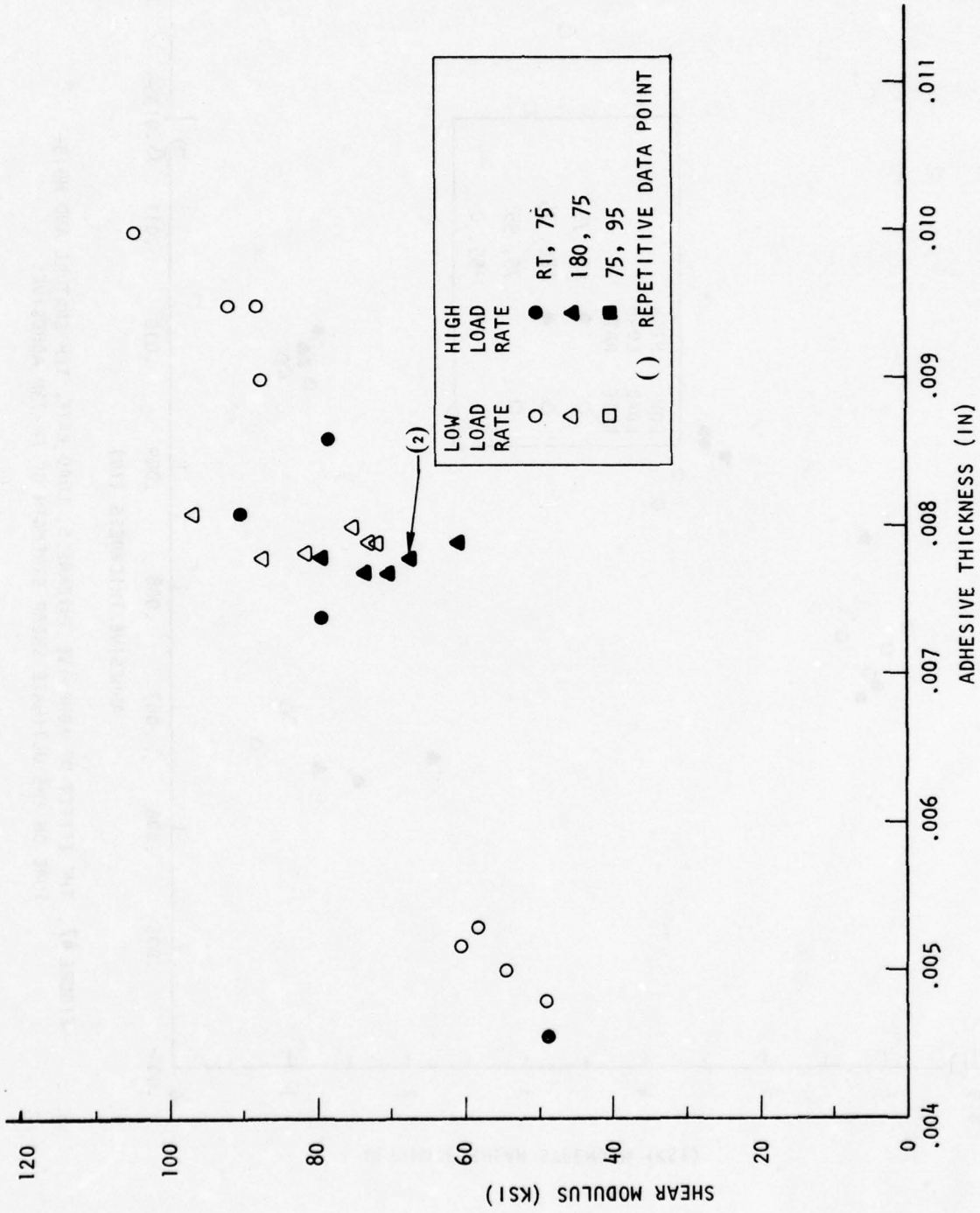
FIGURE 48. THE EFFECT OF ADHESIVE THICKNESS, LOAD RATE, TEMPERATURE AND MOISTURE ON THE SHEAR MODULUS OF FM-400 ADHESIVE.
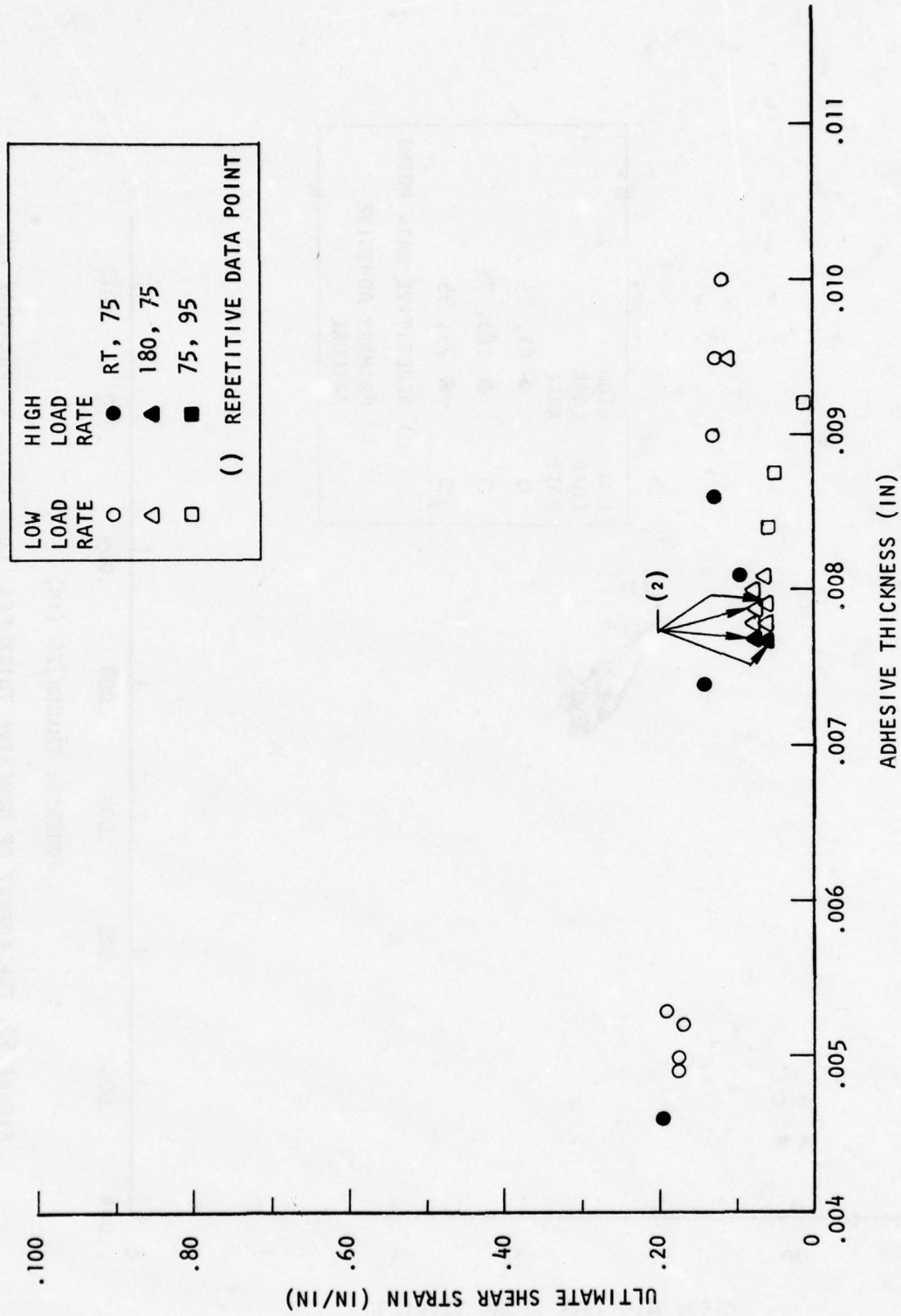
FIGURE 49. THE EFFECT OF ADHESIVE THICKNESS, LOAD RATE, TEMPERATURE AND MOIS- ON THE ULTIMATE SHEAR STRAIN OF FM-400 ADHESIVE.
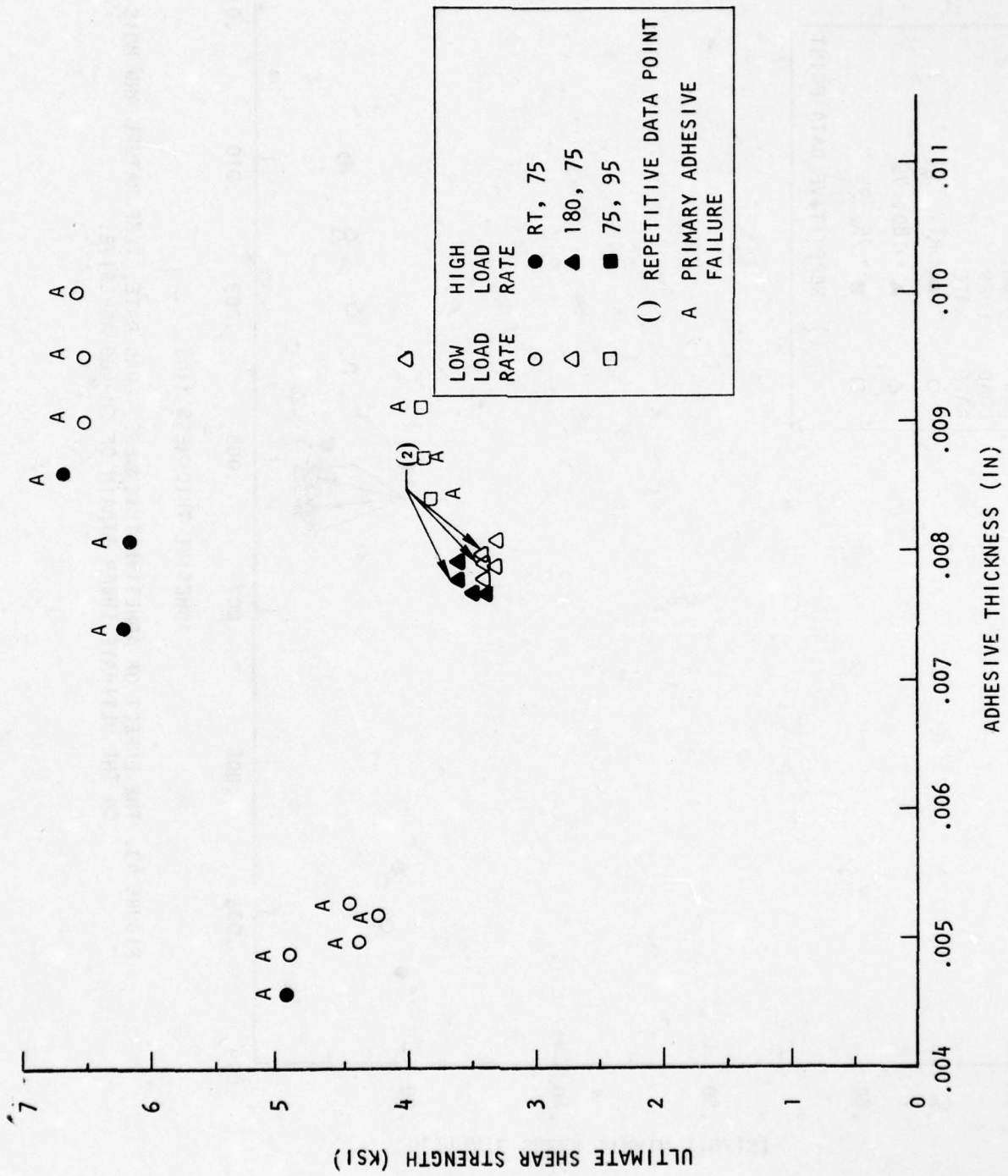
FIGURE 50. THE EFFECT OF ADHESIVE THICKNESS, LOAD RATE, TEMPERATURE AND MOISTURE ON THE ULTIMATE SHEAR STRENGTH OF FM-400 ADHESIVE.

132

That the shear modulus was related to the adhesive thickness for both adhesive materials (ultimate strain of FM-73M) may be attributed to the volume percentage of mat (scrim) vs. adhesive for a particular adhesive thickness. For thinner bondlines one would expect the mat (scrim) to dominate the value of shear modulus (ultimate strain) obtained. As the thickness increases, the influence of the adhesive should tend to become dominant.

The stress-at-failure and strain-at-failure data measured during the constant rate tests have been plotted and are shown in Figure 51. From this figure, it is clear that the trend of the failure envelope is toward lower shear strength and greater strains at the elevated temperature, moisture conditions. This is in agreement with the trends observed when the adhesive film alone (Neat) was tested (see reference 196). Such similarities are encouraging since the stress state within the adhesive layer undoubtedly has residuals from cure shrinkage and cool down, and may well be influenced by the moisture (see reference 197). This area of investigation appears especially promising.

10.2.2 Butt Joint Test Results

Tensile adhesive mechanical properties for FM-73M (Dacron Mat) and FM-400 (Nylon Knit Fabric) adhesive systems have been determined per the Static Test Specification (Volume II). The data obtained reflect two load rates, three temperature levels and three relative humidities. The data presented reveal certain data trends and problems as regards the efficient use of this specimen and deformation measurement device to obtain accurate tensile mechanical properties of the adhesive.

A butt joint test methodology was developed and experimental static and creep data obtained with an optimally designed butt joint test specimen based on the work performed in Section 5.7. Aluminum adherends (7075-T651) were .30" thick 1.1" wide, and 10.0" long. The joint response measurements were extremely sensitive to temperature, moisture and strain rates.

All test specimens were fabricated and their geometries recorded, including adhesive thickness per the Fabrication Specification (Volume II). In general small voids (.005" - .010") were evident in several specimens and are noted under Type of Failure in Table 18.
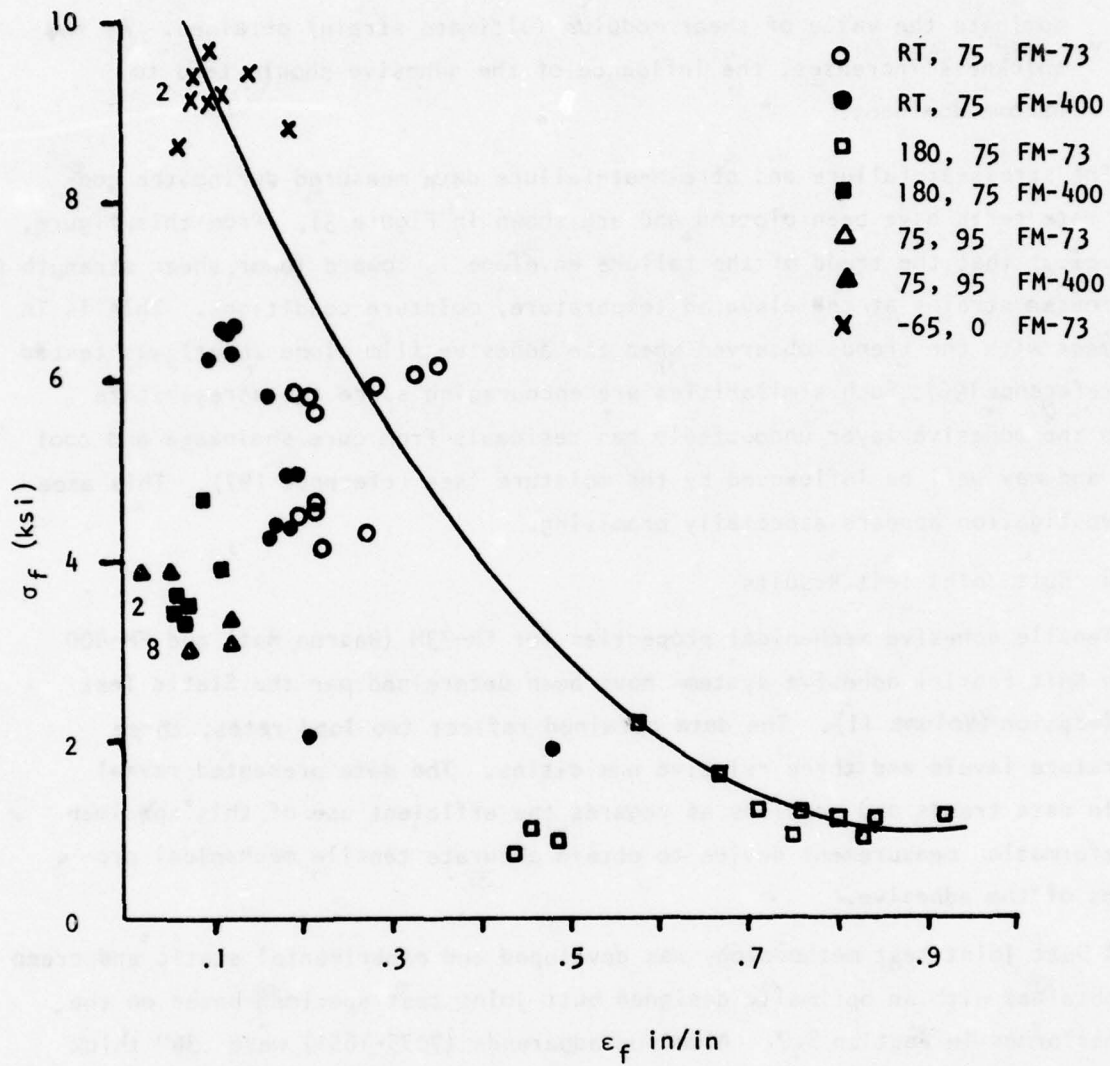
FIGURE 51. SMITH PLOT FOR THICK ADHEREND SHEAR SPECIMENS

TABLE 18

SUMMARY OF BUTT JOINT TENSILE TEST RESULTS

SPECIMEN	ADHESIVE	LOAD RATE (#/SEC)	COND. ENVIRONMENT TEMPERATURE °F R.H. (%)	TIME IN ENVIRONMENT (HRS)	TEST ENVIRONMENT TEMPERATURE °F	R.H. %	$t_{adh.}$ (in)	E_{Sec} (ksi)	MAX. DISP (in)	MAX. STRAIN (in/in)	F_{Tu} (ksi)	TYPE FAILURE	CAP. USED
B-1-04-1	FM-73M	1.6	133°F	336	75	75	.00543	857	.00034	.06317	6.43	Cohesive (Small Voids)	3
-2		1.6	95%		75	75	.00542	1697	.00037	.06840	6.80	"	3
-3		1.6	Then		75	75	.00541	1111	.00031	.05816	6.51	"	3
-4		32.0	133°F		75	75	.00540	1666	.00019	.03495	7.02	"	3
-5		32.0	70%	≈ 2350	75	75	.00539	2086	.00017	.03160	6.79	"	1
-6		32.0			75	75	.00538	2164	.00027	.04950	6.75	"	3
B-7-08-1	FM-73M	1.6	133°F	300	75	75	.00690	1250	.00057	.08309	5.72	" (Numerous Small Voids)	1
-2		1.6	95%		75	75	.00780	706	.00091	.11675	5.58	"	1
-3		1.6	Then		75	75	.00890	267	.00061	.06861	5.40	" (Numerous	3
-4		32.0	75°F	≈ 2350	75	75	.01010	468	.00068	.06708	6.17	" 1/16" Voids)	3
-6		32.0	75%		75	75	.01220	300	.0005	.04160	5.45	" 1/16" = 1/8" Voids	3
B-4-04-2	FM-73	1.6	133°F, 95%	312	75	75	.0042	532.	.0004	.0925	4.95	Cohesive	3
-5		1.6	Then 133°F, 70%	≈ 4400	75	75	.0042	600.	.0012	.3010	5.53	"	3
B-19-04-FI	FM-400	1.6	133°F	300	75	75	.0074	3293	.00001	.0007	7.51	90% Cohesive	1
-F3		1.6	95%		75	75	.0074	614	.0001	.0142	7.74	"	1
-F4		32.0	Then		75	75	.0074	853	.0008	.1102	8.20	"	3
-F5		32.0	75°F	≈ 2350	75	50	.0073		BAD DATA			"	3
-F6		32.0	75%		75	75	.0073	1188	.0005	.0696	8.20	"	3
B-22-04-FI	FM-400	1.6	133°F	336	75	75	.0079	1027.	.0007	.0878	7.58	90% Cohesive	3
B-22-04-F2		1.6	95%		75	75	.0078	4567.	.0004	.0530	7.44	"	3
B-22-04-F3		1.6	Then 75°F 75%	≈ 2350	75	75	.0078	600.	.0003	.0340	7.44	"	3

TABLE 18

SUMMARY OF BUTT JOINT TENSILE TEST RESULTS (CONT'D)

SPECIMEN	ADHESIVE	LOAD RATE (#/SEC)	COND. ENVIRONMENT TEMPERATURE °F R.H.(%)	TIME IN ENVIRONMENT (HRS)	TEST ENVIRONMENT TEMPERATURE °F	R.H. %	$t_{adh.}$ (in)	G (ksi)	MAX. DISP. (in)	MAX. STRAIN (in/in)	F_{Tu} (ksi)	TYPE FAILURE	CAP. USED
B-22-04-F4		32.0	75°F 75%	≈4700	75	75	.0078	1867.	.0004	.0552	8.20	"	3
B-22-04-F5		32.0	75%		75	50	.0077	663.	.0007	.0861	8.20	"	3
B-22-04-F6		32.0			75	50	.0077	330.	.0011	.1474	8.20	"	3
B-4-04-1	FM-73M	1.6	133°F 95%	312	180	75	.0042	14.1	.0102	2.4393	.49	Weird	3
-3		1.6	Then	≈4400	180	75	.0042	2.5	.0048	1.1347	.82	Cohesive	2
-4		1.6	133°F		180	75	.0042	8.2	.0203	4.8308	.98		2
-6		1.6	70%		180	75	.0042	4.2	.0023	.5568	.59	"(Small Voids)2	2
B-12-08-1	FM-73M	.40	133°F	312	180	75	.0089	5.01	.0165	1.8621	.53	"	2
-3		1.6	95%		180	75	.0090	7.4	.0173	1.9314	.78	"	2
-4		1.6	Then		180	75	.0091	10.2	.0305	3.3664	.78	"	2
-5		.40	133°F	≈4300	180	75	.00915	6.3	.0204	2.2998	.50	"	2
-6		1.6	70%		180	75	.0093	4.8	.0261	2.8187	.66	"	2
B-30-04-F1	FM-400	32.	133°F	312	180	75	.0063	240	.0010	.1523	3.81	60% Cohesive	2
2		32.	95%		180	75	.0064	570	.0002	.0260	4.50	70% Cohesive	2
3		32.	Then		180	75	.0065	BAD DATA			4.88	80% Cohesive	2
4		16.	133°F	≈4500	180	75	.0067	400	.0012	.1853	4.83	"	2
5		16.	70%		180	75	.0068	2332.	.0004	.0570	4.83	70% Cohesive (4 1/16" Voids)	2
6		16.			180	75	.0069	2393.	.0001	.0169	3.27	"	2

TABLE 18

SUMMARY OF BUTT JOINT TENSILE TESTS RESULTS (CONT'D)

SPECIMEN	ADHESIVE	LOAD RATE (#/SEC)	COND. ENVIRONMENT TEMPERATURE °F R.H.(%)	TIME IN ENVIRONMENT (HRS)	TEST ENVIRONMENT TEMPERATURE °F	R.H. %	$t_{adh.}$ (in)	E_{Sec} (ksi)	MAX. DISP (in)	MAX. STRAIN (in/in)	F_{Tu} (ksi)	TYPE FAILURE	CAP. USED
B-25-08-F1	FM-400	16.	133°F 95%	≈4900	180	75	.0097	2399.	.0006	.0600	5.01	Cohesive	2
2													
3		16.			180	75	.0099	1521.	.0004	.0428	5.24	"	3
4		32.			180	75	.0100	1300.	.0006	.0571	5.70	"	3
5					BAD DIGISTRIP DATA								2
6		32.			180	75	.0102	BAD DATA			5.73	"	3
B-10-08-1	FM-73M	1.6	133°F 95%		75	95	.0092	2959.	.0030	.3254	3.11	"	2
-2		1.6			75	95	.0092	380.	.0053	.5791	3.47	"	2
-3		1.6	95%	≈7056	75	95	.0092	1524.	.0010	.1106	4.08	"	2
-4		1.6			180	95	.0092	1.0	.0158	1.7217	.26	"	2
B-20-04-F1	FM-400	1.6	133°F 95%		75	95	.0075	BAD DATA	.0002	.0308	?	80% Adhesive	2
-F2		1.6			75	95	.0075	866	.0002		4.06	"	2
-F3		1.6	95%	≈7056	75	95	.0075	2000	.0004	.0484	3.93	"	2
-F4		1.6			180	95	.0075		.0004	.0504	2.50	"	2
B-18-04-1	FM-73M	16.	Dessicated	≈5000	-65	0	.0031				10.49	Cohesive	3
-2		16.			-65	0	.0038	} BAD DATA			10.65	"	3
-3		16.			-65	0	.0046				10.65	"	3
-4		32.			-65	0	.0053				10.68	"	3
-5		32.			-65	0	.0060	410	.0009	.1517	10.82	"	2
-6		32.			-65	0	.0067	BAD DATA			6.55	"	2

137

TABLE 18

SUMMARY OF THICK ADHEREND SHEAR TEST RESULTS (CONT'D)

SPECIMEN	ADHESIVE	LOAD RATE (#/SEC)	COND. ENVIRONMENT TEMPERATURE °F R.H.(%)	TIME IN ENVIRONMENT (HRS)	TEST ENVIRONMENT TEMPERATURE °F	R.H. %	t_{adh} (in)	E_{Sec} (ksi)	MAX. DISP. (in)	MAX. STRAIN (in/in)	F_{Tu} (ksi)	TYPE FAILURE	CAP. USED
B-8-08-1	FM-73M	1.6	133°F 95%	≈ 4900	-65	0	.0082	.2500.	.0007	.0890	7.87	Cohesive	3
2		1.6			-65	0	.0086	500.	.0012	1342	9.53	"	3
3													
4		32.			-65	0	.0093	1022.	.0006	.0690	10.08	"	2
5		32.			-65	0	.0096	1824.	.0013	.1361	9.61	"	2
6		32.			-65	0	.0100	1290.	.0009	.0911	8.64	"	3

138

All test specimens were conditioned in a specific temperature, relative humidity environment for a prescribed time prior to physical testing. In all instances these parameters are defined in Table 18.

The specimens, once removed from the saturated salt chamber had the parallel-plate capacitor attached to them. They were immediately placed in a universal type grip within the controlled environment of the environmental test facility. The long axis of the specimen and the centerline of load pull through the grip assembly ccincided. The recording device was set to the proper sensitivity to record the load vs. deformation results. The load range frequency and strain rate parameters were also set to their desired values. The load was then reduced so as to maintain a small bias load of 25 lbs. on the specimen to preserve all alignment in the assembly prior to applying the test load. The test specimen was then loaded to failure at the prescribed strain rate in the specified environment. The load vs. deformation data was recorded using a multipoint digistrip chart and transferred to a cassette tape for reduction of the data using an HP 9815 mini-computer and HP-9808 plotter.

A summary of the tensile test results is presented in tabular form in Table 18. The data presented for the orthotropic adhesive systems, FM-73M and FM-400 are scattered. These properties are for the adhesive normal to the plane of the scrim.

All FM-73M specimens failed consistently in a cohesive manner as exemplified in Figure 52b. However, most surfaces exhibited a two phase failure pattern of approximately equal surface area. Inspection revealed that one phase involved the scrim begin pulled out of the adhesive while the rest of the surface exhibited a failure in the adhesive yet away from the scrim (Figure 53). The FM-400 specimens failed in an adhesive-cohesive mode (Figure 52a). In several instances minute voids were evident toward one edge of the specimen. This may have been due to a fabrication pressure differential.

In an attempt to identify the reasons for the data scatter, a small study was undertaken. During this study, the secant modulus approach for presenting the test results was tried except for the 180°F. These data are presented in
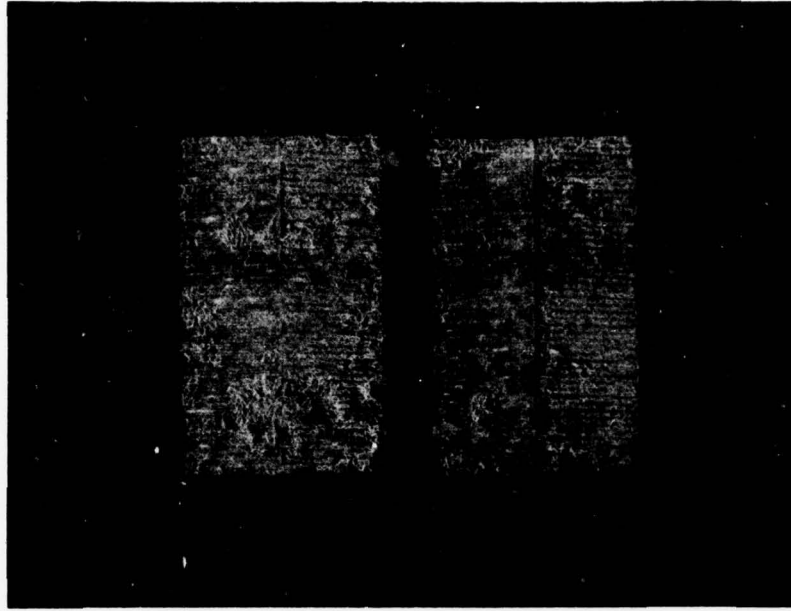
a. FM-400 ADHESIVE TENSILE FAILURE (75°F, 75% R.H.)
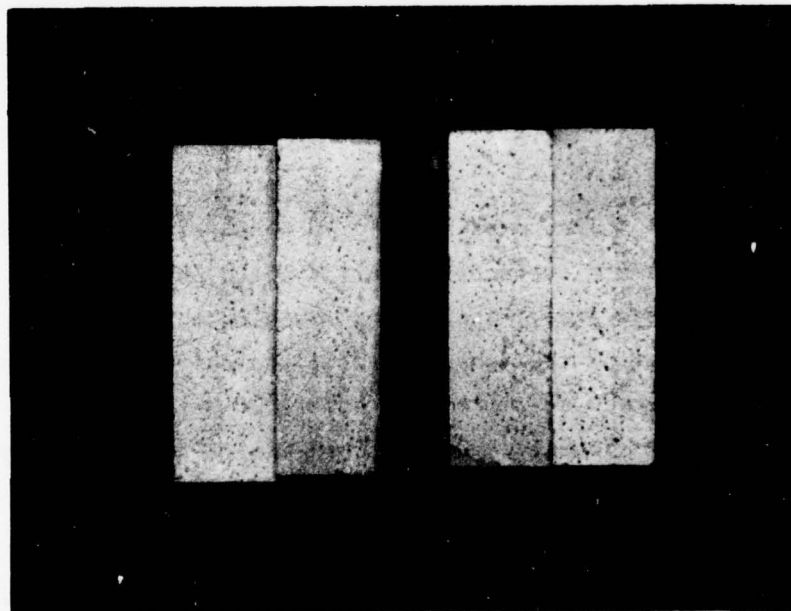
b. FM-73M ADHESIVE TENSILE FAILURE (75°F, 75% R.H.)

FIGURE 52. TYPICAL ADHESIVE TENSILE FAILURE SURFACES.

140
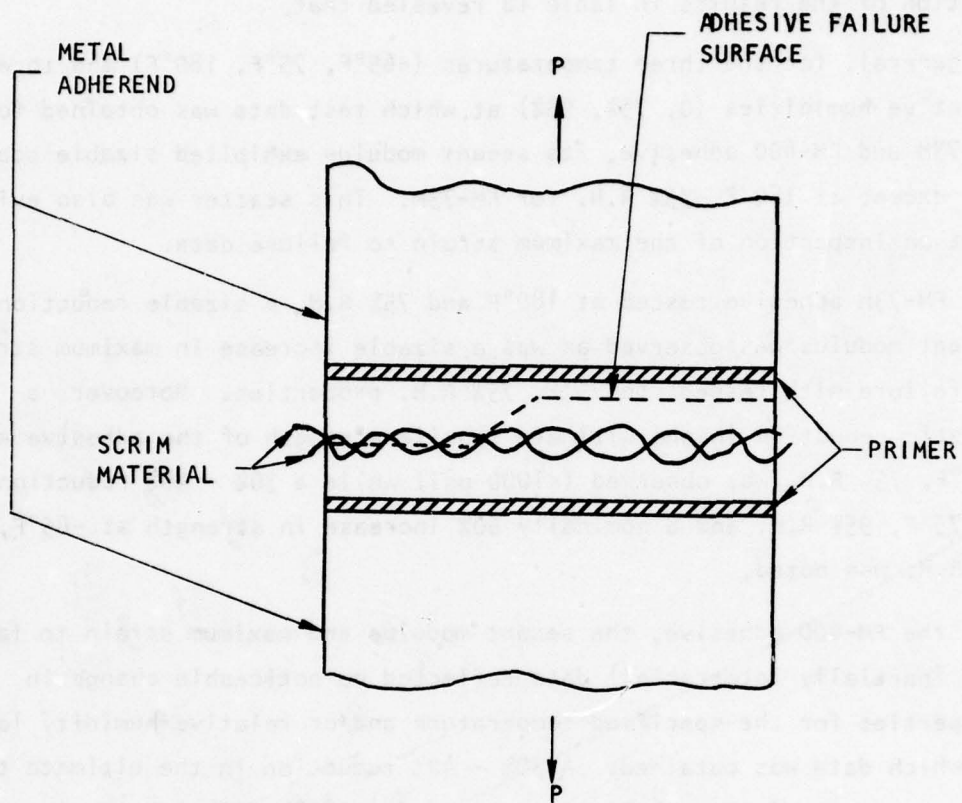
FIGURE 53. BUTT JOINT ADHESIVE FAILURE PATTERN

Table 18, except for the 180°F, 75% condition for which 2 ksi was used for FM-400 data. The adhesive displacement was determined using Equation 8 of the Static Test Specification. The ultimate tensile strength F_{Tu}, was calculated as the ultimate load over the original adhesive area.

Inspection of the results in Table 18 revealed that

O In general, for the three temperatures (-65°F, 75°F, 180°F) and three relative humidities (0, 75%, 95%) at which test data was obtained for FM-73M and FM-400 adhesive, its secant modulus exhibited sizable scatter except at 180°F, 75% R.H. for FM-73M. This scatter was also evident on inspection of the maximum strain to failure data.

O For FM-73M adhesive tested at 180°F and 75% R.H. a sizable reduction in secant modulus was observed as was a sizable increase in maximum strain to failure with respect to 75°F, 75% R.H. properties. Moreover, a drastic reduction in the ultimate tensile strength of the adhesive at 180°F, 75% R.H. was observed (<1000 psi) while a 30% - 40% reduction at 75°F, 95% R.H. and a nominally 60% increase in strength at -65°F, 0% R.H. was noted.

O For the FM-400 adhesive, the secant modulus and maximum strain to failure (partially interfacial) data reflected no noticeable change in properties for the specified temperature and/or relative humidity levels at which data was obtained. A 30% - 40% reduction in the ultimate tensile strength of the material was noted for 180°F, 75% R.H. while nominally a 50% reduction was noted for the 75°F, 95% R.H. condition.

The primary purpose of these tests was to demonstrate the utility, ease of performance, and low cost of recently defined test procedures. However, as evidenced by the consistent scatter in the test data specific improvements in the test methodology are required. As a result of studying this issue the problem areas have been defined that possibly introduced sizable scatter in the adhesive data results. These are:

o Specimen geometry
o Adherend Modulus Variability
o Adhesive void percentage
o Capacitor sensitivity.

142

Specimen geometry is seen as a major reason for the sizable data scatter observed in the secant modulus and ultimate strain to failure data. Due to the small adhesive bondline thickness of typical bonded joints (in this program adhesive thickness varied from 4 to 12 mils) and the inability to attach the capacitor attachment screws no closer than approximately .06 inches from the adhesive-adherend interface, the major component of measured deformation occurring during a tensile test is the aluminum deformation. Table 19 is presented to quantify this and the sensitivity of the adhesive modulus calculated per Equation C-4 of the Static Test Specification (Volume II). The difficulty is due to the small adhesive deformation being measured over an extremely small gage length (i.e. adhesive thickness). As Table 19 points out, an 8-17 percent error is possible due to this specimen geometry problem at ambient conditions for a 1×10^{-6} inch adhesive deformation measurement error. The absolute magnitude of this error is inversely proportional to the magnitude of the modulus. This error could be minimized by redesign of the test specimen.

An additional error of significance is the variability in the adherend Young's modulus. The size of this error is quantified in Table 20. To summarize, as the modulus of the adhesive approaches, in magnitude, the Young's modulus of the adherend material, a sizable error amounting to 100% or more is possible for an adherend modulus variation of from 10×10^6 to 12×10^6 psi. While such a change in magnitude is not believed to be the cause of our present data scatter problem it is believed that a 10-20% variation in adhesive modulus data is possible due to adherend modulus variations. This is an error which could be overcome if the adhesive gage length was increased significantly.

Another source of error is the effect of adhesive void volume on the bulk modulus of the adhesive which can be related to the tensile modulus, albeit, in a rather complicated manner for an orthotropic system. In order to estimate the magnitude of this error the work of Hashin[198] was employed. Assuming a quasi-homogeneous, quasi-isotropic material system, Equation 65 was used to generate the results of Table 21.

$$\frac{K}{K_a} = 1 - \frac{3(1 - \nu) \, C}{2(1 - 2\nu)} \qquad 65$$

K is the bulk modulus from test data with voids, K_a is the bulk modulus from test data without voids, ν is the adhesive Poisson's ratio assumed constant at .38 and C is the void concentration.

143

TABLE 19. SENSITIVITY OF ADHESIVE TENSILE MODULUS AT AMBIENT CONDITIONS TO A 1 × 10⁻⁶ INCH ADHESIVE DEFORMATION DIFFERENCE.

SPECIMEN	LOAD RANGE (LBS)	TOTAL DEFORMATION MEASURED × 10⁻⁶ IN	METAL DEFORMATION × 10⁻⁶ IN	ADHESIVE DEFORMATION × 10⁻⁶ IN	ADHESIVE THICKNESS (IN)	TENSILE MODULUS (KSI)	% ERROR IN TENSILE MODULUS FOR A 1 × 10⁻⁶ INCH ADHESIVE DEFORMATION DIFFERENCE
B-1-04-1	600-1152	49	36	13	.00543	760.	8.4
B-1-04-4	510-980	37	31	6	.00540	1430.	16.7

TABLE 20. BUTT JOINT SENSITIVITY STUDY

SPECIMEN B1-04-5

ASSUMED ADHEREND MODULUS X 10^6 PSI	$E_{ADHESIVE}$ X 10^6 PSI	MAX DISP. (IN)	MAX STRAIN (IN/IN)
10.	2.080	.00010	.01787
11.	1.206	.00011	.02028
12.	.893	.00012	.02228
13.	.732	.00013	.02398

TABLE 21. EFFECT OF VOID CONCENTRATION ON THE BULK MODULUS

C	0	.02	.04	.06	.08	.10
$\frac{K}{Ka}$	1	.922	.845	.767	.690	.612

145

A 10% void concentration can generate a 39% change in bulk modulus. Per the well-known quasi-isotropic formula to relate tensile modulus to bulk modulus, namely:

$$E = 3K(1 - 2\nu) \qquad\qquad 66$$

this can be directly equated to a 39% change in tensile modulus. This is a sizable quantity, yet, this example is meant to point out the sensitivity of adhesive tensile modulus to void content in a qualitative sense only.

A final source of possible error is the capacitors means of attachment to the butt joint test specimen. While the capacitor's design was quite well suited for the thick adherend specimen, we consistently had difficulties in getting a repeatable response from the capacitor on a specimen to specimen basis (possible pin rotation) for the butt joint. It is now believed that when dealing with a device which is designed to measure 300×10^{-6} in/pf, extreme stability and attachment rigidity must be maintained for the capacitor to respond in a consistent manner when a 1×10^{-6} inch variation can result in a sizable error in mechanical property data. With the thin butt joint specimen design, this was not possible. Again, redesign of the test specimen could resolve this problem.

Moreover, the scatter in the maximum strain to failure data is believed to reflect the impact of the capacitor and specimen design difficulties. Yet, adhesive variability inherently introduces a wide band of data results for this parameter.

In summary, a number of sources are believed to be responsible for the scatter observed in the static tensile results. However, it is believed the data do provide realistic bounds for the material parameters of interest and for the environmental parameters within which the tests were run. To obtain data with significantly reduced scatter, additional efforts should be directed at redesigning the butt joint specimen and the attachment of the capacitor to the specimen. The capacitor concept by itself, did perform in a consistent manner over a wide range of temperatures and relative humidities with an extremely sensitive measurement capability.

10.2.3 Scarf Joint Test Results

Adhesive biaxial mechanical properties for FM-73M and FM-400 adhesive systems were determined per the Static Test Specification of (Volume II). Aluminum adherends (7075-T651) were .305" thick by 1.0" wide by 9" long. The bondline angle was 45° with respect to the load pull direction. The load was applied through 1/2" diameter pin holes located in the specimen's ends. A total of twelve specimens were tested, six for FM-73M and six for FM-400 adhesive.

The specimens once removed from their respective environments were immediately placed in a universal type grip within the controlled environment of the environmental test facility with the ATC designed biaxial parallel plate capacitor attached to them. The gage length was equal to the capacitor's attachment point spacing (.230") when mounted on the test specimen. The attachment points were located at the centerline. The recording device was set to the proper sensitivity to record the load vs. deformation results. The load range frequency and strain rate parameters were also set to their desired values. The specimen was preloaded to approximately 900 PSI to align the specimen in the test fixture and eliminate any initial adhesive defects. The load was then reduced so as to maintain a small bias load of 25 lbs. on the specimen to preserve all alignment in the assembly prior to applying the test load. The test specimen was then loaded to failure at the prescribed strain rate in the specified environment.

Load was applied manually at approximately 1.6 lb/sec. This was necessary, as both the parallel and vertical capacitor gages had to be read separately at each load level, to determine fully the biaxial response of the adhesive. Two comparator measurement instruments were not available to read the data simultaneously.

Overall, the biaxial gages response was much more stable under load and the alignment was much easier to maintain than that of the unidirectional model. This enabled direction and linearity of the output signal to be repeatable thereby minimizing data scatter. Again, the tensile data exhibited scatter reminescent of that observed during the tensile test segment of this program. Much of this scatter is again attributed to the specimen and capacitor design.

In general, for 75°F/50% R.H., the shear modulus of FM-73M (Table 22) is shown to be similar in magnitude to that obtained using the thick adherend specimen; that of FM-400 is a factor of two larger vs. the thick adherend test results. The ten-

147

TABLE 22. SUMMARY OF BIAXIAL STATIC TEST RESULTS.

| SPECIMEN	ADHESIVE	CONDITIONING ENVIRONMENT °F/% R.H.	TEST ENVIRONMENT °F/% R.H.	ADHESIVE THICKNESS (IN)	G_{eff}	E_{eff}	U_{ult}	$\varepsilon_{u\ ult}$	ν_{ult}	$\varepsilon_{v\ ult}$	$(F_T - F_S)_{ult}$
S-5-04-1	FM-73M	130°F/75% R.H. ≈ 1680 Hrs. (≈ 80% of Moisture Equilibrium Level)	75/50	.00462	84,287	370,338	.0006	.12921	.00033	.07235	3483
-2			75/50	.00487	81,022	334,258	.00036	.07376	.00015	.03039	3483
-3			75/50	.00512	112,497	-544,346	.00048	.09467	.00001	.00233	3483
S-5-04-4	FM-73M		150/0	.00537	63,626	-481,093	.00166	.30822	.00049	.09049	2049
-5			150/0	.00562	43,779	480,750	.00079	.14078	.00029	.05128	1639
-6			150/0	.00587	40,699	366,263	.00122	.20728	.00033	.05562	1639
S-9-030F-2	FM-400		75/50	.00865	188,689	514,418	.00028	.03256	.00013	.01521	5327
-3			75/50	.00875	220,083	666,414	.00024	.02749	.00006	.00698	4917
-4			75/	.00885	196,383	781,527	.00023	.02587	.00009	.01008	4917
S-8-08-F-4	FM-400	75°F/0% R.H. ≈ 10,000 Hrs.	150/0	.00977	133,899	-780,033	.00039	.03995	.00009	.00930	4507
-5			150/0	.01022	221,710	550,715	.00027	.02597	.00011	.01079	4507
-6			150/0	.01067	176,899	725,842	.00033	.03093	.00005	.00422	4507

*LOAD RATE ≈ 1.6 LB/SEC.

sile modulus data is somewhat lower for the FM-73M adhesive vs. that obtained
using the butt joint while that of the FM-400 adhesive is of a similar magnitude.
The ultimate shear strain for FM-73M adhesive is three to four times that mea-
sured using the thick adherend specimen while the ultimate tensile strains
(normal to the adhesive-adherend interface) are approximately equivalent. Due
to the adhesive-cohesive failure mode for the FM-400 thick adherend specimens,
no similar ultimate shear strain comparison is possible. The ultimate tensile
strains are comparable using the two test specimens. Again, the scarf specimens
design and the parallel-plate capacitors gage length (.230") vs. the adhesive
bondline thickness (.004") result in a condition whereby the adherend deforma-
tion is the dominant movement being measured. Moreover, a one microinch error
in the adhesive deformation measurement can lead to a sizable error in determin-
ing the true adhesive mechanical properties response. Therefore, as with the
butt joint specimens, redesign of the scarf joint specimen and capacitor attach-
ment technique is desirable.

10.3 NEAT ADHESIVE TENSILE TEST RESULTS

10.3.1 Specimen Fabrication

Three ply lay-ups neat adhesive were made against Nylon peel-ply on a
polished aluminum "caul" plate, making sure that no bubbles were sealed between
plys. This was accomplished by rolling each ply on to the other from one edge
to the other. On top of the adhesive layup were placed, in consecutive order,
(1) Nylon peel-ply, (2) 0.020 inch aluminum caul sheet, (3) cotton canvas bleeder
cloth and finally (4) Tedlar vacuum sheet. Evacuation of the bag assembly was
maintained during the entire cure and cool down cycle.

Plates of both adhesives were cut into oversize panels using a high speed
saw. Final sizing (6 inch x 0.75 inch) of the panels was made with the saw-cut
pieces stacked and edge cuts made with an end mill. The end mill was then used
to fashion these panels into a dog bone configuration with ends for tabs being
approximately 1.3 inches in length. The gauge length is approximately 3.4 inches
x 0.375 inches, Figure 54. Tapered aluminum end tabs were applied using M-coat
200 and edge sealed with M-coat C. Conditioning at 130°F and 75% relative
humidity was accomplished using a salt saturated aqueous solution and a labora-
tory oven. The moisture level for FM-73M was approximately 1.40% and for FM-400
1.97%.

149
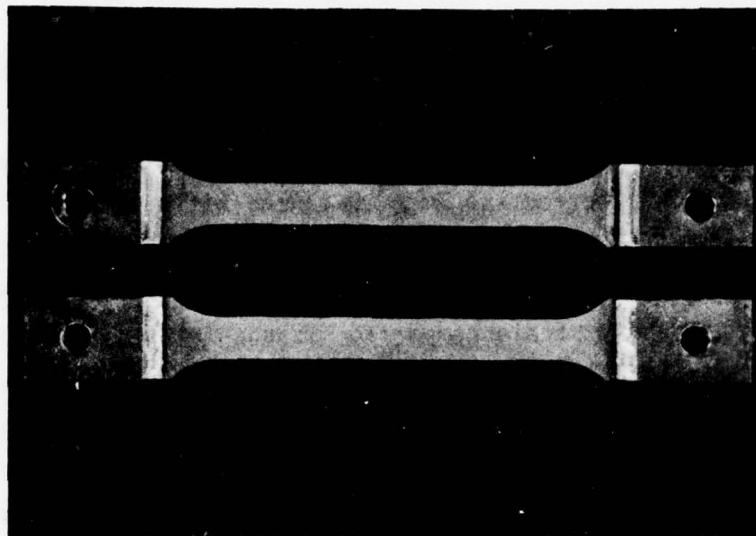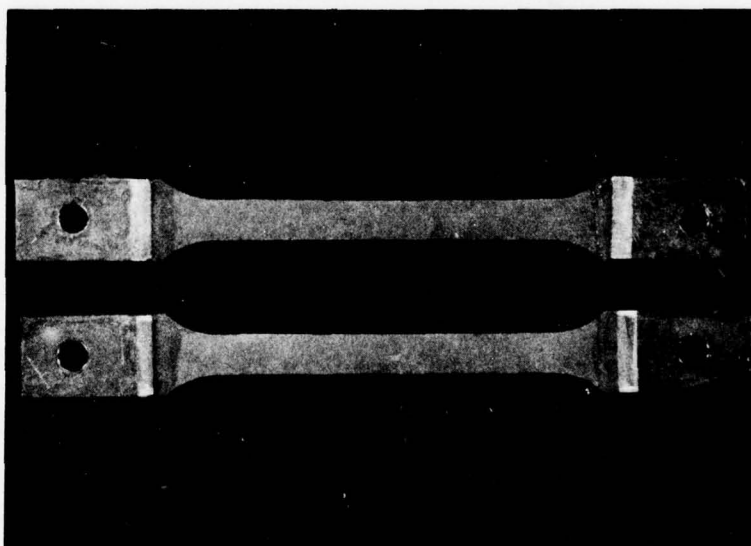
a. FM-73M SPECIMENS

b. FM-400 SPECIMENS

FIGURE 54. BULK TENSILE SPECIMEN GEOMETRY (FM-73M AND
FM-400 ADHESIVE).

10.3.2 Tensile Test Results

Limited tests were performed to evaluate the tensile stress-strain response of neat FM-73M and FM-400 adhesives. Room temperature (75°F) testing was done within one hour after a sample was taken from the chamber. The relative humidity level in the test laboratory was ≅ 40%. Elevated temperature testing was done at the prescribed temperature and relative humidity specified in Table 23. The load rate for all tests was 1.60 lbs/sec. All testing was performed in the Shore Western Environmental Test Chamber. Three specimens were tested for each adhesive and set of environmental conditions. Grip failure was not a problem while overall data scatter is small.

The tensile modulus, maximum strain to failure and ultimate tensile strength data showed far less scatter than the butt joint test results. In general, the tensile modulus and ultimate tensile strength decreased with increasing temperature for both adhesives. The ultimate shear strain increased with temperature for FM-73M while remaining unchanged for FM-400. A direct comparison between the neat and butt joint data was not possible due to the butt joint data scatter and the orthotropic nature of the adhesive; that is for the neat adhesive the load was applied parallel to the scrim; for the butt joint tests, the load was applied normal to the scrim.

10.4 CREEP-RECOVERY TEST RESULTS

To gain insight into the time, temperature, moisture response of adhesive materials, a series of creep-recovery tests were performed per the Creep-Recovery Test Specification in Volume II. Creep-recovery tests were run for thick adherend specimens in shear and butt joint specimens in tension. Neat specimens were loaded in tension only. The bonded and neat specimens were identical to those used in the static tests being fabricated, NDI inspected, and environmentally conditioned along with their static counterparts.

The test assembly including specimen, parallel-plate capacitor (LVDT for neat specimens) and fixture linkages required approximately 45 minutes to stabilize in a given environment. After the test system was stabilized, the specimen was loaded (≅ 10% of it's ultimate load) and unloaded several times (3 ~ 15 times) at the rate of 2 cycles per minute. This exercise is important, in that it will not only mechanically condition the specimen in the chamber, but also enables one to verify the stability of the fixture linkage system so that it will yield reproducible test results.

TABLE 23

SUMMARY OF NEAT ADHESIVE STATIC TENSILE TESTS RESULTS

SPECIMEN	ADHESIVE	LOAD RATE (#/SEC)	COND. ENVIRONMENT TEMPERATURE °F R.H. (%)	TIME IN ENVIRONMENT (HRS)	TEST ENVIRONMENT TEMPERATURE °F	R.H. %	$t_{adh.}$ (in)	E (ksi)	MAX. DISP.* (in)	MAX. STRAIN (in/in)	Tu (PSI)	TYPE FAILURE
2	FM-73M	1.6	SEE NOTE	216	75	75	.0290	300	.0497	.0248	5086	In Central Third of Specimen
4	FM-73M	1.6		240	75	75	.0285	287	.0536	.0268	5153	"
5	FM-73M	1.6		240	75	75	.0304	285	.0484	.0242	5222	"
3	FM-400	1.6		216	75	75	.0333	785	.0082	.0041	3228	"
13	FM-400	1.6		264	75	75	.0339	775	.0070	.0035	2743	"
6	FM-400	1.6		240	75	75	.0344	1112	.0073	.0037	3633	"
7	FM-400	1.6		240	180	75	.0343	564	.0074	.0037	1938	"
8	FM-400	1.6		240	180	75	.0356	538	.0070	.0035	2078	"
9	FM-400	1.6		264	180	75	.0332	594	.0105	.0052	2823	"
10	FM-73M	1.6		264	180	75	.0325	19.	Exceeded LVDT Limit		1630	"
11	FM-73M	1.6		264	150	75	.0299	130.	.1587	.0794	3093	"
12	FM-73M	1.6		264	150	75	.0310	150.	.1479	.0739	3451	"

All specimens conditioned at 130°F, 75% R.H. for 264 hrs. then immersed in 150°F, 75% R.H. per hours listed in table.

*Displacement data obtained using measurement system shown in Figure 32.

The creep-recovery cycle was approximately one hour (15 minutes load - 45 minutes recovery). If creep was observed on the first cycle, a second cycle was run to assess the presence of multiple cycling effects.

Creep and recovery tests of adhesives should be conducted for at least two cycles in order to assess any multiple cycling effects. The transients frequently observed in the creep compliance vs. time response of the material are due to residual stresses and/or flaw effects. After several cycles, the adhesive used in this program responded in a repeatable manner. This was readily verified for a given stress level by inspection of the creep vs. time curve (Figure 55). For a linear viscoelastic material $\varepsilon(t)/\sigma$ is independent of stress and $\varepsilon(t) = \varepsilon(t - t^1)$ where t is the actual time from the initiation of the creep test and t^1 is the time since the stress (load) was removed from the specimen and recovery was initiated.

10.4.1 Thick Adherend (Shear) And Neat Creep - Recovery Test Results

Creep-Recovery tests were conducted using specimens subjected to several temperatures and relative humidities. A summary of the pertinent test parameters are detailed in Table 24, while Figure 55 shows a typical Creep-Recovery response for FM-73M.

For the FM-73M adhesive, creep was observed for temperatures $\geq 120°F$ that had been conditioned in a dessicant. For those specimens conditioned at 75% R.H. a slightly viscous response of the adhesive was observed at 72°F. Creep rupture occured at 160°F, 75% R.H. The FM-400 adhesive experienced a slight time dependent response only at 180°F, 75% R.H.

It was assumed for the FM-73M adhesive that its time-dependent response could be represented by a power law of the form

$$D(t) = D_o (T, R.H.) + D_1 (T, R.H.) t^N \qquad\qquad 67$$

where D_o is the initial compliance and $D_1 t^N$ the time-dependent compliance and D_o, D_1 and N are independent of time. The exponent (N), a material constant, has been determined where possible using the recovery portion of the creep-compliance curve as detailed in Volume II. Linear regression techniques were then used to evaluate D_o and D_1 from the creep test data.
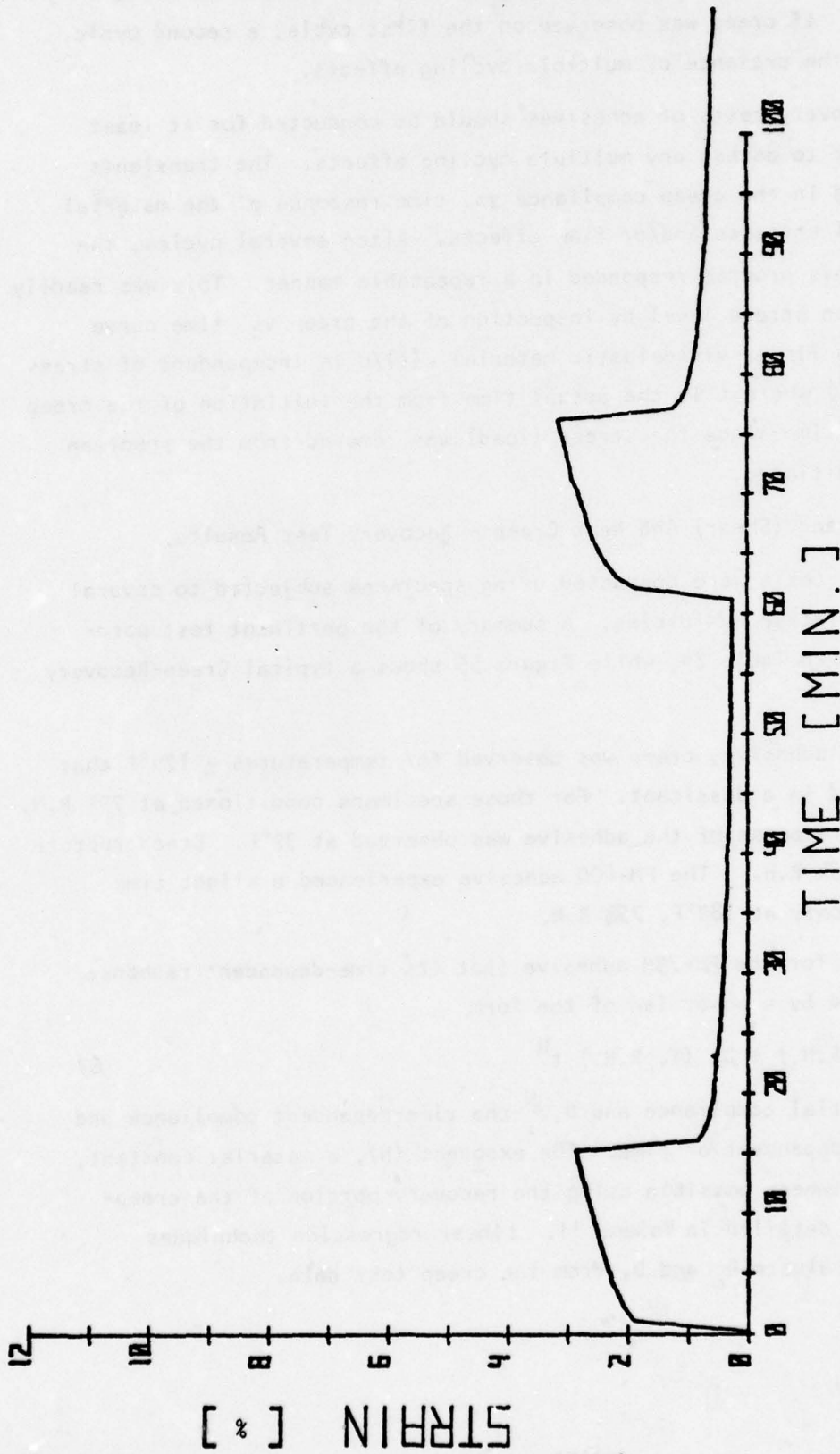
153

FIGURE 55. THICK ADHEREND CREEP-RECOVERY TEST (FM-73M).

TABLE 24

SUMMARY OF THICK ADHEREND SHEAR CREEP TEST RESULTS

SPECIMEN	ADHESIVE	CREEP-RECOVERY LOAD CYCLE	COND. ENVIRONMENT TEMPERATURE °F / R.H. (%)	TIME IN ENVIRONMENT (HRS)	TEST ENVIRONMENT TEMP. °F	TEST ENVIRONMENT R.H. %	t_{adh} (in)	N	STRAIN %	DISP. INCHES	CAP. USED
18L-08-F2	FM-400	15 MIN. @ 20% OF ULT. LOAD; 45 MIN. RECOVERY IF CREEP OBSERVED	DESSICATED	≈ 6216	72	0	.0094		0		3
					120	0			0		3
					160	0			0		3
18L-08-F1	FM-400		DESSICATED	≈ 6216	72	0	.0095		0		2
					120	0			0		2
					160	0			0		2
17L-08-F5	FM-400	15 MIN. @ 20% OF ULT. LOAD; 45 MIN. RECOVERY IF CREEP OBSERVED	133 F 95% R.H. Then 133 F 70% R.H.	336 ≈ 5376	72	75	.0095		0		3
					120	75			0		3
					160	75			0		3
					180	75			.15	.0000142	3
17L-08-F6	FM-400		133 F 95% R.H. Then 133 F 70% R.H.	336 ≈ 5376	72	75	.0095		0		2
					120	75			0		2
					160	75			.2	.000019	2
					180	75			.2	.000019	2

TABLE 24

SUMMARY OF THICK ADHEREND SHEAR CREEP TEST RESULTS (CONT'D)

SPECIMEN	ADHESIVE	CREEP-RECOVERY LOAD CYCLE	COND. ENVIRONMENT TEMPERATURE °F R.H. (%)	TIME IN ENVIRONMENT (HRS)	TEST ENVIRONMENT TEMP. °F	R.H. %	t_{adh} (in)	N	STRAIN %	DISP. INCHES	CAP. USED
14L-08-1	FM-73M	15 MIN. @ 20% OF ULT. LOAD; 45 MIN. RECOVERY IF CREEP OBSERVED	DESSICATED	≈ 6216	150	0	.0102	.35	.15	.0000153	3
					120	0			.18	.0001836	3
					140	0			.3	.0000306	3
					160	0		.35	1.75	.00001785	3
14L-08-2	FM-73M		DESSICATED	≈ 6215	72	0	.0100		0	0	3
					120	0			.2	.00002	3
					140	0		.32	.7	.00007	3
					160	0			1.8	.00018	3
8L-08-2	FM-73M	15 MIN. @ 20% OF ULT. LOAD: 45 MIN. RECOVERY IF CREEP PRESERVED	133°F 95% R.H. Then 133°F 70% R.H.	336 ≈ 5376	72	75	.0101		.1	.0000101	2
					120	75					2
					140	75		.30			2
					160	75		CREEP RUPTURE			2
8L-08-5	FM-73M		133°F 95% R.H. Then 133°F 70% R.H.	336 ≈ 5376	120	75	.0104	.28	.3	.0000312	3
					140	75			1.05	.00001092	3
					160	75		CREEP RUPTURE			

The exponent (N) for FM-73M thick adherend specimens is seen to be approximately .30. N has also been determined from bulk FM-73M and FM-400 creep data. It is .30 for FM-73M and .28 for FM-400 thereby verifying the authenticity of our bonded creep test procedure. The coefficients D_0 and D_1 were also determined selectively using the linear regression procedure for the FM-73M bonded shear specimens at 140°F, 75% R.H.. They were determined to be: D_0 = 9.54 x 10^{-6} psi^{-1}, D_1 = 7.85 x 10^{-6} psi^{-1}. From the bulk FM-73 data at the same temperature and relative humidity D_0 = 21.9 x 10^{-7} psi^{-1} and 6.15 x 10^{-7} psi^{-1}. This is good correlation of bulk vs. bonded joint data for a shear type loading.

If the coefficient information is provided over a wide range of temperatures and humidities, a master curve of creep compliance vs. time can be constructed to enable one to ascertain the effect of a given environment for a given time span on the response of an adhesively bonded structure.

10.4.2 Butt (Tensile) Joint Creep-Recovery Test Results

Butt joint specimens were tested in a creep-recovery type of test for several temperature and two relative humidity levels. A summary of the pertinent test parameters and results are presented in Table 25. Slight creep-recovery response was noted for the FM-73M adhesive with creep rupture occurring at 160°F, 75% R.H. Measurable creep was absent for the FM-400 adhesive for the range of parameters tested. This precluded a comparison of butt joint creep data with the neat tensile data.

For many polymer based systems, which are being characterized well below their T_g level, the Poisson's ratio is ≅ constant. Assuming the material is isotropic, the ratio of shear modulus to tensile modulus will remain approximately constant, implying that the ratio of creep experienced by the material in the linear elastic regime for both shear and tensile loads should remain a fixed percentage of their ultimate strain.

Review of the thick adherend and butt joint test results reveals that the ultimate shear strain for FM-73M is 5.5 times that of its ultimate tensile strain. For the FM-400 adhesive this factor is 3:1, thus a minimal amount of tensile creep strain would be expected. This is what has been observed based on limited test data.

157

TABLE 25

SUMMARY OF BUTT JOINT TENSILE CREEP TEST RESULTS

SPECIMEN	ADHESIVE	COND. ENVIRONMENT TEMPERATURE °F	R.H. (%)	TIME IN ENVIRONMENT (HRS)	TEST ENVIRONMENT °F	R.H. %	$t_{adh.}$ (in)	REMARKS	STRAIN %	DISP. INCHES	CAP. USED.
B-3-04-2	FM-73M	DESSICATED		> 6000	72	75	.0044		0		2
					120	0			.2	.0000088	2
					140	0			.2	.0000088	2
					160	0			.3	.0000132	2
B-3-04-1	FM-73M	DESSICATED		> 6000	140	0	.0044		.2	.0000088	3
					160	0			.3	.0000132	3
B-2-04-1	FM-73M	133°F 95% R.H. Then 133°F 70% R.H.		336 ≅ 5376	120	75	.0055	BAD TEST	0		2
					140	75		(Temp. Drift)			
					160	75		CREEP RUPTURE			
B-2-04-2	FM-73M	133°F 95% R.H. Then 133°F 70% R.H.		336 ≅ 5400	72	75	.0054		0		2
					120	75		BAD TEST			2
					140	75		BAD TEST			2
					160	75		CREEP RUPTURE			2

TABLE 25

SUMMARY OF BUTT JOINT TENSILE CREEP TEST RESULTS

SPECIMEN	ADHESIVE	COND. ENVIRONMENT TEMPERATURE °F R.H. (%)	TIME IN ENVIRONMENT (HRS)	TEST ENVIRONMENT °F	TEST ENVIRONMENT R.H. %	$t_{adh.}$ (in)	REMARKS	STRAIN %	DISP. INCHES	CAP. USED.
B-26-03-F2	FM-400	DESSICATED	> 6000	72	0	.0098		0		2
				120	0			0		2
				160	0			0		2
				180	0			.10	.0000097	2
B-26-08-F1	FM-400	DESSICATED	> 6000	72	0	.0097		0		3
				120	0			0		3
				160	0		TEMP. DRIFT			3
				180	0			0		3
B-33-04-F6	FM-400	133°F 95% Then 133°F 70%	≈ 5900	72	75	.0069		0		2
				120	75		BAD DATA			2
				160	75		BAD DATA			2
				180	75			0		2
B-33-04-F5	FM-400	133°F 95% Then 133°F 70%	≈ 5900	72	75	.0068		0		3
				120	75			0		3
				150	75			0		3
				180	75			0		3

The limited testing was done in order to verify the adequacy of the recommended test procedure and the stability, sensitivity and accuracy of the parallel plate capacitor in the various environments. While this was accomplished, a longer time at load (creep) may have revealed a viscoelastic response of the material at the higher temperatures. Again as with the static tests the capacitance gages response was somewhat unstable at times during the test period. This could be due to moisture, the specimen geometry, or the pin attachment problem discussed in Section 10.2.2
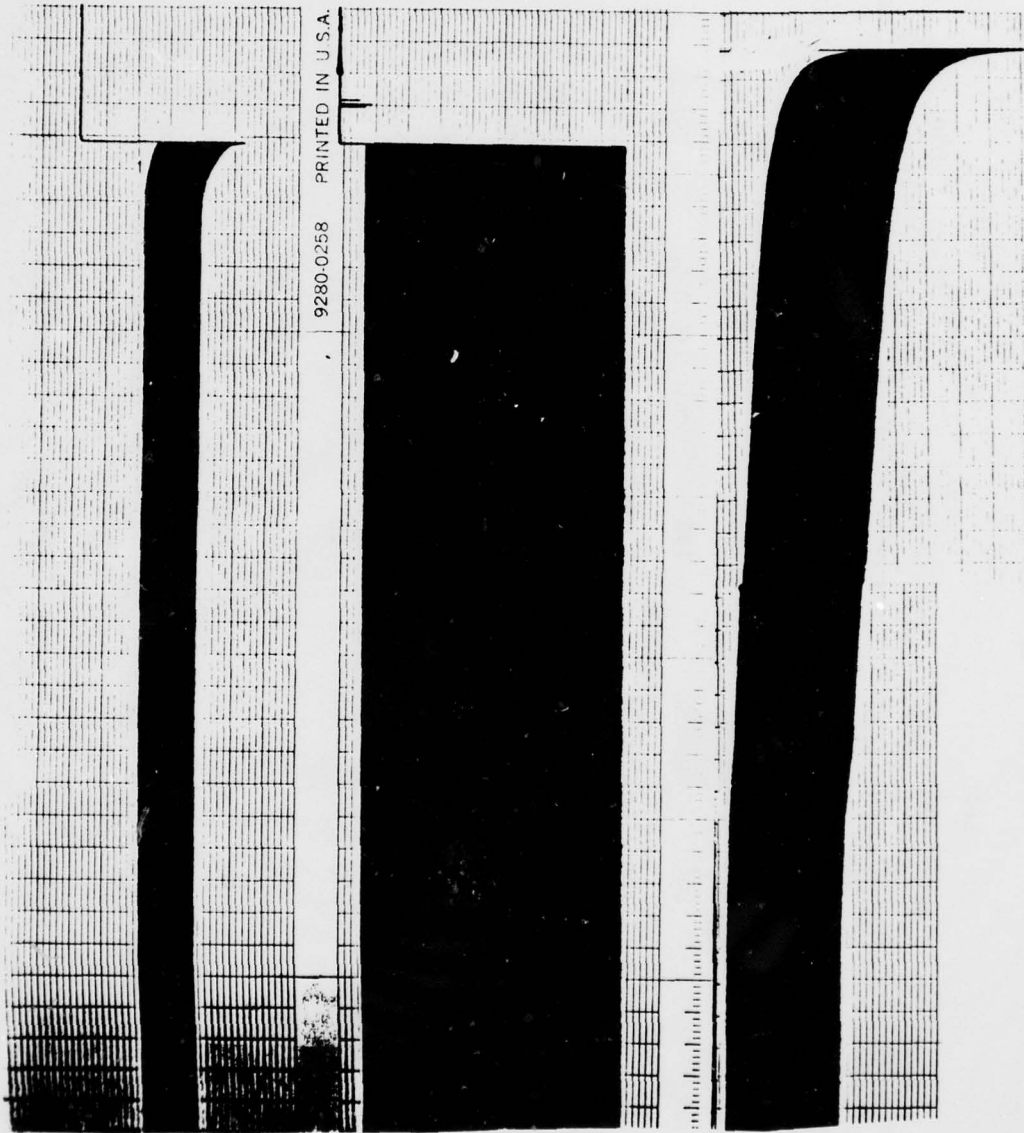
10.5 FATIGUE TEST RESULTS

Limited fatigue tests were run to partially substantiate the correctness of the Fatigue Test Specification (Volume II) and to ascertain the performance of the parallel plate capacitor under a fatigue type load. Both thick adherend and butt joint specimens were tested. All specimens were from the same group used for the static test portion of the program and had been in a dessicant for more than 5000 hours or had attained 95-100% of their moisture equilibrium value (75% R.H. specimens) prior to testing.

The specimens, once removed from the environmental conditioning chamber, were immediately placed in a universal type grip within the controlled environment of the environmental test facility with the ATC designed parallel plate capacitor attached to them. The recording device was set to the proper sensitivity to record the load vs. deformation results. The frequency was 2 Hz while the constant sinusoidal load ratio was + .10 for all tests. Once the capacitor had stabilized in the environment, the test was begun. The load and deformation was monitored continuously on a strip chart recorder (Figure 56).

A summary of the test results are shown in Table 26. Overall, the fatigue endurance of FM-400 was superior to that of FM-73M.

The parallel plate capacitor performed in excellent fashion for both butt and thick adherend test specimens, Figure 56, shows the typical repeatability of the capacitor observed for up to 130,000 cycles (test No. 5) and its ability to measure the creep the adhesive experienced just prior to failure. It is anticipated that the accelerated creep phenomena observed just prior to specimen failure is due to the growth of numerous flaws that have been developed in the material under the fatigue loading mode.

160

FIGURE 56. TYPICAL STRIP CHART RECORD OF FATIGUE TESTS

161

TABLE 26. SUMMARY OF FATIGUE TEST RESULTS

TEST #	SPEC. ID	LOAD (%)			NO. OF CYCLES	TEST ENV. TEMP./R.H.%	COND. ENV. TEMP./R.H.%	REMARKS
		MAX.	ULT.	MIN.				
1	5-L-04-3	720	50.	72	7,900	120°/0%	130°/75%	
2	12-L-08-1	720	50.	72	160,250	120/0%	75°/0%	Residual Static Str. 1350 lbs.
3	12-L-08-2	1008	70	100	236	150/0%	75/0%	
4	12-L-08-3	864	60	86	118	150/0%	75/0%	
5	18-L-08-F-4	720	50.	72	123,000	150/0%	75/0%	
5	18-L-08-F-4	980	65	98	125,000-126,000	150/0%	75/0%	
5	18-L-08-F-4	1120	75	112	126,000-130,548	150/0%	75/0%	
6	18-L-08-F-5	1143	80	114	2,451	150/0%	75/0%	
7	18-L-08-F-6	1143	80	114	7,574	150/0%	75/0%	
8	B-2-04-4	840	70	84	142	150/0%	130°/75%	
9	B-2-04-5	720	60	72	1,400	150/0%	130°/75%	
10	B-2-04-6	480	50	48	79,900	150/0%	150/0%	
11	B-35-08-F-1	686	50	69	146,000	150/0%	75°/0%	Residual Static Str. 1200 lbs.
12	B-35-08-F-2	1097	80	110	7,136	150/0%	75°/0%	
13	B-35-08-F-3	1097	80	110	7,591	150/0%	150/0%	

162

SECTION XI

CONCLUSIONS AND RECOMMENDATIONS

The overall goal of this program was met namely; to assess and develop the low cost test procedures required to generate rigorous engineering structural property data. Significant accomplishments and problem areas include:

o Development of an analytical model to optimize butt and scarf joint test specimen geometry.

o Definition of easily executable Fabrication and Test Specifications to accurately characterize the mechanical response of an adhesive in severe environments, subjected to a variety of load conditions. These were verified by the fabrication and testing of specimens.

o Bondline thickness control and void free bondlines in butt (scarf) joints is difficult to achieve in a consistent manner.

o Neutron Radiography was shown to be superior in detecting voids of 5 mils or less for each test specimen geometry.

o The overall goal to measure the adhesive deformation within $\pm 2 \times 10^{-6}$ inches was not attainable for the butt (scarf) joint specimens. This was primarily due to specimen geometry (small bondline thickness) and capacitor attachment geometry.

o The LVDT extensometer was determined to perform in a superior manner on NEAT specimens in severe environments.

o A unique, highly sensitive, highly accurate uniaxial and biaxial capacitance measurement device was designed. Specific redesign of the biaxial unit as a do it all model should be considered. The specimen attachment concept and the use of a ceramic insulator should be considered during the redesign.

o Based on limited data, promising correlation between NEAT and thick adherend shear specimen test data was found as regards the viscoelastic characterization of an adhesive.

163

Recommendations for future work include:

o   Establish a data base (static, fatigue, viscoelastic) for a specific adhesive; design "real structure" using the data base and attempt to verify the goodness of the data base with a test-theory correlation program.

o   The effect of various combinations of loading and environment on the mechanical and physical response of adhesives needs to be quantified for design purposes (see Section 2.5).

REFERENCES

1. Volkersen, O., "Die Nietraftverteilung in zugbeanspruchten Nietverbindungen mit knostaten Laschenquerschntten," Luftfahrtforschung, Vol. 15, 1938, pp. 41-47.

2. Plantema, F. J., De Schuifspanning in eme lijmnaad, Report M1181, Nat Luchtvaartlaboratorium, Amsterdam, 1949.

3. Goland, M. and Reissner, E., "The Stresses in Cemented Joints", Journal of Applied Mechanics, March 1944, Page A-17.

4. Dietz, A. G. H., Grinsfelder, H., and Reissner, E., "Glueline Stresses in Laminated Wood", presented at ASME Annual Meeting, November 1945.

5. Aleck, B. J., "Thermal Stresses in a Rectangular Plate Clamped Along an Edge", Transactions ASME, Vol. 71, 1949, p. A-118.

6. Norris, C. B. and Ringelstetter, L. A., "Shear Stress Distribution Along Glue Line Between Skin and Cap-Strip of an Aircraft Wing", NACA-TN-2152, July 1950.

7. DeBruyne, N. A. and Houwink R., "Adhesion and Adhesives", Elsevier Publishing Co., 1951.

8. Cornell, R. W., "Determination of Stresses in Cemented Lap Joints", Journal of Applied Mechanics, 20, No. 3, pp. 355-364, September 1953.

9. Niskanen, E., "On The Distribution of Shear Stress in a Glued Specimen of Isotropic or Anisotropic Material", State Institute For Technical Research Report, Finland, 1955.

10. Sherrer, R. E. "Stresses in a Lap Joint with Elastic Adhesive", Forest Products Laboratory Report No. 1864, September 1957.

11. Benson, N. K., "The Mechanics of Adhesive Bonding", Applied Mechanics Reviews, Vol. 14, No. 2, February 1961, Page 83.

12. Bikerman, "The Science of Adhesive Joints", Academic Press, 1961.

13. Hahn, K. F. and Houser, D. F., "Methods of Determining Stress Distribution in Adherends and Adhesives", Journal of Applied Poly. Sci., 6, pp. 145-149, 1962.

14. Goodwin, J. F., "Research on Thermomechanical Analysis of Brazed or Bonded Structural Joints", ASD-TDR-63-447, September 1963.

15. Wang, D. Y., "Influence of Stress Distribution on Fatigue Strength of Adhesive-Bonded Joints", Journal of Experimental Mechanics, June 1964, pp. 173-181.

16. Szepe, F., "Strength of Adhesive-Bonded Lap Joints With Respect to Change of Temperature and Fatigue", paper presented at the Second SESA International Congress on Experimental Mechanics held in Washington, D. C. October 1965.

17. Kelsey, S., and Benson, N. K., Institut fur Statik and Dynamik, Technische Hochschule, Stuttgart, ISD Report No. 10, 1966.

18. Lehman, G. M. and Hawley, A. V., "Investigation of Joints in Advanced Fibrous Composites for Aircraft Structures", Vol. 1, AFFDL-TR-69-43, June 1969.

19. Air Force - Advanced Composite Materials Design Guide, January 1973.

20. Corvelli, N. and Salema, E., "Analysis of Bonded Joints" Grumman Aerospace Corporation, Internal Report No. ADR 02-01-70.1, 1970.

21. Grimes, G. C., et. al., "Experimental Aspects of Adhesive Bonded Joints", Presented at 1970 National SAMPE Technical Conference on "Aerospace Adhesives and Elastomers", October 1970.

22. Erdogan, F. and Ratwani, M., "Stress Distribution in Bonded Joints", Journal of Composite Materials, 5, pp. 378-393, (1971).

23. Grimes, G. C., Blackstone, W. R., Greimann, L. F., and Wah, T., "The Development of Nonlinear Analysis Methods For Bonded Joints in Advanced Filamentary Composite Structures", AD905201-L, AFFDL-TR-72-97, March 1972.

24. Harrison, N. L. and Harrison, W. J., "The Stresses in an Adhesive Layer", Journal of Adhesion, Vol. 3, 1972, pp. 195-212.

25. Dickson, J. N., Hsu, T. M., and McKinney, J. M., "Development of an Understanding of the Fatigue Phenomena of Bonded and Bolted Joints in Advanced Filamentary Composite Material", AFFDL-TR-72-64, Vol. I, June 1972.

26. Pahoja, M. H., "Stress Analysis of an Adhesive Lap Joint Subjected to Tension, Shear Force and Bending Moments", T. & A.M. Report No. 361, August 1972.

27. Wooley, G. R. and Carver, D. R., "Stress Concentration Factors for Bonded Lap Joints", J. Aircraft, 8 (1971), 817-20.

28. Gehring, R. W., Matoi, T. T., and Hughes, E. J., "Evaluation of Environmental and Service Conditions on Filamentary Reinforced Composite Structural Joints and Attachments", AFML-TR-71-194, Volume 1, November 1971.

29. Sainsbury-Carter, J. B., "Automated Design of Bonded Joints", Journal of Engineering for Industry, p. 919, November, 1973.

30. Terekhova, L. P. and Skoryi, I. A., "Stresses in Bonded Joints of Thin Cylindrical Shells", Strength Mater., 4 (1973), 1271-74. Translation of Probl. Proch., No. 10 (1972), 108-10.

31. Barker, R. M. and Hatt, F., "Analysis of Bonded Joints in Vehicular Structures", AIAA Journal, Vol. 11, No. 12, December 1973, page 1650.

32. Hart-Smith, L. J., "Analysis and Design of Advanced Composite Bonded Joints", Douglas Aircraft Company, Inc., McDonnell-Douglas Corporation, Long Beach, California, NASA-CR-2218, 1973.

33. Hart-Smith, L. J., "Adhesive-Bonded Double-Lap Joints", Douglas Aircraft Company, NASA Langley Contract NAS-11234, Report No. NASA CR 112235, January 1973.

34. Hart-Smith, L. J., "Adhesive-Bonded Single-Lap Joints", Douglas Aircraft Company, NASA Langley Contract NASL-11234, Report No. NASA CR 112236, January 1973.

35. Renton, W. J. and Vinson, J. R., "The Analysis and Design of Composite Material Bonded Joints Under Static and Fatigue Loadings", Air Force Office of Scientific Research TR No. 1760-72, August 1973.

36. Renton, W. J. and Vinson, J. R., "The Analysis and Design of Anisotropic Bonded Joints", Report No. 2, AFOSR Report No. 75-0125, August 1974.

37. Sharpe, W. N. and Muha, T. J., "Comparison of Theoretical and Experimental Shear Stress in the Adhesive Layer of a Lap Joint" Proceedings of the Army Symposium on Solid Mechanics, Cape Cod, Mass., 1974: The Role of Mechanics in Design Structural Joints.

38. Adams, R. D. and Peppiatt, N. A., "Stress Analysis of Adhesive-Bonded Lap Joints", Journal of Strain Analysis, Vol. 9, No. 3, July 1974, pp. 185-196.

39. Pirvics, J., "Two Dimensional Displacement-Stress Distribution in Adhesive Bonded Composite Structures", Journal of Adhesion, Vol. 6, 1974, pp. 207-228.

40. Murphy, M. M. and Lenoe, E. M., "Stress Analysis of Structural Joints and Interfaces - A Selective Annotated Bibliography", AMMRC-MS-74-10, Sept. 1974.

41. Renton, W. J. and Vinson, J. R., "Fatigue Response of Anisotropic Adherend Bonded Joints," presented at AMMRC Symposium on Solid Mechanics, Cape Cod, Mass.,1974: The Role of Mechanics in Design-Structural Joints, September 1974.

42. DasGupta, S. and Sharma, S. P., "Stresses in an Adhesive Lap Joint", ASME Publication, 75-WA/DE-18, 1975.

43. Renton, W. J. and Vinson, J. R., "Fatigue Behavior of Bonded Joints in Composite Material Structures", Journal of Aircraft, Vol. 12, No. 5, May 1975, p. 442-447.

44. Renton, W. J. and Vinson, J. R., "The Efficient Design of Adhesive Bonded Joints", Journal of Adhesion, Vol. 7, pp. 175-193, 1975.

45. Renton, W. J. and Vinson, J. R., "Shear Property Measurements of Adhesives in Composite Material Bonded Joints", ASTM STP 580 on Composite Reliability, 1975.

46. Renton, W. J. and Vinson, J. R., "On The Behavior of Bonded Joints in Composite Material Structures", Journal of Engineering Fracture Mechanics, Vol. 7, pp. 41-60, 1975.

47. Srinivas, S., "Analysis of Bonded Joints", NASA TN D-7855, April 1975.

48. Renton, W. J. and Vinson, J. R., "Factors Influencing The Efficient Design of Structural Adhesive Joints", Report No. 3, AFOSR Contract 1760-72, to be published.

49. Hart-Smith, L. J., "Non-Classical Adhesive Bonded Joints in Practical Aerospace Construction", NASA-CR-112238.

50. Mitchell, R. A., Wolley, R. M., and Chwinot, D. J., "Analysis of Composite-Reinforced Cutouts and Cracks", AIAA Journal, Vol. 13, No. 6, June 1975, pp. 744-749.

51. Mitchell, R. A., Wolley, R. M., and Baker, S. M., "Finite Element Analysis of Spotwelded, Bonded and Weldbonded Lap Joints", NBSIR 75-957, December 1975.

52. Kline, S. J., "Similitude and Approximation theory", McGraw-Hill, 1965.

53. Hughes, E. J. and Rutherford, J. L., "Study of Micromechanical Properties of Adhesive Bonded Joints", Technical Report No. 3744, August 1968.

54. Zabora, R. F., et. al., "Adhesive Property Phenomena and Test Techniques" AD-729873, July 1971.

55. Renton, W. J., "The Symmetric Lap Joint-What Good Is It?," presented at the Society of Experimental Stress Analysis Spring Meeting, Silver Spring, Md. May 1976.

56. Schaevitz Engineering, "Handbook of Measurement and Control" 1972.

57. Microstrain in Polycrystalline Metals", N. Brown and K. F. Lukens Jr., Acta Metallurgica, V9, February 1961, page 106

58. Rutherford, J. L., Bossler, F. C., and Hughes, E. J., Review of Scientific Instrumentation "Capacitance Methods for Measuring Properties of Adhesives in Bonded Joints" Vol. 39, No. 5, 1968, page 666.

59. Yeakley, L. M., Lindholm, U. S., "Development of Capacitance Strain Transducers for High Temperature and Biaxial Applications", Experimental Mechanics, August 1974, page 331.

60. Automatic Systems Laboratories Product Summaries.

61. Hi-Tec Systems - Capacitive Strain Gage Technical Data Sheet.

62. CERL Planer High Temperature Technical Data Sheet.

63. General Radio Corporation Catalog #73, p. 147.

64. Schaevitz LVDT Catalog Handbook #HB-72.

65. Tinius Olsen Product Catalog

66. Lion, Kurt S., "Instrumentation in Scientific Research Electrical Input Transducers". McGraw-Hill, 1959.

67. Sharpe, W.N., Jr., "A Short-Gage-Length Optical Gage for Small Strain" Journal of Experimental Mechanics, September 1974, Page 373.

68. Kreiger, R. B., Jr., "Stiffness Characteristics of Structural Adhesives for Stress Analysis in Hostile Environment", American Cyanamid Company Blooming-dale Plant, Havre de Grace, Maryland, presented at Albuquerque, N.M., SAMPE Meeting, October 1975.

69. Shapery, R. A., "Stress Analysis of Viscoelastic Composite Materials," Journal of Composite Materials, Vol. 1, 1967, p. 228.

70. Shen, H. K. and Rutherford, J. L., "Study of The Performance of Adhesive Bonded Joints, Final Report, AD 880416, November 1970.

71. Frazier, T. B., et. al., "Durability of Adhesive Bonded Joints", AFML-TR-74-26 March 1974.

72. Marceau, A. and Scardino, W. M., "Durability of Adhesive Bonded Joints", AFML-TR-75-3, February 1975.

73. Kreiger, R. G., Jr., "Evaluating Structural Adhesives Under Sustained Load In Hostile Environment", paper presented at 5th National Technical Conference of the Society for the Advancement of Material and Process Engineering, October 1973.

74. Norris, C. B., "Plastic Flow Throughout Volume of Thin Adhesive Bonds", Forest Products Laboratory Report No. 2092, March 1958.

75. Fort, T., Private Communication

76. Chmura, M. and McAbee, E., "Correlation of Mechanical Properties of Resins Obtained in an Adhesive Joint and in Bulk Form", Technical Report No. 3330, April 1966.

77. Lindsey, G. H., Schapery, R. A., Williams, M. L., and Zak, A. R., "The Triaxial Tension Failure of Viscoelastic Materials", Aerospace Research Laboratory Report 63-152, 1963.

78. Bikerman, "The Science of Adhesive Joints", Academic Press, 1961.

79. "Treatise on Adhesion and Adhesives", Edited by R. L. Patrick, Volumes I and II, 1969.

80. Parker, R. S. and Taylor, P., "Adhesion and Adhesives", Pergamon Press, 1966.

81. Stanger, A. G. and Blomquist, R. F., "Block Shear, Cross-Lap Tension, and Glueline Cleavage Methods of Testing Glued Joints", Journal of Forest Products, December 1965.

82. Anon, "Solid Propellant Mechanical Behavior Manual", published by the Chemical Propulsion Information AGency, Publication No. 21, November 1963.

83. Kuenzi, E. W. and Stevens, G. H., "Forest Products Laboratory Report No. FPL-011, September 1963.

84. Jones, W. B., Kaelble, D. H., and Knauss, W. G., "Investigation of Fatigue and Crack Propagation Behavior of Adhesives", AFML-TR-72-218, Part I, October 1972.

85. Tellman, S. J. and Soper, V. R., "Measurement of Uniaxial Creep of Selected Adhesives in Free Film Form", Forest Products Laboratory Report No. 0157, March 1967.

86. Wegman, R. F., Devine, A. T., Vacher, C. L., and Anderson, M. D., "Effect of Mechanical Properties of Adherend on Adhesive Bond Strengths", Picatinny Arsenal TR No. 3602, October 1967, AD 661040.

87. "Forest Products Laboratory List of Publications on Glue, Glued Products, and Veneer", U. S. Department of Agriculture Forest Service, April 1968.

88. Bryant, R. W. and Dukes, W. A., "The Effect of Joint Design and Dimensions on Adhesive Strength", Explosives Research and Development Establishment, Report ERDE-5/M/68, (England) 1968.

89. Yalof, Stanley, "Technology in Transition", 20th National SAMPE Symposium and Exhibition, Volume 20, p. 296, April 1975.

90. Hofer, K. E., "Development of Engineering Data on The Mechanical and Physical Properties of Advanced Composites Materials", IIT Research Institute, AD-757, 524, September 1972.

91. "Proceedings of The Second Conference on Fibrous Composites in Flight Vehicle Design", Final Technical Report AFFDL-TR-74-103, May 1974.

92. Hayden, H. W., Moffett, W. G., and Wulff, J., "The Structure and Properties of Materials", Volume III, Wiley and Sons, Inc., 1965.

93. Lin, C. J. and Bell, J. P., Journal of Applied Polymer Science, A-1, 16, 1972.

94. McCarvill, W. T. and Bell, J. P., "Torsional Test Method for Adhesive Joints", Journal of Adhesion, Vol. 6, 1974, pp. 185-193.

95. Teh, J. W., White, J. R., and Andrews, E. H., "Creep-Compensated Fatigue Testing of Polyethylene Under Reversed Loading Conditions", Journal of Materials Science, Vol. 10, 1975, pp. 1626-1635.

96. Rabinowitz, S. and Beardmore, P. "Cyclic Deformation and Fracture of Polymers", Journal of Materials Science, Vol. 9, 1974, pp. 81-99.

97. Dhran, C. K. H., "Fatigue Failure in Graphite Fibre and Glass Fibre-Polymer Composites", Journal of Materials Science, Vol. 10, 1975, pp. 1665-1670.

98. Arad, S., Radon, J. C., and Culver, L. E., "Fatigue Crack Propagation in Polymethylmethacrylate; The Effect of Loading Frequency", Journal Mechanical Engineering Scinece, Vol. 14, No. 5, 1972.

99. Brinson, H. F., Renieri, M. P., Herakvich, C. T., "Rate and Time Dependent Failure of Structural Adhesives", VPI Report E-74-25, September 1974.

100. Federal Test Method Standard No. 175 A "Adhesives-Methods of Testing", 1967.

101. Federal Specification MMM-A-134, "Adhesive, Epoxy Resin, Metal to Metal Structural Bonding", 1970.

102. Lubkin, J. L., Journal of Applied Mechanics, Volume 24, 1957, page 137.

103. Lackman, et. al., "Advanced Composites Data For Aircraft Structural Design-Vol. III; Theoretical Methods", AFML-TR-70-58, 1970.

104. McLaren, A. S. and MacInnes, I., British Journal of Applied Physics, Volume 9, 1958.

105. Dance, W. E., "Neutron Radiographic Nondestructive Evaluation of Aerospace Structures," ASTM Publication STP 586, 1976, page 137.

106. Petersen, D. H., and Dance, W. E., "Detection of Adhesive Bondline Flaws by Neutron Radiography," Proceedings of the Fourth AMMRC Technology Conference, Boston, Mass., "Advances in Joining Technology", September 1975.

107. Kinloch, A. J., "Environmental Failure of Structural Adhesive Joints: A Literature Survey", Technical Note No. 95, Explosives Research and Development Establishment, Ministry of Defense, England, August 1973.

108. Gledhill, R. A. and Kinloch, A. J., "Environmental Failure of Structural Adhesive Joints", Journal of Adhesion, Vol. 6, 1974, pp. 315-330.

109. Kinloch, A. J., Dukes, W. A., and Gledhill, R. A., "Durability of Adhesive Joints", to be published in "Adhesion Science and Technology", Plenum Press, New York, 1975, Ed. L. H. Lee.

110. Kerr, C., MacDonald, N. C., and Orman, S., "Effect of Hostile Environments on Adhesive Joints", British Polymer Journal, Vol. 2, January 1970, pp. 67-70.

111. Orman, S. and Kerr, C., "The Effect of Water on Aluminum-Epoxide Bonds", Aspects of Adhesion, Editor, D. J. Alner, University Press, London, 1969.

112. West, B. S., "Bonded Joints in Composite Structures", AFFDL-TR-73-99, November 1973.

113. MacDonald, N. C., "The Effect of Moisture on Adhesive Bonds", Aspects of Adhesion, Editor, D. J. Alner, University of London Press.

114. Eickner, H. W., Olson, W. Z., and Blomquist, R. F., "Effect of Temperatures From -70° to 600°F on Strength of Adhesive-Bonded Lap Shear Specimens of Clad 24S-T3 Aluminum Alloy and of Cotton-And Glass-Fabric Plastic Laminates", NASA Technical Note 2717, June 1952.

115. Gillespie, R. H., "Accelerated Aging of Adhesives in in Plywood-Type Joints", Forest Products Journal, September 1975.

116. Hall, J. R., "Effect of Salt Spray Environment on Bonded Aluminum Panels Under Complex Stressing", Picatinny Arsenal Technical Memorandum 2112, May 1974.

117. Croke, D. R. et. al., "Test to Determine Corrosion Resistance of Adhesive Primer Systems", Test Methods Forum, January 1971.

118. Kuenzi, E. W., "Strength of Aluminum Lap Joints at Elevated Temperatures", Forest Products Laboratory Report No. 1808, 1954.

119. Black, J. M. and Blomquist, R. F., "Polymer Structure and the Thermal Deterioration of Adhesives in Metal Joints, Part 1, 2, Adhesives Technology.

120. Croke, D. R., Krupp, W. E., Robinson, W. C., and McCurdy, R. N., "A Test to Determine The Corrosion Resistance of Adhesive-Primer Systems", Materials Research and Standards, January 1971.

121. Duckett, R. A., Rabinowitz, S., and Ward, I. M., "The Strain-Rate, Temperature and Pressure Dependence of Yield of Isotropic Poly(methylmethacrylate) and Poly(ethylene terephthalate)", Journal of Materials Science, Vol. 5, 1970, pp. 909-915.

122. Tiezzi, G. J., and Doyle, H. M., "Stress-Strain Behavior of Adhesives in a Lap Joint Configuration at Ambient and Cryogenic Temperatures", Journal of Macromolecular Science-Chemistry, November 1969, pp. 1331-1353.

123. Schwarzl, F., Staverman, A. J., "Time-Temperature Dependence of Linear Visco-elastic Behavior," Journal of Applied Physics, Volume 23, No. 8, 1952, page 838.

124. Schapery, R. A., "Effect of Cyclic Loading on The temperature in Visco-elastic Media With Variable Properties", AIAA Journal, May 1964, page 827.

125. Timoshenko, S., "Theory of Elasticity, McGraw-Hill, 1970.

126. Williams, M. L. and Schapery, R. A., "Studies of Viscoelastic Media", Aerospace Research Laboratory Report 62-366, June 1962.

127. Schapery, R. A., "Deformation and Failure Analysis of Viscoelastic Composite Materials", Chapter 5 in Inelastic Behavior of Composite Materials, C. T. Herakovich, Editor, ASME, 1975.

128. Ferry, J. D., "Viscoelastic Properties of Polymers, 2nd Ed., Wiley, 1970.

129. Schapery, R. A., "Viscoelastic Behavior and Analysis of Composite Materials", Vol. 2, G. P. Sendeckyj, Ed., Academic Press, 1974, p. 85.

130. Schapery, R. A., "On The Characterization of Nonlinear Viscoelastic Materials", J. Polymer Engineering and Sci., Vol. 9, 1969, . 295.

131. Lou, Y. C. and Schapery, R. A., "Viscoelastic Characterization of a Nonlinear Fiber-Reinforced Plastic", Journal Composite Material, Vol. 5, 1971, p. 208.

132. Williams, M. L., "Structural Analysis of Viscoelastic Materials", AIAA Journal, May 1964

133. Lee, E. H., "Stress Analysis In Viscoelastic Bodies", Brown University, Division of Applied Mathematics, TR8, June 1954.

134. Cost, T. L., "Approximate Laplace Transform Inversions in Viscoelastic Stress Analysis", AIAA Journal, December 1964, page 2157.

135. Morland, L. W. and Lee, E. H., "Stress Analysis for Linear Viscoelastic Materials With Temperature Variation", Transactions of The Society of Rheology, Volume IV, 1960, page 233.

136. Kelley, F. N. and Williams, M. L., "The Engineering of Polymers For Mechanical Behavior" Rubber Chemistry and Technology Journal, 1970.

137. Schapery, R. A., "Approximate Methods of Transform Inversion for Viscoelastic Stress Analysis", Proceedings 4th U.S. National Congress Applied Mechanics, ASME (1962).

138. Cuthrell, R. E., "Macrostructure and Environment-Influenced Surface Layer in Epoxy Polymers", Journal of Applied Polymer Science, Vol. 11, 1967. pp. 949-952.

139. "Primary Adhesively Bonded Structure Technology", Alert Technical Bulletin Douglas Aircraft Company, McDonnell Douglas Corporation, USAF Contract F33615-75-C-3016, October 1975.

140. Devine, A. T., Tanner, W. C., Wegman, R. F., Bodnar, M. J., and Anderson, M. D., "Effect of Varying Processing Parameters in The Fabrication of Adhesive-Bonded Structures, Part III: Bonding Glass Reinforced Plastics", Picatinny Arsenal TR No. 4002, December 1970.

141. Bascom, W. D., and Cottington, R. L., "Air Entrapment in The Use of Structural Adhesive Films", Journal of Adhesion, Vol. 4, 1972, pp. 193-209.

142. McIntyre, R. T., Duer, F. L., and Gallagher, E. A., "Effect of Varying Processing Parameters in the Fabrication of Adhesive-Bonded Structures, Part VI: Production Methods, Final Report", Picatinny Arsenal, TR No. 4162, February 1971.

143. Tanner, W. C., "Adhesives and Adhesion in Structural Bonding For Military Material", Applied Polymer Symposia No. 3, 1966, pp. 1-25.

144. Sharpe C. H., "Some Aspects of The Permanence of Adhesive Joints", Structural Adhesive Bonding", pp. 353-359, Applied Polymer Symposium No. 3, Interscience Publisher, 1966.

145. Bascom, W. D., "Adhesive Fracture of Epoxy and Elastomer Epoxy Resins", presented at the 4th AMMRC Army Materials Technology Conference, Boston, September 1975.

146. Jemian, W. A. and Ventrice, M. B., "The Fracture Toughness of Adhesive-Bonded Joints", Journal of Adhesion, Volume 1, July 1969, pp. 190-207.

147. Wilcox, R. C. and Jemian, W. A., "Scanning Electron Fractography of Lap-Shear Joints", Polymer Engineering and Science, Vol. 13, No. 1, January 1973.

148. Jennings, C. W., "Surface Preparation For Adhesive Bonding". To be published in Journal of Adhesion.

149. Wegman, R. F., et. al., "Durability Studies of Adhesive-Bonded Metallic Joints", AD/B000997, December 1974.

150. ASTM D-2095 "Tensile Strength of Adhesives by Means of Bar & Rod Specimens"

151. ASTM D-2094 "Preparation of Bar and Rod Specimens For Adhesion Tests"

152. ASTM D-1002 "Strength Properties of Adhesives In Shear By Tension Loading"

153. ASTM D-3163 "Determining The Strength of Adhesively Bonded Rigid Plastic Lap Shear Joints In Shear By Tension Loading"

154. ASTM D-3164 "Determining The Strength of Adhesively Bonded Plastic Lap-Shear Sandwich Joints In Shear By Tension Loading"
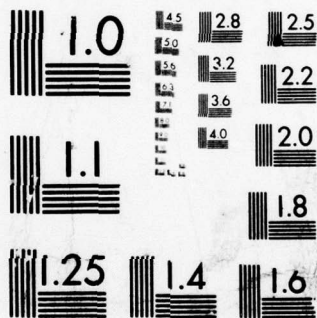
MICROCOPY RESOLUTION TEST CHART

NATIONAL BUREAU OF STANDARDS-1963-A

155. ASTM D-3165 "Strength Properties of Adhesives In Shear By Tension Loading of Laminated Assemblies"

156. ASTM D-2919 "Determining Durability of Adhesive Joints Stressed In Shear By Tension Loading"

157. ASTM D-3166 "Fatigue Properties of Adhesives In Shear By Tension Loading"

158. ASTM D-1780 "Conducting Creep Tests of Metal-to-Metal Adhesives"

159. ASTM D-2294 "Conducting Creep Tests of Metal-to-Metal Adhesives".

160. ASTM D-897 "Tensile Properties of Adhesive Bonds"

161. ASTM D-2557 "Strength Properties of Adhesives In Shear By Tension Loading In The Temperature Range From -267.8 to -55C

162. ASTM D-2295 "Strength Properties of Adhesives In Shear By Tension Loading at Elevated Temperatures"

163. ASTM D-638 "Tensile Properties of Plastics"

164. ASTM E-229 "Shear Strength and Shear Modulus of Structural Adhesives"

165. ASTM D2293-69, "Creep Properties of Adhesives In Shear By Compressor Loading,"

166. Quirk, J. T., Kozlowski, T. T,, and Blomquist, R. F., "Location of Failure In Adhesive Bonded Butt Joints", FPL-0177 (AD663648), December 1967.

167. Foye, R. L., "Inelastic Micromechanics of Curing Stresses in Composites", presented at ASME Annual Meeting, November 1975, Houston.

168. Dukes, W. A. and Bryant, R. W., "The Effect of Adhesive Thickness on Joint Strength", by Explosives Research and Development Establishment, Ministry of Technology, England, 1968.

169. Mahoney, J. W. and Crilly, E. R., "Development of Improved Core Splice Adhesives".

170. Waddoups, M. E., Wolff, R. V. and Wilkins, D. J., "Reliability of Complex Large Scale Composite Structure-Proof of Concept," AFML-TR-73-160, July 1973.

171. Messner, A. M., "Stress Distribution in Poker-Chip Tensile Specimens," Aerojet-General Corporation - personnel communication with Dr. Richard Schapery, 1962.

172. Dixon, J. D., "Photoelastic Analysis of Stress Distributions In Simulated Propellant Under Tensile and Shear Test Specimens," Aerojet-General Corporation Report No. PEL-34, February 1963.

173. Lubkin, J. L. and Reissner, E., "Stress Distribution and Design Date for Adhesive Lap Joints Between Circular Tubes," ASME Paper No. 55-SA-59, April 1955.

174. "Adhesion" Edited by D. D. Eley, Oxford Press, 1961.

175. Dance, W. E. and Petersen, D. H., "Verification of the Structural Integrity of Laminated Skin-to-Spar Adhesive Bondlines by Neutron Radiography," October 1976, Presented at Symposium on Durable Adhesive Bonded Structures Meeting, Picatinny Arsenal, New Jersey.

176. Butt, R. I. and Cotter, J. L., "The Effect of High Humidity on the Dynamic Mechanical Properties and Thermal Transitions of an Epoxy-Polyamide Adhesive," Journal of Adhesion, Vol. 8, pp. 11-19, 1976.

177. Allen, K. W. and Shanahan, M. E. R., "The Creep Behavior of Structural Adhesive Joints - 1", Journal of Adhesion, Vol. 7, pp. 161-174, 1975.

178. Allen, K. W. and Shanahan, M. E. R., "The Creep Behavior of Structural Adhesive Joints - 11," Journal of Adhesion, Vol. 8, pp. 43-56, 1976.

179. Kaplevatsky, Y. and Raevsky, V., "On the Theory of the Stress-Strain State in Adhesive Joints," Journal of Adhesion, Vol. 8, pp. 65-77, 1976.

180. Alwar, R. S. and Nagaraja, Y. R., "Viscoelastic Analysis of an Adhesive Tubular Joint," Journal of Adhesion, Vol. 8, 79-92, 1976.

181. Williams, J. H., Jr., "Stresses in Adhesive Between Dissimilar Adherends," Journal of Adhesion, Vol. 7, pp. 97-107, 1975.

182. Machinery's Handbook, The Industrial Press, 1946.

183. Environmental Chambers, Catalog No. 9400, Webber Manufacturing Company, Inc. P. O. Box 217, Indianapolis, Indiana 46206.

184. Associated Environmental Systems Catalog AES-2, Merrimack St., Lawrence, Mass., 01842,

185. Abbeon Calibration, Inc., Catalog No. 975, Gray Avenue, Santa Barbara, CA. 93101.

186. Blue M Manufacturing Co. Catalog E-176, Blue Island, Illinois 60406.

187. Tenney Engineering, Inc., Bulletins #120A, Union, N.J. 07083.

188. Quinn, F. C., "How to Select Humidity Measuring and Control Equipment," Heating, Piping and Air Conditioning Journal, July 1976, page 107.

189. Hygrodynamics Catalog 672B, Division of American Instrument Co., 8030 Georgia Avenue, Silver Spring, Maryland 20910.

190. Wiederhold, P. R., "Humidity Measurements-Part I: Psychrometers and percent RH Sensors", Reprint From Instrumentation Technology, presented at 21st ISA Analysis Instrumentation Symposium, 1975, King of Prussia, Pa.

191. Quinn, F. C., "The Quality of Water-The 'Other' Raw Materials", Paper Trade Journal, September 4, 1967.

192. Quinn, F. C., "Humidity-The Neglected Parameter", Report from Test Engineering, July 1968.

193. Hygrodynamics Technical Bulletin No. 5. Division of American Instrument Co., 8030 Georgia Avenue, Silver Spring, Maryland 20910.

194. Gent, A. N. Lindley, P. B., "The Compression of Bonded Rubber Blocks," Publication No. 324, Journal of British Rubber Producers Association, Volume 173, 1959.

195. Williams, M. L., Blats, P. J. and Schapery, R. A., "Fundamental Studies Relating to Systems Analysis of Solid Propellants," GALCIT SM 61-5, California Institute of Technology, February 1961, ASTIA Report No. AD256-905.

196. Schjelderup, H. and Jones, W. B., "Mechanical Behavior of Cast Adhesive Film (Neat)," Adhesives Age, 1978.

197. Weitzman, Y., "Effects of Fluctuating Moisture and Temperature on the Mechanical Response of Resin-Plates," J. Applied Mechanics, PP. 571-576, December 1977.

198. Hashin, Z., "The Elastic Moduli of Heterogeneous Materials," Journal of Applied Mechanics, March 1962.